The FLT3 tyrosine kinase receptor ITD mutation controls its expression and drug resistance in acute myeloid leukaemia

Thesis submitted in accordance with the requirements of the University of Liverpool for the degree of Doctor in Philosophy

By

Taha Yahya Alqahtani

February 2021

Dedication

This thesis is dedicated to my father Yahya Alqahtani, my mother Zahra Aljedani, my wife Amal Alsuhaymi and my beautiful kids Saud & Larin

My Mother was so proud when I started PhD study but, unfortunately, did not live to see it finished. I love you Mum!

(الْحَمْدُ لِلَّهِ رَبِّ الْعَالَمِينَ)

All thanks are due purely to God, Lord of the universe

Declaration

I declare that this thesis has been written solely by myself and that it has not been submitted, in whole or in part, in any previous application for a degree. Except where states otherwise the work presented is entirely my own. The work was carried out in the laboratory of Professor David MacEwan, Department of Pharmacology and Therapeutics, Institute of Systems, Molecular and Integrative Biology (ISMIB), University of Liverpool, Liverpool, United Kingdom.

King Khalid University and Saudi cultural bureau in London, Government of Saudi Arabia, funded the PhD work presented in this thesis.

Taha Alqahtani

February 2020

Abstract

In approximately 23% of AML patients, Fms-like tyrosine kinase 3 (FLT3) contains a gain-of-function, internal tandem duplication (ITD) mutation that is associated with an unfavourable prognosis. FLT3 is therefore seen as a promising therapeutic avenue for AML and as a result, a more complete understanding of its function and signalling may lead to additional targets and resistance mechanisms being identified. To date, several FLT3 inhibitors including Quizartinib (AC220), a second-generation ITD-selective tyrosine kinase inhibitor, have been developed, but single-agent clinical trials have not been overwhelmingly successful. In most preclinical studies, the inhibitory effects of FLT3 inhibitors are mainly evaluated using mutant-expressing models, however, most AML patients harbour both a wild-type and mutant *FLT3* allele as well as presenting with high plasma levels of FLT3 ligand (FLT3L). We hypothesized that FLT3L could act through WT-FLT3 to influence the efficacy of FLT3 inhibitors in cells with heterozygous mutations. In this study, we have examined the role of FLT3 inhibition and FLT3L activation on the cellular localisation and downstream signalling in several AML cell lines, some of which express ITD mutations. We also looked at mechanisms by which FLT3L could impair the efficacy of FLT3 inhibitors. Our results revealed that the majority of FLT3 in the MV4-11 and MOLM-13 cells was intracellular. Inhibition of ITD-FLT3 with quizartinib led to a dramatic relocalisation of FLT3 to the cell surface. This effect was more pronounced in MV4-11 ($FLT3^{ITD/ITD}$) than the heterozygous MOLM-13 ($FLT3^{ITD/WT}$) cells that also express WT. This was accompanied by inhibition of ERK, AKT and STAT5 signalling pathways and resulted in cell death. Quizartinib induced cell death only in AML lines expressing FLT3-ITD mutations (MOLM-13 and MV4-11), and this could be antagonised by FLT3 ligand (FLT3L). The largest inhibitory effects were seen in heterozygous cells expressing a mutated and wild-type allele. FLT3 inhibition was associated with downregulation of the anti-apoptotic protein Mcl-1 and upregulation of the pro-apoptotic BH3-only protein, Bim. Our experiments indicated that both of these proteins were regulated by both WT and ITD-FLT3 through the MAPK pathway. These results suggest that activation of FLT3 signalling by FLT3L confers resistance to quizartinib through upregulation of Mcl-1 and suppression of Bim expression.

Taken together, our data suggest that FLT3 cell surface localisation and expression are controlled by ITD mutations and are key components of drug resistance. The data also suggests a novel therapeutic approach in patients with high plasma FLT3L levels, especially when using type II inhibitors such as quizartinib, is to co-target the MAPK/ERK pathway to abrogate the FLT3L-mediated resistance in FLT3-ITD AML.

Acknowledgements

Looking back at this PhD journey, I could not feel more grateful and humbled for what I have been given by so many people. I would like to express my gratitude and admiration for everyone who was part of this incredible experience.

First, I would like to express my deepest appreciation and gratitude to my advisors, Prof. David MacEwan and Prof. Joseph Slupsky, for their guidance, insights and support that made possible this work. Thank you Dave, for inspiring me with your passion for what you do. Your contagious joy and optimism always kept me going! We both know how my experience in the lab, but you have never let me fall. You have trusted in my decisions, guided me, supported me and were always available. I always knew that you believed in me and wanted the best for me. Thank you!

Also I would like to thank Dr. Nicholas Harper, for standing by me and extending a helping hand to me when I needed it most, thank you for reading my thesis and helping me put everything together. To my “lab mates” Dr. Vanessa Marensi and Fiona, I am very happy of being part of such group of people, who were always available to help in any possible way. Thank you all! I’m also very grateful to my dearest friends, Humood, Dr.Jehad, Ammar, and Dr. Anil for their encouragement and precious suggestions.

Finally, I would especially like to thank my family. My wife, Amal has been extremely supportive of me throughout this entire process and has made countless sacrifices to help me get to this point. My children, Saud and Larin, have continually provided the requisite breaks from the science and the motivation to finish my degree with expediency. My parents and whole family, deserve special thanks for always driving me to pursue my scientific passion and cheering me on along the way. Thank you all! Love you!!

Table of Contents

List of Figures

Chapter I:

Chapter III:

Chapter IV:

Chapter V:

List of Tables

Chapter I:

Chapter II:

Abbreviations

Acute Myeloid Leukaemia	AML
Analysis of Variance	ANOVA
Annexin V-Propidium Iodide	AV/PI
Ammonium persulfate	APS
Adenosine triphosphate	ATP
BCL-2-associated death promoter	BAD
BCL-2-homologous antagonist killer	BAK
BCL-2 associated X	BAX
B cell lymphoma 2	Bcl-2
B-cell lymphoma-extra large	Bcl-xL
BCL-2 homology	BH
BH3 interacting-domain death agonist	BID
Bovine serum albumin	BSA
Clustered Regulatory Interspaced Short Palindromic Repeats	CRISPR
Double distilled water	ddH20
Dulbecco Modified Eagle Medium	DMEM
Dimethyl sulfoxide	DMSO
Deoxyribonucleic acid	DNA
Deoxyribonucleotide triphosphate	dNTP
Enhanced chemiluminescence	ECL
Ethylenediaminetetraacetic acid	EDTA
Ethidium bromide	EtBr
French-American-British Classification	FAB
Fluorescence-activated cell sorting	FACS
Fetal Bovine Serum	FBS
Food and Drug Administration	FDA
FMS like Tyrosine Kinase-3	FLT3
Homology Directed Repair	HDR
Horseradish peroxidase	HRP
Haematopoietic stem cell	HSC
Half maximal inhibitory concentration	IC50
Immunoglobulin	Ig
Interleukin	IL
Insertion Or Deletion Mutations	INDEL
Internal Tandem Duplications	ITD
monoclonal antibody	mAb
Myeloid cell leukemia 1	Mcl-1
MAPK/ERK Kinase	MEK
Non-Homologous End Joining	NHEJ
Nucleophosphin 1	NPM1
Tumour protein 53	p53

Poly-ADP ribose polymerase	PARP
Polyacrylamide gel electrophoresis	PAGE
Protospacer Adjacent Motif	PAM
Phosphate-buffered saline	PBS
Polymerase Chain Reaction	PCR
Polyethylenimine	PEI
Pleckstrin homology domain	PH domain
Phosphoinositide-3-kinase	PI3K
Phosphatidylinositol (3,4,5)-trisphosphate	PIP3
Protein Tyrosine kinases	PTKs
p53 upregulated modulator of apoptosis	PUMA
Reactive Oxygen Species	ROS
Roswell Park Memorial Institute	RPMI
Receptor tyrosine kinases	RTKs
Reverse Transcriptase	RT
Sodium dodecyl sulfate	SDS
Short interfering RNA	siRNA
Secondary mitochondrial activator of caspases	SMAC
Signal transducer and activator of transcription 5	STAT5
Spleen focus-forming virus	SFFV
Tris-acetate-EDTA	TAE
Transcription Activator Like Effector Nuclease	TALEN
Truncated BID	tBID
Tris-buffered saline and Tween 20	TBST
Tetramethylethylenediamine	TEMED
Tyrosine kinases	TKs
Trans-activating crRNA	tracrRNA
World Health Organisation	WHO
Carbobenzoxy-valyl-alanyl-aspartyl-[O-methyl]-fluoromethylketone	Z-VAD-FMK

Chapter I

==========

Introduction

1.1 Acute myeloid leukaemia

1.1.1 Haematopoiesis

Haematopoiesis is the process of blood cell formation which occurs during embryonic development and throughout adulthood to produce and replenish the cellular blood components. All hematopoietic lineages originate from the common pluripotent hematopoietic stem cell (HSC)(Baum et al., 1992). HSCs have a long-term self-renewal capability and give rise to multiple hematopoietic types including the myeloid and lymphoid lineages, which possess a limited differentiation capacity (Zhang et al., 2018). Normal haematopoietic cells are organised in a hierarchy, in which long-term reconstituting HSCs (LT-HSCs) differentiate into short-term reconstituting HSCs (ST-HSCs). LT-HSCs are a relatively rare, quiescent population in bone marrow and have full long-term (>3~4 months) reconstitution capacity and are responsible for maintaining self-renewal and multi-lineage differentiation potential throughout life, whereas ST-HSCs can differentiate into multipotent progenitors (MPPs) with reduced self-renewal ability but only have a short-term (< 1 month) reconstitution ability (Orkin and Zon, 2008, Yang et al., 2005). Common myeloid progenitors and common lymphoid progenitors are then derived from MPPs. Common myeloid progenitor cells can differentiate into terminally differentiated haematopoietic cells such as erythrocytes, granulocytes, macrophages, platelets and dendritic cells. Lymphoid multipotent progenitor cells can differentiate into B-cells, T-cells, natural killer cells and dendritic cells that can mediate immune response (Fig 1.1).

Haematopoiesis occurs in two waves; the primitive wave and the definitive wave (Galloway and Zon, 2003). The primitive wave occurs primarily in the yolk sac during the early stages of foetal development and functions to produce primitive red blood cells and macrophages. The main purpose of the primitive wave is to provide and facilitate tissue oxygenation for the rapidly dividing embryonic cells (Palis, 2014). The primitive wave is transitory as these erythroid progenitors are not pluripotent and lack self-renewal capability. By contrast, definitive haematopoiesis occurs later in development and, although it begins in the yolk sac it has the potential to migrate towards the liver and then to the bone marrow which is the final destination for HSCs in adults (Jagannathan-Bogdan and Zon, 2013).

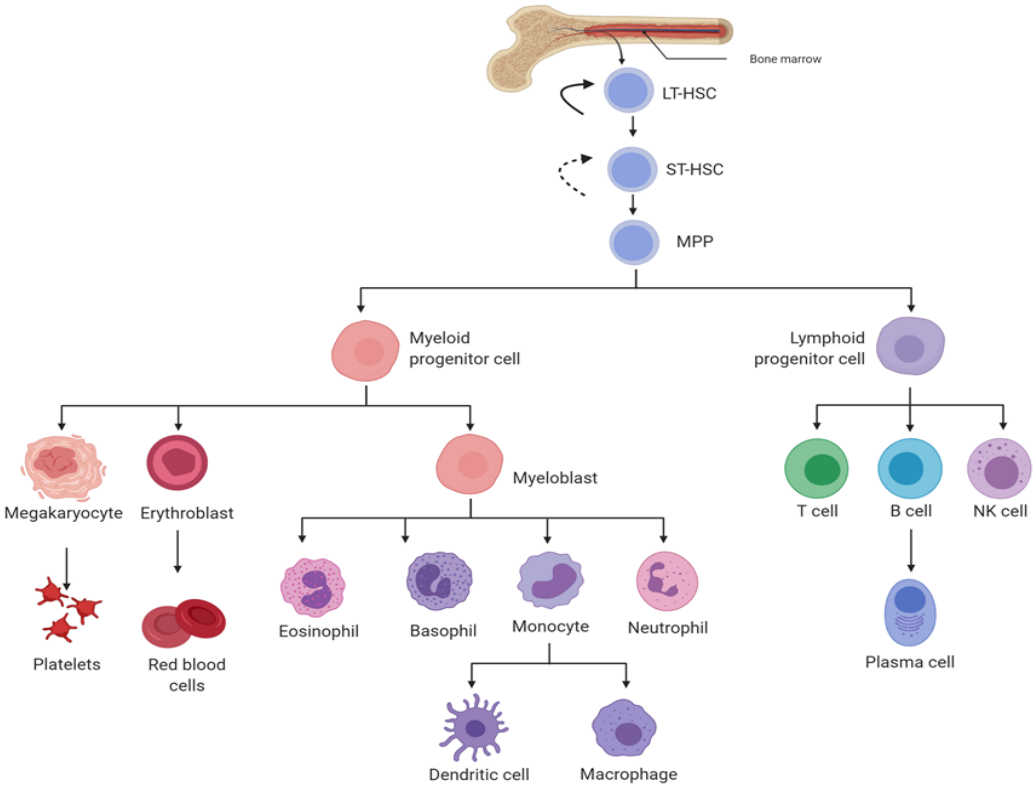

Figure1.1: Haematopoiesis – Schematic of haematopoiesis indicating the origin and common progenitors of all terminally differentiated hematopoietic cell lineages.

Over the past several years, the use of single cell sequencing technologies has led to increased understanding of haematopoiesis and has highlighted more than had previously been appreciated, the complexity of hematopoietic differentiation. In the classical tree-like hierarchy, the HSCs go through defined stages of differentiation as oligo-, bi- and uni-potent progenitors according to their CD34 expression (Kondo et al., 1997, Manz et al., 2002). This model was based on the analysis of predefined flow-sorted cell populations. Single cell sequencing has challenged this classical view and suggested that lineage commitment can bypass the discrete hierarchically organized early progenitor populations (Velten et al., 2017). Sanjuan-Pla et al demonstrated that distinct subsets of HSCs exist that are biased towards platelet generation and sit at the apex of the hierarchy (Sanjuan-Pla et al., 2013). Using single cell RNA-Seq (ScRNASeq), another study indicated that megakaryocyte-erythroid progenitors, a unipotent myeloid lineage-committed progenitor, can be directly derived from HSCs (Yamamoto et al., 2013). Also it was also suggested that MPPs are a heterogeneous population with a potential different lineage-biases and can be sub-divided into MPP1, MPP2, MPP3 and MPP4. MPP1 is similar to IT-HSC and can give rise to all lineages. MPP2/3 are myeloid-biased and MPP4 is lymphoid-biased and exhibit short-term reconstitution ability (Wilson et al., 2008, Pietras et al., 2015). These findings change the view towards the from a step-wise haematopoietic hierarchical pattern to a more fluid continuum model, in which HSCs exhibit a differentiation bias towards different mature blood cells (Fig 1.2).

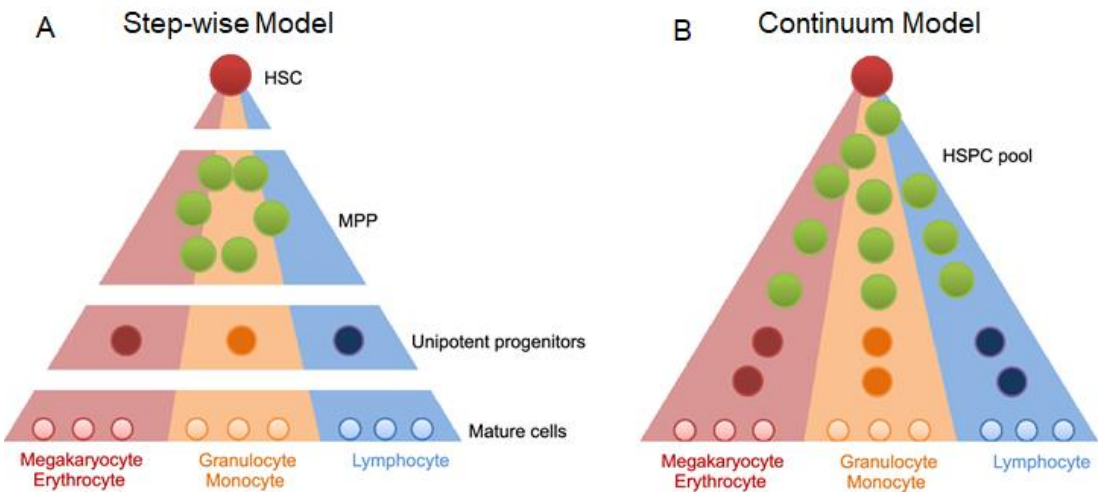

Figure 1.2: Models of HSC Lineage Commitment – A) The step-wise model suggests HSCs differentiation to mature lineages is a stepwise process and with equal contribution to each lineage. **(B)** Recent revised model suggesting haematopoiesis represents a fluid continuum and HSCs exhibit differentiation biases towards one lineage. Reprinted with permission from Protein and Cell, "New paradigms on hematopoietic stem cell differentiation" (Cheng et al., 2020).

1.1.2 Regulation of haematopoiesis by extrinsic and intrinsic factors

During haematopoiesis, key extrinsic and intrinsic factors can precisely maintain the balance between the undifferentiated stem cell state and differentiation into multiple lineages (Trompouki et al., 2011, Zhang and Lodish, 2008). The extrinsic factors include cytokines, growth factors and other environmental factors that can activate multiple cell signalling pathways and trigger changes in a haematopoietic cell's lineage fate. Intrinsic factors include transcription factors that drive key haematopoietic processes, including self-renewal and differentiation. Examples of cytokines and growth factors that regulate haematopoiesis include, Granulocyte-macrophage colony stimulating factor (GM-CSF) which supports the development of macrophages and dendritic cells (Gasson, 1991), Thrombopoietin (Tpo) which is important for

megakaryocyte and platelet production and regulates HSC quiescence (Kaushansky, 1995), Interleukin-1 (IL-1) that regulates the response following injury (Pietras et al., 2016). Tyrosine kinase receptors; such as FLT3 and c-KIT also contribute to lineage determination (Mooney et al., 2017). Cell surface expression of FLT3, and binding of FLT3 ligand control megakaryocyte/erythrocyte lineage development (Tsapogas et al., 2014). Cytokines also activate transcription factors such as C/EBPα and PU.1 that regulate the myeloid progenitor cell's commitment (Iwasaki et al., 2005). Additionally, the balance between the PU.1 and GATA1 transcription factors (TFs) governs the myeloid or the erythroid lineage fate and unbalanced expression of either leads to hematopoietic lineage distortion (Hoppe et al., 2016). As a result, the balance between extrinsic and intrinsic factors needs to be tightly regulated for normal haematopoiesis.

1.1.3 Regulation of HSCs in the bone marrow niche

The primary site of haematopoiesis in adults is the bone marrow (BM), where the HSCs reside, self-renew and differentiate under tightly controlled but dynamic process (Sánchez-Aguilera and Méndez-Ferrer, 2017). The BM has two niches; the endosteal niche and vascular niche. These niches have a complex microenvironment composed of different cell types, growth factors, cytokines, osteoblastic cells, extracellular matrix molecules, and vascular network (Wei and Frenette, 2018). The niche's microenvironment regulates HSC and progenitor cell key processes including survival, differentiation, self-renewal and adhesion (Tamma and Ribatti, 2017) . The osteoblast cells are termed CXCL12-abundant reticular (CAR) cells and as they produce the

soluble and membrane-bound chemokine, CXC chemokine ligand 12 (CXCL12), which promotes the differentiation and proliferation of short-term HSCs (Konopleva and Jordan, 2011). The CAR cells also overexpress vascular cell adhesion molecule-1 (VCAM-1), interleukins (ILs), and platelet-derived growth factor (PDGF), all of which have regulatory roles in cell adhesion and angiogenesis. Pathophysiologically, the environment has also been found to mediate chemotherapy resistance through different mechanisms (Chagastelles and Nardi, 2011, Guerrouahen et al., 2011). In haematopoietic malignancies, interaction of leukaemic cells with the haematopoietic niche is altered. For instance, induction of tumour necrosis factor (TNF)-expression in endothelial cells and the reduction of normal HSC in FLT3-ITD-transgenic mice in transplantation experiments has been linked to FLT3-ITD-induced myeloproliferation. The results indicate that leukaemic blast cells mediate death of stromal cells through the TNF pathway resulting in impaired haematopoiesis (Mead et al., 2017). Furthermore, osteoblasts have been shown to protect AML cells from CXCL12-induced cell death of CXCR4-expressing AML cells residing in the bone marrow (Kremer et al., 2014). The binding of CXCL12 promotes the phosphorylation of CXCR4 and activation of downstream pro-survival signalling pathways, MAPK/ERK, JAK/STAT, and PI3K/AKT pathways. The FLT3-ITDsignalling enhances CXCR4 signalling in leukaemic cells through activation of the serine/threonine kinase Pim1 resulting in phosphorylation of the intracellular domain of CXCR4 enhancing the signalling of the receptor and, enhanced recruitment and localization of FLT3-ITD expressing cells to the perivascular niche (Grundler et al., 2009). Stromal cells can also are also a source of IL-3 and GM-CSF

and these cytokines have been shown to rescue FLT3-ITD cells from TKIs via upregulation of tyrosine kinase receptor, Axl (Dumas et al., 2019). These studies suggest that hematopoietic cells and cells in BM niches can interact with each other during haematopoiesis as well as in hematopoietic malignancies.

1.1.4 Acute Myeloid Leukaemia

Haematological malignancies (HMs) are blood cancers that arise from cells originating in the bone marrow. HMs can be categorised into leukaemia, multiple myeloma, Hodgkin lymphoma, and non-Hodgkin lymphoma. Acute myeloid leukaemia (AML) is an aggressive haematological malignancy arising from genetic alterations in normal HSCs and is characterised by the presence of at least 20% leukemic blasts in the peripheral blood or bone marrow (Kumar, 2011a, Dohner et al., 2010). The defining feature of AML is an accumulation of undifferentiated myeloid blast cells which would normally mature to hematopoietic cells. As a result, the immature, highly proliferative myeloid cells accumulate in the bone marrow, peripheral blood and other sites including liver, lung, central nervous system and spleen (Grove and Vassiliou, 2014). The primary symptoms of AML include bone marrow failure and leucocytosis. Other common symptoms include fatigue, anorexia, and weight loss. People with advanced AML are more vulnerable to excessive bleeding or infection which lead to death if not treated (De Kouchkovsky and Abdul-Hay, 2016).

1.1.5 Classification of AML

As AML is a highly heterogeneous disease, it is classified into different subtypes based on cytogenetic and morphological characteristics. Two systems are used to classify AML. The French-American-British (FAB) classification, was devised in 1976 (Bennett et al., 1976) and revised in 1985 (Bennett et al., 1985). It divides AML into eight subtypes (M0-M7), based on morphological appearance, cytochemical staining and how mature the cells are (Table 1.1). In the FAB classification, the diagnosis of AML is confirmed by the presence of greater than 30% of myeloid blasts in the bone marrow.

Table 1.1 – FAB classification of AML

AML FAB designation	Description
M0	Undifferentiated acute myeloblastic leukemia
M1	Acute myeloblastic leukemia with minimal maturation
M2	Acute myeloblastic leukemia with maturation
M3	Acute promyelocytic leukemia
M4	Acute myelomonocytic leukemia
M4 eo	Acute myelomonocytic leukemia with eosinophilia
M5	Acute monocytic leukemia
M6	Acute erythroid leukemia
M7	Acute megakaryocytic leukemia

FAB classification does not consider prognostic information. In 2001, in order to integrate advances in the diagnosis and treatment of AML, the latest classification from World Health Organization (WHO) has largely replaced the FAB classification as it takes into account different clinical and cytogenetic features. WHO classification splits AML into six major categories including:

“AML with recurrent genetic abnormalities”, “AML with myelodysplasia related features”, “therapy related myeloid neoplasms”, “myeloid sarcoma”, “myeloid proliferation related to Down syndrome” and “AML not otherwise specified” (Arber et al., 2016). In the WHO classification, AML is defined as having at least 20% blasts in the bone marrow. In addition to this, patients with t(8;21)(q22;q22), inv(16)(p13q22) or t(16;16)(p13;q22), and t(15;17)(q22;q12) translocations are considered to have AML regardless of blast percentage. Further subtypes of these categories as well as genetic abnormalities can be found in Table 1.2.

Table 1.2 – World Health Organization Classification of AML

AML with recurrent genetic abnormalities
AML with t(8;21)(q22;q22.1);RUNX1-RUNX1T1
AML with inv(16)(p13.1q22) or t(16;16)(p13.1;q22);CBFB-MYH11
APL with PML-RARA
AML with t(9;11)(p21.3;q23.3);MLLT3-KMT2A
AML with t(6;9)(p23;q34.1);DEK-NUP214
AML with inv(3)(q21.3q26.2) or t(3;3)(q21.3;q26.2); GATA2, MECOM
AML (megakaryoblastic) with t(1;22)(p13.3;q13.3);RBM15-MKL1
Provisional entity: AML with BCR-ABL1
AML with mutated NPM1
AML with biallelic mutations of CEBPA
Provisional entity: AML with mutated RUNX1
AML with myelodysplasia-related changes
Therapy-related myeloid neoplasms
AML, NOS
AML with minimal differentiation
AML without maturation
AML with maturation
Acute myelomonocytic leukaemia
Acute monoblastic/monocytic leukaemia
Pure erythroid leukaemia
Acute megakaryoblastic leukaemia
Acute basophilic leukaemia
Acute panmyelosis with myelofibrosis
Myeloid sarcoma
Myeloid proliferations related to Down syndrome
Transient abnormal myelopoiesis (TAM)
Myeloid leukaemia associated with Down syndrome

1.1.6 AML Pathophysiology

As mentioned previously, AML is a group of haematological diseases characterized by genetic heterogeneity among patients (Grove and Vassiliou, 2014). Clonal transformation of hematopoietic precursors occurs through the acquisition of multiple chromosomal rearrangements and a range of mutations that confer a proliferative and survival advantage as well as impairing hematopoietic differentiation (Tamamyan et al., 2017). Understanding the role of these genetic abnormalities play in disease progression would improve the prognosis and treatment of AML. In majority of cases, AML appears as *de novo* malignancy in previously healthy patients. However, it can also arise in patients as a consequence of prior therapy or in patients with an underlying haematological disorder (Sill et al., 2011).

Studies of key oncogenic events led to the development of the (Knudsen) "two-hit" model of leukemogenesis based on the molecular characterization of leukemic cells from AML patients (Kelly and Gilliland, 2002). This model suggests the development of AML depends on a collaboration between two broad classes of mutations, depending on the type of cellular processes that are affected (Gilliland and Griffin, 2002b, Kihara et al., 2014). The first group of mutations, referred to as class I mutations, are those that promote survival and proliferation. Examples of gain-of-function class I mutations include: FLT3 (internal tandem duplications (ITD), and tyrosine kinase domain (TKD) mutations), c-Kit, BCR-ABL, TP53, K-RAS and N-RAS activating mutations (Network, 2013). The second group of mutations, the class II mutations, are mutations that impair transcription factors essential for differentiation.

Examples include: fusion transcripts such as RUNX1/ETO, CBFβ/MYH11 and PML/RARα, which are generated by recurring chromosomal translocations t(8:21), t(15:17), and inv(16) (Gilliland and Griffin, 2002b, Takahashi, 2011). The resulting disruption of differentiation and proliferation caused by the cooperation of those two groups of mutations results in the transformation of blood forming cells to neoplastic cells and eventually the development of AML.

Recent studies have identified several groups of mutations that do not fit into this framework but still play a crucial role in the leukaemogenesis (Chaudry and Chevassut, 2017, Abdel-Wahab and Levine, 2013). These mutations have been allocated to a new class of epigenetic modifications. These are found in more than 40% of AML cases and include mutations in DNA-methylation and histone modification-related genes such as TET2, IDH1/2, ASXL1 and DNMT3A (De Kouchkovsky and Abdul-Hay, 2016). A revised model of myeloid malignancy pathogenesis has been proposed which considers the mutations in these epigenetic modifiers and the effect on the class I and II mutations (Shih et al., 2012) (Fig 1.3).

The FLT3-ITD is a driver mutation and in itself, does not cause AML rather it acts in cooperation with other oncogenes. In murine and zebra fish models, FLT3 ITD itself is not sufficient to induce AML and another oncogenic event was required to induce leukemogenesis (Skayneh et al., 2019). Using a murine bone marrow transplant model, FLT3 ITD has shown to cooperate with other oncogenic mutations such as the MLL-AF9 fusion protein to initiate and accelerate the onset of human AML-like syndromes (Stubbs et al., 2008).

Another study showed that FLT3-ITD cooperates with mutations in the multifunctional nucleolar protein, nucleophosmin (NPM1) resulting in rapid leukaemogenesis that closely recapitulates the human disease (Mupo et al., 2013). The third most common coincidental mutation is in DNA methyltransferase 3α (DNMT3A). A knock-in mouse harbouring an ITD alone developed a fatal myeloproliferative neoplasm (MPN) rather than full AML. The same group investigated potential cooperativity between ITD and mutant DNMT3A in the same mouse model and showed that genetic deletion of DNMT3A along with subsequent expression of FLT3-ITD in adult mice resulted in the development of AML (Poitras et al., 2016). The clonal heterogeneity of the disease is being elucidated using Single-cell DNA sequencing (scDNA-seq) analysis. In one study, 154 AML samples from 123 patients with different clinical characteristics were analysed. The most frequently detected mutations were in NPM1 (40%), FLT3 (38%) and, DNMT3A (37%) (Morita et al., 2020). Data also showed at the cellular level the co-occurrence and mutual exclusivity among driver mutations. For example, NPM1-FLT3-ITD and DNMT3A-NPM1 often co-occurred, however, IDH1-IDH2 is mutually exclusive. This and similar work would allow systematic investigation of the prognostic impact of clonal diversity in AML.

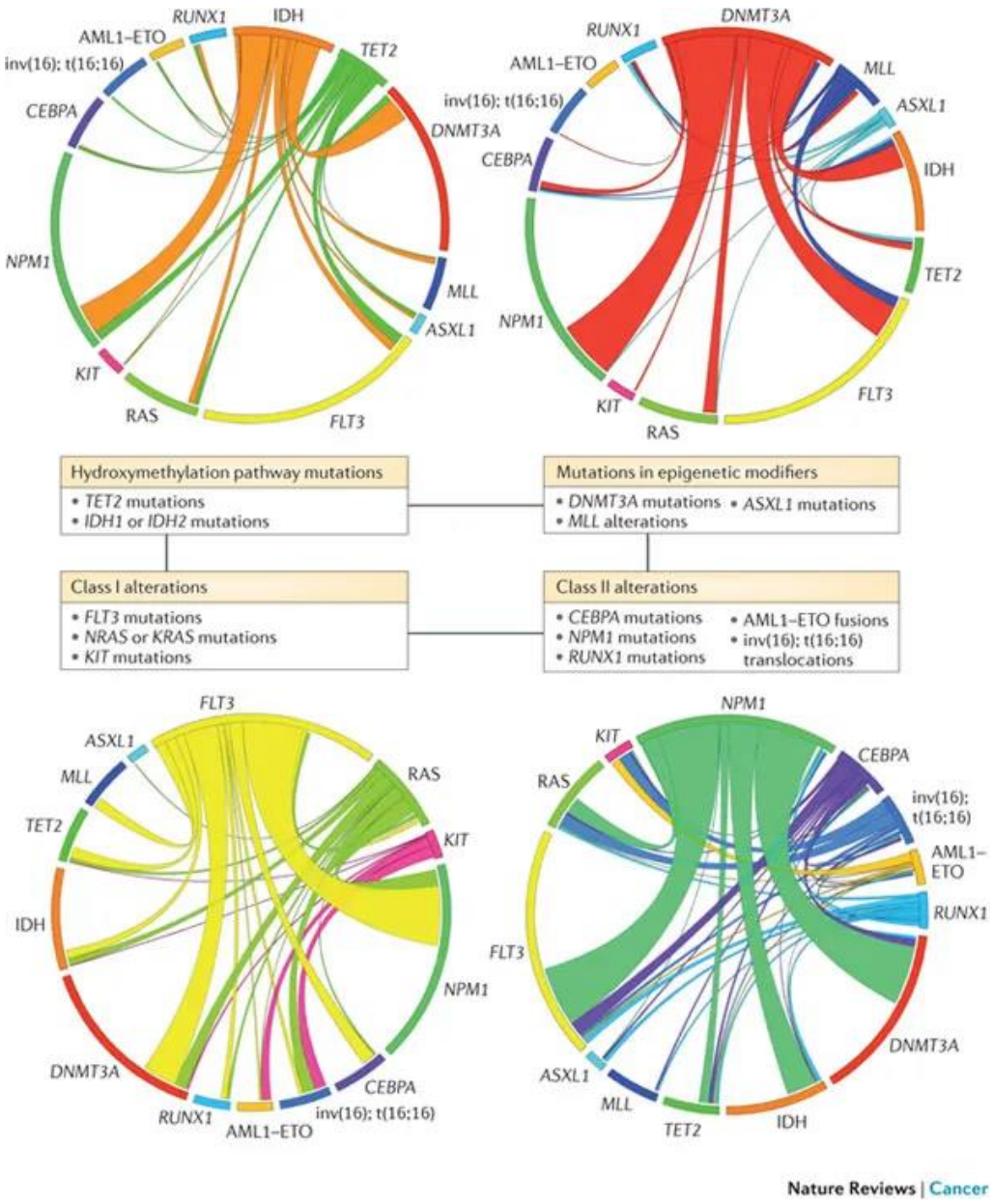

Figure 1.3: Revised model of leukaemogenesis – Myeloid malignancies result as a consequence of multiple mutations in genes involved in the regulation of cell proliferation, survival, and differentiation. The Circos diagrams above indicate the two novel classes of epigenetic modifier genes together with the class I and II alterations that have been found in AML patients. Reprinted with permission from Nature Reviews Cancer, “The role of mutations in epigenetic regulators in myeloid malignancies” (Shih et al., 2012).

1.1.7 Prognostic impact of ITD mutations

The unfavourable impact of FLT3-ITD on AML progression is well established and is keenly associated with a poorer clinical prognosis, high risk of relapse, and shorter overall survival (Port et al., 2014). Mutant-to-wild-type allelic ratio, insertion site, ITD length, as well as co-occurrence with mutations in other AML-mutated genes such as NPM1 and DNMT3A, all appear to have a prognostic impact on newly diagnosed patients presenting with ITD mutations (Garg et al., 2015). In some studies, a higher ITD allelic ratio has been associated with a worse outcome, however, other studies did not support that. For example, a threshold of mutant-to-wild-type ratio of >0.78 was significantly associated with shorter overall survival (Thiede et al., 2002). In another study however, analysis of a large number of patients demonstrated that the ITD allelic ratio did not correlate with risk of relapse in both NPM1-mutated and wild-type cases (Linch et al., 2014).

In addition, the National Comprehensive Cancer Network consensus panel indicates AML patients with FLT3-ITD (low allelic ratio < 0.5) and NPM1 mutations have a favourable prognosis similar to patients with NPM1 mutations in the absence of FLT3-ITD (O'Donnell et al., 2017a). Conversely, other studies have shown that patients who present with either a high or low ITD allelic ratio have a poor prognosis regardless of NPM1 mutational status (Boddu et al., 2019, Sakaguchi et al., 2018). Taken together, the remarkable heterogeneity of AML complicates the prognosis. The European Leukaemia Net (ELN) guidelines are a widely used AML risk stratification guideline and based on cytogenetics and molecular abnormalities (Döhner et

al., 2017). The ELN guidelines stratify AML patients into three risk groups: favourable, intermediate, and poor/adverse (Table 1.3).

Table 1.3 – 2017 ELN risk stratification by genetics

Risk status	Genetic abnormality
Favourable	t(8;21)(q22;q22.1); *RUNX1-RUNX1T1*
	inv(16)(p13.1q22) or t(16;16)(p13.1;q22); *CBFB-MYH11*
	Mutated *NPM1* without *FLT3*-ITD or with *FLT3*-ITD^{low}
	Biallelic mutated *CEBPA*
Intermediate	Mutated *NPM1* and *FLT3*-ITD^{high}
	Wild-type *NPM1* without *FLT3*-ITD or with *FLT3*-ITD^{low}
	t(9;11)(p21.3;q23.3); *MLLT3-KMT2A*
	Cytogenetic abnormalities not classified as favourable or adverse
Adverse	t(6;9)(p23;q34.1); DEK-NUP214
	t(v;11q23.3); KMT2A rearranged
	t(9;22)(q34.1;q11.2); BCR-ABL1
	inv(3)(q21.3q26.2) or
	t(3;3)(q21.3;q26.2);GATA2,MECOM(EVI1) 25 or del(5q);
	27; 217/abn(17p)
	Complex karyotype, monosomal karyotype
	Wild-type and NPM1 and *FLT3*-ITD^{high}
	Mutated RUNX1
	Mutated ASXL1
	Mutated TP53

1.1.8 AML Epidemiology

AML is one of the most common types of leukemia in adults. Despite this, the occurrence is relatively rare, accounting for only about 1 % of all new cancer cases in the UK in 2017 (CancerResearchUK 2015-2017). In the UK, the incidence rate of AML was 4.8/100,000 in 2016, and it has been estimated that around 3,152 new cases are diagnosed with AML leading to around 2,598 deaths in the UK every year with the highest mortality rates in the 85-89 age group (CancerResearchUK 2015-2017). Although AML can develop at any age, it is predominantly a disease of the elderly (average age, 68 years) and its incidence clearly increases with age. In the UK in 2015-2017, 42% of new cases were in people aged 75 and over. AML is also more common in males than females. Based on Cancer Research UK data, the overall 5-year relative survival rate for AML in the UK is only 14% for men and 16% for women. The 5-year survival rate for people aged 65 or older is about 5%. For people younger than 65, this changes to a survival rate of around 40-65%. These survival statistics are poorer than other forms of leukaemias, making AML (although not the most prevalent form of leukaemia) the deadliest. Clearly, the difficulties in successfully treating patients (often elderly) indicate there to be a serious need for much better therapeutic options to be available in the clinic.

1.1.9 Therapy/Therapeutic Options

Accurate assessment of prognosis is a central to AML management. Stratifying patients into well-defined risk groups helps decide the most beneficial therapeutic options (Bloomfield et al., 2018). Although clinical factors like resistance to treatment, comorbidities and age, have proven to play

an important role in therapeutic decisions, cytogenetics has been shown to be strongest prognostic factor of patient outcomes and overall survival (Grimwade et al., 1998, Grimwade et al., 2010). Accordingly, cases with AML can be stratified based on their cytogenetic profile into favourable (good survival), intermediate, and adverse (poor survival) (Estey, 2018).

Induction and consolidation Therapy

The backbone of AML treatment is based on two chemotherapy regimens, induction therapy and consolidation therapy. For induction therapy, patients are given an intensive combination of chemotherapy to achieve a complete remission. This combination is underlined by the “7+3” regimen, which consists of an anthracycline such as daunorubicin or idarubicin and high dose cytarabine, the deoxycytidine analogue. Cytarabine (100 or 200 mg/m^2) is usually given as a continuous infusion for seven days together with either daunorubicin (45-60 mg/m^2) or idarubicin (12 mg/m^2) intravenously, daily, for three days (O'Donnell et al., 2017b). This regimen is given to patients with a favourable or intermediate prognostic risk, in particular younger (< 60 years) and fit elderly patients (Estey, 2018). The aim of induction chemotherapy is to achieve complete morphologic remission and it generally achieves this in approximately 50% of patients above the age of 65 and up to 80% of of young patients (Seval and Ozcan, 2015, De Kouchkovsky and Abdul-Hay, 2016). These rates are not observed in older patients or patients that fall into the adverse prognostic risk group, which subsequently lead to advancement in AML treatment therapies.

The consolidation regimen is usually given after achievement of complete haematological remission (5% or less of leukemic blasts in the bone marrow) to eradicate any remaining leukemic cells and prevent relapse (Medeiros et al., 2019). Consolidation therapy often includes repeated high doses of cytarabine given to patients with a favourable or intermediate prognosis. There is no established optimal approach for elderly patients who are more likely to present with an adverse prognostic risk profile. Individuals over the age of 65 are considered not healthy enough to receive combination therapy and are instead given a low intensity chemotherapy with hypomethylating agents (HMA), or low dose cytarabine, despite this, the prognosis is still poor. Alternatively, Bone Marrow Stem Cell transplant is a consolidation option for elderly patients as well as patients with high risk cytogenetics (Hecker et al., 2018, Almeida and Ramos, 2016). Due to poor prognosis and lack of increased survival rate in elderly AML patients, new therapeutic approaches are required. This can be achieved by targeting specific genetic abnormalities in AML. Hence, FLT3 inhibitors are being investigated in combination with less intensive chemotherapeutic approach as well as monotherapy. The targeted therapy can be used as a front-line, post-transplant maintenance, and in relapse/refractory patients. Such an approach has been used successfully in the treatment of chronic myeloid leukaemia (CML). Targeting the Bcr-Abl fusion protein using TKIs, such as Imatinib, has revolutionized treatment of CML and increased five-year survival rate from ~40% in the pre-imatinib age (1989–2001) to ~90% post-imatinib era (2001–2013) (Beinortas et al., 2016, Brunner et al., 2013). Overall, chemotherapy is tailored by the aggressiveness of the disease, fitness of the patient, and the availability of a stem cell donor.

Alternative treatment strategies

As an induction treatment, decitabine and azacitidine are hypomethylating agents demonstrated to be beneficial for older patients with AML who are not eligible for intensive chemotherapy (Fenaux et al., 2009). The role of hypomethylating agents in the treatment of elderly patients with refractory AML is still not fully understood and is the subject of ongoing, phase II and III studies.

Novel targeted therapies

More recently, the identification of recurrent genetic mutations in AML has led to the development of new inhibitors and selective treatment approaches. Many promising drug candidates have been tested in clinical trials and demonstrated the ability to improve the survival rate either alone or in combination with standard chemotherapy. We will briefly discuss some of the most common targeted therapy for AML.

FLT3-ITD inhibitors

Given the poor prognostic impact of FLT3 mutations and the high incidence in new AML cases, inhibition of FLT3 represents a promising therapeutic avenue. FLT3 inhibitors will be discussed in more detail later.

IDH1/IDH2 small molecule inhibitors

Gain-of-function mutations in the isocitrate dehydrogenase (IDH) 1 and 2 genes are found in about 20% of new AML cases (Network, 2013). Both AG-

120 and AG-221 are IDH inhibitors currently in clinical trials. Preliminary results of phase I/II trials demonstrated an overall response rate of 37% with AG-221 and 31% with AG-120 in relapsed/refractory AML patients (Stein et al., 2015, DiNardo et al., 2015). In 2019, the FDA approved ivosidenib for newly diagnosed AML with IDH1 mutations. Enasidenib was also approved for patients with IDH2-mutated relapsed/refractory AML (Galkin and Jonas, 2019).

Immune therapies

Monoclonal antibodies exert their cytotoxicity either directly or indirectly through conjugation with chemotherapeutic agents or radioactive particles. Monoclonal antibodies being explored for AML treatment include gemtuzumab ozogamicin which binds to CD33, a transmembrane protein expressed on cells of myeloid lineage (Castaigne et al., 2012). The antibody is linked to the potent cytotoxic agent calicheamicin, which is internalized by cells following binding to CD33. In 2017, the FDA approved gemtuzumab ozogamicin for treatment of relapsed or refractory CD33-positive acute myeloid leukaemia in patients 2 years of age and older. Chimeric antigen receptor modified T cells (CAR-T) are T cells engineered to express a receptor that recognizes a specific cell-surface antigen. The antigen binding domain binds to cell surface molecules on the leukaemia, triggers TCR activation which results in cytotoxicity to the leukaemia (Gill et al., 2014). CD33 and CD123 are two attractive antigens in AML as they are predominantly overexpressed in AML blasts (Mardiros et al., 2013). Thirteen CAR-T trials for patients with AML are currently undergoing.

1.2 FMS-like tyrosine kinase 3 (FLT3)

1.2.1 RTKs in hematopoiesis

The receptor tyrosine kinase (RTK) class III, formerly known as the PDGFR (platelet-derived growth factor receptor) family is a most important family involved in HSC function and haematopoiesis. Members of this family include: PDGFR, colony stimulating factor-1 receptor (also known as c-FMS), c-Kit (stem cell factor receptor), and FLT3 (FMS-like tyrosine kinase 3) (Claesson-Welsh et al., 1989, Yarden et al., 1987, Coussens et al., 1986, Rosnet et al., 1993). These receptors span the plasma membrane and contain five immunoglobulin-like domains in the extracellular region, a transmembrane domain, a juxtamembrane (JM) domain and a split tyrosine kinase domain in the intracellular space. RTKs play a pivotal role in normal haematopoiesis through promoting survival, proliferation, and differentiation of early hematopoietic progenitor cells.

FMS-like tyrosine kinase 3 (FLT3)

FMS-like tyrosine kinase 3 (FLT3), also known as cluster of differentiation antigen 135 (CD135) receptor shares ~30% homology with other class III family members. In 1991, two independent groups cloned murine *FLT3* from fetal liver and placental cDNA libraries and it was mapped to chromosome 5 (Matthews et al., 1991, Rosnet et al., 1991a). In 1993, the human gene was isolated from a pre-B cell cDNA library and a CD34 HSC enriched library (Rosnet et al., 1993). The human *FLT3* gene is located on chromosome 13 (13q12) and consists of 24 exons (3,848 bp) extending over more than 100 kb (Rosnet et al., 1991b) (Fig 1.4). The gene encodes for

a protein containing 993 amino acids, which presents as two species when detected by SDS-PAGE and Western blotting. A 160 kDa band is a result of N-linked glycosylation of the extracellular domain and this represents the membrane-bound form. A 130 kDa band is partially glycosylated and located intracellularly (Schmidt-Arras et al., 2005). Glycosylation occurs in two phases, following translation FLT3 undergoes partial glycosylation in the endoplasmic reticulum (ER) resulting in the immature receptor form. This is subsequently processed in Golgi where further modification occurs to produce the mature form that is then transferred to the cell surface.

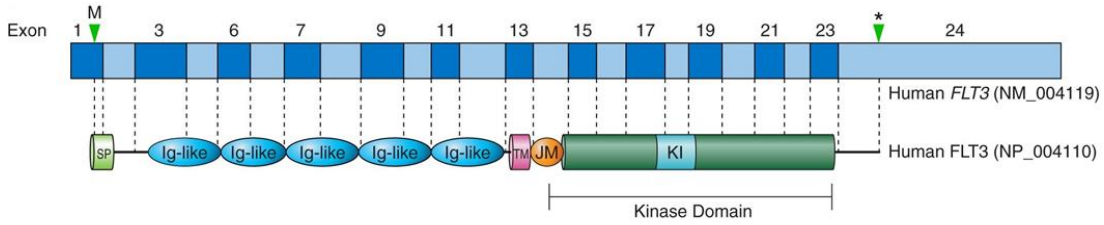

Figure 1.4: Genomic structure and domain arrangement of FLT3 – The human FLT3 gene consists of 24 exons. The translation initiation codon is located in second half of exon 1. An N-terminal signal peptide (SP) is encoded by exons 1 and 2 followed by the extracellular immunoglobulin-like (Ig-like) domains (exons 3–12). Exon 13 encodes the transmembrane domain and the intracellular regions, including the juxtamembrane domain and the kinase domain, are mainly encoded by exons 14–23 and to some extent by exon 24. Reprinted with permission from Physiological reviews, “FMS-like tyrosine kinase 3/FLT3: from basic science to clinical implications” (Kazi and Rönnstrand, 2019).

The extracellular domain of FLT3 consists of five immunoglobulin-like domains D1, D2, D3, D4, and D5 which are essential for ligand recognition. FLT3 also contains a transmembrane domain (TM), a juxtamembrane domain (JM), and two intracellular tyrosine kinase domains (TKD) linked by a kinase insert domain (Fig 1.5). The general structure of tyrosine kinases is composed of a N– and C-lobes flanking an ATP binding pocket , and an activation loop that determines downstream signalling (Modi and Dunbrack, 2019, Kazi et al., 2017).

The juxtamembrane domain (JMD) follows the transmembrane sequence and it is located between lobes. The JMD can be divided into three distinct components; the JM binding motif (Tyr572-Met578), the JM switch motif (Val579–Val592) and a linker peptide (Asp593-Trp603). In the inactivated state, the JMD occupies the active site and prevents the activation loop from adopting an active conformation. The JM switch motif contains several key tyrosine residues (Tyr589 and Tyr591) whose phosphorylation is involved in activation of the receptor (Mol et al., 2003). Ligand-dependent activation causes conformational changes in the JMD, phosphorylation of either Y589 or Y591 and reverts the auto-inhibitory conformation (Griffith et al., 2004). Tyr589 and Tyr591 can also act as a negative regulators of the kinase activity since dephosphorylation of these residues allows JMD to re-adopt its autoinhibitory conformation preventing further catalytic activation (Chan et al., 2003).

The tyrosine kinase domain (TKD) is the catalytic domain that transfers the γ-phosphate of ATP to the hydroxyl group of serine, threonine, or tyrosine

residue on the target protein. The FLT3 kinase domain consists of N-terminal lobe (N lobe) and an α-helical C-terminal lobe (C lobe) linked by a hinge segment. The activation loop is the key conserved structural element required for catalytic activity (Schwartz and Murray, 2011). The structure of the activation loop, including that of a conserved Asp-Phe-Gly element, termed the DFG motif, can adopt active or inactive conformations of FLT3. In the "DFG-in" conformation, the aspartic acid residue, which lies at the N-terminus of the activation loop must be point into the ATP binding site, where it coordinates Mg^{2+} ions and ATP in the active conformation. In the "DFG-out" conformation and as a result of mutations the Asp and Phe residues swap positions and Asp side chain points away from the ATP binding pocket and the Phe points toward the ATP binding pocket keeping the receptor in an inactive state (Kornev et al., 2006). Understanding the different coordination of these residues is a fundamental basis for tyrosine kinase selectivity as Type I inhibitors are classified by this "DFG-in" conformation, whereas, Type II inhibitors are defined by the "DFG-out" conformation (Zhao et al., 2014, Zorn et al., 2015).

Under physiological condition, FLT3 expression is restricted to hematopoietic progenitor cells (human granulocyte-monocyte progenitor (GMP) and common lymphoid progenitor (CLP) cells) in the bone marrow, however, this is usually lost upon differentiation. FLT3 expression has been also detected in thymus, lymph nodes, brain, placenta and liver where its function is unknown (Rosnet et al., 1993, Rosnet et al., 1996a). The expression of FLT3 ligand (FLT3L) is almost ubiquitous and it exists either in a membrane-bound or soluble form

(Hannum et al., 1994, Lyman et al., 1993). Consequently, the function of FLT3L is controlled by the restricted expression of its receptor, FLT3. FLT3 knock-out mice appear healthy with little effect on life span or sign of haematological disease (Mackarehtschian et al., 1995). However, these mice do display a reduction in B lymphoid progenitors, natural killer, and dendritic cells (McKenna et al., 2000).

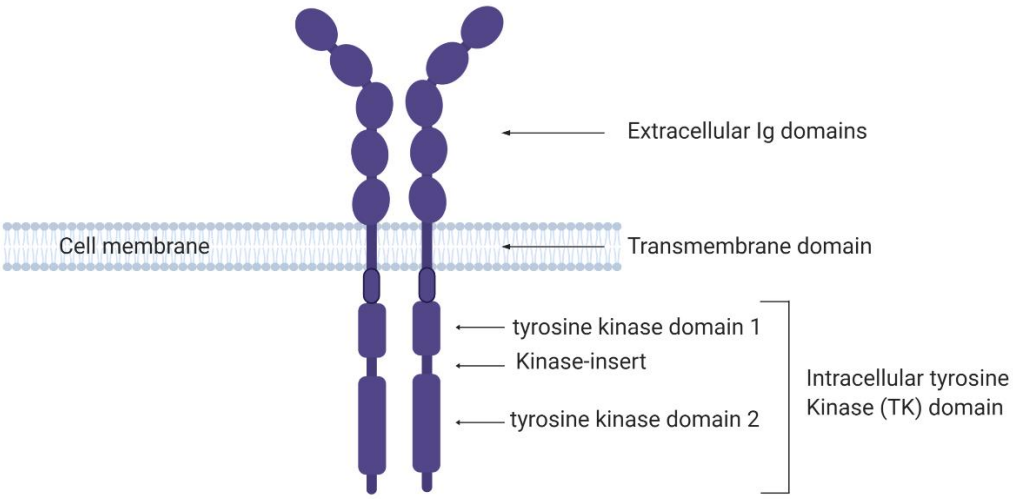

Figure 1.5: Structure of FLT3 receptor – FLT3 consists of five immunoglobulin-like domains in the extracellular region, a transmembrane domain (TM), a juxtamembrane domain (JM), and two intracellular tyrosine kinase domains (TKD) linked by a kinase insert.

Stem Cell Factor Receptor (c-Kit)

As with FLT3, c-Kit (CD117) plays a pivotal role in haematopoiesis as early hematopoietic cells are dependent on c-Kit-mediated signals for proliferation and survival. The *c-Kit* gene located on human chromosome 4q11 contains 21 exons, spanning more than 34 kb (Yarden et al., 1987). c-Kit is commonly

expressed in early hematopoietic cells (including stem cells and progenitor cells), and is downregulated following maturation (Ogawa et al., 1991). Mast and dendritic cells retain high levels of c-Kit expression even when fully differentiated and they rely on c-Kit for their survival and proliferation (Ray et al., 2010).

1.2.2 FLT3 activation and signalling pathways

Inactive FLT3 resides as monomer in the plasma membrane in a conformation described as a “closed” activation loop, and this is maintained by interaction between the juxtamembrane and kinase domains. In this form, phosphorylation sites including Y589, Y591, and Y599 and the ATP-binding site are blocked. The JM domain serves as a critical autoinhibitory loop preventing rotation of the N-lobe towards the C-lobe of the tyrosine kinase domain (TKD) so that dimerization is sterically unfavourable (Griffith et al., 2004)

Binding of FLT3L to the D3 IgG-like domain of two FLT3 monomers, results in dimerization and activation of the receptor. When activated, the receptor stabilizes its open conformation form leading to the activation of its intrinsic kinase activity. This results in exposure of different phosphorylation sites within the tyrosine kinase domain resulting in adoption of the active conformation of the receptor and activation of downstream signalling cascades. FLT3 activates three main signalling pathways: RAS/MAP-kinase, PI3-kinase/AKT and JAK/STAT5 pathways (Stirewalt and Radich, 2003).

The RAS/MAP kinase pathway

The mitogen-activated protein kinases (MAPKs) are a family of serine/threonine kinases that can be activated by FLT3. MAPKs are implicated in a variety of different cellular responses including cell survival, cell cycle and migration. In humans, several MAP kinase subfamilies have been identified including the ERK1/2 (extracellular signal-regulated kinase) family, the p38 MAP kinases, c-Jun amino-terminal kinases (JNK), and the ERK5 family (Pearson et al., 2001).

The MAP kinase pathway is initiated when the membrane-bound GTP-ase Ras is activated after interaction with adaptor proteins such as GRB2/ Sos (Seger and Krebs, 1995). Ras activates a key downstream effector protein Raf-1, which in turn phosphorylates and activates MEK1/2. MEK1/2 in turn phosphorylates ERK1/2 (also known as $p44^{MAPK}$ and $p42^{MAPK}$) on serine and threonine residues. Activated ERK1/2 can then phosphorylate many substrates leading to nuclear translocation of cytosolic transcription factors such as AP-1, which result in diverse biological responses. FLT3 activates the ERK1/2 pathway through the interaction of GRB2/Sos with tyrosine residues (Y768, Y955 and Y969) on FLT3. Association of GRB2 with GAB2 recruits SHP-2 which binds to phosphorylated Y599 in the juxtamembrane region (Masson et al., 2009). The protein tyrosine phosphatase SHP2 (PTPN11) positively regulates Ras activation and therefore mediates ERK1/2 activation by FLT3 (Chong and Guan, 2003). Many studies have shown that ERK is essential for normal haematopoiesis and has been shown to be important for thymocyte differentiation (Miranda et al., 2002, Pagès et al., 1999). Another

study indicated that that ERK plays a crucial role in IL-2 receptor-mediated lineage conversion in common lymphoid progenitors (Hsu et al., 2007).

The PI3-kinase/AKT pathway

Phosphoinositide 3-kinase (PI3-kinase/AKT) is involved in the regulation of a variety of cellular processes including proliferation, cell cycle, survival and differentiation. The PI3K family is divided into three classes but to date, only class I A/B isoforms has been implicated in the regulation of haematopoiesis (Vanhaesebroeck et al., 2005, Buitenhuis and Coffer, 2009). Class I PI3K has been shown to be crucial for both hematopoietic stem cell and progenitor cell development (Polak and Buitenhuis, 2012). PI3-kinase class I A is a lipid kinase which transmits signals from tyrosine kinase receptors and consists of heterodimeric proteins made up of a catalytic p110-kDa α/ β and δ and p85-kDa regulatory subunits. The class 1B isoform consists of a p110*γ* catalytic subunit and a p101 regulatory subunit and is specifically activated by G-protein coupled receptors and Ras (Anderson and Jackson, 2003).

Activation of FLT3 results in tyrosine phosphorylation of adaptor proteins Gab-1, Gab-2 and SHP-2, which in turn bind to the SH2-motif on p85 leading to activation of PI3-kinase at the plasma membrane (Rottapel et al., 1994). The most important substrate for class I PI3Ks is PIP_2 which is converted to PIP_3. The activity of PI3K can be inhibited by the tumour suppressor PTEN which dephosphorylates PIP_3, resulting in the formation of PIP_2. Similarly, Phosphoinositide phosphatases such as SHIP1 can also dephosphorylate PI3K (Vanhaesebroeck et al., 2010, Choi et al., 2002).

Protein kinase B, AKT, has been found to be the most important downstream target of PI3K activated through FLT3. AKT is cytosolic protein which translocates to the plasma membrane through its pleckstrin homology (PH) domains resulting in its phosphorylation following binding to PIP3 (Boudewijn and Coffer, 1995). Activation of AKT requires phosphorylation on both Thr^{308} by PDK1 and Ser^{473} by the MTORC2 complex (Alessi et al., 1997, Sarbassov et al., 2005). HSCs derived from AKT knockout mice revealed that it plays an important role in the maintenance of the long-term, repopulating function of HSCs. Mice deficient in AKT exhibit a persistence of long-term HSCs in the G_0 phase of the cell cycle, suggesting that the functional defects observed in these mice is likely caused by increased quiescence (Juntilla et al., 2010).

AKT substrates include; glycogen synthase kinase 3B (GSK3B), the Forkhead family of transcription factors (FOXO proteins), and serine/threonine kinase mammalian target of rapamycin (mTOR). Inactivated FOXO transcription factors contribute to apoptosis and phosphorylation of FOXO proteins by AKT leads to disruption of its activity and ultimately to induced cell growth (Brunet et al., 1999). Deletion of FOXO proteins in mice results in in a defective long-term HSCs repopulating capacity (Tothova et al., 2007). GSK3B negatively regulates cyclin D1, however, AKT can phosphorylate GSK3B and promote G1/S-phase entry to cell cycle (Manning and Cantley, 2007). The third important mediator of AKT is mTOR which unlike GSK-3 and FOXO is activated by AKT. The GTPase activating protein TSC2/TSC1 complex suppresses mTORC1 activation through hydrolysis of GTP- to GDP-bound

Rheb. AKT inhibition of TSC1/2 leads to a subsequent activation of mTORC1 complex (Sengupta et al., 2010). Studies in TSC1 and GSK3-deficient mice demonstrated that these proteins are essential for HSC maintenance and lineage development (Huang et al., 2009, Chen et al., 2008).

JAK/STAT5 signalling pathway

The Janus-activated kinase (JAK/ STAT5) pathway is also activated by FLT3 however, not by the wild-type receptor, but exclusively through ITD mutations (Choudhary et al., 2005). Signal transducer and activator of transcription (STAT5) is phosphorylated by JAK proteins following binding of cytokines such as IL-2/-4 to their cognate receptors. Activated JAKs phosphorylate tyrosine residues in the receptor, resulting in binding of monomeric STAT5 through its SH2 domain. Recruited STAT5 is phosphorylated on Y641/699 by JAKs, undergoes dimerization then translocates to the nucleus (Calò et al., 2003, Benekli et al., 2003). Studies in STAT5 knockout mice reveal the importance of STAT5 during foetal erythropoiesis. Embryos from mice with STAT5A/B knock-out develop foetal anaemia due to decreased responsiveness to the anti-apoptotic effect of Epo (Socolovsky et al., 1999). STAT5 is also require for IL-7 signalling during early B-cell development through induction of Mcl-1 and knock-out mice display severe B cell developmental arrest, likely due to loss of Mcl-1 expression (Yao et al., 2006).

1.2.3 FLT3 ligand (FLT3L)

FLT3L is a member of a small family of growth factors that stimulate the proliferation of hematopoietic cells. This family includes the colony-stimulating

factor 1 (CSF-1), interleukin-3 (IL-3) and granulocyte macrophage colony-stimulating factor (GM-CSF) (Lyman and Jacobsen, 1998). Similar to stem cell factor (c-Kit ligand), FLT3L can exist as membrane-bound or soluble form as a result of proteolytic cleavage from the cell surface (McClanahan et al., 1996). Both are biologically active and able to activate FLT3. FLT3L consists of a signal peptide which is absent from the mature protein, an extracellular domain, a transmembrane domain, and a cytoplasmic tail.

FLT3L is produced by many hematopoietic cells and regulates early hematopoiesis through FLT3. Its release is tightly regulated as the T-lymphocytes produce and store FLT3L for release upon certain stimuli (Chklovskaia et al., 1999). FLT3L can act synergistically with other growth factors to enhance the cell growth and proliferation. In contrast to the receptor, the expression of FLT3L is ubiquitous, and as mentioned previously its function is most likely determined by restricted receptor expression. Under normal physiological conditions, the plasma level of soluble FLT3L is low (14 ±31 pg/ml), but it is elevated during pathological conditions or following chemotherapy (Lyman et al., 1995). Normally, FLT3L promotes survival and proliferation of haematopoietic progenitors. Mice deficient in FLT3L are viable but exhibit a reduction in all leukocytes including: B cell progenitors, dendritic cells and natural-killer cells (McKenna et al., 2000).

1.2.4 RTKs in Leukaemia – c-KIT and FLT3

c-Kit activating mutations have been observed in 2-5% of total AML cases, however, the most frequent observed gain-of-function RTK mutations occur in

FLT3 (Speck and Gilliland, 2002). Several studies observed increased expression of c-Kit in AML cases (60–80%) (Cole et al., 1996). c-KIT is commonly mutated in core-binding factor acute myeloid leukaemia (CBF-AML), which occurs in patients with inv(16) and t(8;21) and is associated with high relapse risk and poor prognosis (Paschka et al., 2006).

The most common receptor involved in AML pathogenesis is FLT3 which is overexpressed in 90% of leukemic blasts (Drexler, 1996). Two different alterations in FLT3 lead to a change in its signalling. In the presence of its ligand, overexpression of the wild-type receptor results in elevated activation in malignant cells. The other is mutations are in FLT3 itself and result in constitutive activation of the receptor and these are considered the strongest single predictor for AML relapse after intensive chemotherapy (Ozeki et al., 2004). Mutated FLT3 is observed in about 30% of AML patients (Meshinchi et al., 2001).

1.2.5 Mutations and oncogenic signalling of FLT3 in AML

There are two types of FLT3 mutations found in AML: internal tandem duplications within the juxta-membrane domain (FLT3-ITD) and point mutations in the activation loop in the kinase domain (FLT3-TKD).

FLT3-ITD

In 1996, Nakao et al. described the presence of a novel mutation in the FLT3 gene in a small number of AML patients. These mutations were reported as in-frame tandem duplications (ITDs) of 3–400 base pairs in the

juxta-membrane (JM) region and have been extensively studied since as they represent one of the most common mutations in AML (Nakao et al., 1996). ITDs are in-frame mutations caused by duplication of various fragments of sequence in exons 14 and 15 that code for the JM domain. The length of ITD insertion can differ between patients and influences prognosis with poorer outcomes generally associated with larger inserts. This may also explain the response of different mutations to FLT3 inhibitors. The ITD causes the receptor to lose its auto-inhibitory function and so it dimerizes, auto-phosphorylates and activates the kinase domains in a ligand-independent manner (Kiyoi et al., 2002). The underlying mechanism of ITD mutation is still obscure, however, it has been proposed that it's a result of DNA replication error (Kiyoi et al., 1998a). Although ITD mutations have been identified in wider regions of the intracellular domain, two main residues, Y589 and Y591 in the JM domain are found to be the crucial sites for FLT3 oncogenic activation (Vempati et al., 2008). Most of the mutations in the JM domain are ITDs, but there several studies reporting other deletions and insertion mutations in this region.

To study the oncogenic signalling as a result of constitutive activation of ITD, many studies have used cell lines overexpressing the mutated receptor. Although there are signalling overlaps between wild-type and oncogenic FLT3, there are crucial differences between them. Wild-type FLT3 signals at the plasma membrane, however, ITD-FLT3 displays an altered localisation and ultimately initiates additional signalling pathways. Knockdown of FLT3 in MV4-11 and MOLM-14 AML cells was shown to prevent

phosphorylation of ERK1/2 and decrease proliferation and survival (Cauchy et al., 2015). PI3K activation by FLT3 leads to AKT activation and inhibition of the FOXO3a transcription factor in 32D myeloid progenitor cells. Restoration of FOXO3A expression reversed the effects of the ITD mutation (Brandts et al., 2005). PI3K also controls the AKT-MDM2-p53 axis, and targeting the negative regulator of p53, MDM2 is a novel approach to restore the crucial tumour suppressor function of p53 in AML cells (Kojima et al., 2005). Idasanutlin (RG7833) is a second generation MDM2 inhibitor and currently being investigated in phase III clinical trial as a combination therapy in relapse and refractory AML (Khurana and Shafer, 2019).

As MAPK and PI3K/AKT signalling is initiated at the cell membrane, the WT and ITD receptors both activate those pathways (Kiyoi et al., 1998a). By contrast, ITD-FLT3 also localises to the ER and has been shown also to activate STAT5 (Fig 1.6) (Hayakawa et al., 2000, Mizuki et al., 2000). As a result, ITD-FLT3 activates STAT5 controlled cell-cycle regulating genes and myeloid differentiation transcription factors, such as PU1 and C/EBPα (Mizuki et al., 2003, Zheng et al., 2004). In addition, aberrant activation of STAT5 appears to promote an overall elevation in reactive oxygen species which has been associated with genomic instability through enhancing the frequency of double-strand DNA breaks (Fan et al., 2010, Woolley et al., 2012). Another effect of STAT5 activation is to promote survival and proliferation of AML cells by inducing phosphorylation and subsequent suppression of the pro-apoptotic regulator FOXO3a (Scheijen et al., 2004).

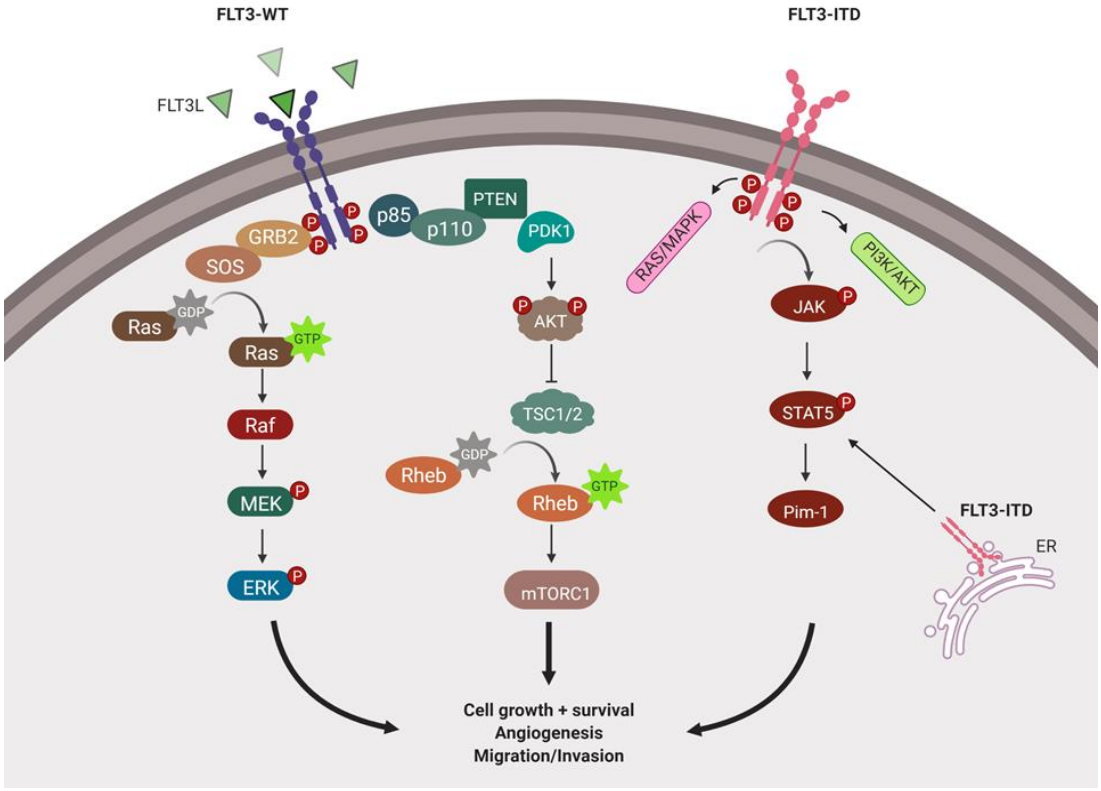

Figure 1.6: Schematic of WT and ITD-FLT3 signalling – binding of FLT3 ligand to WT FLT3, causes activation of RAS/MAPK and PI3K/AKT pathways leading to a cascade of pathways promoting proliferation, growth, migration, and survival. FLT3-ITD signals via the RAS/MAPK and PI3K/AKT pathways but also activates STAT5.

FLT3-TKD

Point mutations in the tyrosine kinase domain are the second most common FLT3 mutation found in AML patients. The most common of these are missense mutations in residue D835 within the activation loop of TKD2 which results in an amino acid change (Abu-Duhier et al., 2001). FLT3-TKD point mutations also promote ligand-independent activation of the receptor (Yamamoto et al., 2001). Although these mutations can have distinct biological functions, the downstream signalling appears to be different to ITD-FLT3 and they also have a weaker transforming potential (Choudhary et al., 2005).

Prognosis and overall survival are also significantly higher in patients with TKD compared to ITD mutations. Mice harbouring FLT3-TKD mainly develop an oligoclonal lymphoid disorder, in contrast to ITD-expressing mice which develop a myeloproliferative disorder (Grundler et al., 2005). In agreement with this, FLT3-TKD mice present with a less aggressive malignancy than FLT3-ITD. The reason behind this difference may be that TKD mutations do not activate STAT5 while ITD mutations do.

1.3 Treatment of FLT3-driven leukaemia

1.3.1 Chemotherapy

AML is an intrinsically chemotherapy-resistant disease. Therapeutic approaches produce a relatively high remission rate, however, newly diagnosed patients, especially those who harbour FLT3 mutations and receive standard chemotherapy, commonly experience relapse. In case of a FLT3 mutated patient, chemotherapy should be administered in combination with a FLT3 inhibitor. There are several early phase trials for using “7+3” induction chemotherapy in combination with FLT3-TKIs with high response outcome.

Since the approval of midostaurin by the FDA in April 2017, chemotherapy is administered in combination with midostaurin for the treatment of adult patients with newly diagnosed FLT3-mutated AML. The recommended dose of midostaurin is 50 mg twice daily on days 8 to 21 of each cycle of induction with cytarabine and daunorubicin and days 8 to 21 of each cycle of consolidation with high dose cytarabine (Stone et al., 2017b). Table 1.4

summarises some of the clinical trial protocols of chemotherapy-combination therapy for newly diagnosed AML patients with FLT3 mutations (ITD/TKD).

Table 1.4 – Studies of FLT3 inhibitors and chemotherapy for newly diagnosed FLT3-mutated AML patients

Protocol	Phase	Endpoints	Ref.
7+3 induction followed by 2 cycles of intermediate/ high dose cytarabine consolidation+ sorafenib or placebo	Phase III	Median overall survival: 15 months for placebo vs 13 for sorafenib	(Serve et al., 2013)
1–2 cycles of induction chemotherapy followed by 3–4 cycles cons + Lestaurtinib or placebo	Phase III	5-year overall survival: lestaurtinib 46% vs placebo 45%	(Knapper et al., 2017)
Crenolanib + 7 + 3	Phase II	complete remission: 83%	(Wang et al., 2017)
Gilteritinib+ induction (idarubicin/ cytarabine)	Phase I	composite complete remission: 100%	(Pratz et al., 2018)

Based on the high response rate achieved with the next generation FLT3 inhibitors, two phase III randomized trials are ongoing to investigate quizartinib combined with “7 + 3” chemotherapy, and crenolanib vs midostaurin and 7 + 3 chemotherapy (Erba et al., 2016, Stone et al., 2019). A promising recent phase III study (ADMIRAL study) compared gilteritinib as a single therapy versus four salvage chemotherapy regimens. In this study, Gilteritinib a single oral agent at 120 mg daily led to significantly longer overall survival and increased safety profile (9.3 months) over salvage chemotherapy (5.6 months) (Perl et al., 2019a). This study may lead to a paradigm shift for using single oral agents to replace standard chemotherapy as the primary therapy for relapsed or refractory FLT3-mutated patients (Zhao et al., 2019).

1.3.2 Tyrosine/ serine, threonine kinase inhibitors

Targeted kinase inhibitors have been developed in the hope to improve selectivity with less side-effects than conventional chemotherapy. Here, we will discuss the main inhibitors that have been used or are being developed to interfere with abnormal signal transduction in acute leukaemia.

FLT3 Tyrosine Kinase Inhibitors

It has been reported that high-dose daunorubicin and gemtuzumab ozogamicin might help AML patients with FLT3-ITD mutations, and patients with unfavourable cytogenetics, however, a retrospective analysis showed that allogeneic hematopoietic stem cell transplantation (allo-HSCT) showed no beneficial effect on the poor prognosis of FLT3-ITD mutation patients (Luskin et al., 2016, Schlenk et al., 2008). Therefore, Given the importance of FLT3 mutations in AML pathogenesis, FLT3 inhibition is a key therapeutic target in AML, and clinical trials of FLT3 inhibitors have been ongoing for a decade (Pemmaraju et al., 2011). Small molecule inhibitors targeting FLT3 are categorised based on their mechanism of interaction with FLT3. Type I inhibitors (such as midostaurin and gilteritinib) bind to the active or inactive conformation of the FLT3 receptor either near the activation loop or the ATP-binding site, while type II compounds (such as sorafenib and quizartinib) bind to the inactive receptor in a region adjacent to the ATP-binding site (Ke et al., 2015). As a result, type I inhibitors are active against ITD and TKD mutations, while type II inhibitors have activity against ITD but not TKD mutations (Smith et al., 2015). The inhibitors can be further classified based on their specificity for FLT3 into first generation and second generation (Larrosa-Garcia and

Baer, 2017). First-generation FLT3 inhibitors, including lestaurtinib, sunitinib, sorafenib, ponatinib, and midostaurin are relatively nonspecific for FLT3 receptor with additional activity involving other targets such as c-Kit, platelet-derived growth factor receptor (PDGFR), vascular endothelial growth factor receptor (VEGFR) and JAK2 kinases (Weis et al., 2019)). The lack of specificity of first-generation FLT3 inhibitors may contribute to the higher toxicity profile and limited clinical efficacy, especially as monotherapy (Larrosa-Garcia and Baer, 2017). The plasma inhibitory activity (PIA) assay, a novel index for evaluating the clinical efficacy of FLT3, showed that the first-generation FLT3 inhibitors did not effectively suppress the phosphorylation status of mutant FLT3 even at the desired blood concentration(Levis et al., 2011). Therefore, using of these molecules as a monotherapy has been discontinued. However, when used as combination with chemotherapy the clinical outcome has improved and ended-up in the approval of midostaurin in combination with standard chemotherapy. On the other hand, second-generation inhibitors, such as quizartinib, gilteritinib, and crenolanib, were designed to be more specific and potent against FLT3 receptor with improved tolerability. Small molecule kinase interaction maps for FLT3 inhibitors are represented in (Fig 1.7).

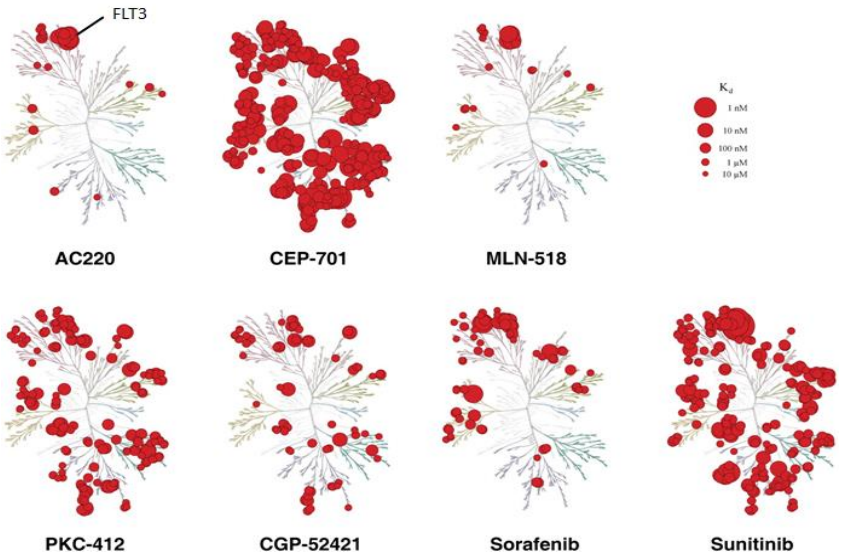

Figure 1.7: KinomeScan binding plots for FLT3 TKIs – Red circles represent kinases inhibited by the indicated drug and the relative size of the circle is inversely proportional to the binding affinity. Compounds with a smaller number of binding sites are said to be more 'specific' with fewer 'off target effects'. Reprinted with permission from Blood, The Journal of the American Society of Hematology, "AC220 is a uniquely potent and selective inhibitor of FLT3 for the treatment of acute myeloid leukemia (AML)" (Zarrinkar et al., 2009a).

Reviewed a data over 15 years (from 2000 to 2014) suggest that there was an improvement in outcome in poor prognostic, FLT3- ITD mutated AML patients. This is probably due to advancement in treatment strategies over time, including the incorporation of FLT3 inhibitors in the treatment approach (Badar et al., 2015). This lead to an increasing in the interest of using FLT3 inhibitors as first line therapy for FLT3 mutated AML with a new therapeutic paradigms for AML with FLT3 mutations (Fig 1.8).

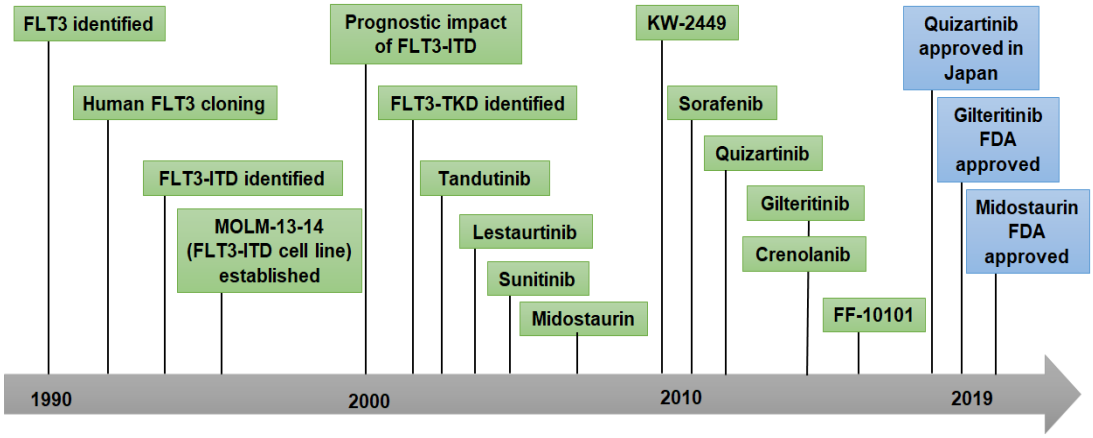

Figure 1.8: History timeline of FLT3 to start times of clinical trials and practical use – Adapted from "FLT3 mutations in acute myeloid leukaemia: Therapeutic paradigm beyond inhibitor development" (Kiyoi et al., 2020).

Quizartinib (AC220), is a novel second-generation type II FLT3 inhibitor with high selectivity for mutated FLT3 and additional inhibitory activity of KIT and PDGFR. Before quizartinib, numerous other compounds (lestaurtinib, midostaurin, tandutinib and sorafenib) were under investigation however they were not effective as single agents. In addition, most of them had short plasma half-life, which delays the efficacy (Levis, 2014, Pratz et al., 2009). Then, a bis aryl-urea derivative was identified as potent and selective FLT3 inhibitor. After, improving its pharmacokinetic profile, this compound was designated as AC220 or quizartinib which was the first small molecule to be identified and developed as an orally active FLT3 inhibitor. Also, quizartinib has long half-life and sustained inhibition against FLT3(Levis, 2014, Fathi and Chen, 2011). In contrast, quizartinib does not have an effect against TKD mutations when compared with other FLT inhibitors like midostaurin, crenolanib and gilteritinib which is due to resistance in quizartinib-treated patients (Smith et al., 2012a). Multiple independent studies shows that this drug is a promising agent in treatment of AML by inhibiting FLT3, however, there is a concern of side

effects and drug resistance among patients with high expression of RUNX1, which is mainly involved in cell proliferation and myeloid differentiation (Hirade et al., 2016). Clinical trials show that quizartinib is well tolerated with a favourable prognosis and demonstrates efficacy in improving clinical outcomes as a single agent in relapsed/ refractory AML patients. A phase II study showed that 44-53% of patients with ITD-FLT3 achieved the composite complete remission (Grunwald and Levis, 2013). The QuANTUM Phase III trial is ongoing to examine the efficacy of quizartinib as monotherapy or in combination with standard induction chemotherapy (Erba et al., 2016, Cortes et al., 2018b). The addition of quizartinib to standard chemotherapy is under study in the randomized phase 3 trial QuantumFirst and results expected in 2022. In Japan, quizartinib has been approved for the treatment of relapsed or refractory AML patients with ITD mutations (Cortes et al., 2019). There are about ten ongoing clinical trials with quizartinib in the US, and quizartinib might be eventually obtain FDA approval as part of combination treatment in near future (Fletcher et al., 2020).

Gilteritinib is a second-generation type I FLT3 inhibitor with activity against both ITD and TKD mutations, EML4-ALK as well as AXL (Ueno et al., 2014). Recent data reveals that gilteritinib has longer overall survival and remission in relapse or refractory FLT3 mutated AML patients than salvage chemotherapy (Perl et al., 2019b). In a phase I/II clinical trial in refractory or relapsed AML patients, the overall response rate was 55%, 17% and 62% in patients with ITD, TKD mutations or both, respectively (Perl et al., 2016). A phase III randomized trial is undergoing comparing gilteritinib to other salvage

chemotherapy. In 2018, as the first non-chemotherapy drug, gilteritinib was approved as monotherapy to treat adult patients who have relapsed or refractory AML with mutated FLT3 (Perl et al., 2019b).

Midostaurin (PKC-412), is a staurosporine derivative and first-generation type I FLT3 inhibitor capable of targeting ITD and TKD mutations. It displays multitargeted kinase activity against protein kinase C, vascular endothelial growth factor (VEGFR), c-KIT, and platelet derived growth factor (PDGFR) (Propper et al., 2001, Weisberg et al., 2002). Studies confirmed that synergy between chemotherapy and midostaurin, a phase 1b study of newly identified AML patients was performed and examined that oral midostaurin could be administered at a dose of 50 mg twice each day for 14 days. This regimen had promising efficacy in patients with a FLT3 mutation. Various other studies determined that midostaurin is safe and improved outcomes in younger patients with AML and FLT3 mutation (Stone et al., 2012). Midostaurin significantly extended the survival of FLT3-mutated AML patients in a phase III clinical trial (Schlenk et al., 2019). Kaplan–Meier curves for median overall survival of (RATIFY) trial in the midostaurin group and the placebo group showed 74.7 months vs 25.6 months, respectively (Stone et al., 2017a). As a consequence, it is the first TKI to be approved by the FDA for treatment of newly diagnosed FLT3-mutated AML in combination with conventional induction and consolidation chemotherapy (Stone et al., 2017a). Data from the RATIFY trial showed patients with all FLT3 mutation subtypes (i.e., TKD, ITD low allelic ratio, and ITD high allelic ratio) benefited from midostaurin and this might be related to its multiple kinase activity along with FLT3 inhibition.

Furthermore, FLT3-TKD mutations can be found in about 7% of AML patients, however, the number of population in this study with FLT3-TKD mutation was about 23% which is larger than the percentage of TKD occurrence in AML and this could lead to a biased outcome in favour of patients with a FLT3-TKD mutation. Of note, median age of patients in this trial was 47.9 years which is younger than typical patients with newly diagnosed AML, highlighting the importance for more data regarding midostaurin safety and effectiveness in elderly fit and unfit patients (Schlenk et al., 2016). Despite limitations, the RATIFY trial was the first study to show significant improvements in overall survival and event-free survival with the addition of a targeted therapy to standard chemotherapy in AML population.

Sorafenib is a first-generation type II FLT3 inhibitor again with multi-target kinase activity. Several studies indicate that sorafenib has greater activity against FLT3-ITD than the wild-type receptor (O'Farrell et al., 2003). A phase II trial of sorafenib combined with azacitidine showed an overall response rate of 46% in patients with relapsed or refractory AML. A recent study has shown that sorafenib administration in a post-hematopoietic stem cell transplant setting (SORMAIN study) lead to improved maintenance and prolonged relapse-free survival (Burchert et al., 2018). Table 1.5 summarises a panel of other TKIs in development for use in AML (Fernandez et al., 2019).

Recently, a promising novel FLT3 inhibitor, FF-10101, has been designed to form a covalent binding between the C695 residue of FLT3. This covalent bond formation of FF-10101 maintains the ability to bind to both the active and

inactive conformations of FLT3 and shows high efficacy against AML cells with FLT3 mutations including quizartinib-resistant activation loop mutations and its effective against the gatekeeper mutation F691L. It also showed a potential growth inhibition of primary AML cells harbouring either FLT3-ITD or FLT3-D835 mutation in vitro and in vivo (Yamaura et al., 2018).

Table 1.5 – Other TKIs in Development for AML

Drug	Main Target	Development Status
Crenolanib	FLT3	Phase III
Sunitinib	FLT3	Phase II
Lestaurtinib	FLT3	Phase III
FF-10101	FLT3	Phase II
Dasatinib	KIT	Phase III
SU5416	KIT	Phase II
Bemcentinib	AXL	Phase II
Cabozantinib	AXL	Phase I
Entospletinib	SYK	Phase II
SAR103168	SFK	Phase I
Ibrutinib	BTK	Phase III
Pacritinib	JAK-STAT	Phase II
CG-806	FLT3 / BTK	Phase I

About 50% of AML patients with adverse prognosis are not candidates for intensive chemotherapy. Therefore, another interesting approach of using FLT3 inhibitors with hypomethylating agents has been emerged for unfit FLT3

mutated AML patients. The combination of sorafenib and azacitidine in FLT3 mutated AML patients in a phase II trial lead to overall response rate of 78% and a median overall survival of 8.3 months (Ohanian et al., 2018). Similarly, other FLT3 inhibitors including quizartinib and gilteritinib in combination with azacitidine are being evaluated in different clinical trials, and the data showed that the combination appears safe and may improve both response rate and survival (Cortes et al., 2017, Swaminathan et al., 2017). Gilteritinib has been reported to be more effective in a combination with azacitidine (DiNardo et al., 2019), and according to a presentation by Eunice S. Wang, MD, of Roswell Park Comprehensive Cancer Center, at the virtual 62nd American Society of Hematology (ASH) Annual Meeting and Exposition (2020), an ongoing, phase 3, open-label, randomized trial investigating gilteritinib plus azacitidine in adults with newly diagnosed FLT3 mutated AML who were ineligible for intensive induction chemotherapy revealed a composite complete remission rate of 67%.

The MAPK and PI3K/AKT/ mTOR have been described extensively in the literature as oncogenic pathways in AML. Targeting protein serine/threonine kinases in multiple pathways in combination with FLT3 inhibitors is therefore considered a promising strategy to improve AML therapy and minimize drug resistance. A summary of common serine/threonine kinase inhibitors in trials for AML is summarized in Table 1.6 (Ling et al., 2017).

Table 1.6 – Ser/Thr kinase inhibitors in development for AML

Drug	Main Target	Development Status
Everolimus	mTORC	Phase I
Temsirolimus	mTORC	Phase II
Pimasertib	MEK1/2	Phase II
U0126	MEK1/2	Preclinical
Trametinib	MEK1/2	Phase II
A674563	Akt/FLT3	Preclinical
Mk-2206	Akt	Preclinical
Flavopiridol	CDK	Phase II

1.3.3 Resistance to FLT3 inhibitors

Despite the encouraging improvement in identification of molecular targets in AML and development of novel therapeutic strategies, relapse is a significant cause of treatment failure (Daver et al., 2015). Due to the heterogeneity of the disease, mechanisms of resistance are multifaceted, but mainly involve emergence of kinase domain mutations and/or some other pathway adaptation that counteracts FLT3 inhibition. There are two potential mechanisms underlying drug resistance to FLT3 inhibition. Intrinsic mechanisms occur within leukemic blasts and can be a primary (occurring before treatment) or secondary resistance (induced by a FLT3 inhibitor). The other is through an extrinsic mechanism e.g. microenvironmental cues.

Intrinsic mechanisms

The primary mechanism of intrinsic resistance to FLT3 inhibitors is lack of addiction of leukemic cells harbouring FLT3-ITD to FLT3 signalling. This occurs due to the variation in levels of mutated FLT3 in leukemic clones. A study of five FLT3 inhibitors demonstrated that AML patients with a high allelic burden or those that have relapsed respond better to FLT3 inhibitors (Pratz et al., 2010). The presence of additional TKD mutations reduces affinity conferring resistance to type II FLT3 inhibitors such as quizartinib (Smith et al., 2012a). The presence of a FLT3-ITD627E mutation is linked to upregulation of antiapoptotic proteins such Mcl-1 resulting in resistance (Breitenbuecher et al., 2009a). Upregulation of the other anti-apoptotic proteins such as Bcl-2 through FLT3-independent pathways is also reported to confer resistance to FLT3-TKIs in AML (Kohl et al., 2007).

Development of TKD secondary, intrinsic mutations confers resistance to type II inhibitors (e.g. quizartinib) that do not have significant activity against TKD mutations. These mutations usually occur following treatment with FLT3 inhibitors and may include those at the activation loop (e.g. D835) or the gate-keeper residue (F691) depending on type of inhibitor being used (Smith et al., 2015, Daver et al., 2015). Non-FLT3 mutations also have been found to mediate resistance during FLT3 inhibitor treatment. For example, mutations in the TP53 and RAS pathways have been reported in R/R FLT3-ITD AML patients who relapsed after treatment with crenolanib or gilteritinib (Zhang et al., 2019, McMahon et al., 2019).

Rapid clonal evolution through genomic instability in AML patients treated with FLT3 inhibitors following relapse represents another potential mechanism of resistance (Fan et al., 2010). Upregulation of other oncogenic kinases has been implicated and these then serve as rational targets to combine with FLT3 inhibitors. For example, increased phosphorylation of AXL was observed in cells expressing FLT3-ITD following treatment with FLT3 inhibitors and AXL inhibition and/or knockout was shown to overcome resistance (Park et al., 2015). Notably, AXL is also a target of gilteritinib, in addition to FLT3. Expression of Pim kinase, a signalling molecule downstream of ITD signalling, has been shown to upregulated in primary AML cells with acquired resistance to sorafenib, in these cells inhibition of Pim restored the sensitivity of ITD-expressing cells to FLT3 inhibition (Green et al., 2015). Constitutive activation of PI3K/AKT/mTOR, MAPK/ERK and STAT5 pathways is known to contribute to resistance in both FLT3 inhibitor-resistant ITD-expressing cell lines and primary AML blasts (Lindblad et al., 2015). This suggest that at this stage of resistance, the survival of some cells is independent of FLT3 and these other pathways may serve as a potential therapeutic avenues. Targeting these pathways in combination with FLT3 inhibitors is also under investigation (Piloto et al., 2007).

Extrinsic mechanisms

The bone marrow microenvironment plays an important role in mediating extrinsic resistance to FLT3 inhibitors. Enhanced secretion of cytokines from bone marrow stromal cells has been shown to protect AML blasts from the cytotoxic effect of FLT3 inhibitors and conventional chemotherapy (Yang et

al., 2014). Serum levels of FLT3L were shown to increase after chemotherapy and FLT3 inhibitor treatment. AML cells remain responsive to FLT3L despite constitutive activation through the mutated receptors and this ligand-dependent signalling subsequently decreases the sensitivity of cells to FLT3 inhibition. In a recent study, large increases in FLT3L levels in the newly diagnosed patients were observed following intensive induction chemotherapy as well as after subsequent courses of treatment (Sato et al., 2011). Similarly, the stromal cells are sources of fibroblast growth factor 2 (FGF2) and CXCL12-CXCR4. FGF2 binds to fibroblast growth factor receptor 1 in ITD-FLT3 AML cells and induces resistance to FLT3 inhibitors through activation of MAPK pathway (Traer et al., 2016). Upon chemotherapy treatment, CXCL12-CXCR4 was reported to promote resistance to FLT3 inhibitors as a consequence of the highly expressed CXCR4 in FLT3-ITD AML which resulted in increased production of CXCL12, a pro-survival cytokine (Fukuda et al., 2005). Other extrinsic resistance mechanisms are through the hepatic enzymes which result in inadequate drug concentrations in the plasma leading to suboptimal efficacy of the FLT3 inhibitors. Several preclinical studies have demonstrated that CYP3A4 expressed primarily in hepatocytes and bone marrow stromal cells may enhance drug metabolism and reduce drug bioavailability (Teo et al., 2015).

1.4 Regulation of cell death by the Bcl-2 family

1.4.1. Apoptosis overview

Apoptosis is a form of tightly regulated cell death that maintains cellular homeostasis, particularly of rapidly renewing cells such as those in the hematopoietic system. Evading apoptosis is seen as a crucial step for malignant tumour progression (Hanahan and Weinberg, 2000). Following detection of cellular abnormalities such as DNA damage or ER stress, different signalling pathways are initiated ultimately leading to activation of the apoptotic machinery (Kastan et al., 1991). During DNA damage, activation of tumour suppressor p53 is crucial for initiating specific cellular responses such as senescence, transient cell cycle arrest and apoptosis to determine ultimately the fate of the cell. Cancers arise as cells accumulate a series of mutations that result in uncontrolled growth and the avoidance of apoptosis (Muller and Vousden, 2013).

Apoptosis occurs through two mechanisms; the intrinsic and extrinsic pathways (Fig 1.9). The extrinsic pathway is activated by external factors at the cell surface and typically involves binding of ligands of TNF family to their respective receptors which in turn activate downstream adaptor proteins, and the initiator caspases -8 and -10 (Wallach et al., 1999, Sheikh and Huang, 2004). The active initiator caspases then cleave and activate effector caspases -3 and -7 to induce apoptosis. In some cases, cells require the extrinsic pathway to combine with the intrinsic mitochondrial pathway through cleavage of the Bcl-2 protein, Bid (Li et al., 1998, Milhas et al., 2005).

Truncated Bid can then engage the mitochondrial apoptosis pathway amplifying a weak external stimulus.

In contrast to the extrinsic pathway, the intrinsic pathway triggers apoptosis directly, as a result of changes in mitochondrial integrity. Diverse cytotoxic stimuli such as DNA damage, ER and oncogenic stress affect the delicate balance of anti-apoptotic and pro-apoptotic Bcl-2 family members ultimately tipping the balance towards initiation of apoptosis (Ashkenazi et al., 2017). Activation of the intrinsic pathway involves an increase in the permeability of the outer mitochondrial membrane, resulting in the release of proapoptotic factors such as cytochrome c, HtrA2, and SMAC that normally reside in the mitochondrial intermembrane space (Green and Reed, 1998). Of these, the key protein which activates the cell death pathway is cytochrome c (Saelens et al., 2004). For cytochrome c to be released from the mitochondria, the pro-apoptotic Bcl-2 proteins Bak and Bax cluster into large oligomers forming pores in the outer mitochondrial membrane. Cytochrome c escapes through these pores into the cytosol where it binds to APAF-1, inducing its oligomerisation and subsequent recruitment of the initiator pro-caspase-9 in a complex known as the apoptosome (Bratton et al., 2001). Following activation, caspase-9 in turn activates the effector caspases -3 and -7 which are responsible for cleavage of many cellular proteins causing the morphological changes associated with apoptotic cell death (Volkmann et al., 2014). SMAC is also released from the mitochondria and acts to repress the inhibitor of apoptosis proteins (IAPs), which are believed to prevent activation of some pro-caspases (Du et al., 2000).

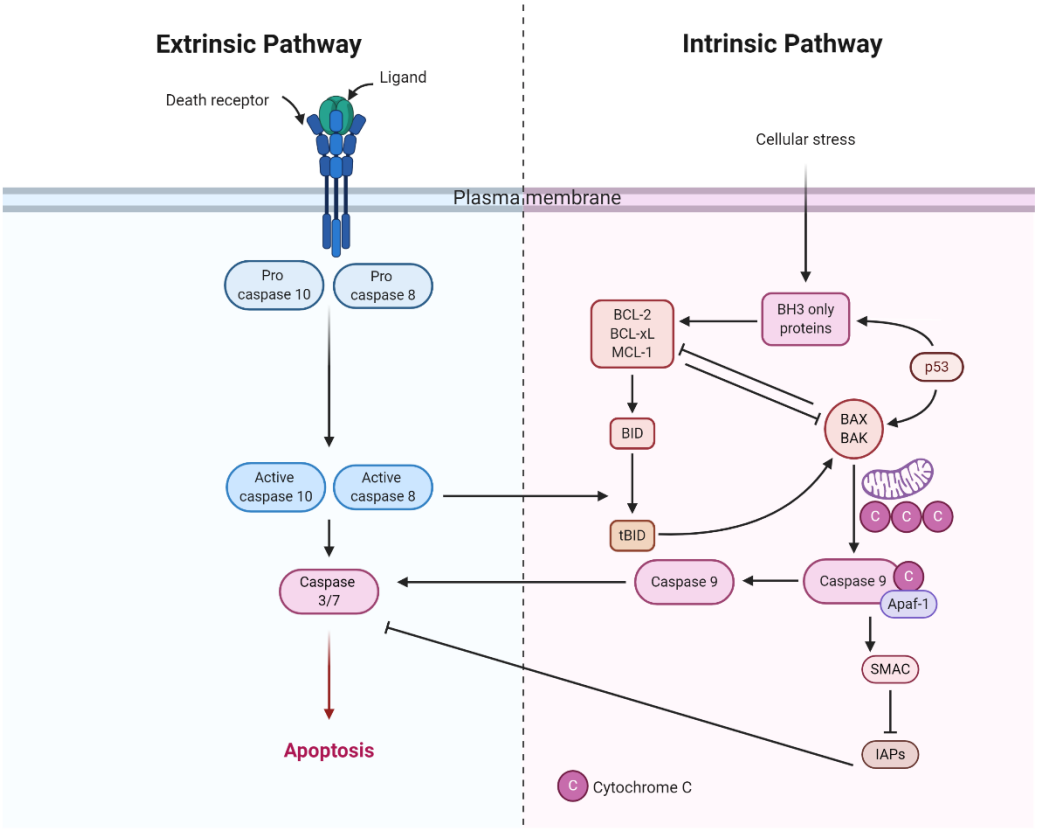

Figure 1.9: Schematic representation of the Extrinsic and Intrinsic apoptosis pathways – The intrinsic apoptotic pathway acts directly at the mitochondria leading to apoptosome formation, whereas the extrinsic pathway can activate caspases independently of the mitochondria. The two pathways can converge at the Bcl-2 protein, Bid, which when cleaved translocates to the mitochondria to activate Bax or Bak. Ultimately, activation of either pathway leads to cleavage of effector caspases, leading to the coordinated breakdown of the cellular structure and death.

1.4.2 The Bcl-2 family and apoptosis induction

Activation of the intrinsic pathway is controlled by Bcl-2 family members (Czabotar et al., 2014). The Bcl-2 family includes at least 25 members, which can be classified based on their function into either pro-apoptotic (promote activation of the apoptotic signalling pathway) or anti-apoptotic (prevent a cell

from death). The dynamic interactions of these different pro- and anti-apoptotic proteins under various physiological or pathological stimuli forms a central checkpoint to determine cell fate (Kale et al., 2018).

Bcl-2 proteins share a strong structural homology due to the presence of highly conserved regions termed Bcl-2 homology (BH) domains. Anti-apoptotic members of the Bcl-2 family (Bcl-2, Bcl-xL and Mcl-1) contain BH1, BH2, BH3 and BH4 domains. These proteins can bind and sequester the pro-apoptotic family members to prevent the initiation of apoptosis (Chan and Yu, 2004). The pro-apoptotic Bcl-2 family members can be subdivided into two functionally and structurally distinct classes, the effectors (multi-domain) and the activators and/or sensitisers (the BH3-only proteins). The effector proteins Bax and Bak contain BH1, BH2 and BH3 domains and when activated adopt a pro-death conformation to form pores in the outer mitochondrial membrane facilitating the release of cytochrome c (Shamas-Din et al., 2013). Other pro-apoptotic Bcl-2 family members such as Puma, Bim, Bid, Bad, Bik, Bmf, Hrk, and Noxa contain only the BH3 domain. BH3-only proteins are able to bind to certain anti-apoptotic proteins antagonising their function. In addition to inhibiting anti-apoptotic members, BH3-only activator proteins such as Bid and Bim interact with, and activate Bax and Bak (Fleischer et al., 2003). Sensitiser BH3 proteins such as Bad and Noxa displace activator BH3-only proteins from antiapoptotic proteins to promote apoptosis (Youle and Strasser, 2008).

The intrinsic apoptotic pathway in leukaemia

Disrupting the delicate balance between cell proliferation and cell death is involved in the pathogenesis of several diseases including leukaemia (Hanahan and Weinberg, 2000). The key role of apoptosis in the pathogenesis of AML has been discussed since the 1990s with several papers implicating the role of Bcl-2 proteins in promoting leukaemogenesis (Delia et al., 1992, Bradbury and Russell, 1995). Bcl-2 family proteins have been reported to be overexpressed in AML and consequently confer resistance to conventional chemotherapy as well as more targeted therapies (Kornblau et al., 1999, Mehta et al., 2013). AML patients with the favourable t(8;21) karyotype display downregulation of the anti-apoptotic protein Bcl-2, and it was found to be overexpressed in AML patients with low rate of remission (Banker et al., 1998, Del Poeta et al., 2003). Additionally, a high Bcl-2:Bax ratio was found to be associated with poor prognosis (Venditti et al., 2004). The anti-apoptotic protein Mcl-1 has been shown to be a critical regulator of early hematopoietic development and overexpression of both Bcl-xL and Mcl-1 have been shown to play a crucial role in AML progression (Kaufmann et al., 1998).

1.4.3 BH3 mimetics in cancer

Over the past three decades, greater understanding of the intrinsic apoptotic pathway led to the development of BH3 mimetic drugs. Following on from successful results in lymphoid neoplasms, targeting the apoptotic pathway has been seen as a promising approach for the development of novel AML therapies to overcome the issue of acquired resistance. BH3 mimetics are small molecule inhibitors that mimic the pro-apoptotic BH3-only members by

docking into the binding groove of the anti-apoptotic members to displace the sequestered pro-apoptotic proteins (Besbes et al., 2015, Hata et al., 2015). These compounds therefore induce apoptosis in a Bak/Bax-dependent manner by nature of their strong affinity for BH3 domains in the anti-apoptotic Bcl-2 family members (Lessene et al., 2008).

ABT-737 (Oltersdorf et al., 2005) and ABT-263/navitoclax (Tse et al., 2008) represent a breakthrough in the development of BH3 mimetics and display high binding affinities for Bcl-2, Bcl-xL and Bcl-w but not Mcl-1. Both induce cytochrome c release and apoptosis in haematopoietic cancer cell lines and supress tumour growth in xenograft models. While ABT-263 improved patient's survival its clinical usage was limited due to thrombocytopenia linked to Bcl-xL inhibition in megakaryocytes (Delbridge et al., 2016). To circumvent this, the drug was re-engineered to generate ABT-199/Venetoclax, a Bcl-2 -specific inhibitor (Souers et al., 2013). ABT-199 is clinically successful and has been trialled extensively for treatment of many haematological malignancies including AML. ABT-199 shows promising activity as single agent or in combination with chemotherapy in primary AML samples and patient trials (Konopleva et al., 2014). ABT-199 binds poorly to Mcl-1, an essential regulator for AML cell survival, and as expected leukemic cells expressing high levels of Mcl-1 are resistant to ABT-199 as well as a variety of other chemotherapeutic agents (Gores and Kaufmann, 2012). Venetoclax is now approved by FDA in combination with Low-dose cytarabine or azacitidine in older AML patients ineligible for intensive chemotherapy. Development of selective and potent BH3 mimetics to inhibit Mcl-1 has become a key

therapeutic avenue for treatment of refractory malignancies (Yecies et al., 2010). This has proved to be more difficult and progress has been slow as the Mcl-1 BH3 binding groove is more rigid compared to other anti-apoptotic Bcl-2 family members (Czabotar et al., 2007). Additionally, Mcl-1 displays a strong binding affinity for its endogenous BH3-only protein binding partners (Lee et al., 2009). S63845 is a promising Mcl-1 inhibitor with several studies demonstrating its potency when used in synergy with other chemotherapeutic (Moujalled et al., 2019, Leverson et al., 2015).

1.5 Genome editing

1.5.1 Introduction/Overview

Genome editing technologies have advanced significantly over the past few years allowing us to manipulate precisely specific loci within the genome. These approaches using programmable nucleases can potentially correct or delete single genes responsible for disease (Capecchi, 1989, Capecchi, 2005).

In the last decade, three genome-editing platforms have been used to create DSBs: Zinc-Finger Nucleases (ZFNs), Transcription Activator-Like Effector Nucleases (TALENs) and Clustered Regularly Interspersed Short Palindromic Repeats (CRISPR)/Cas9 (Wood et al., 2011, Mali et al., 2013). Regardless of their differences, all three technologies share the common theme of targeting nucleases to cause double-strand cleavage of DNA at specific genomic loci. DSBs can be repaired by one of two distinct endogenous repair pathways: non-homologous end-joining (NHEJ) or homology-directed repair (HDR) with the opposing DNA strand or a template (donor). In the absence of an exogenous repair template, NHEJ is efficient but error-prone resulting in small insertions or deletions (indels) at the point of cleavage during the normal repair process (Rodgers and McVey, 2016). These indels can disrupt target genes by causing frame-shift mutations, resulting in an unstable mRNA or the introduction of a premature stop codon (Weterings and Chen, 2008). In contrast, HDR requires donor DNA strand that serves as a template to guide the repair enabling precise modification of the genomic sequences. HDR-based gene editing can therefore theoretically be used to repair disease-

causing mutations or to generate a “knock-in” of a desired sequence of DNA into the genome (Kakarougkas et al., 2014). Both repair mechanisms are used by cells to maintain genomic integrity.

The difference between the editing methods employed is in the recognition of the genomic sequence. Sequence recognition by ZFNs and TALENs occurs through protein-DNA interactions. ZFN technology involves creating chimeric protein fusions of zinc-finger DNA binding domains with the catalytic domain of the FokI nuclease (Carroll, 2011). The binding domain can be engineered to target any defined sequence providing DNA binding specificity (Gaj et al., 2013). In general, ZFNs are reported to have relatively low editing efficiency as they are very sensitive to epigenetic modifications such as methylation.

TALENs, similar to ZFNs, use a sequence of transcription activator-like effector repeats for DNA binding coupled to the same FokI nuclease used in ZFNs (Joung and Sander, 2013). While TALENs have been effective, the design, construction and effective expression of these molecules in mammalian cells can be challenging due to their size and the repeated sequences have a high rate of recombination making them unsuitable for viral delivery methods (Wang et al., 2016b).

1.5.2 CRISPR-Cas9

Since the discovery of its basic components, Clustered regularly interspaced short palindromic repeats (CRISPR) and its associated Cas9 protein has emerged as a pioneering new tool for gene editing at the forefront of current

biological research. This system functions as an adaptive immune pathway in bacteria protecting them from viruses and invading plasmids (Wiedenheft et al., 2012). The invading viral DNA is cleaved by the Cas complex, into smaller fragments (spacers) which are integrated into the CRISPR locus in the bacterial genome. These are transcribed and the pre-cRNA is processed into shorter, separate crRNA, complementary sequences when invading viruses are recognised and targeted by Cas proteins (Rath et al., 2015, Koonin and Wolf, 2015). Through repurposing, CRISPR/Cas9 has recently emerged as the preferred system for achieving site-specific DNA targeting.

CRISPR/Cas systems can be divided into two classes, Class 1 (which encompasses approximately 90% of Cas loci) and Class 2. Class 1 (encompassing type I, III and IV) Cas systems requires several Cas proteins to form an effector complex that can target either DNA or RNA. By contrast Class 2 (encompassing type II, V and VI) only requires one Cas protein, making them useful for gene editing (Koonin et al., 2017, Makarova et al., 2015). The most commonly Cas enzyme used in genome editing is that found in Streptococcus pyogenes (SpCas9) which belongs to the Class 2, type II system. The Cas9 endonuclease contains two nuclease domains, RuvC and HNH, responsible for cleavage of the non-complimentary and complimentary strand, respectively (Sternberg et al., 2015). The other two components required for this system, the CRISPR RNA (crRNA) and the trans-activating crRNA (tracrRNA) provide the DNA recognition (Deltcheva et al., 2011). The crRNA, also known as protospacer, possesses an 18–20-nucleotide guide sequence which recognises target sites within the genome, while the tracrRNA

hybridizes with the crRNA providing a scaffold for Cas9 binding (Pellagatti et al., 2016). The Cas9-tracRNA (trans-activating crRNAs) complex is directed to the region of DNA complementary to the corresponding crRNA sequence. The tracrRNA and crRNA can be fused by a short synthetic linker to create a single guide RNA (sgRNA) and is widely used in plasmid-based delivery systems (Jinek et al., 2012).

A protospacer adjacent motif (PAM) is required for Cas9 DNA binding, with SpCas9 the target must be upstream of a 5'-NGG-3' site. Assuming the crRNA sequence is complementary to the DNA sequence preceding the PAM site, Cas9 binding partially unwinds then cleaves the DNA 3 bp downstream of the PAM (Graham and Root, 2015, Jiang and Doudna, 2017). As mentioned previously once a DSB has occurred, cells employ one of two pathways to repair the damage, NHEJ or HDR (Ran et al., 2013). A single gRNA is commonly utilised for gene knockouts that result in non-homologous end joining (NHEJ) DSB repair. During NHEJ random insertion or deletion of nucleotides occurs which usually results in frameshift mutations potentially knocking out the gene of interest. However, these mutations can remain in-frame which contributes to a low efficiency (Christin and Beckert, 2016).

A)

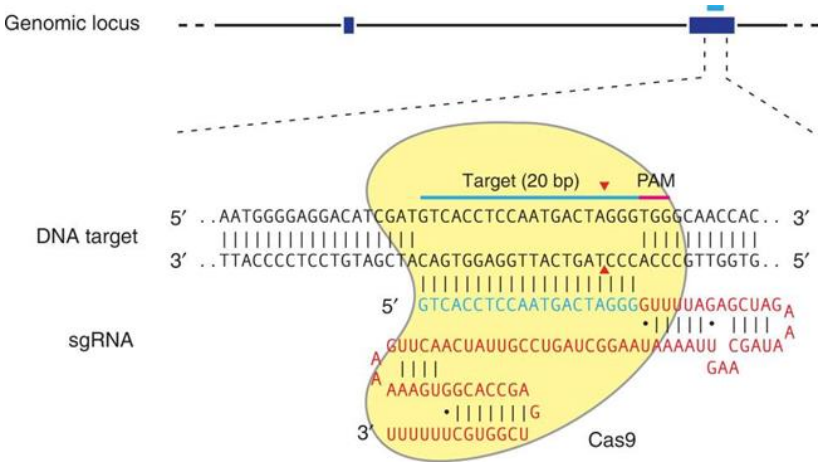

B)

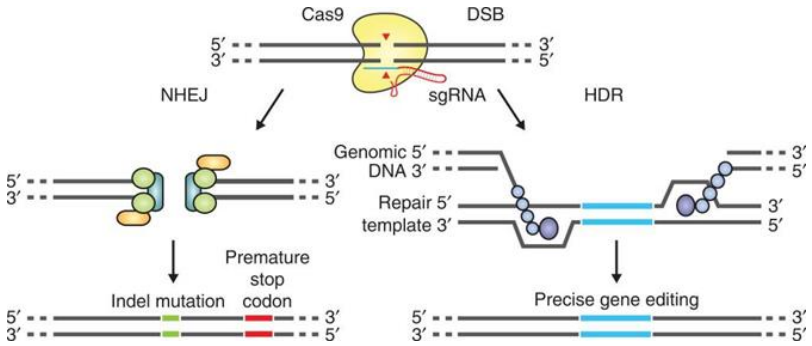

Figure 1.10: Overview of Gene editing with CRISPR-Cas9 – A) Cas9 binds to DNA complementary to the sgRNA (in blue), upstream of an NGG PAM site. Triangles indicate location of double strand break. **B)** A Cas9 induced DSB can be resolved either through the NHEJ pathway resulting in random small insertions and deletions or via HDR in the presence of a suitable repair template allowing precise alterations to be made. Adapted with permission from Springer Nature: Nature Protocols (Ran et al., 2013).

1.5.3 Therapeutic Applications of Gene Editing

All three genome editing tools have been successfully used to modify the genome in human cells with different haematological abnormalities (Porteus, 2015, Meissner et al., 2014). Targeted nucleases are being used in drug discovery and development to understand better molecular mechanisms of several diseases, including cancer. T-cell engineering and transduction using an array of genetic tools is currently the subject of many clinical trials. Recent work in ALL has shown the potential for TALENs in the treatment of chemotherapy-resistant B-ALL children where CAR-T cells with TALEN-modified target TCRαβ, were used as a novel treatment option (Reardon, 2015). An alternative approach utilises ZFNs to disrupt permanently CCR5 expression. Mutations in CCR5, a crucial receptor for HIV entry, have shown to increase viability of CD4 T-cells, and provide resistance to HIV (Wang and Cannon, 2016).

The CRISPR/Cas system has not yet been used for *in vivo* applications, however, in the past decade improved understanding of this system was a breakthrough in the study of cancer genes in human cells and mouse models. Recently the CRISPR-Cas9 system has been utilized to simultaneously disrupt up to eight alleles in mouse embryonic stem (ES) cells in a single step generating mice carrying multiple gene mutations (Wang et al., 2013). In *vivo* delivery of a CRISPR/Cas9 plasmid with single guide RNAs targeting the tumor-suppressor genes PTEN and p53 were successfully to derive a hepatic cancer model (Xue et al., 2014). Combining the CRISPR-Cas9 system with a lentiviral model to modify multiple genes in single mouse HSC and generating

AML model that can be used for better understating the complexity of human AML disease (Heckl et al., 2014).

The potential of the CRISPR-Cas9 system as a powerful genome-editing platform has almost endless applications, and can be used to inhibit, repress, activate, translocate, invert or duplicate any target gene. This offers numerous exciting opportunities to better understand cancer biology by modelling the disease and potentially treating patients with an optimal targeted therapy (Kannan and Ventura, 2015).

1.6 Thesis aims

Fms-like tyrosine kinase 3 (FTL3) is mutated in approximately 23% of AML cases resulting in an internal tandem duplication (ITD) within Exons 14/15. ITD mutated FLT3 (FLT3-ITD) is constitutively activated and confers an unfavourable prognosis. Targeting FLT3-ITD is therefore seen as a promising therapeutic avenue. The overall aim of this work is to better understand the biochemical signalling and therapeutic relevance of the FLT3-ITD mutations present in human AML cells. We will gain a more complete understanding of its function and signalling hopefully leading to additional future strategies for treating AML, and assist in identifying potential drug resistance mechanisms.

Quizartinib (AC220) is the first FLT3-ITD inhibitor to show excellent potency, selectivity and pharmacokinetic properties in clinical trials. The clinical response to TKI monotherapy remains limited by the high risk of relapse. To overcome this resistance it is crucial to improve the understanding of how

FLT3-ITD mutations affect cellular signalling in AML and how they respond to these targeted drugs, which this thesis aims to inform.

In this study, we will investigate:

- The effects of quizartinib and FLT3L on the expression, localisation and downstream targets of FLT3 and FLT3-ITD in human AML cell lines.
- The effect of FLT3 mutational status on sensitivity to quizartinib and downstream FLT3L signalling.
- The potential mechanisms of FLT3L-mediated drug resistance.
- Introduce a mutated/altered signalling component in AML cells by gene-editing.

Chapter II

==========

Materials and Methods

2.1 Materials

2.1.1 Reagents and Kits

A list of reagents and kits used in this thesis can be found in Appendix (Table A2). All regents and kits were purchased from either Sigma-Aldrich (Poole, UK) or Thermo Fisher (Loughborough, UK) unless otherwise stated.

2.1.2 Buffers

A list of buffers used in this thesis can be found in Table 2.1.

Table 2.1 – Buffers and composition

Name	Constituents
1 x Annexin V binding buffer	10 mM HEPES/NaOH (pH 7.4), 140 mM NaCl, 2.5 mM CaCl2
1 x TAE buffer	40 mM TRIS, 20 mM acetic acid and 1 mM EDTA
10 x Running buffer	1% (w/v) SDS, 1.92 M glycine, 0.25 M Tris
10 x TBS	10 mM Tris-HCl, 150 mM NaCl, pH 8.0
10 x Transfer buffer	0.25 M Tris, 1.92 M glycine
Resolving gel buffer	1.5 M Tris-HCl, 0.4% (w/v) SDS, pH 8.8
Stacking gel buffer	0.5 M Tris-HCl, 0.4% (w/v) SDS, pH 6.8
Tail lysis buffer	50 mM Tris/HCL (pH 7.5), 150 mM NaCl, 1 mM EDTA
TBST	1 x TBS, 0.1% tween 20
5% BSA Blocking buffer for (WB)	1 g BSA in 20 ml TBS-T

2.1.3 Antibodies

All primary and secondary antibodies were purchased from Cell Signalling Technology (CST) through New England Biotech (NEB, Hitchin, UK), Santa Cruz Biotechnology (Heidelberg, Germany) and Abcam (Cambridge, UK). A table of antibodies used in this thesis is found in Table 2.2.

Table 2.2 – Primary and secondary antibodies

Antibody	Source	Cat. No.	Dilution	MW (kDa)	Species
β-Actin	Sigma	A5316	1:20000	42	Mouse
STAT5	CST	25656	1:1000	90	Rabbit
STAT5A	CST	4807	1:1000	90	Mouse
STAT5B	CST	34662	1:1000	90	Rabbit
p-STAT5	CST	9351	1:1000	90	Rabbit
p44/42 MAPK	CST	9102	1:2000	42,44	Rabbit
p-p44/42 MAPK	Santa Cruz	SC7383	1:2000	42,44	Mouse
AKT	CST	2920	1:2000	60	Mouse
p- AKT	CST	4060	1:2000	60	Rabbit
FLT3	CST	3462	1:1000	130,160	Rabbit
Mcl-1	Abcam	ab32087	1:1000	35,40	Rabbit
Bcl-2	CST	4223	1:2000	26	Rabbit
Bax	CST	5023	1:2000	20	Rabbit
Bak	CST	12105	1:2000	25	Rabbit
Bim	CST	2933	1:2000	12,15,23	Rabbit

Bcl-xL	CST	2762	1:2000	30	Rabbit
PARP	CST	9532	1:1000	116	Rabbit
Caspase-3	CST	9662	1:1000	32	Rabbit
Cleaved-caspase-3	CST	9661	1:1000	17, 19	Rabbit
Anti-rabbit IgG	CST	7074S	1:3000	n/a	Goat
Anti-mouse IgG	CST	7076S	1:3000	n/a	Horse

2.1.4 Cell lines

AML cell lines U937, MV4-11, THP-1 and MOLM-13 were purchased from the Deutsche Sammlung von Mikroorganismen und Zellkulturen GmbH (DSMZ) (Braunschweig, DE). Table 2.3 shows characteristics of the AML cell lines used as models in this study. Classification was according to France-American-British Classification (FAB) that separates AML into 7 subclasses (M0-M7) according to their genetic characteristics.

Table 2.3 – Characteristics of cell lines used in this study

Cell line	Cell type	Patient age/sex	Leukaemia subtype	Doubling time (h)
U937	Histiocytic lymphoma	31/ Female	AML FAB M5	30-40
THP-1	Acute monocytic leukemia	69/ Female	AML FAB M5	35-50
MV4-11	Biphenotypic B myelomonocytic leukemia	61/ Male	AML FAB M5a	50
MOLM-13	Acute monocytic leukemia	70/ male	AML FAB M5a	50

2.2 Maintenance of cell lines

2.2.1 Cell culture

Cells were maintained in Roswell Park Memorial Institute (RPMI) medium containing foetal bovine serum (10% v/v), penicillin (1000 units/ml) and Streptomycin (1 mg/ml) in a humidified incubator at 37°C with 5% carbon dioxide (CO2). All cell lines were cultured and maintained in vented flasks and handled under aseptic conditions within a Class II tissue culture cabinet.

HEK-293T cells were cultured in Dulbecco's Modified Eagle Medium (DMEM), supplemented with 10% FBS and 1% Penicillin/Streptomycin. The adherent cell line HEK-293T had to be enzymatically treated to detach cells from the culture flask surface prior to passaging. When cells were confluent, the medium was removed, cells washed once in phosphate-buffered saline (PBS) before the addition of 2 mL of trypsin (0.05% w/v) EDTA (0.02% w/v). After

incubation for 5 min at 37°C / 5% CO_2 an equal volume of growth medium was added to the cells to inactivate trypsin. Cells were then transferred to a 15 ml conical tube and pelleted at 113 x g for 3 min. The supernatant was removed, and cells were resuspended in 5 ml of growth medium. Part of the media containing cells was transferred to the culture flask and cells were further diluted with growth medium.

2.2.2 Cell counting

Cell counts were determined by dye exclusion assay. Trypan blue passes through ruptured cell membranes in non-viable cells, staining them dark blue. Live/viable cells with intact membranes are impermeable and appear as a shiny bright halo under the microscope. Cells are diluted 1:1 with trypan blue (0.1% (w/v)) in PBS and counted using a haemocytometer.

2.2.3 Cryopreservation of cell lines

Stocks of each cell line at low passage number were prepared for use throughout the study. For preservation, cells were harvested by centrifugation (2,000 x g, 5 min), culture medium was removed, the cell pellet resuspended in freezing media (10% DMSO in FBS) and transferred to cryovials (Corning, UK). Cells were placed in a 'Mr Frosty' freezing container (Thermo-Fisher) and kept at -80ºC for 24 hours before being transferred to liquid nitrogen for long-term storage.

2.2.4 Thawing of cryopreserved cell lines

To recover cells from liquid nitrogen, cryovials were quickly thawed in a 37°C water bath. Cells were then transferred to a fresh tube and “washed” with 10 ml of complete medium (to dilute out the DMSO in the freezing medium). Following centrifugation (2,000 rpm for 5 min) to remove dead cells and debris cells were resuspended in appropriate volume of complete media then transferred to appropriate cell culture vessel and incubated in a humidified incubator at 37°C with 5% CO_2.

2.2.5 FLT3 inhibitors and FLT3L treatment of AML cells

AML cell lines were seeded in 6/12 well plates at density of 2 $x10^6$ cells per well in RPMI and incubated overnight at 37°C. The next day cells were treated with of FLT3L (100 ng/mL) or different concentrations of FLT3 inhibitors for indicated times and incubated at 37°C. After treatment cells were pelleted (500 x g for 1 min) at 4°C and whole cell protein extraction performed as described in cell lysis section. Lysates were analysed by SDS-PAGE and Western blotting.

2.3 RNA interference

All siRNAs (small interfering RNA oligoduplexes) were purchased from Qiagen (Cambridge, UK) (Table 2.5). Knockdowns were performed in Opti-MEM Reduced Serum Media (Life Technologies), using Interferin™ (Polyplus, Illkirch, France) (Table 2.6). Cells were seeded at optimal density and transfected with Interferin™ and the respective siRNA (10 nM final concentration) according to the manufacturer’s instructions. Cells were

incubated for 72h before protein knockdown efficiency was verified by Western blotting.

Table 2.5 – siRNA sequences and target regions: targeted region is highlighted. Grey bars indicate the coding sequence of the gene. The negative control has no known target gene in the cells.

Protein targeted	Cat. No.	Sequence Targeted
Mcl-1	SI02781205	CCCGCCGAATTCATTAATTTA 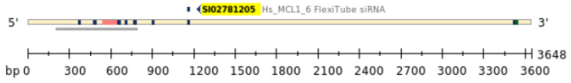
Bim	SI02655359	CGGAGACGAGTTTAACGCTTA 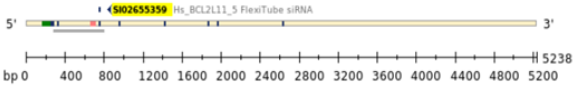
STAT5A	SI00048419	CGGCACATTCTGACAATGAA 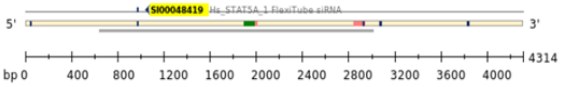
STAT5B	SI00100408	CCGCTTGGGAGACTTGAATTA 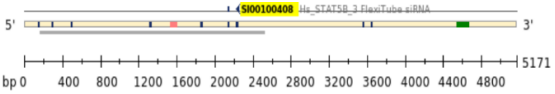
FLT3	SI02659608	CCGGCTTGAGTGAATTGTGTA 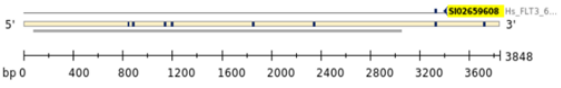
Non-targeting control	1022076	AATTCTCCGAACGTGTCACGT

Table 2.6: – Volumes of siRNA, OptiMEM and Interferin used for siRNA transfection

Well numbers	Total volume/well	OptiMEM	siRNA (CONC)	Interferin
12 wells	1ml	200 µl	1.2 µl	4 µl
6 wells	2 ml	400 µl	2.4 µl	8 µl
10 cm dish	10ml	1000 µl	10 µl	24 µl

2.4 NanoString nCounter analysis

Nanostring™ technology (NanoString Technologies, Inc) was used for kinase mRNA quantification. Cells were collected, counted, washed in PBS and snap-frozen until required. Pellets were thawed and resuspended at a concentration of ~6,500 cells/µl in RLT buffer (Qiagen). The equivalent of ~10,000 cells (~1.5 µl) was employed for direct kinase mRNA quantification, without the need for mRNA purification or amplification. mRNAs were hybridised to NanoString™ human kinome barcode probes and control code sets, and mRNA levels quantified using the nCounter colour barcoding system after count normalisation with internal housekeeping genes and eight negative controls.

2.5 Protein analysis

2.5.1 Cell lysate preparation

Lysates were prepared by harvesting cells in Eppendorf tubes on ice. Following centrifugation (550 × g for 5') at 4°C, pellets were washed twice with 0.5 ml ice-cold PBS and lysed with clear sample buffer (CSB) (125 mM Tris

(pH 6.8) containing 1% SDS (w/v), 5 mM EDTA and 10% (v/v) glycerol) containing Complete™ protease inhibitor cocktail (Roche). Lysed cells were sonicated on ice and lysates cleared by centrifugation for 5 min at 14000 *g*. The protein concentration of samples was determined and lysates stored at -20°C prior to use in Western blotting.

2.5.2 Protein quantification by Bradford assay

Total protein concentration was determined using a Bio-Rad DC protein assay kit (Bio-Rad laboratories Ltd, UK) according to the manufacturers' instructions. In brief, a series of pre-made BSA protein standards were prepared. First, 5 µL of sample or standard (in triplicate) was placed in a 96-well plate. Then, reagent A and reagent S were prepared at a 1:50 dilution and 25 µL of this mixture was added to each well followed by the addition of 200 µL of reagent B. The plate was gently agitated to ensure the reagents were mixed then plates incubated at room temperature for 15 minutes. The absorbance was measured at 650 nm using a plate reader (Bio-Tek, UK).

2.5.3 Sample preparation

The volume of cell lysate required to load 10 to 30 µg of total protein was calculated and the volume made up to 20 µL with CSB and 5x loading dye (625 mM Tris (pH 6.8) containing 5% SDS, 50% glycerol, 5% β-mercaptoethanol and 0.04% bromophenol blue). Samples were heated at 95°C for 5 minutes and analysed by SDS-PAGE and Western blotting.

2.5.4 Protein separation by SDS-PAGE

Proteins were separated by electrophoresis according to their molecular weight. Different percentages of polyacrylamide gels were used according to size of the target protein (Table 2.7).

Table 2.7 – Resolving and Stacking gel recipes for 2 gels

Ammonium Persulphate (APS) and Tetramethylethylenediamine (TEMED) were added last to initiate polymerisation. Resolving Buffer: 1.5 M Tris/HCl (pH 8.8) containing 0.4% SDS. Stacking Buffer: 0.5M Tris/HCl (pH 6.8) containing 0.4% SDS.

	Resolving gel			**Stacking gel**
%	10%	12%	15%	5%
ddH2O	8.3 ml	7 ml	5 ml	2.9 ml
Acrylamide (30%)	6.7 ml	8 ml	10 ml	0.85 ml
Resolving/Stacking buffer	5 ml	5 ml	5 ml	1.25 ml
10% APS	250 µl	250 µl	250 µl	30 µl
TEMED	25 µl	25 µl	25 µl	10 µl

When polymerised, gels were assembled in the Mini-PROTEAN® Tetra Vertical Electrophoresis Cell (Bio-Rad) and placed into a tank filled with SDS running buffer (25 mM Tris, 192 mM glycine and 0.1% (w/v) SDS). Then equal amounts of protein (calculated as described previously) were added to the wells along with the Page Ruler Plus™ protein ladder (Thermo Fisher) in the

first lane of each gel. Empty wells were filled with an equal volume of 1X loading dye. Finally, the apparatus was connected to a power supply to run the gels at a constant voltage of 100 V for up to 2 hours.

2.5.5 Western Blotting

Following electrophoresis, the gels were soaked in transfer buffer (25 mM Tris and 192 mM glycine) (Geneflow, UK) for 10 min prior to transfer. Proteins resolved by SDS-PAGE were then transferred to Hybond-ECL nitrocellulose (Amersham) at 400 mA for 70 minutes. Following transfer, the membranes were washed with Tris-buffered saline containing 0.1% Tween 20 (TBST) then blocked in TBST containing 5% (w/v) non-fat milk or 5% (w/v) Bovine Serum Albumin (BSA) (TBSTB) for 1 hour at room temperature. Following this blocking step membranes were incubated with the appropriate primary antibody diluted TBSTB and incubated overnight at 4 ºC. The membrane was then washed three times with TBST prior to incubation with an appropriate horseradish peroxidase (HRP)-conjugated secondary antibody diluted in TBSTB for 1h at room temperature. Following this, membranes were washed three times with TBST followed by a wash with TBS before being developed with enhanced chemiluminescence (ECL) (Millipore). Membranes were visualized using the ChemiDoc imaging system (Bio-Rad).

2.5.6 Quantification of protein expression by densitometry

The relative abundance of specific proteins was determined by quantifying the immune reactive bands detected on ChemiDoc. Densitometric analysis was accomplished using ImageJ (National Institute of Health (NIH), Version 1.48n)

and plotted with GraphPad Prism. Densitometry was performed and phospho-proteins were normalised relative to the respective total protein (eg. pERK with ERK). Mcl-1 and Bim were normalised to β-Actin.

2.6 Functional Assays

2.6.1 Annexin V and Propidium Iodide staining

Apoptosis was measured by flow cytometry using Annexin V/ PI staining. Cells were harvested by centrifugation at 300 g for 5 min. The pellet was washed twice with PBS and resuspended in 100 µl Annexin V binding buffer (10mM HEPES, 140 mM NaCL, and 2.5 mM $CaCl_2$). Then, 2 µl of Annexin V-FITC (BD Biosciences, UK) was added and tubes incubated for 8 min. 5 µl of propidium iodide (1 mg/ml) was then added followed by incubation in the dark at room temperature for a further 5 min. Annexin V/PI staining was measured using an Attune NxT flow cytometer (ThermoFisher) 10,000 events were captured per sample and at least three replicates were analysed for each experiment. The percentage of apoptotic cells was calculated by combining the early apoptotic (positive for Annexin V and negative for PI) and late apoptotic/secondary necrotic (positive for both PI and Annexin V) events.

2.6.2 Measurement of cell proliferation

Carboxyfluorescein succinimidyl ester (CFSE) staining was used to measure cell proliferation according to the manufacture instructions. The fluorescence intensity of the dye reduces as cells divide and this was monitored by flow cytometry at indicated time points. Cells were harvested at a density of 3×10^6 cells/ml and re-suspended in PBS. CFSE stain (CellTrace™ Cell Proliferation

Kits (C34554) (Thermo Fisher Scientific, UK)) was added to the cells at an effective 1:1000 dilution (stock concentration: 0.5 mM), and cells incubated for 30 min in a 37°C water bath. Cells were centrifuged at 500 g for 5 min, re-suspended in fresh RPMI and incubated for 15 min at 37°C. Cells were further centrifuged and resuspended in RPMI at a concentration of 5 $\times 10^6$ cells/ml and incubated overnight. The zero time-point was collected immediately following staining together with an unstained control. Time points were collected over 72h and analysed by flow cytometry.

2.6.3 Cell cycle analysis

Cell cycle analysis was performed with propidium iodide (PI) staining and flow cytometry. Cells were harvested, washed with ice-cold phosphate-buffered saline (PBS) and fixed in 70% ethanol for 30 minutes on ice. Samples were washed twice in PBS and treated with RNase (50 µl of (100µg/ml stock) at 37˚C for 30 minutes. Samples were stained at room temperature with 20 µL of PI (1mg/ml stock) for 5 minutes under light-protective conditions and analysed by flow cytometry.

2.6.4 Cell surface expression of FLT3 receptor by flow cytometry

Cells were pelleted at 500 x g for 5 min then re-suspended in 100 µL of PBS. To assess cell surface FLT3, cells were stained with 1 µg of a CD135-PE antibody or 2.5 µg of an isotype control mouse IgG2a-PE antibody for 20 min before being washed once with PBS. Pellets were re-suspended in PBS and cells analysed by flow cytometry. Total FLT3 levels (cell surface and

internalized receptor) were measured by first permeabilizing and fixing cells with Cytofix/Cytoperm buffer (BD Biosciences) for 30 minutes prior to staining.

2.7 Molecular Biology Techniques

2.7.1 Plasmids

All plasmid backbones were originally purchased from Addgene (Boston, MA). Modifications to LentiCRISPR to generate LentiCRISPR SFFV mod gRNA and pLeGO with multiple cloning sites were performed by Dr. Nicholas Harper (University of Liverpool, UK).

2.7.2 Preparation of Competent cells

Competent NEB “Stable” *E.coli* (New England Biolabs) were generated using the Mix and Go E.coli transformation buffers (Zymo Research, Cambridge Bioscience, Cambridge). 5 ml of SOB culture medium (10% Tryptone, 5% Yeast Extract, 1 mM $MgCl_2$, 1 mM $MgSO_4$ and 0.5 mM KCl) was inoculated and incubated overnight. Next day this was used to inoculate a 50 ml culture (1/400 dilution) in a 500 ml flask. *E.coli* were then grown at 24°C until an OD 600nm between 0.4-0.6 was reached. Bacteria were then rapidly chilled and diluted in the Zymo buffers according to the manufacturer’s instructions. Competent cells were then aliquoted and stored at -80°C.

2.7.3 Transformation of *E.coli*

DNA was added to a tube containing 50 µl of competent *E.coli*, the tube was then briefly vortexed followed by incubation on ice for 20 min. *E.coli* were then heat-shocked (42°C, 45 sec) and recovered on ice. SOC medium (SOB

including 1% glucose) was added and tubes incubated at 37°C with shaking for 1 hour. For plasmid transformation 50 µl of this culture was then plated on Luria Broth (LB)-Agar plates containing the required antibiotic or for ligation transformations, bacteria were pelleted (5000 rpm, 5 min) resuspended in a small volume of LB medium and the whole culture then plated. Plates were then incubated overnight at 37°C.

2.7.4 Plasmid DNA isolation

Plasmid isolation was carried out using kits according to the manufacturer's instructions. Mini-preps were carried out using the Qia-Quick Mini-Prep kit (Qiagen). 4 ml of an overnight culture was routinely used. Briefly the pellets were resuspended in 250 µl of Buffer P1 then lysed with an equal volume of P2, protein and genomic DNA was then precipitated with 350 µl of Buffer N3. This precipitate was removed by centrifugation (13,000 rpm, 10 min) and the resulting supernatant added to the spin columns. Plasmid DNA was bound following centrifugation and after several sequential wash steps with Buffers PB and PE was eluted by the addition of DNA/RNase-free water.

Where larger amounts of DNA were required MAXI-preps were performed using the PureLink HiPure Plasmid Filter Maxiprep Kit (Invitrogen, ThermoFisher Scientific). A 5 ml starter culture was inoculated and grown for 6-8 h at 37°C, this was then used to inoculate 200 - 400 ml cultures of LB medium (depending on plasmid copy number). The larger cultures were then grown overnight and pelleted the following day. Plasmid DNA was then isolated according to the manufacturer's instructions with modifications.

Briefly, pellets were resuspended in Buffer R3, followed by lysis with Buffer L7 and neutralization/precipitation with Buffer N3. The resulting precipitate was removed by filtration through glass wool and applied to the provided Maxi-prep columns (which had been previously equilibrated). When the lysate had been applied, columns were washed successively with Buffer W8 and bound DNA eluted with Buffer E4. DNA was then precipitated with an equal volume of isopropanol overnight at -20°C. The following day DNA was pelleted by centrifugation at 4000 rpm for 1h. DNA pellets were transferred to 1.5 ml Eppendorfs and washed with 70% Ethanol before being resuspended in DNA/RNase-free water. Isolated DNA was quantified using a Nanodrop (Thermo).

2.7.5 DNA Electrophoresis

Agarose gel electrophoresis was performed to analyse PCR reactions and purify DNA. Agarose was dissolved in TAE buffer (40 mM TRIS, 20 mM acetic acid and 1 mM EDTA) using a microwave. The percentage of agarose was dependent on the size of the DNA to be analysed (for a typical PCR this would be 1.5 % (w/v). Ethidium bromide (EtBr) was then added before pouring the gel. DNA samples and an appropriate DNA “ladder” were mixed with a 6x loading dye (NEB) and gel ran at 135 V until sufficient separation was seen. Gels were then visualized on a ChemiDoc imager (Bio-Rad).

2.7.6 Polymerase chain reaction (PCR)

PCR was performed to analyse genomic DNA, colony PCR to check correct insertion of guide oligonucleotides or cassettes into plasmids and to amplify

guide cassettes for cloning. For routine PCR on genomic DNA or colony PCR on bacteria we used the OneTaq PCR master mix (NEB). For cloning of guide cassettes, we used the high fidelity Q5 polymerase (NEB). Typical PCR reactions are shown in Table 2.8. Reactions were cycled according to the manufacturer's instructions.

Table 2.8 – Typical PCR reactions

	One-Taq	Q5
PCR Buffer	5 µl (2x buffer)	10 µl (5x buffer)
DNA/RNase free water	2 µl	31 µl
dNTPs (10 µM)	n/a	1 µl
Forward primer (5 µM)	1 µl	2.5 µl
Reverse primer (5 µM)	1 µl	2.5 µl
Template	n/a	1 µl
Q5 enzyme	n/a	1 µl

2.7.7 Restriction Digestion of Plasmid DNA

Plasmid DNA or PCR amplified DNA (insert) were digested with restriction enzymes. Typically, 5 µg of plasmid was digested with the appropriate enzyme (NEB). Undigested and single enzyme controls were used for all multiple enzyme reactions to ensure enzyme activity. Digests were incubated for up to 4h (depending on the enzyme) at 37°C, before being analysed by agarose electrophoresis and gel extracted or, for the inserts, just directly using the Wizard SV Gel and PCR Clean-up system (Promega).

2.7.8 Ligation of digested DNA fragments

Ligation of plasmid and PCR product or oligonucleotides was performed using a T4 DNA ligase (NEB). Table 2.9 shows a typical ligation reaction which

varies the ratio of plasmid to insert. Reactions were incubated at 4°C overnight before transformation.

Table 2.9 – Typical ligation reaction (V – vector, plasmid DNA. I – insert)

	V+L	V:I ratio (1:2)	V:I ratio (1:4)
Digested plasmid	25 ng	25 ng	25 ng
Insert	n/a	100 ng	200 ng
T4 ligase	0.5 µl	0.5 µl	0.5 µl
2x ligase buffer	5µl	5 µl	5 µl
DNA/RNase-free water	to 10µl	to 10 µl	to 10 µl

2.7.9 Colony PCR

Colony PCR was performed on bacterial colonies obtained following ligation transformations to ensure presence and correct orientation of cloned inserts. A One-Taq master mix containing the appropriate primers was aliquoted into PCR tubes and bacterial colonies picked and added to each tube. Plates which had colonies picked were placed back in the incubator to allow colony regrowth. PCR was then performed, and results analysed by agarose gel electrophoresis. Positive colonies were marked before being picked for further processing.

2.7.10 Transfection of DNA into Mammalian Cells

Plasmid DNA was transfected into adherent cells (HEK293Ts) using Polyethylenimine (PEI) (Sigma). 4 $\times 10^5$ cells were plated into 6-well plates 16h before transfection. The following day 100 µl of 150 mM NaCl was mixed with 4 µl PEI (1 mg/ml in DNA/RNase-free water). In another tube 100 µl of NaCl was mixed with the plasmid 1-2 µg of plasmid DNA. The PEI mix was then

added to the plasmid DNA mix and vortexed vigorously. After 20 minutes at room temperature the DNA/PEI complexes were added to the cells dropwise and the plates returned to the incubator. An EGFP-expressing plasmid was routinely used to ensure transfection was working as cells could be visualized by fluorescence microscopy.

2.7.11 Isolation of Genomic DNA

Transfected cells were scraped in medium in the 6-well plates and transferred to a 1.5 ml Eppendorf tube. Cells were then pelleted and washed once with PBS. Cell pellets were then lysed in 300 µl of “tail” buffer (50 mM Tris/HCL (pH 7.5), 150 mM NaCl, 1 mM EDTA and 0.2% SDS) supplemented with 20 mg/ml proteinase-K and 50 mg/ml RNaseA. Digestion was performed overnight at 55°C. Proteinase K was inactivated at 95 °C for 10 min then lysates left to cool on ice before the addition of glycogen (1 µl of a 100 mg/ml stock) and 400 µl of isopropanol to precipitate the DNA. Tubes were incubated on ice for up to 1 h (or left at -20 °C overnight) before DNA recovered by centrifugation at 20,000 x g for 1h. The DNA pellet was then washed in 70% ethanol before being resuspended in DNase/RNase-free water. Samples could be incubated at 55°C to aid resuspension. DNA was then quantified by nanodrop and normalized to 500 µg/ml

2.7.12 Gene Editing

Guide RNA design and cloning

Guide RNAs were designed to target Exon 1 and the intergenic region upstream of the ATG of the STAT5A gene using the CRISPOR tool

(http://crispor.tefor.net/). Guide oligonucleotides were obtained from IDT (Leuven, Belgium).

Table 2.10 – 5'- 3' Guide oligonucleotide sequences

STAT5A Exon 1	Forward oligo	Reverse oligo
guide#1	CACCGCCGCGGTCCAGGGATAGGT	AAACACCTATCCCTGGACCGCGGC
guide#2	CACCGGCCATGGCGGGCTGGATCC	AAACGGATCCAGCCCGCCATGGCC
guide#3	CACCGCGCCAGATGCAGGTGCTGTA	AAACTACAGCACCTGCATCTGGCGC

Oligonucleotides were designed such that when annealed they would contain "sticky" ends compatible with the LentiCRISPR plasmid and therefore didn't require digestion for cloning. Oligonucleotides were reconstituted at 100 µM in DNA/RNase-free water and phosphorylated using a T4 polynucleotide kinase (PNK) for 30 minutes at 37°C (Table 2.11).

Table 2.11 – Phosphorylation of guide oligonucleotides

Forward oligo (100 µM)	1 µl
Reverse oligo (100 µM)	1 µl
2x Ligase buffer	5 µl
ATP (1 µM)	0.5 µl
PNK	0.5 µl
DNA/RNase-free water	2 µl

Oligos were then denatured and PNK inactivated by incubating tubes at 95°C for 10 minutes in a heat-block. The heat-block was then removed and allowed to cool to room temperature to anneal the oligonucleotides. Annealed oligonucleotides were then diluted 1:25 prior to ligation. Annealed oligonucleotides were ligated into a modified LentiCRISPR plasmid that had previously been digested with BsmBI and alkaline phosphatase. Resulting clones were screened by colony PCR using a U6 forward primer (5'

GAGGGCCTATTTCCCATGATTCC 3') and the respective reverse guide oligo (Table 2.10). Plasmids were sequenced prior to use.

2.7.13 Genotyping

Primers recognising ~500 bp spanning Exon 1 of STAT5A were designed and synthesised (IDT) Table 2.12. PCR was performed on genomic DNA from transfected cells as described in 2.7.9.

Table 2.12 – STAT5A Exon 1 genotyping primers

STAT5A Exon 1 For #1	5' TCTTTCAGTTTCTGGCCGTCC 3'
STAT5A Exon 1 For #2	5' TCCACTCCTCACCATCTCTGTTC 3'
STAT5A Exon 1 Rev #1	5' CCAGCAGCTCCACAGACATCC 3'
STAT5A Exon 1 Rev #2	5' CCACCATGAGTAAAACTAGAGGCC 3'

2.7.14 Single cell clone Isolation

Single cell clones were isolated by growing cells in methylcellulose. 2.4 g of sterilised methylcellulose 4000 cP dry powder was added to 50 mL of sterile water and gently simmered for several hours with constant stirring. The solution was then cooled to 50°C and diluted 1:1 with 2 x RPMI medium. To allow the methylcellulose to fully solubilise the solution was stirred overnight at 4°C. The following day the solution was transferred to a 50 mL conical tube and centrifuged at 920 x g for 60 min to clear any particles that had not solubilised. The methylcellulose solution was stored at -20°C in 10 mL aliquots until used.

50 µL of non-essential amino acids (NEAA), 50 µL of 10 U/mL Penicillin/Streptomycin and 1.5 mL FBS were added to 1.5 mL of media containing (6000 cells/ml). 3 mL of Methylcellulose / RPMI was added to the cells and mixed with a 5 mL syringe and 12-gauge needle. This was then left to stand for the bubbles to disperse before the cells were seeded in 12 well plate (1 mL/well) (1500 cells/well). Plates were left for 10-14 days after which colonies were picked under a microscope using a 10 µL pipette and transferred to a 96 well plate for expansion. Images were acquired using an EVOS FLOID system (Bio-Rad). Scale bar 100 µM.

2.8. Lentivirus

2.8.1 Virus production in HEK-293T cells

The plasmids necessary for virus production are packaging plasmid psPAX2, an envelope plasmid encoding VSV-G (pMD2.G) and a lentiviral transfer plasmid, pCW Cas9-blast plasmid. 3.5 x 106 HEK-293T cells were seeded in 10 cm3 dishes and allowed to adhere overnight. Culture medium was changed 4h prior to transient transfection. Transfection mixture was prepared by combining 150 µL of 150 mM NaCl with 20 µL of 1 mg/mL Polyethylenimine (PEI) in one tube and 150 µL of 150 mM NaCl with 4 µg of transfer plasmid and 2 µg of each of the packaging and envelope plasmids in a second tube. The NaCl/PEI mix was added to the NaCl/plasmid mix, vortexed and left for 20 min at room temperature before it was added dropwise to the HEK-293T cells. Medium was changed the next morning and 72 hours post-transfection, the media (containing the viral particles) was removed, cleared using a 0.45 µm filter and concentrated on the day of harvesting by Ultracentrifugation at

4°C for 1.5 h at 25000 rpm using an SW41Ti rotor in a Beckman Ultracentrifuge. The supernatant was then removed and the pellet air dried then resuspended in 200 µl OptiMEM (ThermoFisher Scientific) and stored at -80°C.

2.8.8 Transduction with Lentivirus

Medium of target cells was changed 24 h before transduction. Six-well plates were set up with target cells. Polybrene (1 µg/ml), sodium butyrate (4mM) ,and 20 µl of concentrated virus was added to each well and the cells were transduced via spinoculation for one hour at 400 x g, then incubated at 37°C. 24 h after the transduction, medium was replaced and cells incubated for a further 48 h and cells were pooled and transferred into a T25 tissue culture flask for selection/expansion or used immediately for experiments.

2.9 Real-time PCR

2.9.1 RNA extraction

RNA extraction was carried out using the RNeasy Mini Kit (Qiagen). We followed the manufacturer protocol but essentially cells were pelleted in 1.5 ml microcentrifuge tubes and washed in PBS. Cells were lysed in RLT buffer using the included QiaShredder columns. 70% ethanol was added to the lysate which was then applied to an RNeasy Spin Column. The column was washed with the buffers RW1 and RPE. After which the empty spin column was centrifuged to remove any traces of ethanol before being eluted using 30 µl DNase/RNase-free water. The concentration of the extracted RNA was determined by nanodrop.

2.9.2 Reverse Transcription

RNA was converted to cDNA using the Qiagen Quantitect Reverse Transcription Kit (Qiagen) according to the manufacturer's instructions. Briefly the purified RNA sample is incubated in gDNA Wipeout Buffer at 42ºC for 5 minutes to remove any genomic DNA contamination (Table 2.13).

Table 2.13 – Genomic DNA (gDNA) elimination reaction

Component	Volume/reaction	Final concentration
gDNA Wipeout Buffer, 7x	2 µl	1x
RNA	1 µg	
RNase-free water	Variable	
DNA/RNase-free water	to 14 µl	-

After genomic DNA elimination, cDNA was prepared using the Quantiscript Reverse Transcriptase (Table 2.14).

Table 2.14 – Reverse-transcription reaction components

Component	Volume/reaction	Final concentration
Reverse-transcription master mix Quantiscript Reverse Transcriptase Quantiscript RT Buffer, 5x RT Primer Mix	 1 µl 4 µl 1 µl	1x
Template RNA genomic DNA elimination reaction	14 µl	
DNA/RNase-free water	to 20 µl	-

Reactions were incubated at 42ºC for 20 minutes (required for cDNA synthesis) followed by 95ºC for 5 minutes (to inactivate the reverse transcriptase).

2.9.3 Quantitative real time-PCR (qPCR)

qPCR was used to quantify gene expression in cells. cDNA was diluted 1:4 to make up the working solution. A typical qPCR reaction is shown below (Table 2.15). Reactions were plated into white-walled 96-well plates (Roche). Plates were then sealed with PCR sealing foil (Roche) and briefly centrifuged. The qPCR reaction was performed on a Stratagene Mx3005P qPCR machine (Thermo Fisher) for 45 amplification cycles. Results were normalized to GAPDH expression and quantified using the following formula = 2 – (ΔCT gene of interest ΔCT GADPH).

Table 2.15 – Example of a typical 20µl qPCR reaction using 5x EvaGreen buffer

Component	Amount
5x EvaGreen® qPCR buffer	4 µl
Forward primers (10 µM)	1 µl
Reverse primers (10 µM)	1 µl
DNase/RNase-free water	12 µl
cDNA	2 µl

All primers were designed and purchased from Integrated DNA Technologies (www.idtdna.com) and subjected to BLAST (NCBI) analysis (https://blast.ncbi.nlm.nih.gov/Blast.cgi) to ensure specificity.

Table 2.16 – 5’- 3’ Primer sequences used for qPCR

Gene	Forward Primer	Reverse Primer
GADPH	GAPDH was purchased from Qiagen	
STAT5A	CAGTGGTTTGACGGGGTGAT	GTCGTGGGCCTGTTGCTTAT
STAT5B	CAGAACACGTATGACCGCTG	CTGGAGAGCTACCATTGTTGG

2.10 Statistics

The data in this thesis were analysed by using GraphPad Prism 8 and ImageJ (western) software. Details of analyses are indicated in the relevant results section.

Chapter III

==========

Effect of quizartinib and FLT3-ligand on the regulation of FLT3 signalling in ITD-expressing AML cell lines

3.1 Introduction

Approximately one-third of acute myeloid leukemia (AML) patients carry an “activating” mutation in the FMS-related tyrosine kinase 3 (FLT3) gene, most commonly an internal tandem duplication (ITD) (Smith et al., 2012b, Yokota et al., 1997). FLT3-ITD mutated AML is associated with an unfavorable prognosis, characterized by shorter overall survival and high risk of relapse making it difficult to treat effectively (Kottaridis et al., 2001). Despite extensive research, no single agent, specific, FLT3 inhibitor has been approved for patients harbouring ITD mutations.

On a cellular level, the ITD mutation causes constitutive activation of FLT3. This results in activation of a number of signalling pathways including extracellular signal-regulated kinase (ERK), PI3K/Akt kinases, and the signal transducer and activator of transcription 5 (STAT5), which in turn can promote proliferation of hematopoietic stem and myeloid progenitor cells (Meshinchi and Appelbaum, 2009, Choudhary et al., 2005). ITD mutations lead to conformational changes in the receptor, resulting in impaired maturation of the protein and intracellular accumulation of incompletely glycosylated FLT3-ITD protein (Gilliland and Griffin, 2002a). For these reasons, development of FLT3-ITD targeted therapies is being actively pursued either as a single-agent or an adjuvant to conventional chemotherapy.

Many small molecule inhibitors targeting FLT3-ITD have been evaluated in clinical trials (Knapper, 2007). However, a substantial number of patients develop resistance due to the failure to completely eradicate all ITD-mutated

cells (Small, 2006). Quizartinib (AC220) is the first FLT3-ITD inhibitor to demonstrate potency, selectivity and pharmacokinetic properties in clinical trials (Zarrinkar et al., 2009b, Chao et al., 2009). Despite this the clinical response to monotherapy remains limited due to a high risk of relapse that can occur within months. To overcome this resistance, it is crucial to improve the understanding of how ITD mutations affect FLT3 signalling and how cells harbouring these mutations respond to these targeted drugs.

Aberrant ITD signalling appears to be dependent on subcellular localization. For example, THP-1 cells express wild-type FLT3 which localises primarily to the cell surface (Takahashi, 2019). In these cells FLT3 ligand (FLT3L) is required to activate ERK, and PI3K/Akt. In contrast, MV4-11 cells have a homozygous ITD mutation resulting in constitutively active FLT3 which localises almost exclusively to the endoplasmic reticulum (ER). As well as ERK and PI3K/Akt, this mutation also causes activation of STAT5 pathway (Spiekermann et al., 2003a). The effect of FLT3 inhibition by quizartinib and activation by FLT3L on signalling and subcellular localisation of the receptor and its ITD mutants has not yet been examined systematically.

3.1.1 Aims

This chapter will focus on the effects of quizartinib and FLT3L on the expression, localisation and downstream targets of FLT3 and its ITD mutants in different AML cell lines.

3.2 Results

3.2.1 Characterization of FLT3 mutations in common AML cell lines

Four AML cell lines that differ in FAB classification and FLT3 mutational status were used (Table 3.1) (Quentmeier et al., 2003). The ITD mutation in the MV4-11 cell line is well described and comprises a 30 bp duplication in Exon 14 but the mutation in the MOLM-13 cell line is more obscure (Quentmeier et al., 2003). To characterise the mutational status of FLT3 in each of the AML cell lines prior to use, genomic DNA was extracted and Exon 14 amplified by PCR and resulting products analysed, first by DNA-PAGE.

The MV4-11 cells clearly showed a single PCR product larger than the corresponding bands in the wild-type-expressing THP-1 and U937 cell lines (Fig 3.1A). This agrees with these cells being homozygous for a 30 bp ITD mutation. The MOLM-13 cells exhibited two bands, one corresponding to the wild-type product and an additional band, larger than wild-type but smaller than that obtained in the MV4-11s. This would agree with these cells harbouring a heterozygous ITD mutation that differed from the one found in the MV4-11 cells.

To further characterize these bands the PCR products were excised from Agarose gels and sequenced. The MOLM-13 products could not be successfully, separated on Agarose gels and therefore they were cloned into pBluescript prior to sequencing. Sequences obtained from both THP-1 and U937 cells as expected corresponded to wild-type sequence with no mutations in Exon 14 (Fig 3.1B).

The MV4-11 sequence had a 30 bp insertion in Exon 14 which has previously been described. This sequence is homozygous as determined by the single product following PCR and the single trace obtained with sequencing. Several pBluescript plasmids were sequenced following cloning of the PCR products from the MOLM-13 cell line and two sequences were obtained. The first was wild-type but the second had a 21 bp insertion in Exon 14 (Fig 3.1B). In conclusion the genotyping shows that two of the lines (U937 and THP-1) have wild-type FLT3 ($FLT3^{ITD-/-}$), MV4-11 cells have a homozygous 30 bp ITD ($FLT3^{ITD+/+}$), and the MOLM-13s have both a wild-type and an ITD allele ($FLT3^{ITD-/+}$) which differs from that found in the MV4-11s.

A)

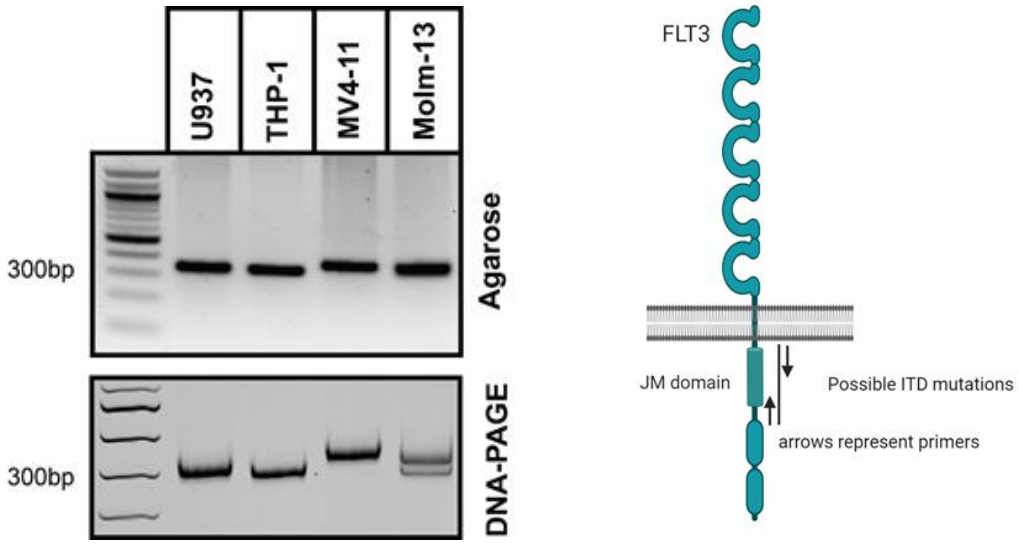

B)

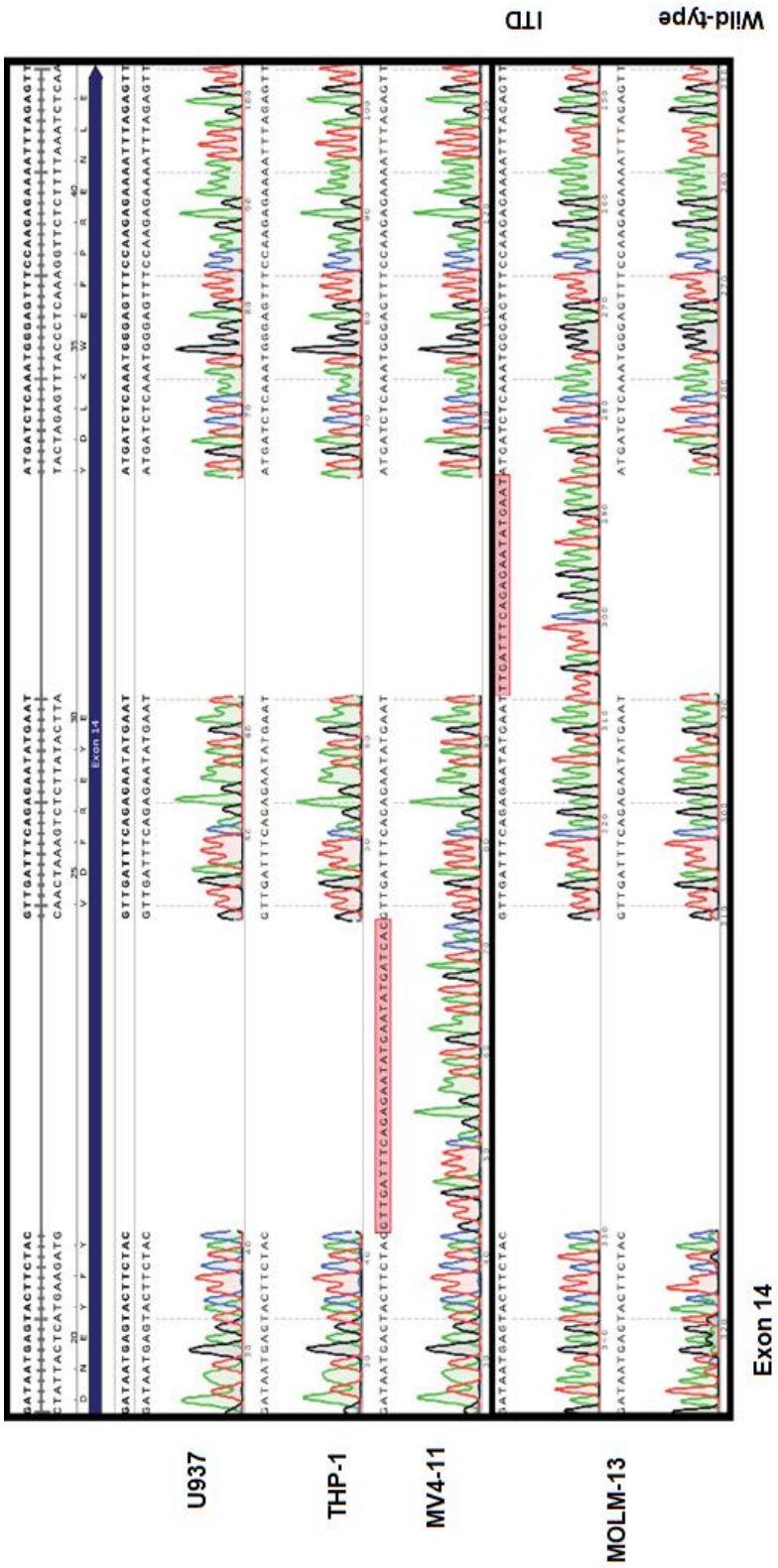

Figure 3.1: Identification of FLT3-ITD mutations in common AML cell lines – A) Exon 14 of FLT3 was amplified from genomic DNA isolated from AML cell lines and products separated by Agarose gel electrophoresis (upper panel) and DNA-PAGE (lower panel). The doublet observed in the MOLM-13's indicates a heterozygous mutation. **B)** Sanger sequencing of PCR products. MOLM-13 products were first cloned into pBluescript prior to sequencing several clones.

3.2.2 Quizartinib induces apoptosis only in ITD-expressing AML cell lines

Having characterized FLT3 mutations in the AML cell lines (Fig 3.1) their response following treatment with the FLT3 inhibitor quizartinib was assessed using Annexin-V/PI. The effect of quizartinib was analysed with increasing concentrations (0.01–10 μM) over a four-day period. Treatment with quizartinib induced apoptosis and decreased cell viability in the ITD expressing MV4-11 and MOLM-13 cell lines in a time and concentration-dependent manner. In contrast, the wild-type FLT3 expressing, THP-1 and U937, cells were not sensitive (Fig 3.2A). The IC_{50} values of quizartinib after 72h are summarized in Table 3.1. The pan-tyrosine kinase inhibitor, midostaurin, was also tested, and all AML lines appeared to exhibit some sensitivity following treatment (Fig 3.2B). These data suggest that the Type II TKI quizartinib is selective for ITD-expressing AML cells whereas the type I TKI midostaurin effectively induce apoptosis in all AML cell lines irrespective of FLT3 mutational status.

Table 3.1 – IC50 of quizartinib on AML

Cell lines	FAB	FLT3 status	IC50 (72h)
MV4-11	M5a	$FLT3^{ITD+/+}$	31 nM
MOLM-13	M5a	$FLT3^{ITD-/+}$	6 nM
THP-1	M5	$FLT3^{ITD-/-}$	N/A
U937	M5	$FLT3^{ITD-/-}$	N/A

A)

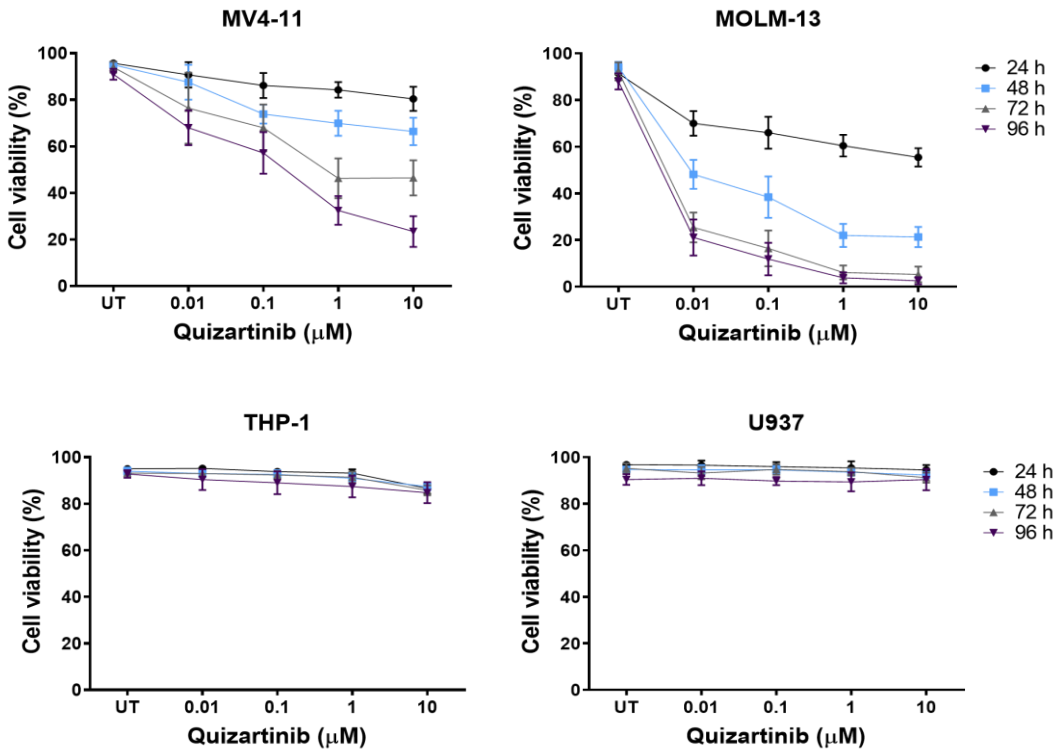

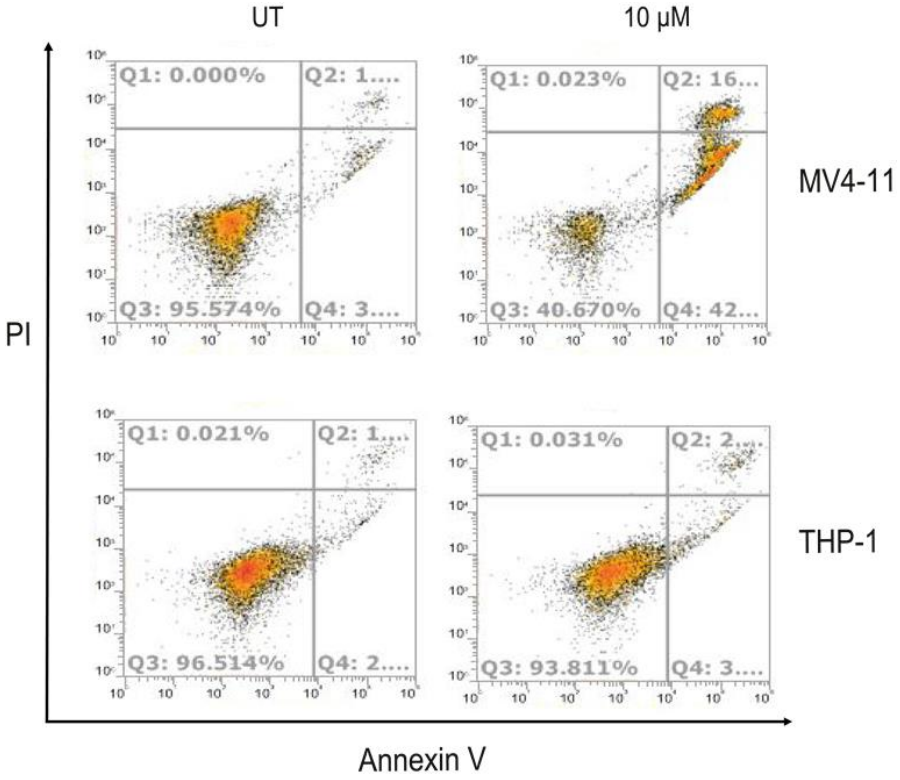
UT
10 µM
MV4-11
THP-1
PI
Annexin V
Q1: 0.000%
Q2: 1....
Q3: 95.574%
Q4: 3....
Q1: 0.023%
Q2: 16...
Q3: 40.670%
Q4: 42...
Q1: 0.021%
Q2: 1....
Q3: 96.514%
Q4: 2....
Q1: 0.031%
Q2: 2....
Q3: 93.811%
Q4: 3....

B)

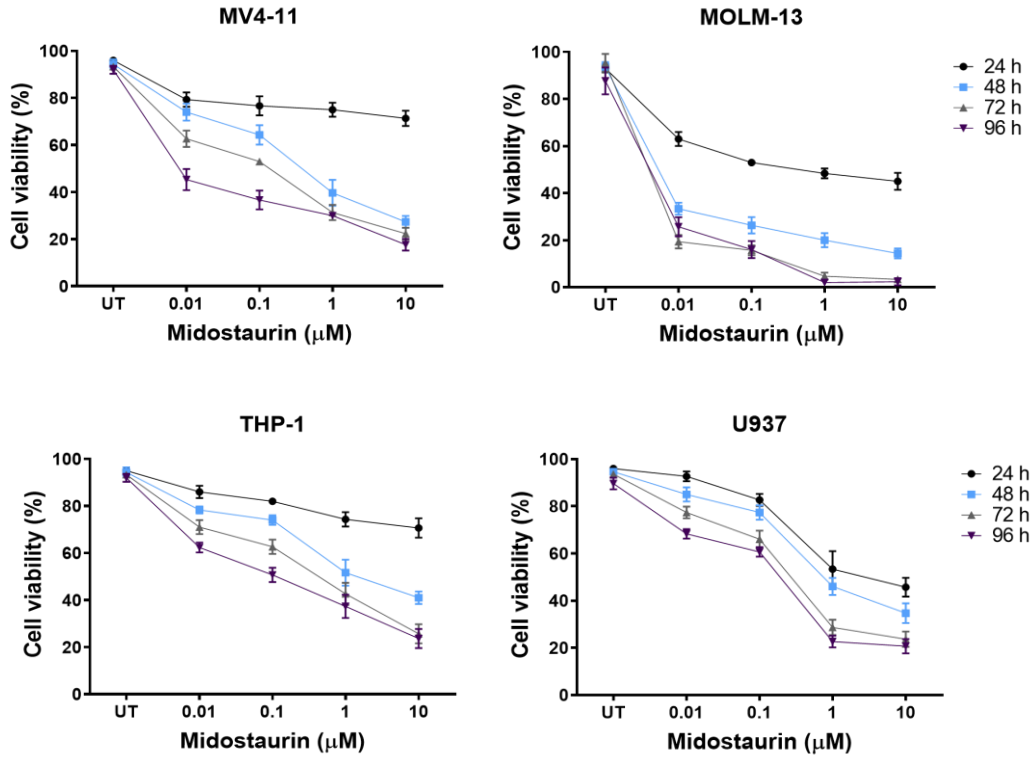
MV4-11
MOLM-13
THP-1
U937
Cell viability (%)
Midostaurin (µM)
UT
0.01
0.1
1
10
24 h
48 h
72 h
96 h

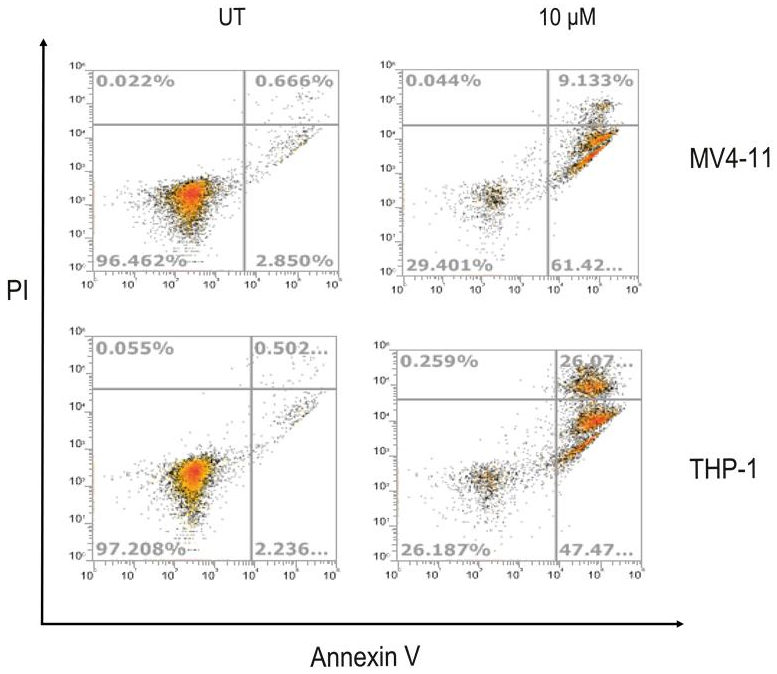

Figure 3.2: Quizartinib selectively induces apoptosis in FLT3-ITD expressing cells – MV4-11, MOLM-13, THP-1, and U937 cells were incubated with increasing concentrations of **A)** quizartinib or **B)** midostaurin. Apoptosis was measured at indicated times using Annexin-V/PI staining. Results represent the mean +/- SEM for 5 independent experiments. Scatter plots are representative of cells at 72h with quizartinib or midostaurin.

3.2.3 Quizartinib inhibits FLT3 signalling in ITD-expressing Cells

As the AML cell lines displayed a differential sensitivity to quizartinib but not midostaurin, we looked at the effect of quizartinib on FLT3 signalling pathways in ITD, compared to WT cells. Again, cells were incubated with increasing concentrations of quizartinib (0.01–10 µM) and the phosphorylation status of known FLT3 signalling intermediates analysed by Western blotting. Both ERK1/2 and AKT were constitutively phosphorylated in MV4-11 and MOLM-13 cells and this was inhibited by quizartinib indicating these pathways were downstream of FLT3. Cells displayed constitutive phosphorylation of STAT5, and this was also inhibited by quizartinib, again indicating this was dependent

on ITD signalling in these cells (Fig 3.3A). ERK1/2 and AKT were also constitutively phosphorylated in the WT-FLT3 expressing THP-1 and U937 cells, and this was unaffected by quizartinib (Fig 3.3B).

To confirm the inhibition in signalling observed is a result of ITD inhibition and not a secondary effect due to cell death, we examined the effect of quizartinib on FLT3 signalling at earlier time points (Fig 3.3C). Consistent with the previous results, quizartinib inhibited constitutive phosphorylation of STAT5, ERK1/2, and AKT in MV4-11. Inhibition was observed as early as 30 minutes after treatment with 1µM quizartinib but 0.1 µM and even 0.01 µM was effective with later time points.

Western blotting results examining FLT3 inhibition by quizartinib for all AML cell lines correlated well with the Annexin-V/PI data. Taken together, these results show that inhibition of FLT3-ITD by quizartinib is accompanied by potent inhibition of FLT3 signalling pathways within 30 minutes of TKI treatment leading to cell death.

A)

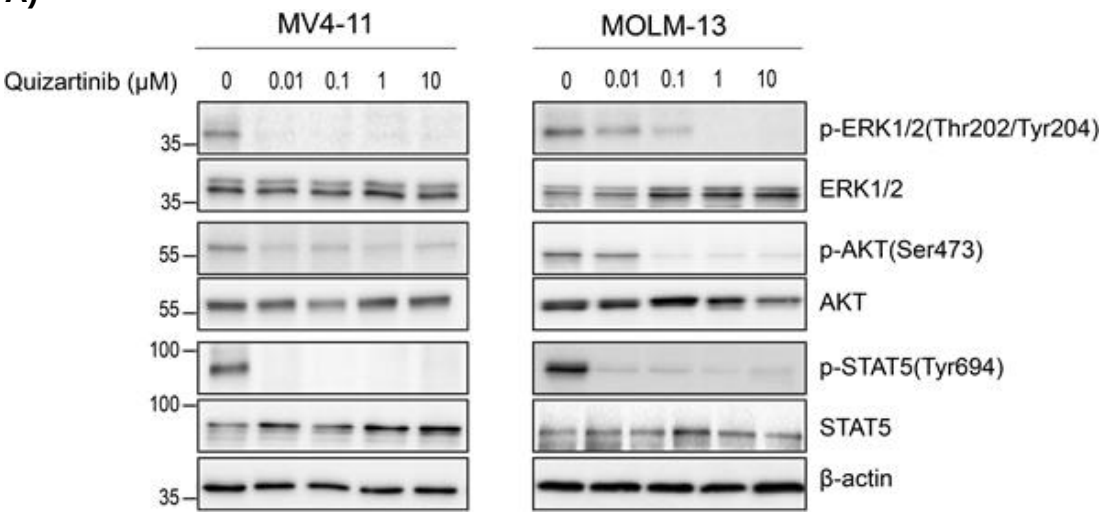
MV4-11
MOLM-13
Quizartinib (μM)
0 0.01 0.1 1 10
35
35
55
55
100
100
35
p-ERK1/2(Thr202/Tyr204)
ERK1/2
p-AKT(Ser473)
AKT
p-STAT5(Tyr694)
STAT5
β-actin

B)

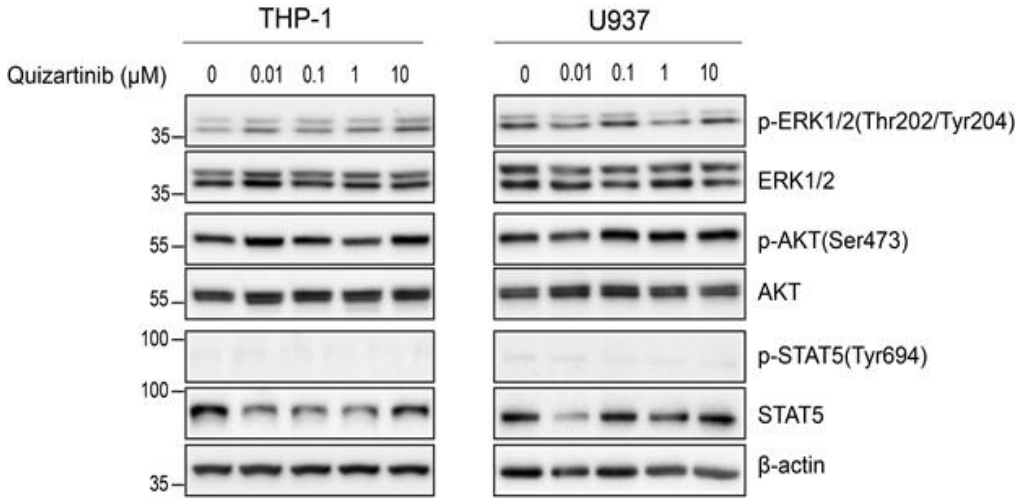
THP-1
U937
Quizartinib (μM)
0 0.01 0.1 1 10
35
35
55
55
100
100
35
p-ERK1/2(Thr202/Tyr204)
ERK1/2
p-AKT(Ser473)
AKT
p-STAT5(Tyr694)
STAT5
β-actin

C)

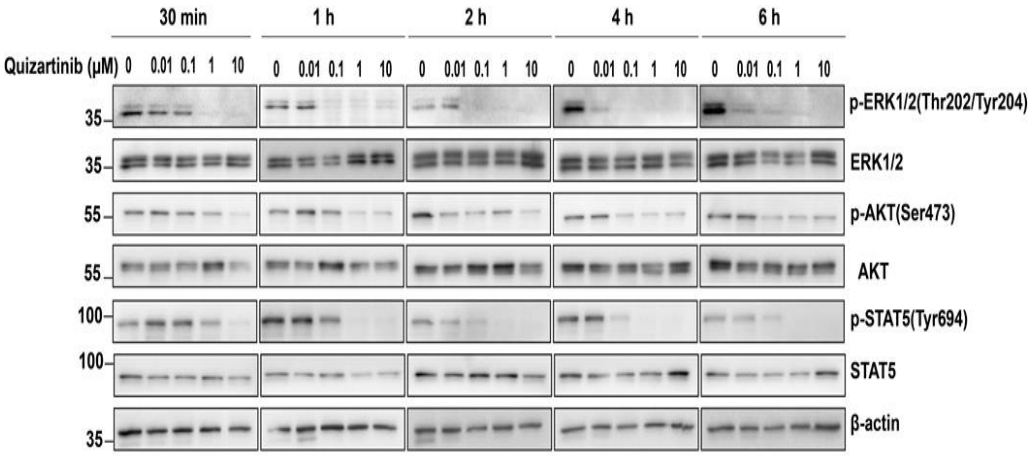
30 min
1 h
2 h
4 h
6 h
Quizartinib (μM) 0 0.01 0.1 1 10
35
35
55
55
100
100
35
p-ERK1/2(Thr202/Tyr204)
ERK1/2
p-AKT(Ser473)
AKT
p-STAT5(Tyr694)
STAT5
β-actin

Figure 3.3: Quizartinib inhibits FLT3 signalling in ITD expressing cells – A) MV4-11, MOLM-13 and **B)** THP-1, and U937 cells were treated with quizartinib for 24h for indicated concentrations. **C)** Effect of quizartinib on MV4-11 cells at shorter time periods. Total cellular protein extracts were separated by 10% SDS-PAGE and subjected to immunoblot analysis with antibodies against known FLT3 signalling intermediates; phospho-STAT5, -AKT, -ERK1/2 and their unphosphorylated forms. β-actin was used as a loading control. Results are representative of 3 independent experiments.

3.2.4 Effect of quizartinib on cell cycle progression and proliferation of AML cell lines

To further confirm the selectivity of quizartinib in ITD expressing cells, we looked at its effect on cell cycle progression and proliferation using flow cytometry. In MV4-11 and MOLM-13 cells, incubation with quizartinib for 24h resulted in an increased in the population of G1 phase cells, and for 72h a higher percentage of cells in (sub-G1) than untreated cells were observed. This was accompanied by a decrease in proportion of cells in S and G2/M phases (Fig 3.4A). By contrast, quizartinib appeared to have no effect of on cell cycle status in THP-1 or U937 cells.

This was further confirmed using a CFSE-based cell proliferation assay. The mean fluorescence intensity (MFI) of viable CFSE-stained cells was obtained for untreated and treated cells. CFSE staining decreases following cell division, as it is diluted within the daughter cells. Thus inhibition of cellular division results in higher MFI levels of the CFSE in cells. As with the previous data, quizartinib only affected proliferation in the ITD-expressing cells but not THP1 or U937s (Fig 3.4B). Of the two ITD lines effects were more pronounced

in the MOLM-13s. These results demonstrate that quizartinib induces cell cycle arrest and has an anti-proliferative effect in ITD but not WT-FLT3 cells, which is in agreement with the apoptosis and inhibition of FLT3 signalling observed previously (Fig 3.2).

A)

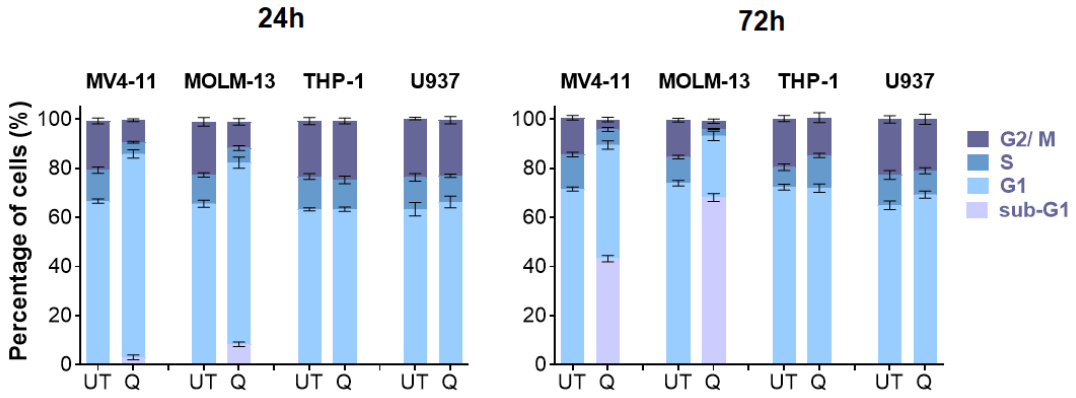

B)

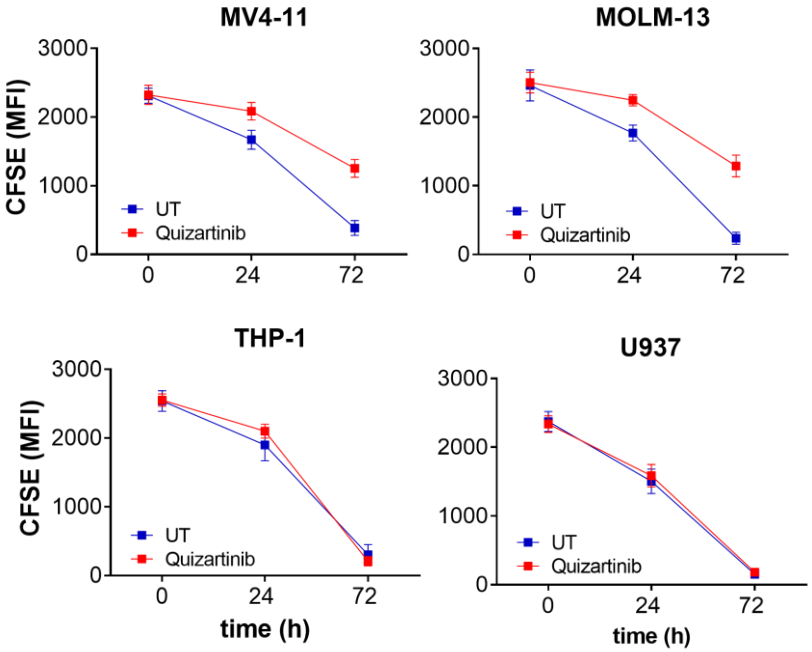

Figure 3.4: Quizartinib induces cell cycle arrest and displays anti-proliferative activity only in FLT3-ITD expressing cells – A) MV4-11, MOLM-13, THP-1, and U937 cells were treated with quizartinib (Q) (0.1 μM) for 24h-72h and cell cycle analysis was performed on fixed cells using PI staining followed by flow cytometry. **B)** Proliferation was measured by CFSE staining after treatment for 24 and 72h. Results represent the mean +/- SEM for 3 independent experiments and are expressed as mean fluorescence intensity (MFI).

3.2.5 FLT3 localisation in AML cell lines

It has been reported that FLT3 mutational status affects it subcellular localisation as well as its signalling. To further investigate this, AML cells were stained with a FLT3 (CD135) antibody and cell surface receptor localisation evaluated by flow cytometry. MOLM-13 ($FLT3^{ITD-/+}$) and THP-1 ($FLT3^{ITD-/-}$) cells exhibited significantly higher cell surface expression of FLT3 (MFI 3.6 and 4.3) than that observed with MV4-11 cells ($FLT3^{ITD+/+}$) (MFI 1.7). No cell surface staining of FLT3 was detected in U937 cells (Fig 3.5 A-B).

To compare total FLT3 expression to cell surface localisation, cells were permeabilized prior to staining. Permeabilization resulted in an increase in FLT3 staining in the ITD expressing MV4-11 and MOLM-13 cells indicating a significant proportion of the FLT3 in these cells is intracellular (Fig 3.5 C-D). In the THP-1 cells, permeabilization did not increase staining above that seen in intact cells indicating the majority of the FLT3 in these cells is on the cell surface. In the U937 cells, permeabilization did not increase the FLT3 staining and, given that there is also no FLT3 on their cell surface strongly suggests these cells do not express FLT3 protein. These results indicate that in

homozygous ITD-expressing cells the majority of FLT3 is intracellular, suggesting these mutations may impair trafficking of the receptor to the cell membrane.

Furthermore, mRNA from each of the cell lines was analysed using NanoString nCounter^{TM} gene expression system. In agreement with the flow cytometry data no mRNA was detected in the U937 cells again indicating these cells don't express FLT3. Of the other cells, the FLT3 mRNA transcript level was higher in the ITD expressing MOLM-13 and MV4-11 cells compared to the THP-1 cells (Fig 3.5E). Despite only expressing a single ITD allele, mRNA levels were considerably higher in MOLM-13 cells compared to the THP-1s.

Western blot analysis on whole cell lysates showed that the AML cell lines expressed the different glycosylated forms of FLT3 (Fig 3.5F). THP-1 ($FLT3^{ITD-/-}$) presented as two species; partially glycosylated (130 kDa), corresponding to the intracellular form and fully glycosylated (160 kDa) that is present at the cell surface (Choudhary et al., 2009b). In MV4-11 cells ($FLT3^{ITD+/+}$) only the partially glycosylated (130 kDa) form was present agreeing with the flow-cytometry data demonstrating receptor is predominantly intracellular in these cells. FLT3 in MOLM-13s presents as a doublet which includes the partially glycosylated 130 kDa form and another closely related species. Genotyping suggests this cell line could potentially express 2 species and these bands could possibly be the WT and ITD (21 bp insertion corresponding to approximately a 3 kDa difference) forms. Although there was no clearly defined 160 kDa species a smear of

immunoreactivity is clearly visible above the two major bands which may represent the cell surface form. As expected, given the flow cytometry results, FLT3 protein was undetectable in the U937 cells again indicating FLT3 is absent in these cells.

A)

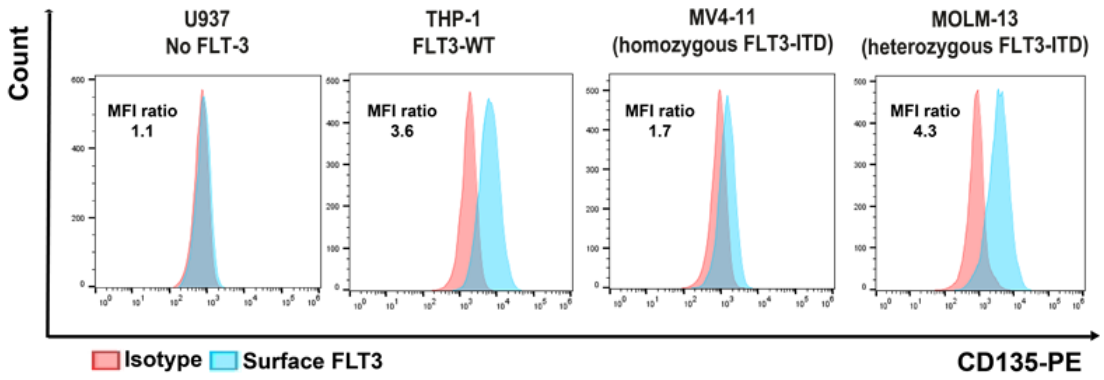

B)

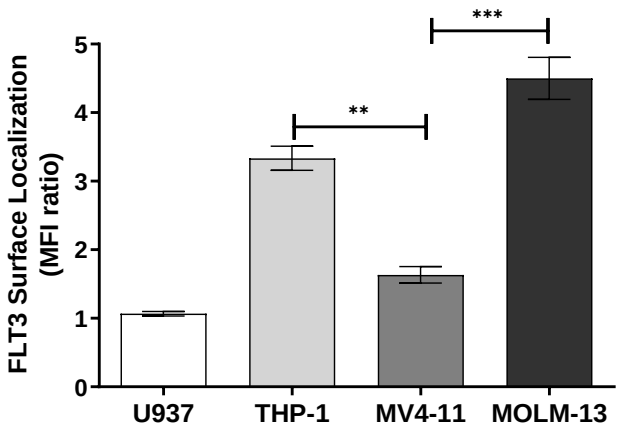

C)

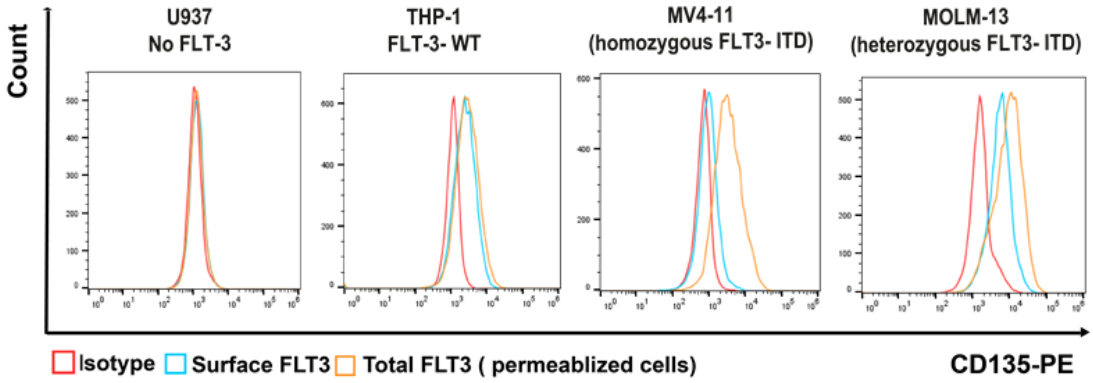
Count
U937
No FLT-3
THP-1
FLT-3- WT
MV4-11
(homozygous FLT3- ITD)
MOLM-13
(heterozygous FLT3- ITD)
Isotype
Surface FLT3
Total FLT3 (permeablized cells)
CD135-PE

D)

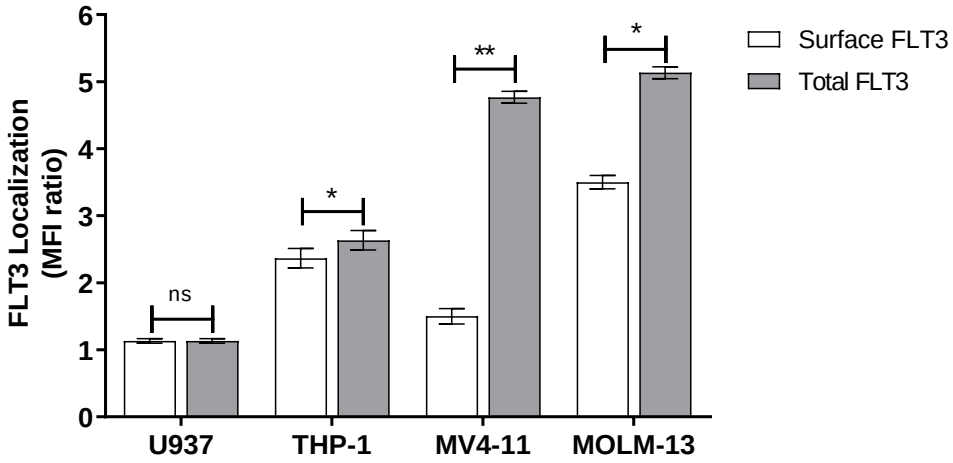
FLT3 Localization
(MFI ratio)
0
1
2
3
4
5
6
ns
*
**
*
U937
THP-1
MV4-11
MOLM-13
Surface FLT3
Total FLT3

E)

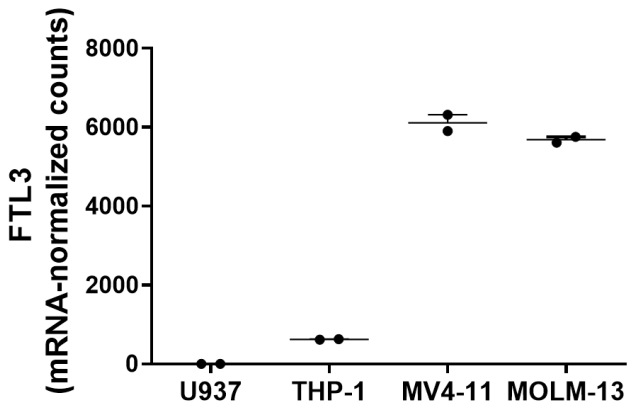
FTL3
(mRNA-normalized counts)
0
2000
4000
6000
8000
U937
THP-1
MV4-11
MOLM-13

F)

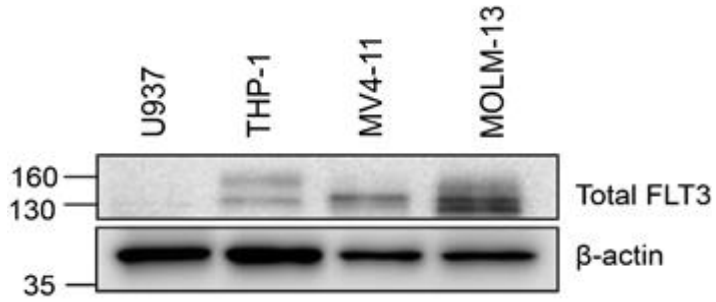

Figure 3.5: Localisation of FLT3 in AML lines depends on ITD status – A-B) U937, THP-1, MV4-11, and MOLM-13 cells were stained with anti-CD135-PE antibody and cell surface FLT3 assessed using flow cytometry. IgG-PE was used as an isotype control and results presented as MFI ratio compared to control. Significance testing was done by two-tailed unpaired *t*-test (n=3), ***p* ≤ 0.01 and ****p* ≤ 0.001**. C-D)** cells were first permeabilized with BD Cytofix/Cytoperm buffer prior to staining to assess total (cell surface + intracellular) FLT3. Significance testing was done by two-tailed paired *t*-test (n=3),**P* ≤ 0.05, ***P ≤ 0.01, ns, not significant.* Results represent the mean +/- SEM for 3 independent experiments **E)** Nanostring analysis of FLT3 mRNA in AML cell lines. mRNA level was normalized against several internal reference genes. Results represent the mean +/- SEM for 2 independent experiments. **F)** Total cellular protein (20 µg) from the AML cell lines was separated by SDS-PAGE and subjected to immunoblot analysis with a FLT3 antibody. β-actin was used as a loading control.

3.2.6 Role of FLT3 activation and inhibition on receptor localisation and signalling in AML cell lines.

3.2.6.1 FLT3L and FLT3 antibody binding experiment

As we wished to use the FLT3 (CD135) antibody to detect FLT3 localisation following FLT3L treatment we needed to ensure whether FLT3L would interfere with binding of the CD135 antibody. For this purpose, we used the

THP-1 cells as they express WT-FLT3, which almost exclusively resides on the cell surface in unstimulated cells (Fig 3.5C). THP-1 cells were incubated on ice for 30 minutes before being treated with FLT3L for a further 30 minutes, this allows the ligand to bind the receptor in the absence of activation or internalization. The cells are washed in ice-cold PBS and subsequently stained with the CD135 antibody. As we have seen previously, THP-1 cells bound the CD135 antibody demonstrating they express FLT3 on their cell membrane. Staining was unaffected by preincubation of the cells with FLT3L indicating that FLT3L does not compete with the anti-FLT3 antibody (Fig 3.6).

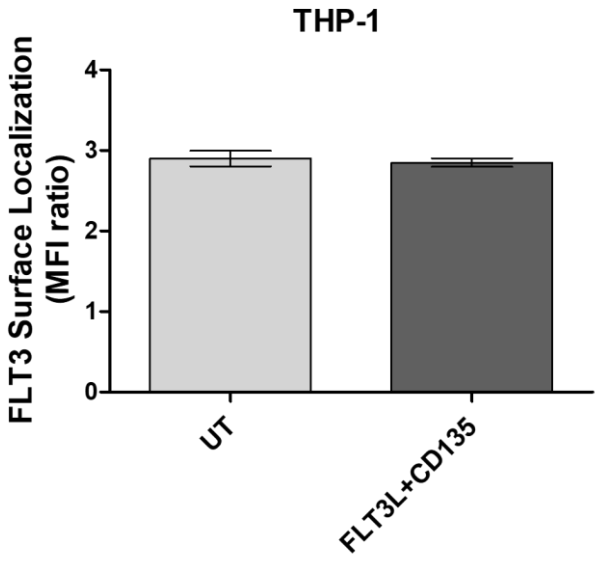

Figure 3.6: The FLT3L does not compete with the anti-FLT3 (CD135) antibody – THP-1 cells were treated with FLT3L for 30 minutes on ice (to block receptor internalization) before washed with PBS and stained with anti-CD135-PE and IgG-PE antibodies to detect FLT3. Cells were analysed for cell surface FLT3 expression by flow cytometry and mean fluorescence intensity plotted. Results represent the mean +/- SEM for 2 independent experiments.

3.2.7 Activation of FLT3 receptor in AML cells by exogenous FLT3L

As the FLT3-WT and ITD appeared to be differently localised in the unstimulated AML cells, the effect of FLT3L on cell surface expression was determined by flow cytometry. Treatment with FLT3L decreased cell surface expression of FLT3 in THP-1 and MOLM-13, but not MV4-11 cells. This agrees with results obtained with related receptors such as c-kit which is rapidly internalized following engagement with ligand (Yee et al., 1994). In MV4-11s the FLT3 would have no access to the exogenous FLT3L as it's primarily intracellular, and therefore its subcellular localisation would be expected to remain unchanged. U937 cells showed no staining with or without ligand (Fig 3.7A-B).

We next investigated the effect exogenous FLT3L had on activation of FLT3 signalling by examining phosphorylation of ERK1/2, AKT, and STAT5. As seen before, many of these pathways were constitutively active in all the AML lines in the absence of ligand. Enhanced phosphorylation of ERK1/2 and AKT by FLT3L was observed in the THP-1 cells however, no STAT5 phosphorylation was apparent (Fig 3.8A). No effect of exogenous ligand was observed in U937s as these cells don't express FLT3. In MV4-11 and MOLM-13 cells, the ITD causes ligand-independent activation of FLT3 and this likely results in the constitutive phosphorylation of ERK1/2 and AKT, and STAT5 in these cells. Despite this, we observed that the FLT3L could further activate the ITD cells leading to increased phosphorylation of ERK1/2 and AKT but not STAT5 (Fig 3.8B). This data suggests that the addition of FLT3L activates WT-FLT3 and can augment the activation of ITD-FLT3 receptors resulting in

additional activation of ERK1/2 and AKT. The data also confirmed that only ITD but not ligand-activated WT-FLT3 is able to activate STAT5.

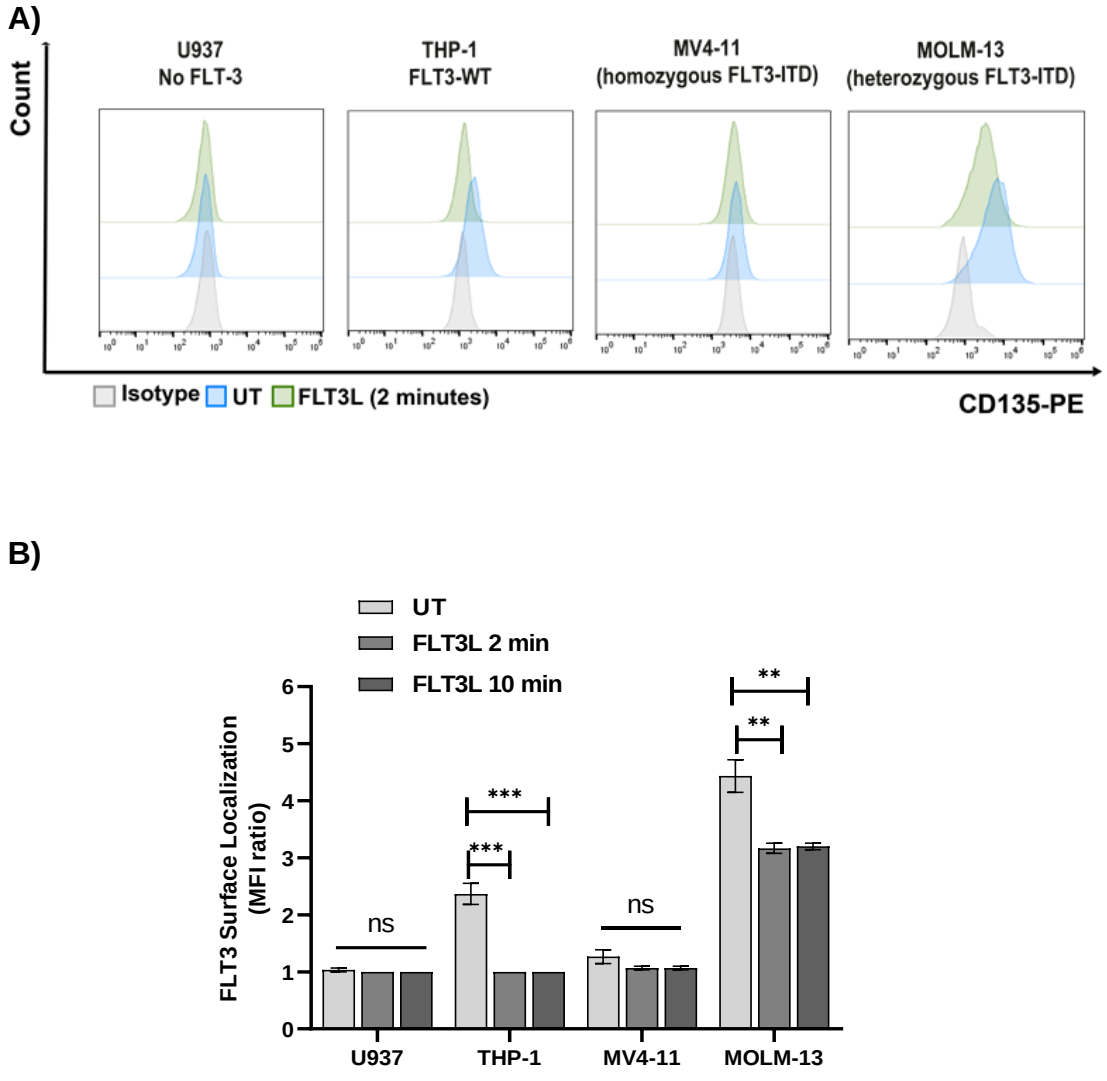

Figure 3.7: FLT3L reduces cell surface levels of FLT3 – A-B) U937, THP-1, MV4-11, and MOLM-13 cells were stimulated with FLT3L for indicated times. Cell surface FLT3 expression was measured by staining with anti-CD135-PE or isotype control (IgG-PE) antibodies and analysing stained cells by flow cytometry. Results are presented as the mean fluorescence intensity (MFI) and represent the mean +/- SEM of 3 independent experiments. Significance testing was done by one-way ANOVA with Dunnette's multiple comparison test (n=3), ***P ≤0.01, ***P ≤0.001, ns, not significant.*

A)

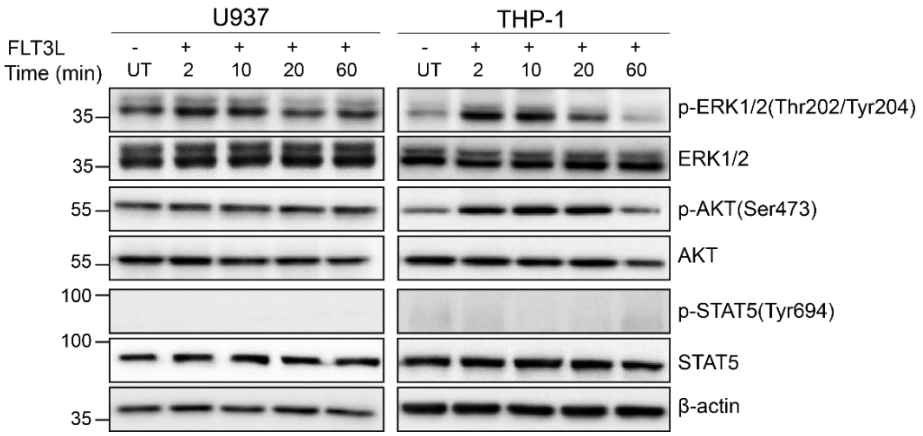
U937
THP-1
FLT3L
Time (min)
- + + + +
UT 2 10 20 60
35
35
55
55
100
100
35
p-ERK1/2(Thr202/Tyr204)
ERK1/2
p-AKT(Ser473)
AKT
p-STAT5(Tyr694)
STAT5
β-actin

B)

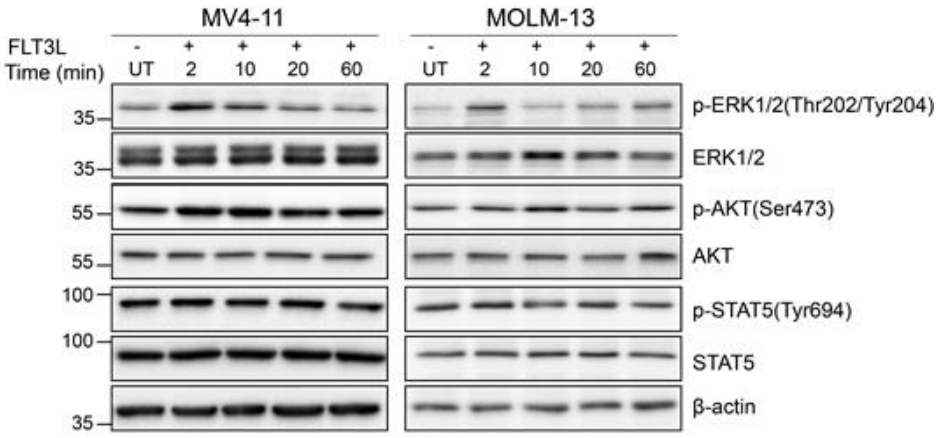
MV4-11
MOLM-13
FLT3L
Time (min)
- + + + +
UT 2 10 20 60
35
35
55
55
100
100
35
p-ERK1/2(Thr202/Tyr204)
ERK1/2
p-AKT(Ser473)
AKT
p-STAT5(Tyr694)
STAT5
β-actin

C)

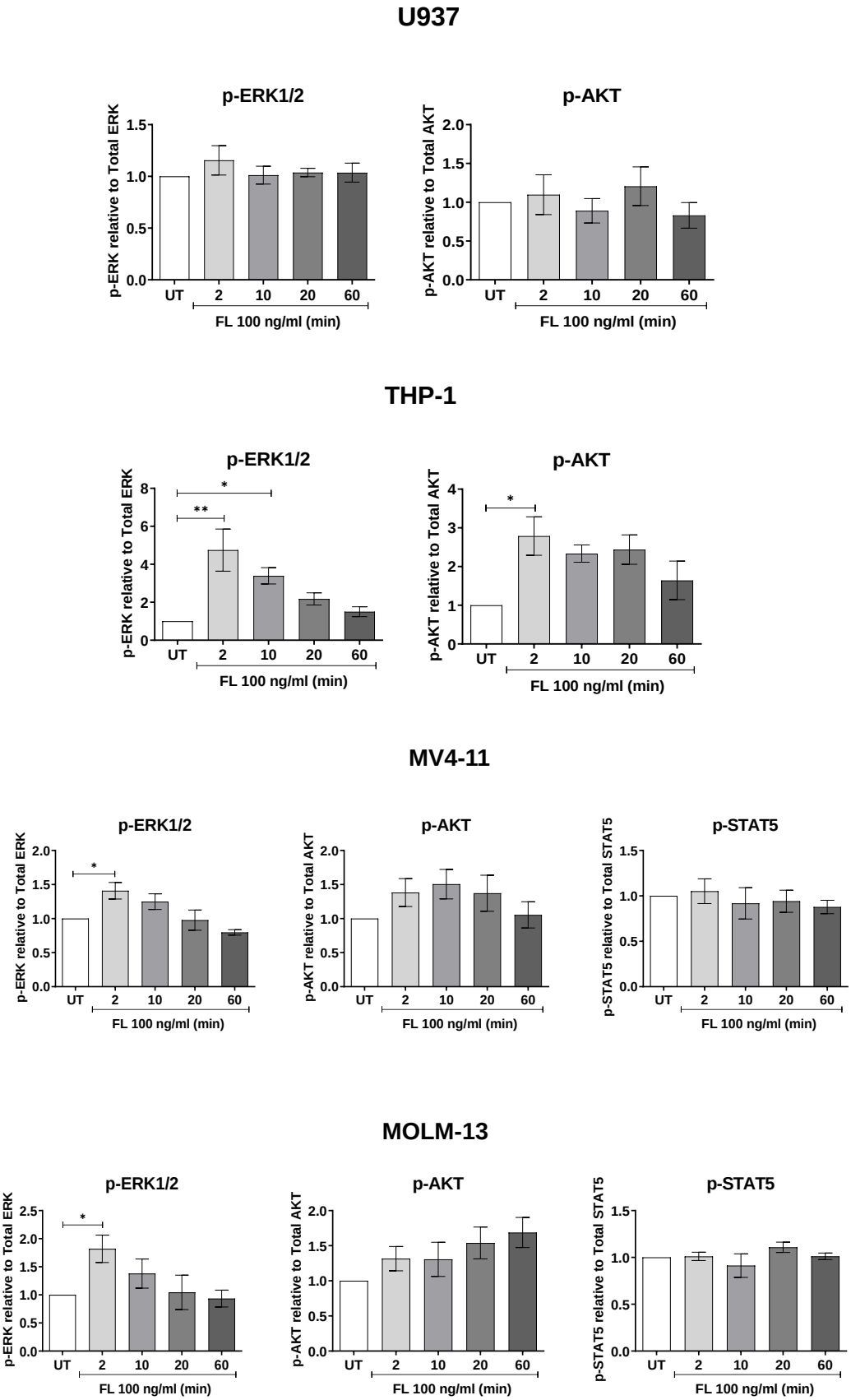
U937
p-ERK1/2
p-ERK relative to Total ERK
1.5
1.0
0.5
0.0
UT
2
10
20
60
FL 100 ng/ml (min)
p-AKT
p-AKT relative to Total AKT
2.0
1.5
1.0
0.5
0.0
UT
2
10
20
60
FL 100 ng/ml (min)
THP-1
p-ERK1/2
p-ERK relative to Total ERK
*
**
8
6
4
2
0
UT
2
10
20
60
FL 100 ng/ml (min)
p-AKT
p-AKT relative to Total AKT
*
4
3
2
1
0
UT
2
10
20
60
FL 100 ng/ml (min)
MV4-11
p-ERK1/2
p-ERK relative to Total ERK
*
2.0
1.5
1.0
0.5
0.0
UT
2
10
20
60
FL 100 ng/ml (min)
p-AKT
p-AKT relative to Total AKT
2.0
1.5
1.0
0.5
0.0
UT
2
10
20
60
FL 100 ng/ml (min)
p-STAT5
p-STAT5 relative to Total STAT5
1.5
1.0
0.5
0.0
UT
2
10
20
60
FL 100 ng/ml (min)
MOLM-13
p-ERK1/2
p-ERK relative to Total ERK
*
2.5
2.0
1.5
1.0
0.5
0.0
UT
2
10
20
60
FL 100 ng/ml (min)
p-AKT
p-AKT relative to Total AKT
2.0
1.5
1.0
0.5
0.0
UT
2
10
20
60
FL 100 ng/ml (min)
p-STAT5
p-STAT5 relative to Total STAT5
1.5
1.0
0.5
0.0
UT
2
10
20
60
FL 100 ng/ml (min)

Figure 3.8: Activation of FLT3 signalling in AML cells by FLT3 Ligand – A) U937, THP-1 and **B)** MV4-11 and MOLM-13 cells were stimulated with recombinant human FLT3L (100 ng/ml) and incubated for indicated times. Total cellular protein extracts were separated by 10% SDS-PAGE and subjected to immunoblot analysis with antibodies against known FLT3 signalling intermediates; phospho-STAT5, -AKT, -ERK1/2 and their unphosphorylated forms. β-actin was included as a loading control. **C)** Densitometric levels of phosphorylated protein band intensity was normalized with its total protein then each value was calculated in relative to untreated cells. Significance testing was done by one-way ANOVA with Dunnette's multiple comparison test (n=3), **P ≤0.05 and **P ≤0.01.* Results represent the mean +/- SEM for 3 independent experiments.

3.2.8 Inhibition of ITD signalling affects subcellular localisation of FLT3

We next examined the effect of ITD inhibition with quizartinib on FLT3 localisation. Cells were first cultured in the presence of the quizartinib, and surface FLT3 expression measured by flow cytometry. In ITD-expressing cells, FLT3 surface expression altered significantly following inhibition with quizartinib.

In MV4-11 cells, the FLT3-ITD protein appears entirely intracellular. Quizartinib treatment resulted in redistribution of FLT3 with significantly higher levels of cell surface expression compared to untreated cells (Fig 3.9A). MOLM-13s already display some cell surface FLT3 expression in untreated cells presumably due to the presence of inactive, WT-FLT3. In these cells surface levels were increased by quizartinib likely through inhibition and redistribution of the ITD variant to the cell surface (Fig 3.9B). The increase in surface FLT3 was larger in MV4-11 compared to the MOLM-13 cells. THP-1

cells did not response to quizartinib, and the surface level remained unchanged (Fig 3.9C), suggesting redistribution of FLT3 following quizartinib occurred only in ITD expressing cells.

When cells were treated with the pan-tyrosine kinase inhibitor (midostaurin), FLT3 surface expression levels remained essentially unaltered even in the ITD-expressing cell lines which suggests that this inhibitor does not specifically affect ITD-mutated FLT3 (Fig 3.10).

A)

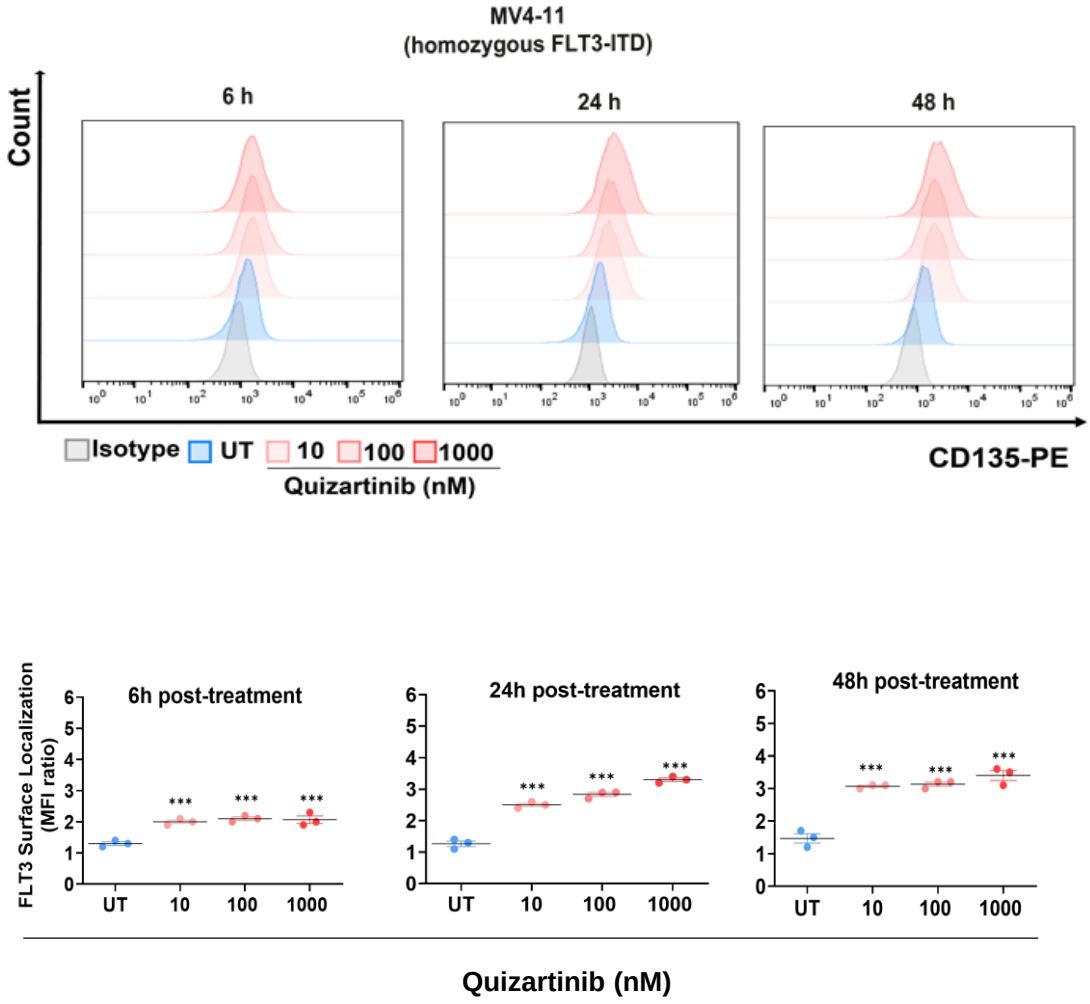

B)

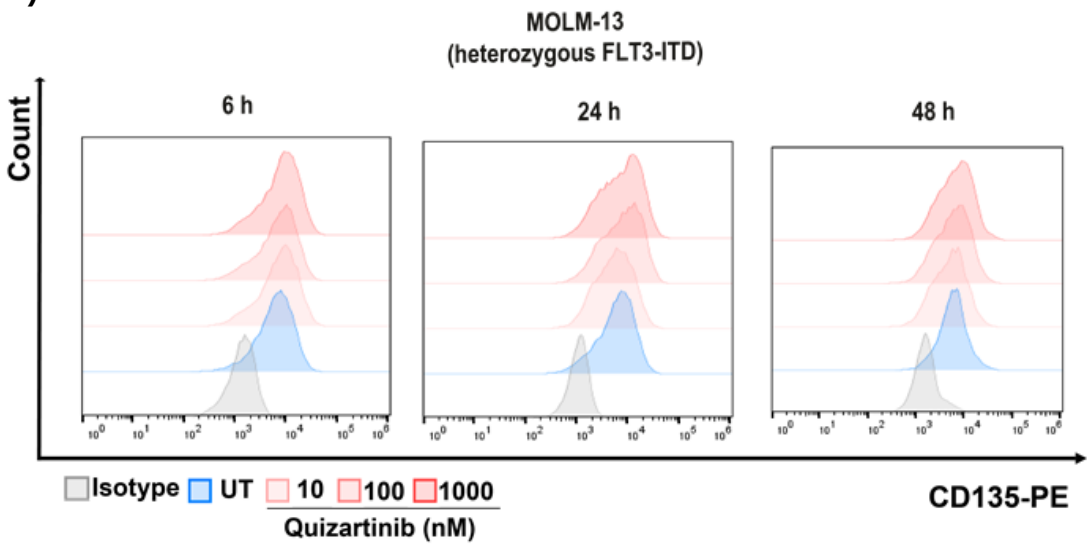
MOLM-13
(heterozygous FLT3-ITD)
6 h
24 h
48 h
Count
Isotype
UT
10
100
1000
Quizartinib (nM)
CD135-PE

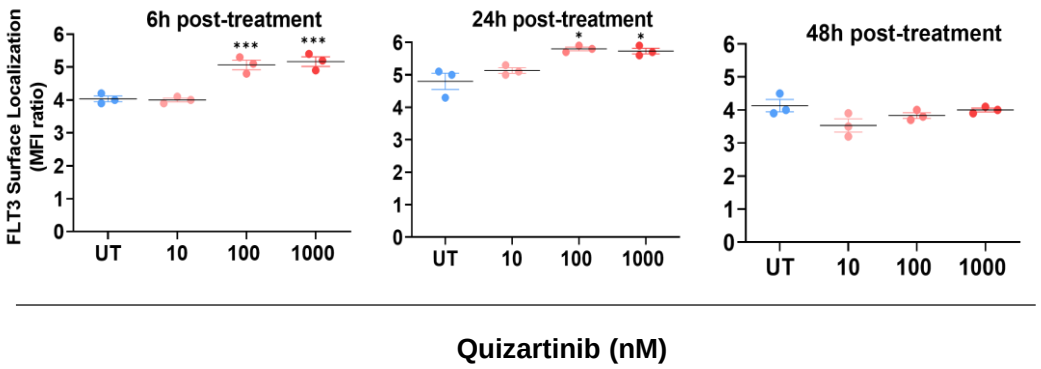
FLT3 Surface Localization
(MFI ratio)
6h post-treatment
24h post-treatment
48h post-treatment
UT
10
100
1000
Quizartinib (nM)

C)

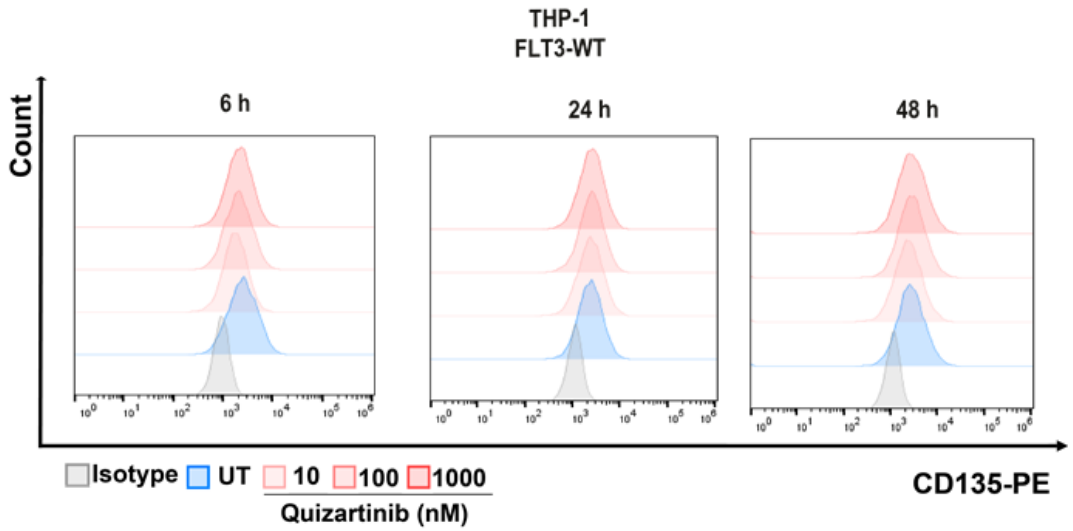
THP-1
FLT3-WT
6 h
24 h
48 h
Count
Isotype
UT
10
100
1000
Quizartinib (nM)
CD135-PE

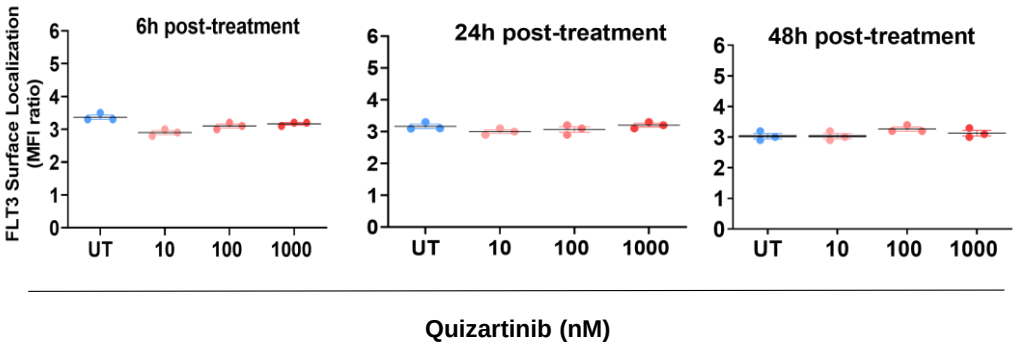

Figure 3.9: Quizartinib alters FLT3-ITD localisation – A) MV4-11, **B)** MOLM-13 and **C)** THP-1 cells were treated with increasing concentrations of quizartinib for indicated times. Cell surface FLT3 expression was measured by staining with anti-CD135-PE or isotype control (IgG-PE) antibodies and analysing stained cells by flow cytometry. Results are presented as the mean fluorescence intensity (MFI) and represent the mean +/- SEM of 3 independent experiments. Significance testing was done by one-way ANOVA with Dunnette's multiple comparison test (n=3), **P ≤0.05 and ***P ≤0.001* shows statistical higher significant difference versus untreated cells.

A)

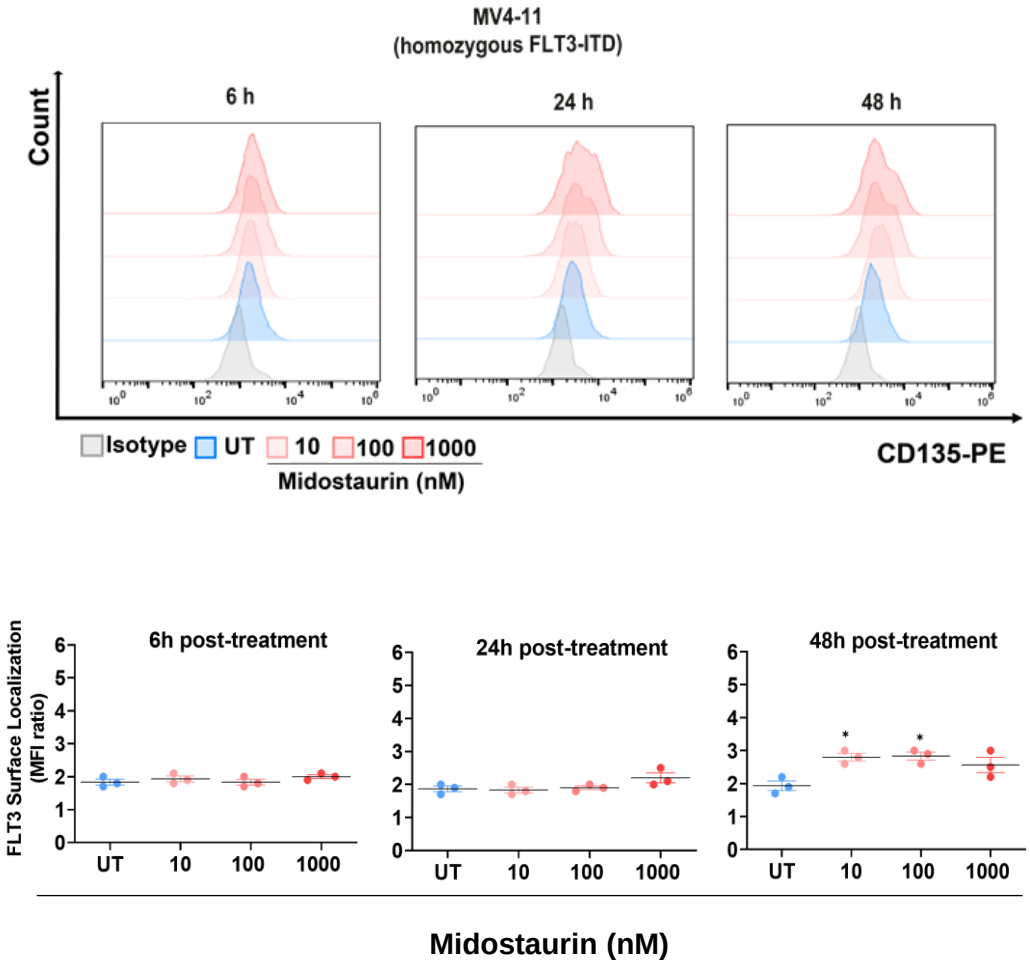
MV4-11
(homozygous FLT3-ITD)
6 h
24 h
48 h
Count
Isotype UT 10 100 1000
Midostaurin (nM)
CD135-PE
FLT3 Surface Localization
(MFI ratio)
6h post-treatment
24h post-treatment
48h post-treatment
UT
10
100
1000
Midostaurin (nM)

B)

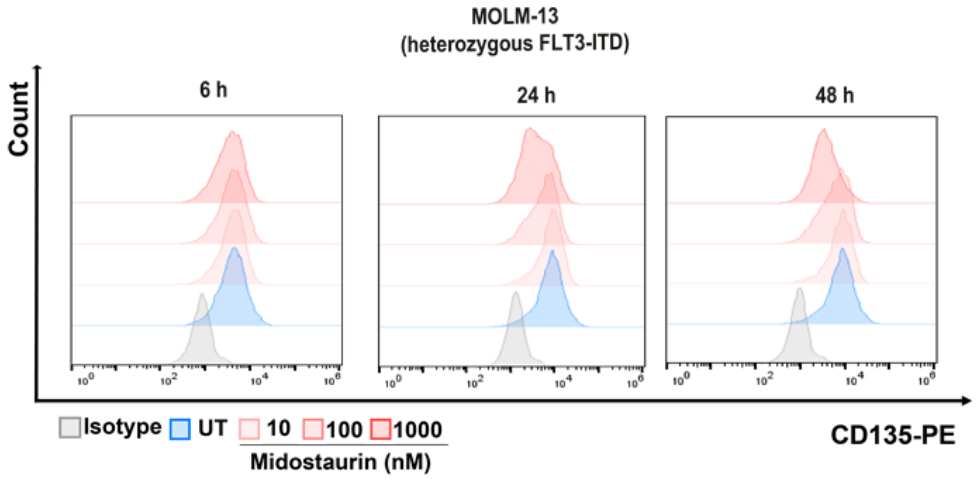
MOLM-13
(heterozygous FLT3-ITD)
6 h
24 h
48 h
Count
Isotype UT 10 100 1000
Midostaurin (nM)
CD135-PE

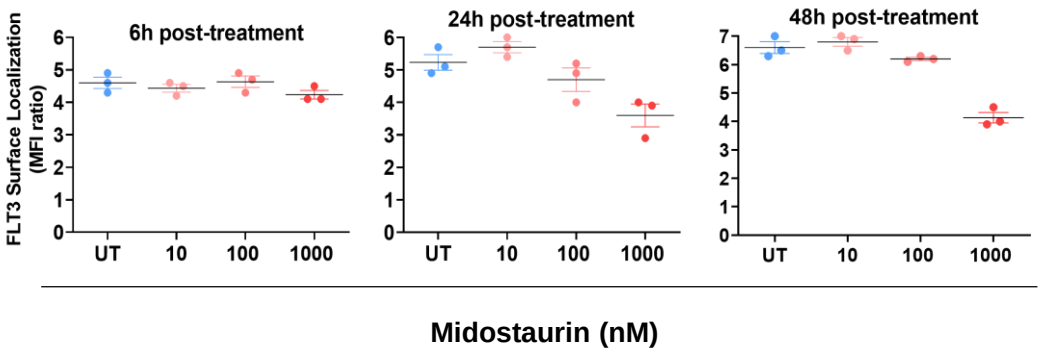
FLT3 Surface Localization (MFI ratio)
6h post-treatment
24h post-treatment
48h post-treatment
UT
10
100
1000
Midostaurin (nM)

C)

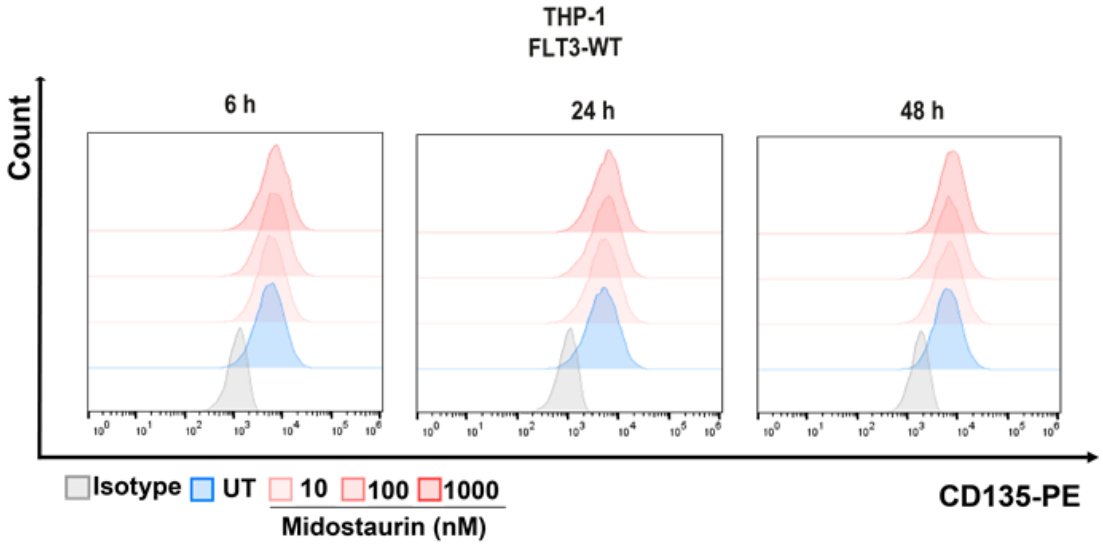
THP-1
FLT3-WT
Count
6 h
24 h
48 h
Isotype
UT
10
100
1000
Midostaurin (nM)
CD135-PE

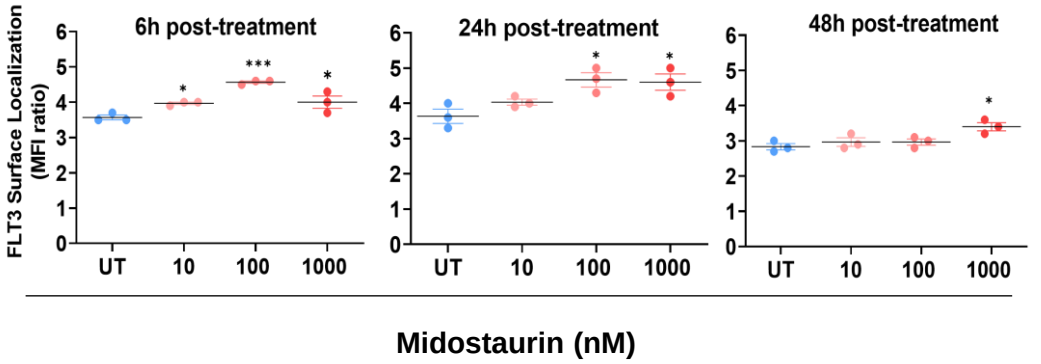
FLT3 Surface Localization (MFI ratio)
6h post-treatment
24h post-treatment
48h post-treatment
UT
10
100
1000
Midostaurin (nM)

Figure 3.10: The pan-tyrosine kinase inhibitor Midostaurin does not change FLT3 localisation – A) MV4-11, **B)** MOLM-13 and **C)** THP-1 cells were treated with increasing concentrations of midostaurin for indicated times. Cell surface FLT3 expression was measured by staining with anti-CD135-PE or isotype control (IgG-PE) antibodies and analysing stained cells by flow cytometry. Results are presented as the mean fluorescence intensity (MFI) and represent the mean +/- SEM of 3 independent experiments. Significance testing was done by one-way ANOVA with Dunnette's multiple comparison test (n=3), **P ≤0.05 and ***P ≤0.001* shows statistical higher significant difference versus untreated cells.

3.2.9 The role of FLT3 activation and inhibition on signalling in wild-type and ITD-expressing AML cells

We have previously shown that quizartinib alters the cell surface expression of FLT3-ITD but fails to affect levels in WT-expressing cells. We next wished to relate the changes seen in subcellular localisation to FLT3 signalling in the presence of quizartinib or following activation with FLT3L.

As shown before, results indicate that THP-1s display high surface expression of FLT3 and as expected, these were unaffected following treatment with quizartinib (Fig 3.11A-B). Activation with FLT3L resulted in a decrease in cell surface staining which was unaffected by quizartinib pre-treatment. FLT3L activation was accompanied by a reduction in the 160 kDa membrane-localised glycosylated form. An increase in phosphorylation of both ERK1/2 and AKT indicated the receptor was available for activation with exogenous ligand and this was unaffected by the presence of quizartinib (Fig 3.11C).

Inhibition of ITD-FLT3 in MV4-11 cells resulted in an increase in cell surface FLT3 (Fig 3.11A-B). Adding FLT3L to the quizartinib pre-treated MV4-11 lead to a slightly decrease in the surface localized ITD receptor when compared to quizartinib only treated condition. Western blot analysis indicated a corresponding increase in the fully glycosylated (160 kDa), mature form together with a decrease in the partially glycosylated form, likely as a consequence of relocalisation of the receptor from an intracellular compartment to the cell surface (Fig 3.11C). Inhibition was also accompanied by a reduction in phosphorylated ERK1/2, AKT and STAT5. This indicate that the FLT3L can cause internalization of homozygous FL3-ITD, however, for the time point we used for FLT3L stimulation (2 min), this was not enough to rescue ERK1/2 and AKT dephosphorylation that caused by quizartinib pre-treatment.

The MOLM-13s already have high levels of cell surface FLT3 expression and there was only a small increase following quizartinib treatment (Fig 3.11A-B). As with the MV4-11s quizartinib resulted in inhibition of basal phosphorylation of ERK, AKT and STAT5 indicating these were due to ITD signalling. Addition of FLT3L caused an increase in activation of these pathways which is presumably due to the presence of WT-FLT3 in these cells. This enhanced activation was unaffected by quizartinib reinforcing the fact that quizartinib can only affect ITD but not WT-FLT3 signalling (Fig 3.11C).

The fully glycosylated mature (160 kDa) form was reduced in MOLM-13 upon FLT3L stimulation; however, no changes in MV4-11 were detected due to an

undetectable amount of cell surface FLT3. Interestingly as shown in Fig 3.11B, when FLT3L was added to quizartinib pre-treated MV4-11 cells, the surface localisation of FLT3 reduced compared to cells treated with quizartinib alone and this reduction matched the level of untreated cells. Unlike in the MOLM-13s, the co-treatment in MV4-11 was not accompanied by an increase in FLT3 signalling independent of that inhibited by quizartinib. The rapid activation by exogenous FLT3L must there be causing ligand-dependent internalization of the receptor, but this is not accompanied by an increase in signalling in the MV4-11 cells as they only express the quizartinib-inhibited ITD form.

A)

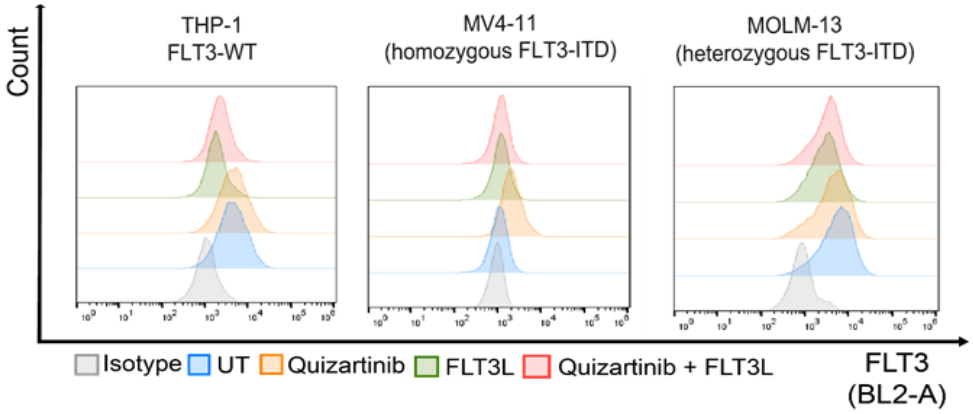

B)

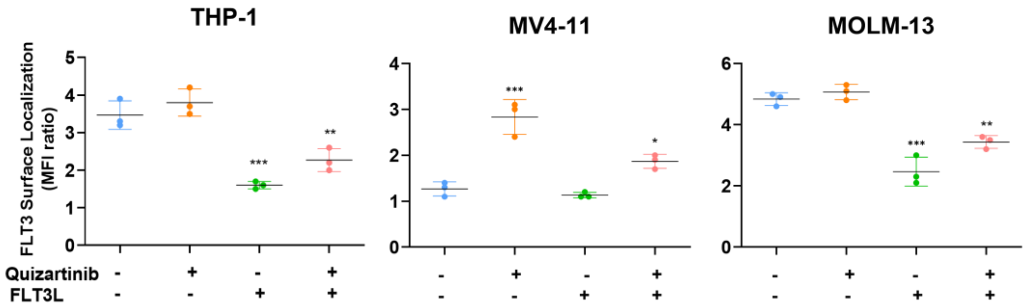

C)

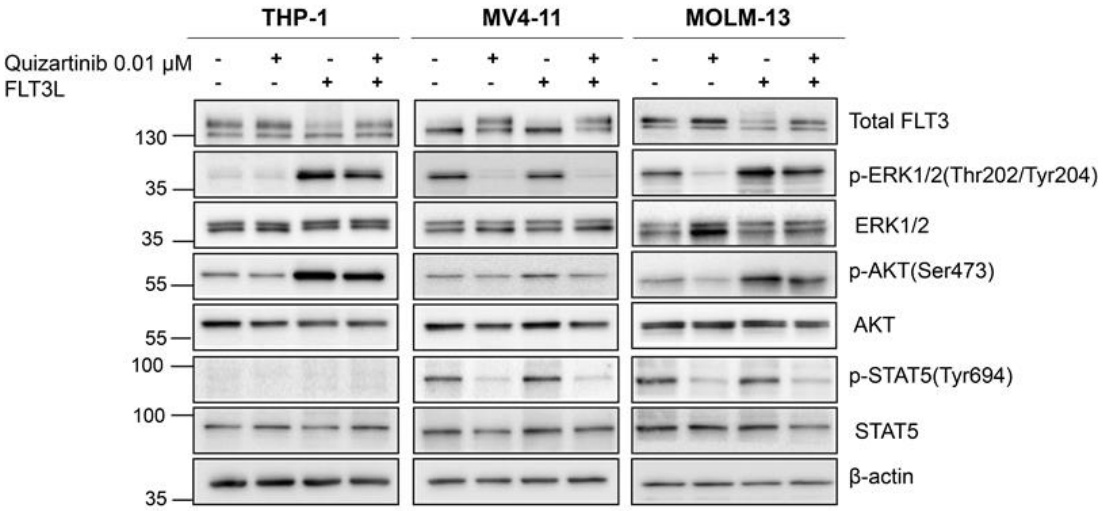

Figure 3.11: FLT3L alters cell surface localisation and signalling of FLT3-ITD – A-B) THP-1, MV4-11, and MOLM-13 cells were treated with quizartinib (10 nM) for 24h before being stimulated with FLT3L (100 ng/ml) for 2 minutes. Cells were stained with anti-CD135-PE to detect FLT3 and IgG-PE as an isotype control. Cell surface FLT3 expression was measured by FACS analysis, and the mean fluorescence intensity plotted. **C)** THP-1, MV4-11, and MOLM-13 cells were treated with quizartinib (10 nM) for 24h. The following day cells were stimulated with FLT3L (100 ng/ml) for 2 minutes. Total cellular protein extracts (20 µg) were separated by 10% SDS-PAGE and subjected to immunoblot analysis with phospho- STAT5, -AKT, -ERK1/2, and their unphosphorylated forms. β-actin was included as a loading control. Results represent the mean +/- SEM for 3 independent experiments. Significance testing was done by one-way ANOVA with Dunnette's multiple comparison test (n=3), **P ≤0.05, **P ≤0.01 and ***P ≤0.001* shows statistical significant difference versus untreated cells.

3.2.10 Short term FLT3L treatment cannot rescue quizartinib inhibition of homozygous FLT3-ITD

In the previous result, FLT3L (2 minutes) stimulation of MV4-11 pre-treated with quizartinib caused the decrease in cell surface ITD-FLT3 but did not rescue signalling as was observed in the MOLM-13s. MV4-11 cells have constitutive, basal activation of FLT3 and quizartinib appears to inhibit signalling, in part, by increasing the surface localisation of fully glycosylated ITD-FLT3. To further study this, MV4-11s were treated with quizartinib (10 nM, 24 h) a concentration that has been previously shown in to increase the surface localised ITD-FLT3 (Fig 3.10) followed by a “wash-out” to remove unbound drug. Results showed that re-localisation of ITD-FLT3 induced by quizartinib remained unchanged and only STAT5 phosphorylation was partially restored. This is indicative that the binding of quizartinib to ITD is irreversible. We then wished to see whether FLT3L (2-10 minutes stimulation) could restore signalling following “wash-out”, as these cells would have cell surface ITD-FLT3 available for ligand binding. This treatment failed to restore signalling indicating that the surface re-localisation and kinase activity inhibition is not affected by FLT3L after quizartinib “wash out”. However, restoration of STAT5 activation following quizartinib “wash out” could be the de novo synthesis. This suggests a mechanism by which STAT5 inhibition is a result of a shift in ITD-FLT3 localisation from an intracellular space to the plasma membrane (Fig 3.12). The concentration of TKIs and the number of washing steps could affect the accumulation of TKIs inside the cell as described by (Lipka et al., 2016). Therefore, this experiment can done thoroughly in the future using multiple concentrations and washing procedure.

A)

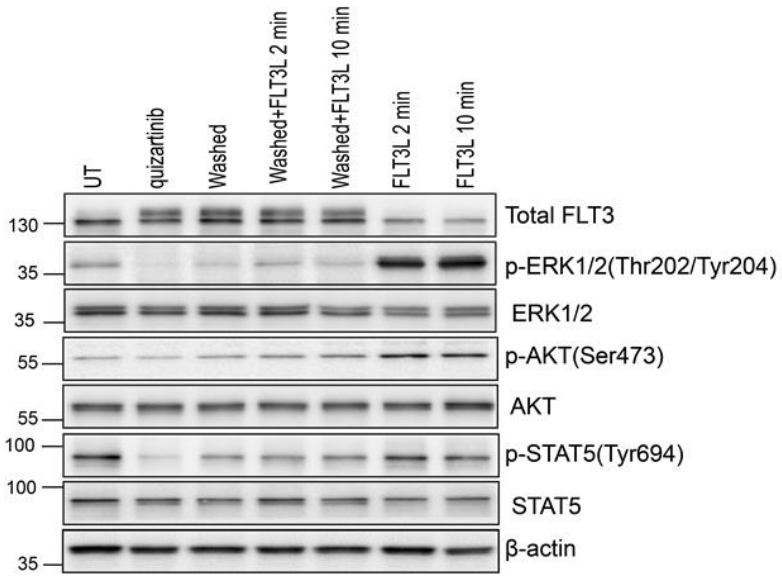
UT
quizartinib
Washed
Washed+FLT3L 2 min
Washed+FLT3L 10 min
FLT3L 2 min
FLT3L 10 min
130
Total FLT3
35
p-ERK1/2(Thr202/Tyr204)
35
ERK1/2
55
p-AKT(Ser473)
55
AKT
100
p-STAT5(Tyr694)
100
STAT5
35
β-actin

B)

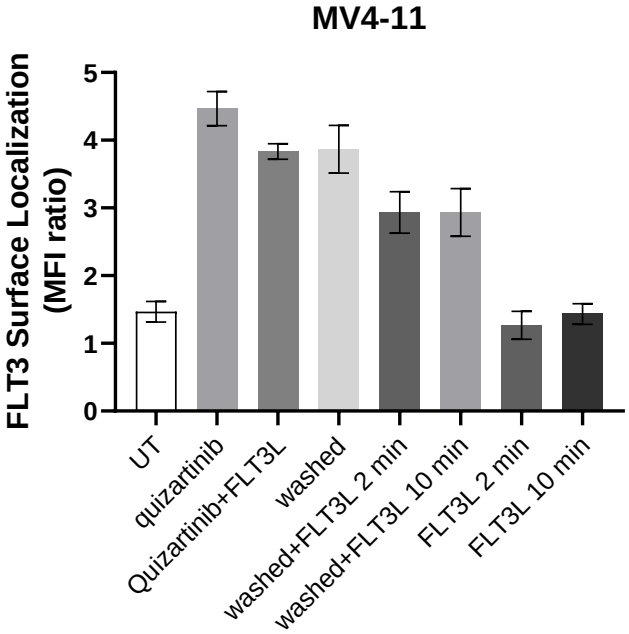
MV4-11
FLT3 Surface Localization (MFI ratio)
0
1
2
3
4
5
UT
quizartinib
Quizartinib+FLT3L
washed
washed+FLT3L 2 min
washed+FLT3L 10 min
FLT3L 2 min
FLT3L 10 min

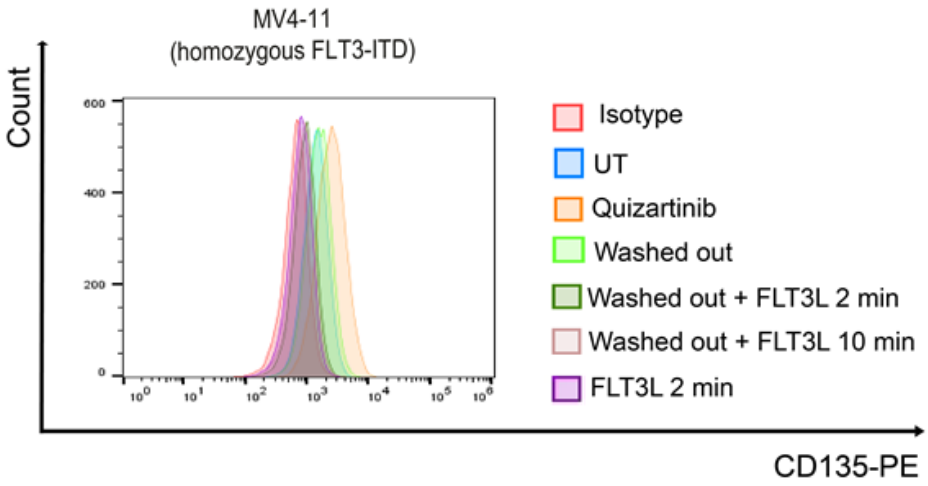

Figure 3.12: FLT3L cannot restore FLT3 inactivation by quizartinib – A) MV4-11 cells were treated with 10 nM quizartinib for 24h. The following day, the cells were washed and incubated in fresh media for 3h followed by treatment with FLT3L (100 ng/ml) for indicated times. Total cellular protein extracts were separated by 10% SDS-PAGE and subjected to immunoblot analysis with antibodies against known FLT3 signalling intermediates; phospho-STAT5, -AKT, -ERK1/2. β-actin was included as a loading control. **B)** MV4-11 cells were treated with 10 nM of quizartinib for 24h and then cells were washed and left untreated for the indicated times followed by treatment with FLT3L for 2 and 10 minutes. Cells were stained with anti-CD-135-PE and an isotype control IgG-PE and analysed for cell surface FLT3 expression by FACS analysis. The mean fluorescence intensity (MFI) was plotted and results represent the mean +/- SEM of 2 independent experiments.

3.2.11 Quizartinib cannot restore FLT3L-mediated reduction in surface localisation of FLT3 in THP-1 cells

Quizartinib leads to a redistribution and increase in cell surface localisation of FLT3 both in MV4-11 and MOLM-13 but not THP-1 cells whose FLT3 is almost exclusively at the cell surface (Fig 3.5D). Unlike the ITD-expressing cells, THP-1 cells lack any FLT3 mutations and therefore require exogenous ligand to activate the receptor. We next wanted to examine if quizartinib had any effect

on WT-FLT3 localisation in the THP-1 cells. As expected, treatment with quizartinib for 24h did not affect surface localisation of FLT3. To induce FLT3 internalization, THP-1 cells were treated with FLT3L for 10 minutes, this resulted in a large decrease in cell surface FLT3 staining (Fig 3.13). Pretreatment of cells for 10 minutes with FLT3L prior to quizartinib treatment for 24h failed to restore surface FLT3 localisation indicating that quizartinib can only affect FLT3-ITD localisation and not FLT3L internalized WT-FLT3.

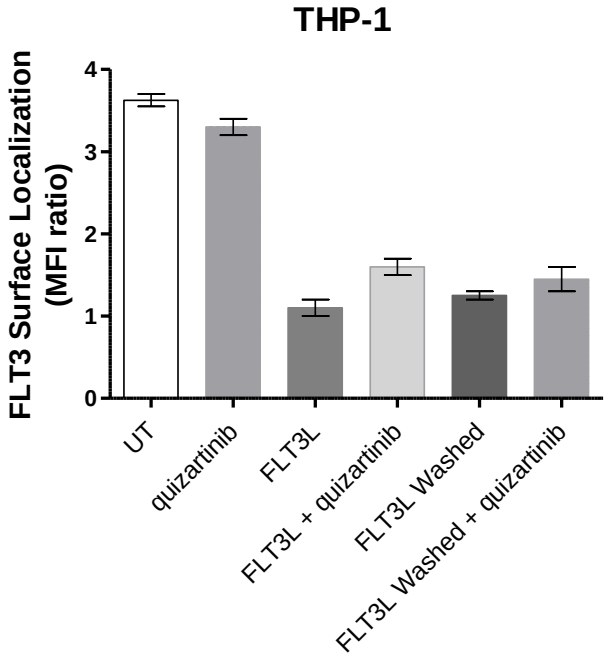

Figure 3.13: Quizartinib cannot restore FLT3 surface localisation in THP-1 cells following FLT3L – THP-1 cells were treated with quizartinib (10 nM) for 24h or FLT3L for 10 minutes. Cells also treated with FLT3L for 10 minutes followed by quizartinib treatment for 24h. The cells also stimulated with FLT3L for 10 minutes and washed by PBS prior to re-suspending in fresh growth medium and left untreated or treated with quizartinib for 24h. Cells were stained with anti-CD-135-PE and IgG-PE antibodies to detect FLT3 and isotype control, respectively. Cells were analysed for cell surface FLT3 expression by FACS analysis, and the mean fluorescence intensity (MFI) was plotted. Results represent the mean +/- SEM for 2 independent experiments.

3.3 Discussion

The FLT3 receptor has been reported to be mutated in around 30% of AML patients (Kiyoi et al., 1998b). The most common FLT3 mutations are internal tandem duplications, which result in a constitutive activation of the receptor and are associated with an adverse impact on disease progression and overall survival (Kottaridis et al., 2001). For this reason, targeting FLT3 is one of the most recent strategies to treat AML. In order to compare the impact of different FLT3 genotypes on the therapeutic response to FLT3 kinase inhibitors, we investigated the functional aspects of targeting multiple FLT3 mutational genotypes; wild-type, homozygous, heterozygous, and FLT3-negative in AML cell lines. As this project was focused on the signalling of FLT3 and its mutant form ITD, We wished to characterize our cells model as it's important for all further work in this thesis.

We first genotyped four common AML cell lines and confirmed ITD mutations in two of them by Sanger sequencing. Mutations in the MV4-11 and MOLM-13 cells were both in Exon 14 in the juxtamembrane region but were not equivalent, one being a homozygous 30bp insertion (MV4-11), the other a 21bp heterozygous insertion (MOLM-13s). We next confirmed FLT3 localisation, expression, and mRNA level in our model lines; U937 (FLT3-negative), THP-1 (WT-FLT3), MV4-11 and MOLM-13 (ITD-FLT3). FLT3 mRNA was detected in the cell lines but transcript expression was much higher in the ITD expressing cells (MV4-11 and MOLM-13) than the wild-type THP-1 cells. The U937 cells did not express any FLT3 protein or mRNA and therefore acted as a FLT3-negative control line.

Midostaurin (PKC412) and quizartinib (AC220) are examples of first and second generations FLT3 inhibitors, respectively. We analysed their activity using flow cytometry protocol involves the use of fluorescein isothiocyanate (FITC)-conjugated Annexin V and PI staining, a gold standard technique for apoptosis measurements and more accurate than MTT or cell count techniques (Schutte et al., 1998). Midostaurin is a pan-kinase inhibitor and has been approved to treat newly diagnosed, FLT3-mutated AML patients, in combination with standard chemotherapy (Stone et al., 2005). As midostaurin is not selective for just FLT3, all AML cells were highly sensitive. Quizartinib is currently in phase III clinical trials to treat relapsed/refractory patients expressing FLT3-ITD. Only the MV4-11 and MOLM-13 cells with ITD were sensitive to quizartinib and unlike midostaurin, the drug did not induce cytotoxicity in the FLT3-negative U937 or the WT-FLT3 THP-1 cell lines. Quizartinib induced cell cycle arrest in ITD-expressing cells and inhibited proliferation. We were able to track proliferation even when cells have only 20% viability. This was done by gating on the viable cell population using CFSE staining, which originally developed to track lymphocyte migration studies (Weston and Parish, 1990) then start to be used in *Vitro* and in *Vivo* studies (Marchesi et al., 2004, Jetani et al., 2018). The proliferation of quizartinib treated cells at 72h was markedly decreased compared to untreated cells, however, this still has implications for the cell's response to FLT3L and the resistance seen in AML patients. Even though the cell cycle analysis using PI was an indicative of cell cycle arrest, the interpretation would be improved by using two parameter such as (Hoechst vs PI) (Kim and Sederstrom, 2015).

In the model we used sensitive to TKI treatment and this may be related to various factors including; the length and location of ITD insertion (21bp vs 30bp in MV4-11), the different genetic background with gene fusions MLL-MLLT3; MLL-AF9 vs MLL-AFF1; ALL-1/AF4 in MV4-11 We also know that MOLM-13 has both ITD and WT alleles and so there is the possibility that heterogeneity in receptor composition (WT/WT, ITD/ITD or ITD/WT) may also influence signalling and sensitivity of the cells to the inhibitors. As a result, it would be expected to see variation in response to treatment among AML cell lines due to individual cell-specific factors and this would be interesting to address in future studies.

The results also confirmed that quizartinib is highly selective against FLT3-ITD–mutated AML cells as all downstream signalling was inhibited following treatment. Given the selectivity of quizartinib, this confirms that the basal activation of ERK1/2, AKT and STAT5 observed is through the constitutively active ITD-FLT3expressed in these cells. This is further reinforced with observations in the THP-1 (inactive WT-FLT3 and U937s (FLT3-expression-negative) which were resistant to quizartinib. Although these cells have high basal activation levels of AKT and ERK1/2 (two pathways activated by FLT3) they must be activated by additional factors in these cells. It has been reported that quizartinib inhibits KIT and PDGFR, and this activity explains its effects on cell lines with genetic alterations of KIT and PDGFR such as the FLT3-WT cell lines Kasumi-1 (Heterozygous for KIT) and EOL-1 (Gene fusion FIP1L1-PDGFRA) (Kampa-Schittenhelm et al., 2013). As THP-1 and U937 cells don't carry KIT or PDGFR mutations, but PTEN, TP53 and NRAS genetic

alterations, it would be of interest to study in future the effect of FLT3L and quizartinib in FLT3-WT cell lines with KIT and PDGFR genetic alteration and compare that to our model in this project.

An additional aspect of FLT3 expression regulation is glycosylation status and subcellular localisation which we looked at using Western blotting and FACS analysis. It was crucial for us to determine the different localisation of wild-type FLT3 and FLT3 ITD in human AML cell lines. This has been reported previously using murine myeloid progenitor cell line, 32D and homozygous ITD (Choudhary et al., 2009a). We took this further by using wild-type FLT3 and heterozygous FLT3 mutation cells along with other cells and also looked into mRNA, surface and total FLT3 expression and how this could affect the responsiveness of cells to kinase inhibition with or without FLT3L stimulation which may improve our understanding of FLT3 signalling. Different maturation status of FLT3 has been previously reported, partially glycosylated FLT3 species at 130 kDa and the fully glycosylated mature form at 160 kDa (Schmidt-Arras et al., 2005). This is particularly important concept when study any receptor tyrosine kinases (RTKs). The constitutively active RTKs including FLT3, Stem-cell factor receptor (c-Kit), fibroblast growth factor receptor 3 (FGFR3) and others are recognized as an active in a ligand-independent manner, and impaired in the normal processing of RTKs N-glycosylation lead to mislocalised subcellular localisation and subsequent aberrant signalling (Lievens et al., 2006, Tabone-Eglinger et al., 2008). In our cells model, two glycosylated forms were detected in THP-1 and MOLM-13, while MV4-11 expressed only the partially glycosylated form. We noted that a strong signal

for 130 kDa-sized FLT3 protein that could be detected in FLT3-ITD expressing cells (MV4-11 and MOLM-13) compared to WT-FLT3 cells (THP-1). We also employed the flow cytometry to evaluate the cell surface localisation of FLT3 using CD135 antibody conjugated to phycoerythrin (PE), and WT-FLT3 and FLT3-ITD expressing cells exhibited different cell surface expression levels with the WT cells being higher than those containing ITD mutations. Therefore, the lower surface level of FLT3 in MV4-11 is a consequence of different cellular distribution rather than transcript or protein expression differences. Indeed, MV4-11 has more mRNA level than THP-1 and upon permeabilization the surface FLT3 level was increased dramatically. This may has an implication in drug resistance as the ITD receptor can be traffic to the cell surface as a result of kinase inhibition.

Physiologically, FLT3 is normally expressed at low levels in hematopoietic progenitor cells (Rosnet et al., 1996b). In AML patients, in addition to being mutated, the leukemic cells frequently overexpress FLT3 with 90% of the patients found to have overexpressed the FLT3 receptor (Carow et al., 1996, Rosnet et al., 1996b). FLT3 activity depends on the binding of FLT3L, which is not exclusively expressed in hematopoietic cells, rather it is expressed in a variety of tissues (Brasel et al., 1995, Meierhoff et al., 1995). Together, these observations suggest that the expression level and localisation of mutated or wild-type FLT3, and the FLT3L can influence the development of AML. We showed that the capacity for further stimulation of ITD-FLT3 by FLT3L was directly proportional to the presence of cell surface FLT3. In fact, a study suggests that FLT3 mutations result in differential subcellular localisation of

the receptor as explained by (Köthe et al., 2013), in which K-Ras and N-Ras are equally activated by ligand stimulation of WT-FLT3 and ITD can mediate Ras activation at the surface level but not the mislocalised intracellular pool of ITD and this ultimately lead to cell transformation. We were interested to investigate the possible variation of signalling network in response to FLT3L. WT-FLT3 (THP-1) was mainly located on the cell surface and showed a strong response to FLT3L. By contrast, FLT3 in ITD expressing cells (MV4-11 and MOLM-13) was mainly retained intracellularly and this resulted in a weaker response to FLT3L. As has been reported before constitutive activation of STAT5 by FLT3-ITD in MV4-11 and MOLM-13 cells occurred is independent of FLT3L. Many studies have provided insights into intracellular signalling pathways mediated by the FLT3, but only few studies pay attention to the differential response of differing FLT3 genotypes to FLT3L (Rosnet et al., 1996a, Steelman et al., 2008). Additionally, FLT3 signalling in ITD-expressing cells have been reported in the literature mainly looking at signalling in a ligand independent manner (Choudhary et al., 2005). As FLT3 mutations appear exclusively in intracellular domains it is conceivable that the extracellular domain remains available for FLT3L binding or sequestration. One group has shown that the mutated FLT3 can be further activated by treatment with FLT3L which led to a slight increase in phosphorylation of STAT5 and AKT but not MAPK in MV4-11s, whereas, in BaF3/ITD cells only MAPK was affected (Zheng et al., 2011). This work has shed a light in the possibility of activation of FLT3-ITD by exogenous ligand. We explored this idea further using a time course of ligand treatment as well as different cells expressing different FLT3 genotypes. Following stimulation with FLT3L, we observed that AKT and

ERK1/2 are signalling pathways of the membrane-bound WT-FLT3 (THP-1). We also found that the surface-bound FLT3-ITD is required for the full activation of AKT and ERK1/2 but not STAT5 in FLT3-ITD mutant cell lines. However, this was not the case with ITD in all experiments we have done as for example in Fig 3.11C we didn't observe activation of ERK1/2 upon ligand stimulation but in Fig 3.8B it does. The basal level of ERK1/2 or AKT phosphorylation in MV4-11 cells (ITD) could affect the final activation of these kinases by ligand stimulation. We observed that in case if the cells presented with high basal level of ERK1/2 or AKT phosphorylation, the cells most likely won't response to 2-10 minutes FLT3L stimulation. On the other hand, THP-1 and MOLM-13 cells were always sensitive to FLT3L and further activation of ERK1/2 or AKT were presented in all experiments. Our result was in agreement with what it has been reported previously that STAT5 activation occurs with the ITD variant but not ligand stimulated WT receptor and in an intracellular compartment, as STAT5 was exclusively activated by ITD, in which the majority of receptor is localized intracellularly (Zhang and Broxmeyer, 2000, Choudhary et al., 2007, Choudhary et al., 2005). This particularly has been studied in AML patient's samples as the work done by Seedhouse and Cao et al groups. (Seedhouse et al., 2009, Cao et al., 2019), or in 32D and BaF3 with FLT3-ITD construct and has been linked to the transforming potential of leukemogenesis (Mizuki et al., 2000, Spiekermann et al., 2003b). In the model we used, STAT5 was only phosphorylated in ITD expressing cells but not in FLT3-WT like THP-1 cells even though the cells has high level of total STAT5. One possible explanation of this was explained by Rocnik et al as STAT5 activation is a consequence of ITD mutation. The

finding suggest that disruption of juxtamembrane structure by ITD lead to expose of two candidate STAT5 SH2 docking phosphorylation sites (Y589 and Y591) and allowed activation of STAT5 (Rocnik et al., 2006). Our work also indicated that STAT5 does not response to stimulation by FLT3L at detectable levels by immunoblotting in both wild-type and ITD receptor, at least in the cell lines we used, and that STAT5 may not be regulated by surface localised FLT3.

The wide range of signalling responses to FLT3 ligand in MV4-11 versus the consistent response in THP-1 or MOLM-13 observed in this chapter highlighted the crucial concept of AML molecular heterogeneity and how this underlie the various response to FLT3 stimulation and ultimately management and clinical outcome of AML patients. The different observations between our work and Zheng et al group could explain the importance of studying ITD response to FLT3L and how this might change the sensitivity of AML cells to kinase inhibition. One of the limitation of signalling results in this chapter is that we used a semi-quantitative approach (immunoblotting), and given the important of the signalling in a diseases like AML it's crucial to employ more sensitive proteomic platforms to analyse the biologic complexity of FLT3 signalling in response to FLT3L.

The exact mechanism by which inefficient glycosylation of FLT3 occurred is yet unknown. However, a work led by Schmidt-Arras and his group indicate that the inefficient maturation of FLT-3 ITD and as a result it's low surface localisation caused by the constitutive kinase activity of the receptor itself

(Schmidt-Arras et al., 2005). The next logical question is that what happen if the receptor exposed to kinase inhibition, is that going to change the localisation from intracellular compartments to cell surface?. This was presented as an observation during several previous studies (Yee et al., 2002, Scheijen et al., 2004), but not until a recent work ,published while we are investigating the effect of kinase inhibition, showed that tyrosine kinase inhibition increases the cell surface localization of FLT3-ITD and taking the advantage of this phenomenon by employing FLT3-directed immunotherapy as a result of upregulation of the FLT3 target antigen caused by TKIs (Reiter et al., 2018).

We next looked into this as if we re-localised FLT3-ITD or WT-FLT3 by TKIs or FLT3L using different FLT3 genotypes, what are the possible consequences of FLT3L stimulation on surface FLT3 level and also on the downstream cascades. We were interested on how the different pools of FLT3 (both the intracellular and the plasma membrane forms) will react to the kinase inhibition and subsequently FLT3L stimulation. That’s to our knowledge has not been studied before. The change in cell surface localisation of FLT3 in non-permeabilized cells after treatment with quizartinib was tested at several time points. MV4-11 and MOLM-13 showed an increased cell surface localisation following FLT3 inhibition. This increase may be due to an increase in FLT3 expression or possibly the binding of quizartinib to the cytosolic portion of FLT3-ITD facilitates glycosylation resulting in increased trafficking to the plasma membrane. This effect was not seen with the Type I inhibitor, midostaurin, which did not affect FLT3 surface localisation in any of the cells

but could block signalling. This data suggest a mechanism by which quizartinib induces cytotoxicity through FLT3-ITD by promoting cell surface localisation of FLT3 in the MV4-11 and MOLM-13 cells and accompanied by inhibition of FLT3 signalling. The regulation of signal transduction relies on the receptor localisation and expression. It is well documented that FLT3-ITD is largely retained in the ER and causes constitutive activation and phosphorylation of the receptor (Schmidt-Arras et al., 2009a). Because quizartinib facilitates full glycosylation of FLT3 and trafficking to the plasma membrane, we investigated the consequences of changes in FLT3-ITD localisation in the MV4-11 and MOLM-13 cells induced by quizartinib but also in the presence of ligand. We also studied the effect of FLT3L and quizartinib in the activation of ERK1/2, AKT and STAT5, the main representative proteins of FLT3 signalling cascade.

In THP-1 and MOLM-13s, the cell surface localisation is reduced following treatment with FLT3L, which is indicative of ligand-induced receptor internalization and recycling as seen with other RTKs such as c-KIT (Blume-Jensen et al., 1991). However, there was no changes in MV4-11s, presumably as these cells have a homozygous ITD mutation leading to the receptor residing almost exclusively inside the cells. In THP-1 and MOLM-13 which express WT-FLT3, ERK1/2 and AKT were activated upon stimulation with FLT3L; however, this effect was hardly observed in MV4-11s which exhibited constitutive ERK1/2 and AKT activation. Since quizartinib has no effect on THP-1 cells, ERK1/2 and AKT activation were sustained by FLT3L. Short term FLT3L stimulation (2 minutes) to quizartinib pre-treated MOLM-13s and MV4-11s lead to decrease in the surface localised FLT3 when compared to

quizartinib only treated condition, yet restoration of ERK1/2 and AKT activation only observed in MOLM-13s but not MV4-11s. MOLM-13 cell harbours a heterozygous ITD mutation and therefore still expresses WT-FLT3 which can be activated by the ligand. This data and in consistent with published data suggests that the phosphorylation of ERK1/2 and AKT is driven mainly from the activation of WT-FLT3 expressed on the cell surface and not the intracellular ITD form. It also shows the disparity between the homozygous and heterozygous ITD mutations. It is also tell us that FLT3L is able to induce both surface bound-ITD and WT-FLT3 internalization, even though the internalization of FLT3 was more efficient with WT form. Several studies described that only the ER localised FLT3-ITD can activate STAT5 (Yoshimoto et al., 2009). As expected, STAT5 in ITD cells does not respond to FLT3L, and its phosphorylation was inhibited by quizartinib treatment.

Of note, most studies examining FLT3-ITD in cell lines, have introduced the FLT3 mutations into BaF3 or 32D cells (Mizuki et al., 2000, Tse et al., 2000). These models do have the benefit of expressing ITD mutations on the same cellular background, making delineation of signalling events attributed to FLT3 and ITD signalling much easier. They also have their drawbacks as they are based on overexpressed receptors and even when stably expressed, depending on the promoter of the plasmid, used they will have much higher expression than endogenous. This may lead to a different data interpretation when compare to AML cell lines as in Zheng et al work that discussed above. They are also of murine origin, may contain murine FLT3 and this could potentially heterodimerise with the human receptor or bind the human ligand

this is in addition to containing their own unique genetic background of mutations that could similarly affect FLT3 signalling. Although the human and murine FLT3 is highly conserved, some studies have indicated that there are potentially biologic differences in downstream signalling pathways for instance (Zhang and Broxmeyer, 2000, Beslu et al., 1996). Both are IL-3 dependent, which amongst other pathways strongly activates STAT5 and therefore they require starvation prior to experimentation. IL-3 withdrawal induces apoptosis in both lines so getting the balance between starvation to reduce signalling, but not initiate early apoptosis, whose cleavage events can start hours before any common markers (Annexin V staining) are seen, can make interpretation difficult. ITD expression is also sufficient to transform these cells which is different to the action of FLT3 in AML in humans as additional mutations are required (Mizuki et al., 2000). This may be due to expression levels as mentioned above. On the other hand, the genetic background is more complicated in human AML cell lines and the ITD mutation usually occurs with other molecular abnormalities. In the context of our project, the expression of human FLT3 in a murine cellular context may not represent the molecular biology of FLT3 in a human leukemic cell. We therefore believed that using human AML cell lines that have naturally occurring FLT3-ITD mutations for signalling study could represent the significant of AML heterogeneity status as appeared in patients. Accordingly, using cell models of chronic myelogenous leukaemia (CML) have been essential for better understanding the biology of the diseases and led to advancement in therapeutic approaches like imatinib, the most commonly used TKI for CML (Druker et al., 1996).

Collectively, changes in the subcellular localisation of FLT3 induced by quizartinib and FLT3L impacts the function of FLT3 and downstream signalling. We showed that FLT3L can promote ITD activation of its signalling (ERK1/2 and AKT), and also that the ligand can bind to and internalize the replenished cell surface receptor pool following TKI treatment In the MOLM-13s, ERK1/2 and AKT signalling was restored meaning the WT receptor must be available for signalling and as quizartinib has no effect on this form, FLT3L would act to promote proliferation in quizartinib-treated patients with heterozygous ITD/WT mutations. This can be utilized more to further clarify the different biological response of FLT3 mutants and WT forms and suggests new avenues for therapeutic approaches to treat ITD-mutated AML. The second-generation inhibitor, quizartinib had a greater effect on cell surface re-localisation than multi-kinase inhibitors such as midostaurin. In this context, second generation ITD inhibitors may show reduced efficacy in ITD mutation (homozygous or heterozygous) positive patients when these patients also present with high serum levels of FLT3L. The disparities in response to TKIs and FLT3L reinforce the importance of assessing the modulation of intracellular signalling and also to characterize the biology of individual AML patents in the context of genetic alterations for the best prognostic outcome. Overall, these data suggest that FLT3L is able to act on both WT- and ITD-FLT3, possibly contributing to drug resistance in AML. In next chapter we will be looking to possible resistance mechanisms induced by FLT3L in both homozygous and heterozygous ITD cells.

Chapter IV

==========

Investigating the mechanism of resistance to quizartinib mediated by FLT3-ligand

4.1 Introduction

FMS-like Tyrosine Receptor 3 (FLT3) plays a critical role in the differentiation and survival of hematopoietic stem cells in bone marrow. An internal tandem duplication (ITD) in the juxtamembrane domain of FLT3 is an important driver mutation in AML and has been reported in approximately 25-30% of patients. The prognosis for AML patients with this mutation, particularly those who have lost the wild-type (WT) allele, is far worse than patients possessing only the WT receptor (Whitman et al., 2001).

FLT3L exists as a transmembrane homodimer consisting of two short chain α-helical bundles. FLT3L is constitutively made by fibroblasts and endothelial cells, and is abundantly expressed in most human tissues, including the bone marrow and peripheral blood. As FLT3 expression is mainly restricted to early progenitor cells and FLT3L expression is relatively ubiquitous, FLT3 signalling is dictated more by the presence of FLT3 rather than FLT3L (Matthews et al., 1991).

FLT3 resides in an inactive state at the cell membrane as a result of the autoinhibitory conformation of the JM domain. Binding of FLT3L to inactive FLT3 induces receptor homodimerization to produce the active dimer form and stabilizing the receptor in an open conformation (Turner et al., 1996). This then promotes auto-phosphorylation of the receptor at several locations.

ITD mutations disrupt the autoinhibitory activity of the JM domain and stabilize the receptor in the ‘open,’ ATP-binding conformation resulting in ligand-independent, constitutive dimerization and activation of the FLT3 signal transduction cascade (Kiyoi et al., 2002). Whereas, normal FLT3 activation requires binding of FLT3L, and the ITD mutants are constitutively active despite this exogenous FLT3L can also further activate both homozygous and heterozygous ITD to different extents as we previously showed.

The biological and clinical significance of mutated FLT3 in leukaemia makes it a promising avenue for the treatment of patients with FLT3 mutations. For this reason, several selective FLT3 inhibitors have been developed; including the first-generation multi-targeted kinase inhibitors, such as midostaurin, sunitinib and lestaurtinib, and more selective second-generation kinase inhibitors, such as quizartinib, gilteritinib and crenolanib (Larrosa-Garcia and Baer, 2017, Garcia and Stone, 2017). Despite promising responses in preclinical models, most of the clinical trials using FLT3 inhibitors as single agents or in combination with conventional cytotoxic chemotherapies have not been completely successful (Weisberg et al., 2010).

Several mechanisms of resistance have been identified which negatively impact inhibitor efficacy compromising FLT3-targeted therapeutic strategies. One such mechanism in refractory AML patients is treatment-induced elevation of plasma levels of FLT3L that appear to antagonise the efficacy of the FLT3 inhibitors (Levis et al., 2011).

4.1.1 Aims

It has been reported that following chemotherapy or FLT3 inhibitor treatment many AML patients are found to express increasing serum levels of FLT3L (Sato et al., 2011, Levis et al., 2011). Given most FLT3-ITD mutations are heterozygous many cells are likely to express one wild-type copy of the FLT3 gene that would respond to FLT3L. FLT3L-FLT3 responses are known to have a proliferative effect on cells, however the effect of FLT3L on the inhibitory action of quizartinib is unclear.

The aim of this chapter is to discover the mechanism by which FLT3L may cause resistance to FLT3 inhibitors. We will also uncover how the FLT3 genotype might play a role in the observed resistance to FLT3 inhibition. Resulting future strategies to overcome the effect of FLT3L on FLT3 inhibition will also be discussed and developed.

4.2 Results

4.2.1 Effect of FLT3-ligand on quizartinib-induced apoptosis in FLT3-ITD AML cells

FLT3L is constitutively expressed in the bone marrow, whether a cell is affected depends on its FLT3 expression. FLT3L-FLT3 interactions are known to have a proliferative effect on early hematopoietic progenitor cells, dendritic cells and NK cells (McKenna et al., 2000). Pathologically, an increase in FLT3L as a cellular response to chemotherapy, FLT3 inhibitors or BH3 mimetics has been reported as a cause of resistance to FLT3-targeted therapy (Zhou et al., 2009, Stölzel et al., 2010). We first tested the effect of FLT3L on quizartinib treatment in different FLT3-ITD–mutated cells (homozygous and heterozygous ITD). MV4-11 and MOLM-13 were used as we have previously shown that these cells are sensitive to FLT3-ITD inhibition.

Cells were treated with quizartinib (0.1 µM) in the presence or absence of FLT3L (100 ng/ml) for 48h and the effect on cell death measured using Annexin V staining. Quizartinib alone induced about 32% and 49% apoptosis in MV4-11 and MOLM-13 cells respectively. Co-treatment with both quizartinib and FLT3L resulted in a significant reduction in apoptosis by 30% in MOLM-13 compare to 11% in MV4-11 cells (Fig 4.1A).

Treatment with increasing concentrations of quizartinib (0.01-10 µM) resulted in an increase in the cell death that was reduced in the presence of FLT3L (Fig 4.1B). The IC50 of quizartinib against homozygous ITD MV4-11 cells was 31 nM compared with 97 nM in the presence of exogenous FLT3L.

In heterozygous ITD-expressing MOLM-13 cells the protective effect of FLT3L was more pronounced as the IC50 increased from 6 nM to 49 nM (Table 4.1).

Table 4.1 – IC50 of quizartinib on ITD expressing cells

Cell line and Cytogenetics	compound	IC50 (72h)
MV4-11(FLT3-ITD$^{+/+}$)	Quizartinib	31 nM
	Quizartinib + FLT3L	97 nM
MOLM-13 (FLT3-ITD$^{-/+}$)	Quizartinib	6 nM
	Quizartinib + FLT3L	49 nM

To determine whether the concentration of FLT3L used was important, cells were treated with a fixed concentration of quizartinib (0.1 µM) in the presence of increasing concentrations of FLT3L. Reduction of quizartinib-induced cytotoxicity by FLT3L did not vary significantly between FLT3L doses ranging from 5-100 ng/ml. The largest inhibition was observed at 100 ng/ml and therefore this was used for subsequent experiments (Fig 4.1C). Time course analysis indicated that co-treatment of 0.1 µM quizartinib and 100 ng/ml FLT3L resulted in a significant reduction in cell death when compared with quizartinib treated cells. This effect was more pronounced in the MOLM-13s compare to MV4-11s which is likely due to the association of exogenous FLT3L with the WT-FLT3 on the cell surface in these cells (Fig 4.1D).

Next, we wanted to assess whether FLT3L can have a similar inhibitory effect on the multi-kinase inhibitors, (which can inhibit WT-FLT3 in addition to ITD-FLT3). To explore this further, MV4-11, MOLM-13 and THP-1 cells were treated with different FLT3 inhibitors including midostaurin, gilteritinib, and sorafenib. Midostaurin and sorafenib are classified as first-generation inhibitors, whereas gilteritinib is a second-generation FLT3 inhibitor like quizartinib.

We have previously shown that quizartinib is selective for ITD-FLT3 and consequently has no effect on cells expressing WT-FLT3 alone or on FLT3L signalling in these cells. Midostaurin, however, has similar potency against WT and ITD (Figs 3.2). To test the response of FLT3 mutational status to sorafenib and gilteritinib, we first measured apoptosis induction by these inhibitors in the absence of ligand (Appendix Fig A1). Results show that sorafenib has more selectivity towards ITD-FLT3 as in THP-1s, no significant apoptosis was observed with up to 10 µM sorafenib. Gilteritinib inhibit both ITD and WT with more selectivity against ITD.

Unlike with quizartinib (Appendix Fig A2), the addition of FLT3L was unable to rescue midostaurin and gilteritinib treated cells, however, the FLT3L reduces the cytotoxicity of sorafenib (Fig 4.1E). The IC50 of all four inhibitors in the presence of FLT3L is summarized in (Fig 4.1F).

A)

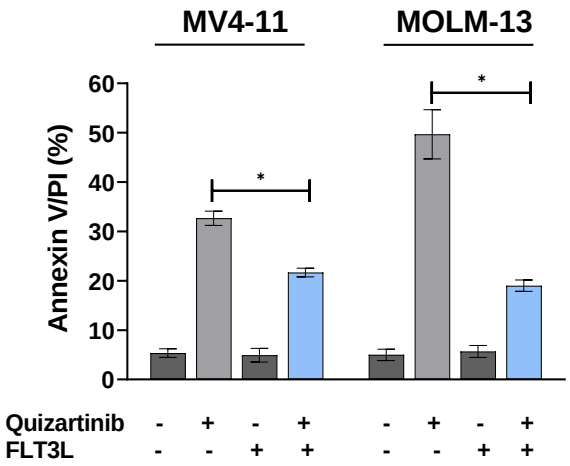
MV4-11
MOLM-13
Annexin V/PI (%)
60
50
40
30
20
10
0
*
*
Quizartinib - + - + - + - +
FLT3L - - + + - - + +

B)

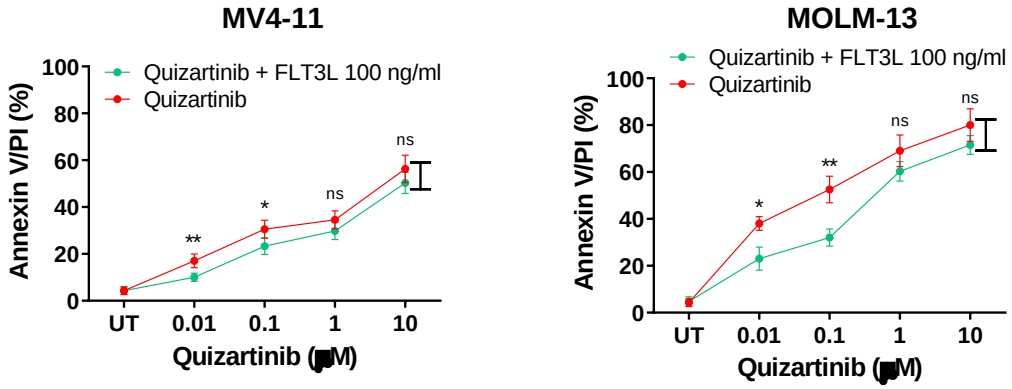
MV4-11
Quizartinib + FLT3L 100 ng/ml
Quizartinib
Annexin V/PI (%)
100
80
60
40
20
0
**
*
ns
ns
UT
0.01
0.1
1
10
Quizartinib (μM)
MOLM-13
Quizartinib + FLT3L 100 ng/ml
Quizartinib
Annexin V/PI (%)
*
**
ns
ns
UT
0.01
0.1
1
10
Quizartinib (μM)

C)

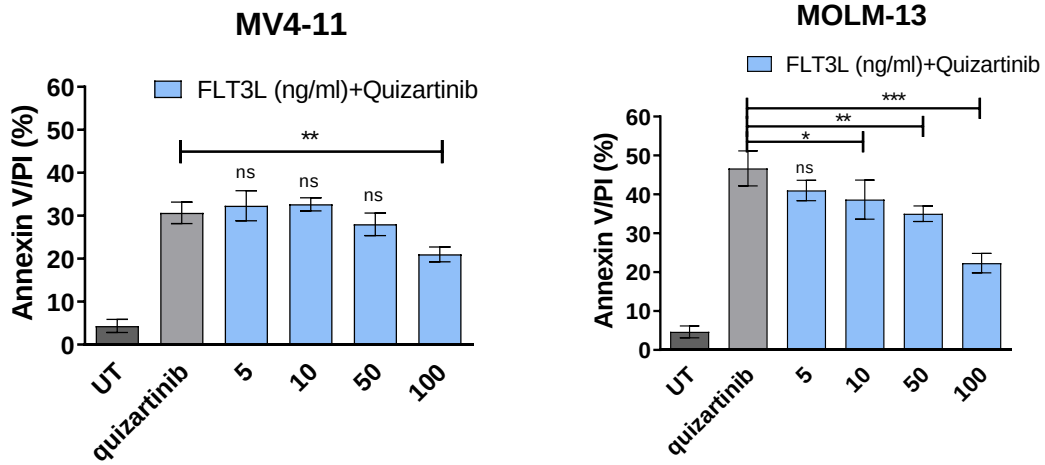
MV4-11
FLT3L (ng/ml)+Quizartinib
Annexin V/PI (%)
60
50
40
30
20
10
0
**
ns
ns
ns
UT
quizartinib
5
10
50
100
MOLM-13
FLT3L (ng/ml)+Quizartinib
***
**
*
ns
Annexin V/PI (%)
UT
quizartinib
5
10
50
100

D)

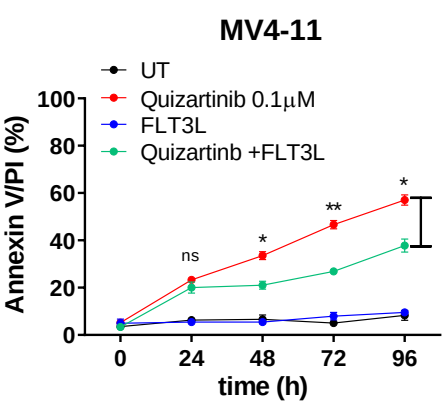
MV4-11
UT
Quizartinib 0.1μM
FLT3L
Quizartinb +FLT3L
Annexin V/PI (%)
100
80
60
40
20
0
0
24
48
72
96
time (h)
ns
*
**
*

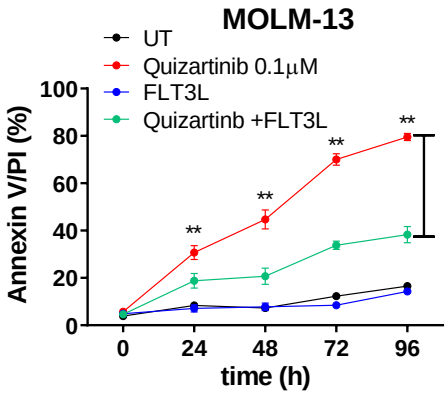
MOLM-13
UT
Quizartinib 0.1μM
FLT3L
Quizartinb +FLT3L
Annexin V/PI (%)
100
80
60
40
20
0
0
24
48
72
96
time (h)
**
**
**
**

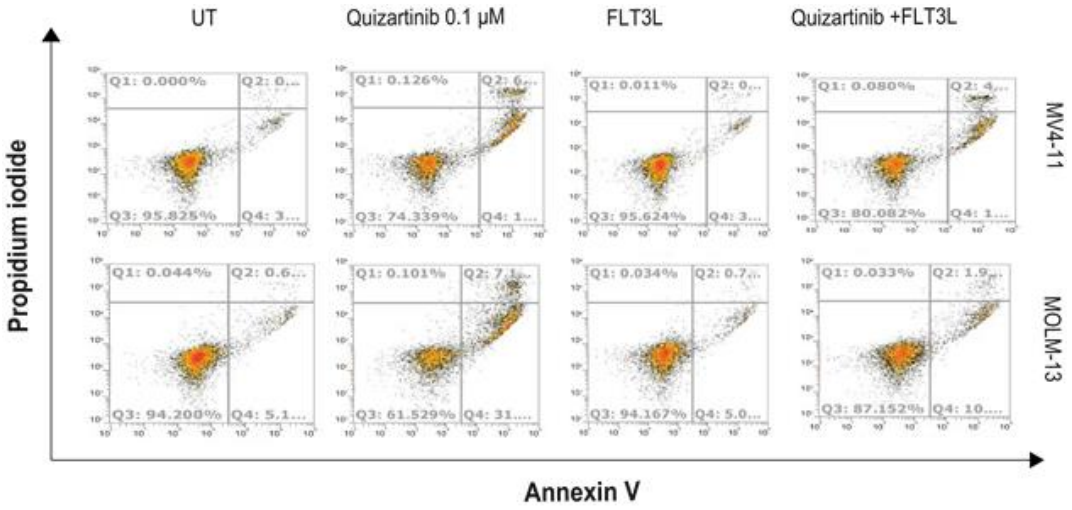
UT
Quizartinib 0.1 μM
FLT3L
Quizartinib +FLT3L
Propidium iodide
Annexin V
MV4-11
MOLM-13
Q1: 0.000%
Q3: 95.825%
Q1: 0.126%
Q3: 74.339%
Q1: 0.011%
Q3: 95.624%
Q1: 0.080%
Q3: 80.082%
Q1: 0.044%
Q3: 94.200%
Q1: 0.101%
Q3: 61.529%
Q1: 0.034%
Q3: 94.167%
Q1: 0.033%
Q3: 87.152%

E)

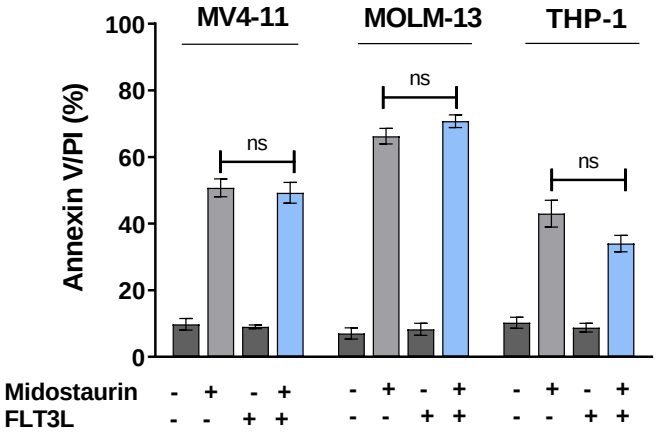
MV4-11
MOLM-13
THP-1
Annexin V/PI (%)
100
80
60
40
20
0
ns
ns
ns
Midostaurin - + - + - + - + - + - +
FLT3L - - + + - - + + - - + +

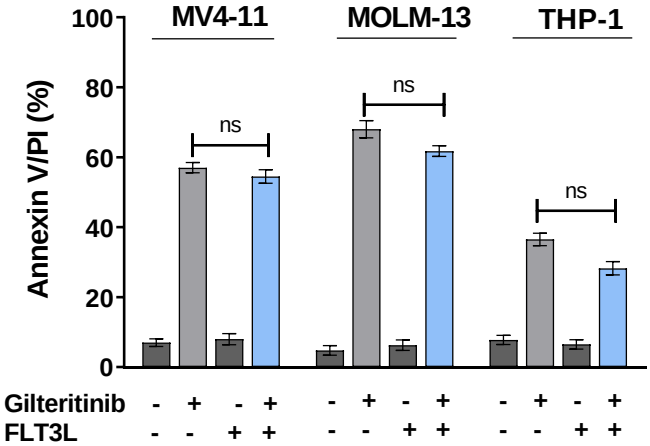
MV4-11
MOLM-13
THP-1
Annexin V/PI (%)
100
80
60
40
20
0
ns
ns
ns
Gilteritinib - + - + - + - + - + - +
FLT3L - - + + - - + + - - + +

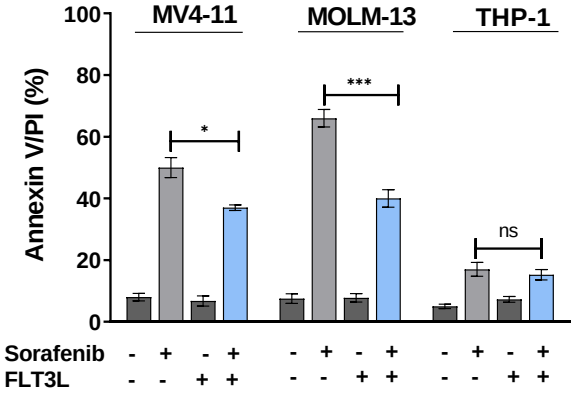
MV4-11
MOLM-13
THP-1
Annexin V/PI (%)
100
80
60
40
20
0
*
***
ns
Sorafenib - + - + - + - + - + - +
FLT3L - - + + - - + + - - + +

F)

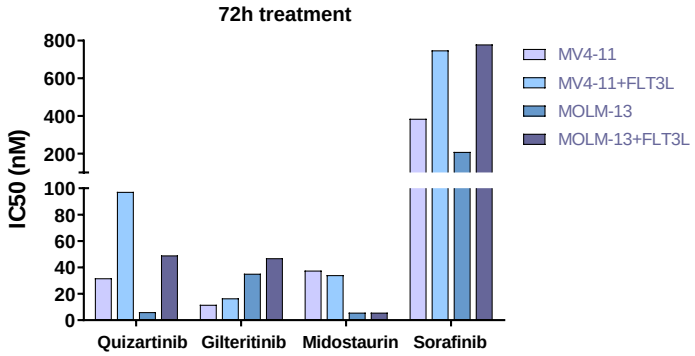

Figure 4.1: Effect of FLT3L on apoptosis induction by FLT3 inhibitors in FLT3-ITD expressing cells – A) MV4-11 and MOLM-13 cells were treated with quizartinib (0.1 µM) in the presence of FLT3L (100 ng/ml) for 48h following which apoptosis was assessed by Annexin V/PI staining. **B)** Cells were exposed for 48h to the indicated concentrations of quizartinib in combination with FLT3L (100 ng/ml) and cell death measured by flow cytometry. **C)** Cells were treated with increasing concentrations of FLT3L in combination with quizartinib (0.1 µM) for 48h after which apoptosis measured using Annexin V/PI staining. Results represent the mean +/- SEM for 3 independent experiments. Significance testing was done by one-way ANOVA with Dunnette's multiple comparison test (n=3), *$P \leq 0.05$, **$P \leq 0.01$ *and* ***$P \leq 0.001$. **D)** Cells were treated with quizartinib (0.1 µM) and/or FLT3L (100 ng/ml) for indicated times and assessed by AV/PI. Scatter plots are representative of cells after 48h treatment). **E)** MV4-11, MOLM-13, and THP-1 were treated with midostaurin (0.1 µM), gilteritinib (0.1 µM), sorafenib (1 µM) in the presence of FLT3L (100 ng/ml) for 72h. Apoptosis was measured at indicated times using Annexin V/PI. Significance testing was done by two-tailed paired *t*-test (n=5),*$P \leq 0.05$, **$P \leq 0.01$, ***$p \leq 0.001$ and *ns, not significant.* Results represent the mean +/- SEM for 5 independent experiments. **F)** IC50 of FLT3 inhibitors against AML cells in the presence of/absence of FLT3L.

4.2.2 Effect of FLT3-ligand on proliferation of quizartinib treated ITD expressing cells

To further investigate the mechanism by which FLT3L can impair the efficacy of ITD inhibition, we treated MV4-11 and MOLM-13 cells with quizartinib and analysed cell survival and proliferation following quizartinib treatment in the presence of FLT3L. Survival assays performed by counting viable cell numbers demonstrated that exogenous FLT3L promoted the survival of quizartinib treated cells. MOLM-13s, in particular, exhibited significant protection when cultured in the presence of FLT3L. These data are consistent with previous results suggesting that FLT3L can contribute to resistance to FLT3 inhibition by prolonging the survival of cells expressing ITD-FLT3 in the presence of quizartinib (Fig 4.2A).

Proliferation is a critical process for the maintenance and progression of cancer. We measured the effect of quizartinib combined with FLT3L on proliferation of the AML cells using a CFSE dilution assay monitored by flow cytometry. In untreated cells the fluorescence intensity of CFSE was reduced in both cell lines in a time-dependent manner. This indicated the cells were proliferating normally as the concentration of the dye, and hence the fluorescence, reduces with each division.

In the presence of quizartinib, the loss of fluorescence was markedly slowed indicating that proliferation was reduced in these cells. Co-treatment with quizartinib and FLT3L did not appear to alter proliferation compared to

quizartinib treatment alone indicating that FLT3L did not reverse the decrease in proliferation caused by quizartinib (Fig 4.2B).

A)

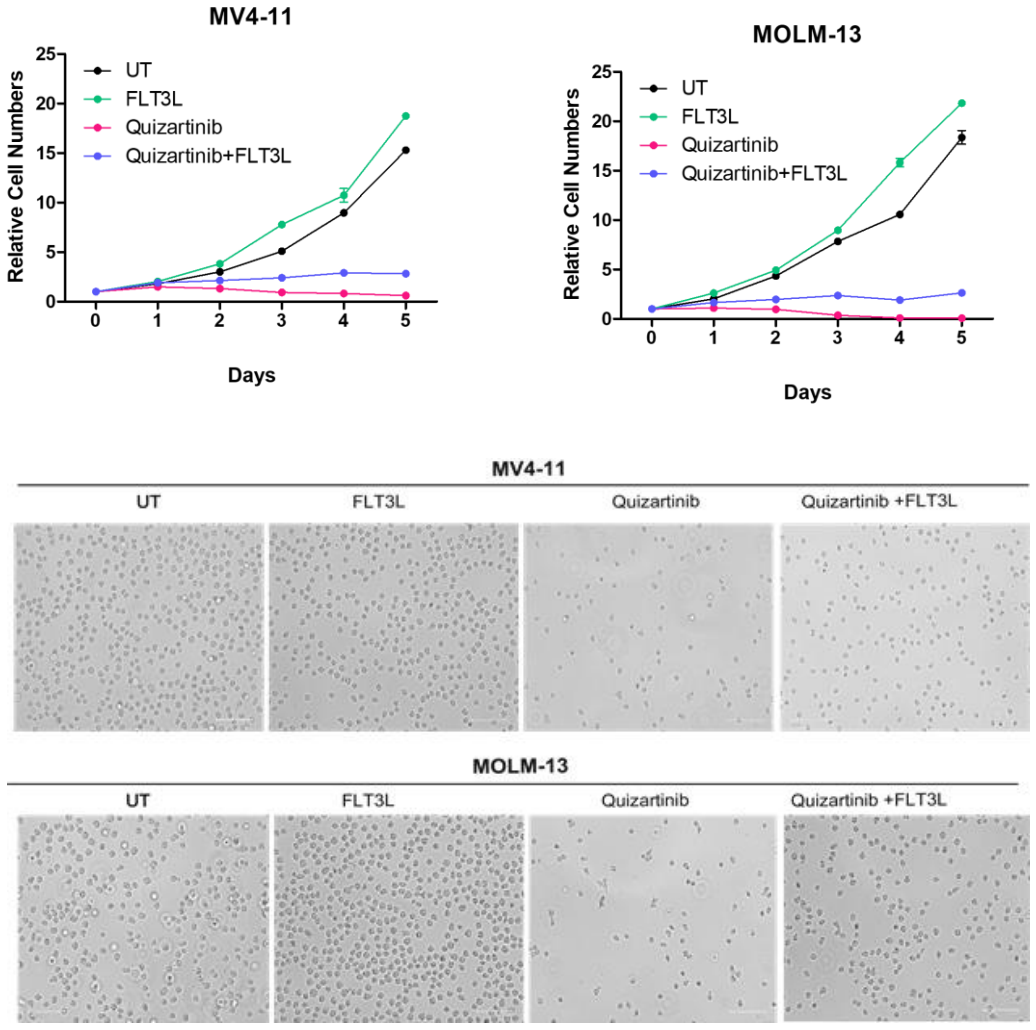

B)

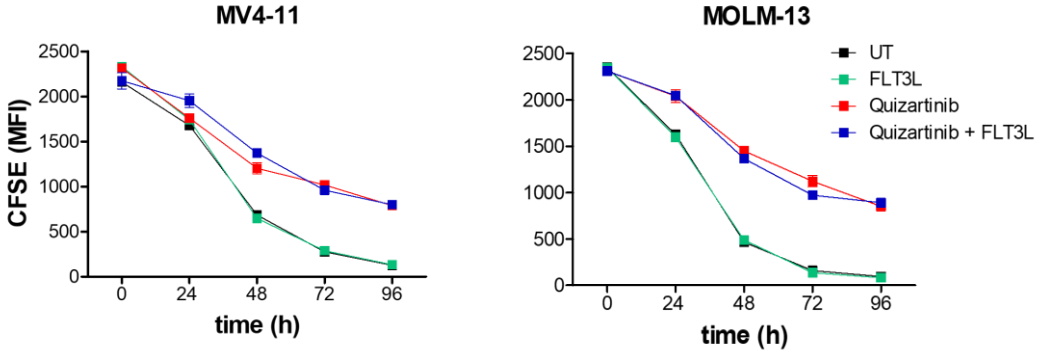

Figure 4.2: Effect of FLT3-ligand on proliferation of FLT3-ITD expressing cells – MV4-11 and MOLM-13 cells were treated with quizartinib (0.1 μM) in the presence of FLT3L (100 ng/ml) for indicated times. **A)** Cell numbers were assessed by trypan blue exclusion assay. **B)** Proliferation was measured using CFSE staining. CFSE results are expressed as mean fluorescence intensity (MFI). Results represent the mean +/- SEM of 3 independent experiments.

4.2.3 Effect of FLT3-ligand and quizartinib on cell cycle progression in FLT3-ITD expressing cells

We next looked at the effects quizartinib and FLT3L had on cell cycle progression in the ITD-expressing AML cells. Cell cycle analysis was performed on treated and fixed cells using propidium iodide staining followed by flow cytometry. MV4-11 and MOLM-13 cells were treated with quizartinib (0.1 μM) or FLT3L (100 ng/ml) or a combination of both for 48-72h following which cell cycle distribution was analysed (Fig 4.3).

As the result shown in previous chapter, 24h treatment with quizartinib alone resulted in G0/G1 cell cycle arrest. Here we presented the result of 48-72h as we started to see the effect of FLT3L on quizartinib. In both cell lines the increase in the sub-G1 population likely representing cells undergoing apoptosis. As was observed previously the MOLM-13 cells appeared more sensitive. Co-treatment of the cells with FLT3L and quizartinib for 72h decreased the sub-G1 population. This protective effect was much more pronounced in the MOLM-13s as the sub-G1 peak decreased (from 75 to 16 %) compared to the MV4-11s (from 33 to 26 %) again likely due to the fact that these cells expressing WT as well as ITD-FLT3. These data support previous findings that suggest the role of FLT3L in drug resistance and suggests that

FLT3L expression could be responsible for quizartinib resistance in ITD-expressing cells. FLT3L alone did not affect cell cycle progression in either cell line for all time points used 24 to 72h. Taken together, these data support the previous findings suggesting a role for FLT3L in quizartinib resistance which seems to be mediated through anti-apoptotic effect.

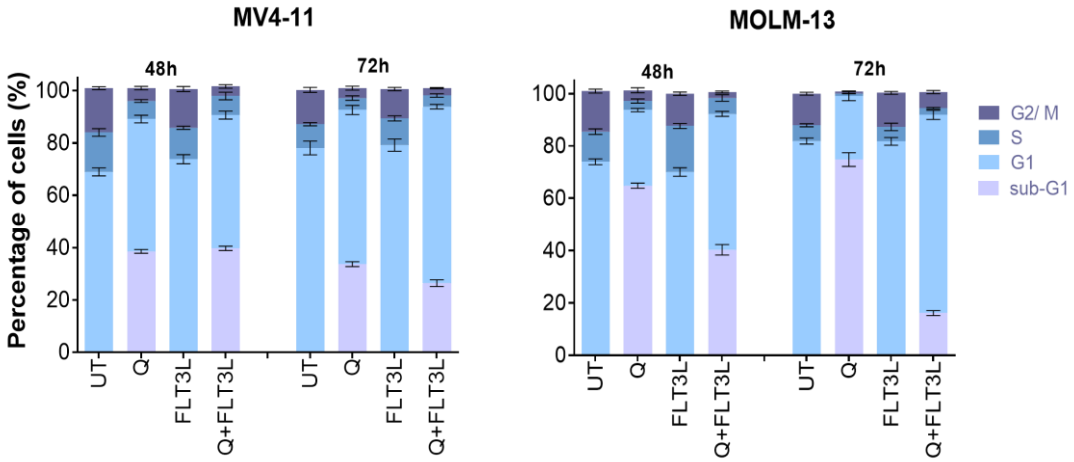

Figure 4.3: FLT3L decreases quizartinib-induced cell cycle arrest in FLT3-ITD$^{-/+}$ cells – MV4-11 and MOLM-13 cells were treated with quizartinib (0.1 µM) in the presence of FLT3L (100 ng/ml) for indicated times. Cell cycle analysis was performed on fixed cells using PI staining followed by flow cytometry. Results represent the mean +/- SEM of 3 independent experiments.

4.2.4 Role FLT3 localisation plays in quizartinib resistance in FLT3-ITD expressing cells

It is known that FLT3 is partially glycosylated in the ER before being transported to the Golgi complex where further modification takes place (Schmidt-Arras et al., 2005). Only the fully glycosylated form is trafficked to the cell surface. We have previously shown that FLT3 is present in the AML cells

in a partially glycosylated form (130 kDa) which represents that residing in an intracellular compartment or as a fully glycosylated form (160 KDa) representing that expressed at the cell surface. We next investigated whether the localisation of these different FLT3 species plays a role in the differential sensitivity observed with quizartinib and the protective effect of FLT3L.

FLT3L can activate WT and ITD-FLT3 at the plasma membrane level, however only the ITD form is potentially active before reaching the cell surface. To investigate if FLT3 cell surface localisation can alter the effect of FLT3L-mediated resistance, cells were treated with either the glycosylation inhibitors, Tunicamycin or Brefeldin A (BFA) which blocks ER to Golgi transport prior to FLT3 inhibition (Helenius and Aebi, 2004).

Tunicamycin inhibits glycosylation at the ER so will impair production of both 130 and 160 kDa forms of the receptor. BFA will inhibit maturation of the receptor from the 130 kDa to the 160 kDa forms in the Golgi. First, we checked the effectiveness of glycosylation inhibition to modulate FLT3 surface localisation and its signalling in our AML cell model. MV4-11 (ITD) and THP-1(WT) cells were treated with BFA or Tunicamycin and the FLT3 signalling analysed by immunoblotting. Both inhibitors resulted in the loss of 130 kDa or 160 kDa FLT3 forms in ITD and WT cells as indicated in total FLT3 blot in Figure 4.4, which indicate the loss of surface localisation of FLT3 as confirmed by FACS in next section Fig 4.5B. However, phosphorylation of ERK1/2 and AKT was inhibited. Notably, in ITD-expressing cells Tunicamycin or BFA appeared to enhance STAT5 phosphorylation.

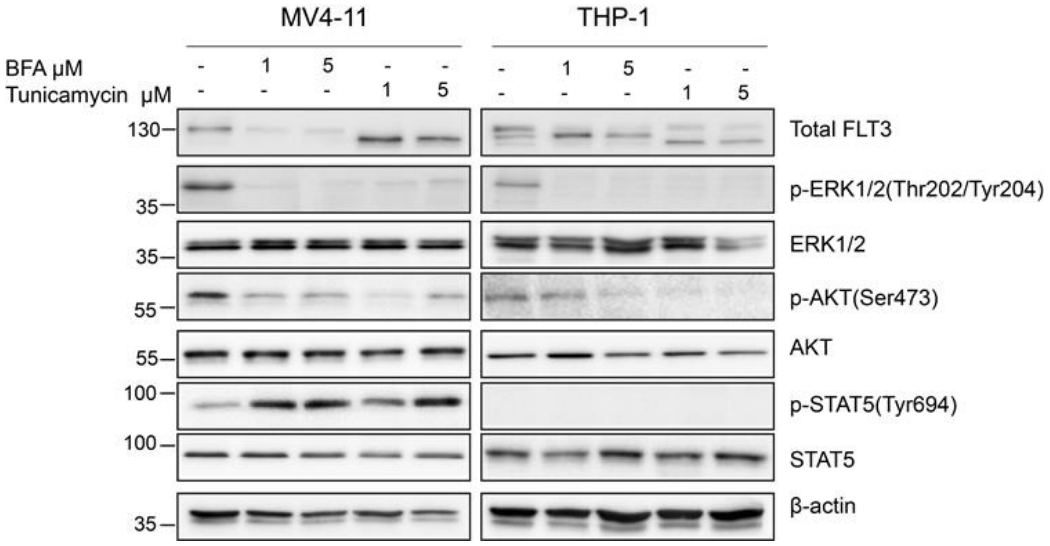

Figure 4.4: Tunicamycin and BFA alter glycosylation state and modulate FLT3 signalling – MV4-11 and THP-1 cells were treated with indicated concentrations of Tunicamycin or BFA for 24h. Total cellular protein extracts were separated by 10% SDS-PAGE and subjected to immunoblot analysis with antibodies against known FLT3 signalling intermediates; phospho-STAT5, -AKT, -ERK1/2, and their unphosphorylated forms. β-actin was used as a loading control. n=1.

Treatment with Tunicamycin or BFA results in ER stress through the accumulation of unfolded proteins in the ER. Therefore, we tested the cytotoxicity of these inhibitors in MV4-11 and MOLM-13 cells and observed a dose and time-dependent induction of cell death with increasing concentrations of both drugs over three-day period (Fig 4.5A).

Flow cytometry results showed that starting from 0.1 µM concentration, brefeldin A and tunicamycin treatment caused a reduction in cell surface FLT3 (CD135) expression, and this was more pronounced in the MOLM-13 cells as we have previously shown that MV4-11 cells have low levels of FLT3 on the

cell surface in untreated cells (Fig 4.5B). Western blot analysis of total FLT3 indicated that tunicamycin lead to the complete inhibition of FLT3 glycosylation and resulted in accumulation of the unglycosylated form (110-120 kDa) (Fig 4.5C). As expected BFA treatment only resulted in inhibition of the fully glycosylated form.

To check whether the inhibition of FLT3 glycosylation and cell surface localisation would prevent the FLT3L induced ERK1/2 and AKT activation, we treat MOLM-13 cells with 0.1 µM BFA in the presence of quizartinib for 24h following by FLT3L stimulation for 2 minutes. Activation of ERK1/2 and AKT by FLT3L was blocked in the presence of BFA (Fig 4.5D). Annexin V/PI staining showed that the reduction in quizartinib-induced apoptosis by FLT3L was also attenuated following BFA or tunicamycin treatment (Fig 4.5E-F). These results indicate that cell surface localisation of FLT3 is crucial for FLT3L to cause resistance to quizartinib. Inhibition of FLT3 trafficking to the cell surface abrogates the protective effect of FLT3L on quizartinib.

A)

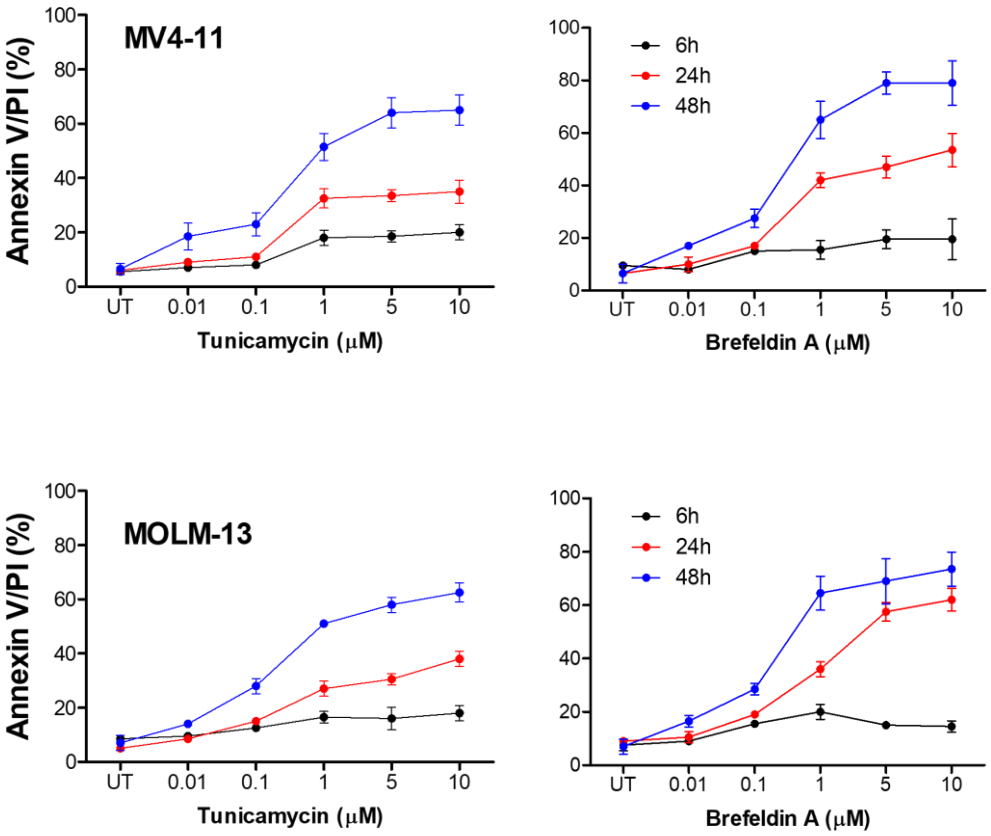
MV4-11
Annexin V/PI (%)
Tunicamycin (μM)
Brefeldin A (μM)
6h
24h
48h
UT
0.01
0.1
1
5
10
MOLM-13

B)

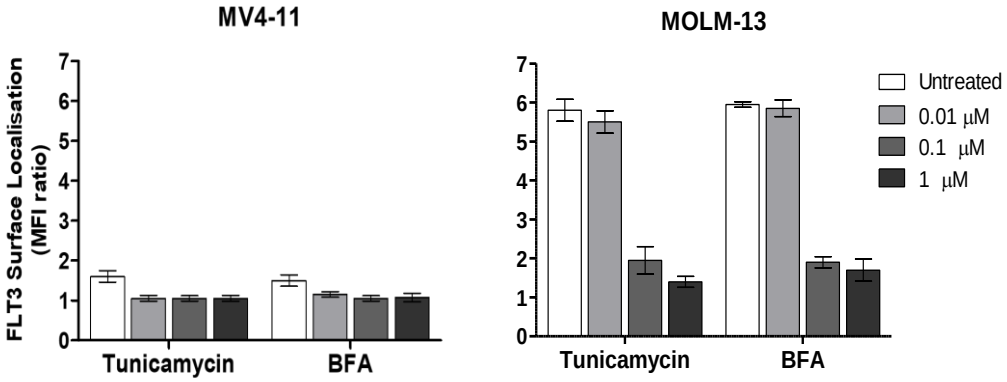
MV4-11
MOLM-13
FLT3 Surface Localisation (MFI ratio)
Tunicamycin
BFA
Untreated
0.01 μM
0.1 μM
1 μM

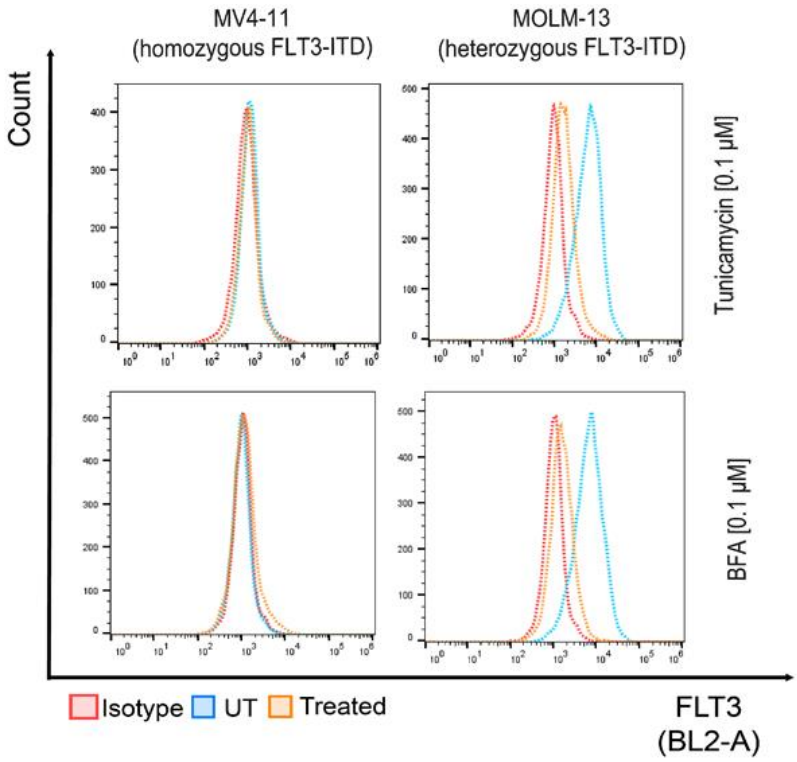
MV4-11
(homozygous FLT3-ITD)
MOLM-13
(heterozygous FLT3-ITD)
Count
Tunicamycin [0.1 µM]
BFA [0.1 µM]
Isotype
UT
Treated
FLT3
(BL2-A)

C)

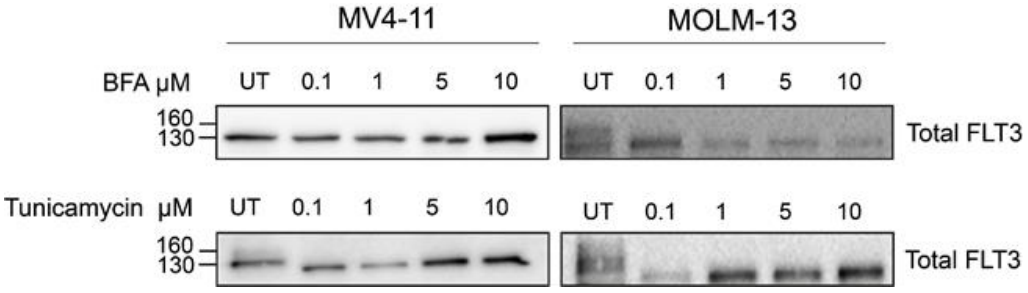
MV4-11
MOLM-13
BFA µM
UT
0.1
1
5
10
160
130
Total FLT3
Tunicamycin µM
UT
0.1
1
5
10
160
130
Total FLT3

D)

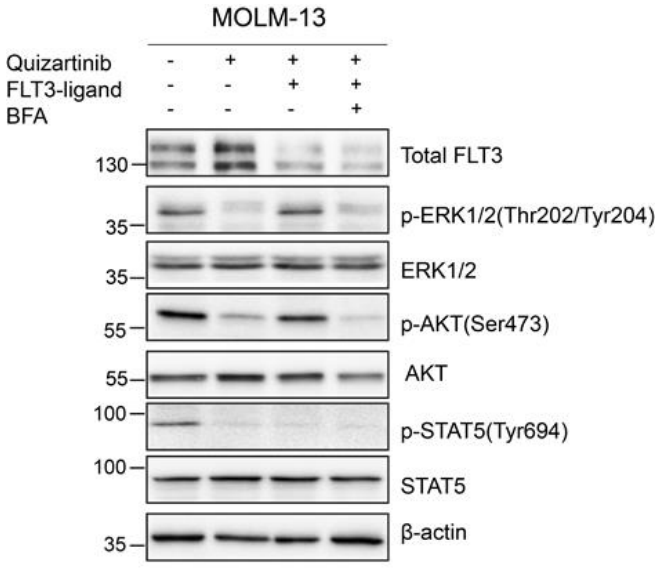
MOLM-13
Quizartinib
FLT3-ligand
BFA
130
Total FLT3
35
p-ERK1/2(Thr202/Tyr204)
35
ERK1/2
55
p-AKT(Ser473)
55
AKT
100
p-STAT5(Tyr694)
100
STAT5
35
β-actin

E)

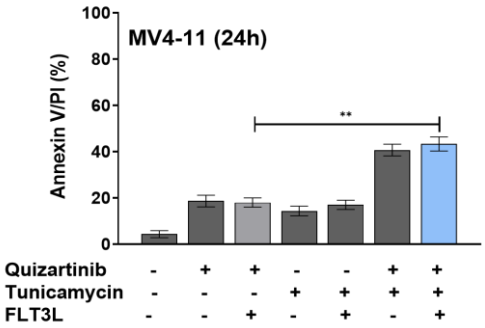
MV4-11 (24h)
Annexin V/PI (%)
100
80
60
40
20
0
**
Quizartinib - + + - - + +
Tunicamycin - - - + + + +
FLT3L - - + - + - +

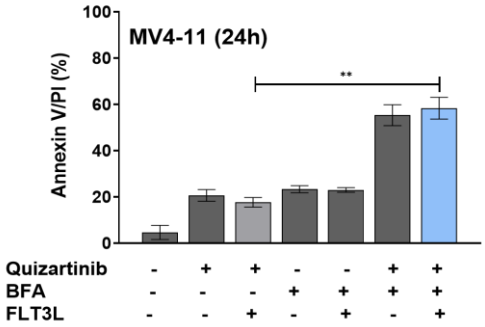
MV4-11 (24h)
Annexin V/PI (%)
100
80
60
40
20
0
**
Quizartinib - + + - - + +
BFA - - - + + + +
FLT3L - - + - + - +

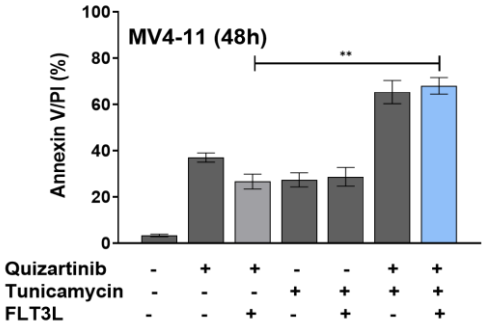
MV4-11 (48h)
Annexin V/PI (%)
100
80
60
40
20
0
**
Quizartinib - + + - - + +
Tunicamycin - - - + + + +
FLT3L - - + - + - +

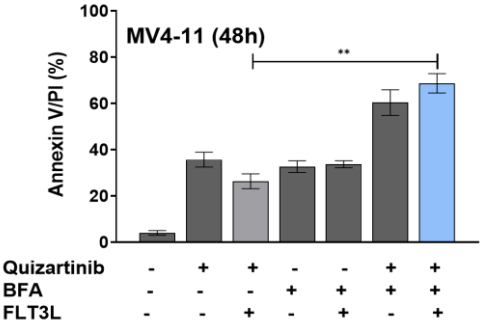
MV4-11 (48h)
Annexin V/PI (%)
100
80
60
40
20
0
**
Quizartinib - + + - - + +
BFA - - - + + + +
FLT3L - - + - + - +

F)

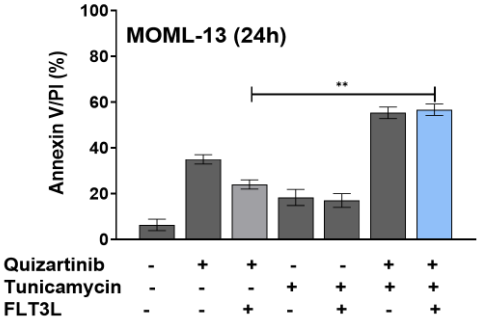
MOML-13 (24h)
Annexin V/PI (%)
100
80
60
40
20
0
**
Quizartinib - + + - - + +
Tunicamycin - - - + + + +
FLT3L - - + - + - +

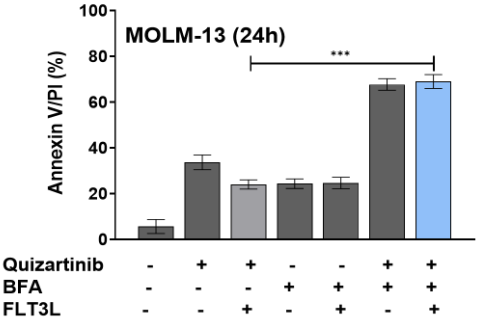
MOLM-13 (24h)
Annexin V/PI (%)
100
80
60
40
20
0
***
Quizartinib - + + - - + +
BFA - - - + + + +
FLT3L - - + - + - +

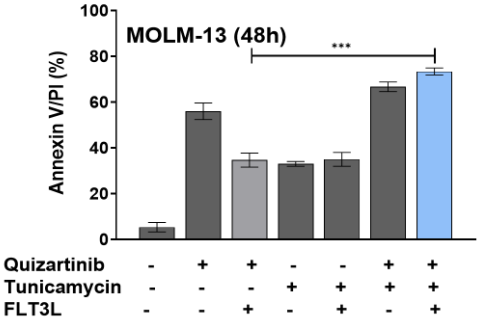
MOLM-13 (48h)
Annexin V/PI (%)
100
80
60
40
20
0
***
Quizartinib - + + - - + +
Tunicamycin - - - + + + +
FLT3L - - + - + - +

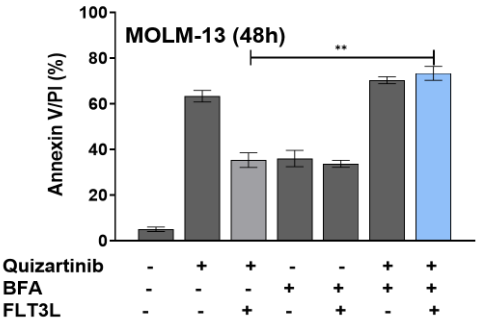
MOLM-13 (48h)
Annexin V/PI (%)
100
80
60
40
20
0
**
Quizartinib - + + - - + +
BFA - - - + + + +
FLT3L - - + - + - +

Figure 4.5: Tunicamycin and BFA abrogates FLT3L protective effect on FLT3 inhibition by quizartinib – A) MV4-11 and MOLM-13 cells were incubated for indicated times with increasing concentrations of Tunicamycin or BFA Following which apoptosis was measured using Annexin V/PI staining. **B)** Cells were treated with increasing concentrations of Tunicamycin or BFA for 12h followed by staining with CD-135-PE (anti-FLT3) or IgG-PE (control) antibodies. Cells were then analysed for cell surface FLT3 expression by flow cytometry, n=2. **C)** MOLM-13 cells were treated with tunicamycin and BFA for 12h and total protein (20 µg) was subjected to immunoblot analysis with a FLT3 antibody. β-actin was used as a loading control. **D)** MOLM-13 cells were treated with BFA (0.1 µM) and quizartinib (0.1 µM) for 24h. Next day, the cells were stimulated with FLT3L (100 ng/ml) for 2 minutes. Total protein extracts were separated by 10% SDS-PAGE and subjected to immunoblot analysis with indicated antibodies. **E-F)** Cells were incubated for 24 and 48h with of Tunicamycin (0.1 µM), BFA (0.1 µM), and quizartinib (0.1 µM) with or without FLT3L as indicated. Apoptosis was measured at indicated times using Annexin V/PI. Significance testing was done by two-tailed paired *t*-test (n=3), ***P ≤ 0.01* and ****p ≤ 0.001.* Results represent the mean +/- SEM for 3 independent experiments.

4.2.5 Role of the Bcl-2 protein family in cell death induced by quizartinib in ITD cells

In many cancer types, the balance between pro- and antiapoptotic Bcl-2 family members is disrupted leading to chemoresistance. To examine the potential role Bcl-2 proteins play in both the cytotoxicity-induced by quizartinib and the protective effect of FLT3L we first looked at their expression in the ITD-expressing cells.

Both cell lines expressed a number of anti-apoptotic proteins including Bcl-2, Bcl-XL and Mcl-1 as well as the pro-apoptotic effector proteins Bak and Bax

(Fig 4.6A-B). Basal levels of Bim, a pro-apoptotic BH3-only protein, were very low in untreated cells. Treatment with quizartinib caused a decrease in Mcl-1 expression in both cell lines but this was more pronounced in the MOLM-13s. Downregulation of Mcl-1 was accompanied by a marked increase in the expression of Bim. No significant change was observed in the other Bcl-2 family proteins following treatment. FLT3L increased Mcl-1 expression in both lines but again levels of the other Bcl-2 proteins remained unchanged. Co-incubation of FLT3L with quizartinib did not affect the MV4-11 cells as Mcl-1 levels were still reduced and Bim levels increased similar to treatment with quizartinib alone. In FLT3L treated MOLM-13s ,however, Mcl-1 levels were slightly higher than in those treated with quizartinib and the increase in Bim observed following FLT3 inhibition was abrogated (Fig 4.6A-B).

A)

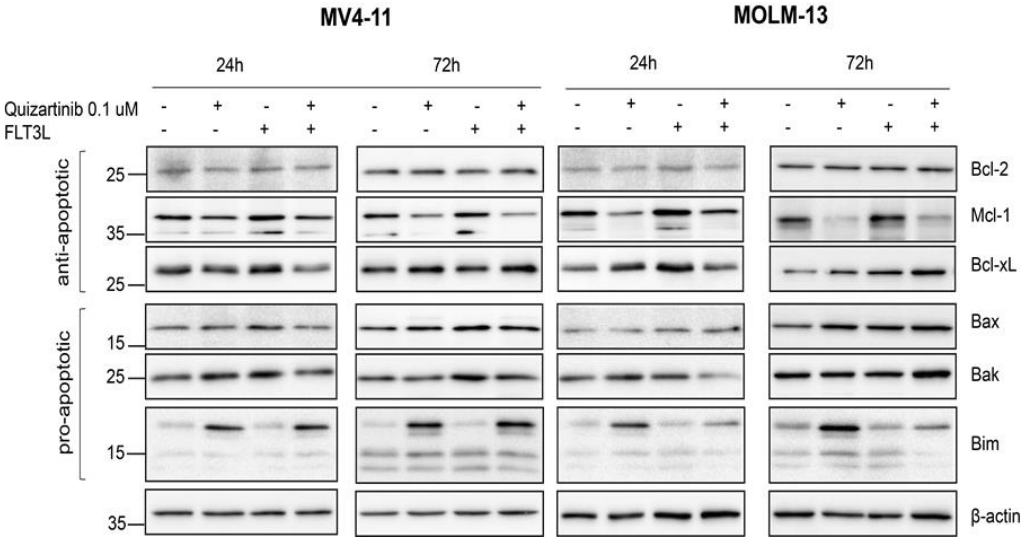

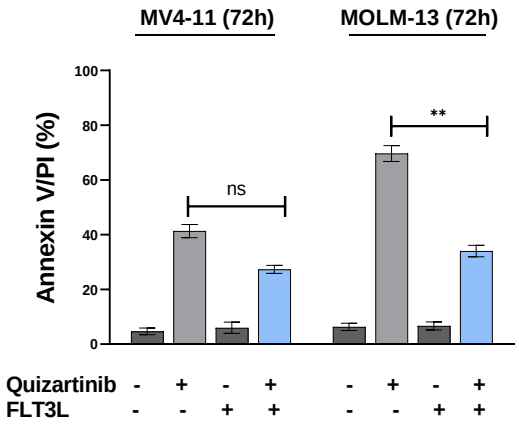

B)

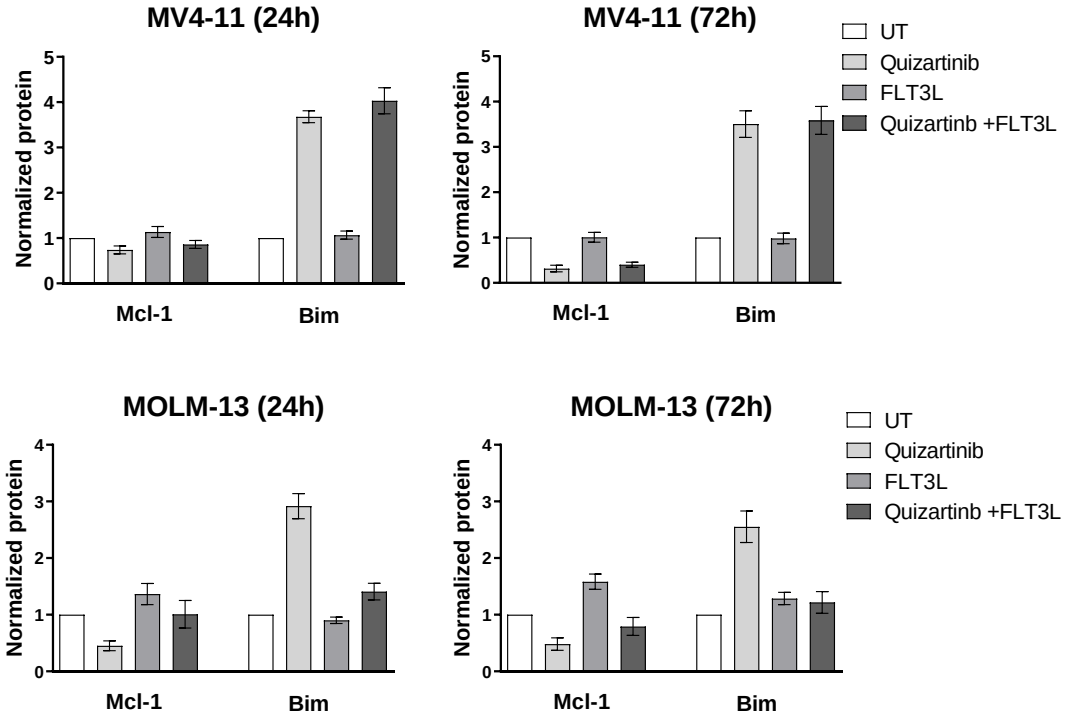

Figure 4.6: Mcl-1 and Bim levels are modulated by FLT3 inhibition and activation – A) MV4-11 and MOLM-13 cell lines were treated with quizartinib (0.1 µM) and/or FLT3L (100 ng/ml) for 24 and 72h, followed by immunoblotting with indicated antibodies. β-actin was used as a loading control. Apoptosis was measured at indicated times using Annexin V/PI. Significance testing was done by two-tailed paired *t*-test (n=3), ***P ≤ 0.01* and *and ns, not significant.* **B)** Densitometric levels of protein bands intensity in (A) was normalized to β-actin then each value was calculated in relative to untreated cells. Results represent the mean +/- SEM for 3 independent experiments.

4.2.6 Role of Mcl-1 in ITD-expressing AML

Down regulation of Mcl-1 with a concomitant upregulation of Bim could potentially be one mechanism through which quizartinib induces apoptosis in ITD-expressing cells. This would mean that FLT3 potentially regulates both Mcl-1 and Bim.

To investigate whether Mcl-1 can be regulated by FLT3 we first analysed its expression in THP-1s and the ITD-expressing AML cell lines. The results indicated that FLT3-ITD cells (MV4-11 and MOLM-13) express high basal levels of Mcl-1 compared to WT-FLT3 cells such as the THP-1s (Fig 4.7A). However, when FLT3 was activated in the THP-1s with FLT3L, we observed a significant upregulation of Mcl-1. This effect was specific to Mcl-1 as no change was observed in Bcl-2 following FLT3L treatment. This indicates that FLT3L can regulate Mcl-1 expression through WT-FLT3 and suggests that the high basal level of expression seen in the MV4-11 and MOLM-13 cells is likely due to the constitutively active ITD-FLT3.

We have previously seen downregulation of Mcl-1 in both ITD-expressing cell lines following ITD inhibition and this could provide a potential mechanism for quizartinib-induced cell death. Upregulation of Mcl-1 could also explain the pronounced protective effect of FLT3L seen in the WT-FLT3-expressing MOLM-13 cells (Fig 4.6). To confirm ITD-regulation of Mcl-1 we used FLT3 siRNA in the MV4-11 and MOLM-13 cell lines. FLT3 siRNA effectively knocked down FLT3 in both cell lines as judged by Western blotting (Fig 4.7B). This was accompanied by a decrease in Mcl-1 levels, again in both cell lines.

Mcl-1, as well as being an antiapoptotic protein is also a caspase substrate during induction of apoptosis, and therefore the possibility exists that the downregulation seen following ITD inhibition or FLT3 siRNA was a consequence of cell death rather than direct downregulation through FLT3 signalling pathways.

To investigate this, ITD cells were treated with quizartinib together with the broad-spectrum caspase inhibitor, z-VAD-FMK (Fig 4.7C). Inhibition of FLT3-ITD was confirmed by a reduction in STAT5 phosphorylation. As expected, quizartinib induced Mcl-1 downregulation, Bim upregulation, and procaspase 3 cleavage in both cell lines with both Mcl-1 and Bim levels modified within 24h of ITD inhibition. z-VAD-FMK abrogated procaspase 3 processing but also rescued Mcl-1 suggesting this may be linked to caspase activation. Interestingly, Bim was upregulated even in the presence of z-VAD-FMK demonstrating this was independent of cell death. AV/PI results showed that Z-VAD-FMK attenuated the apoptosis induced by quizartinib. Taken together, these findings suggest that down regulation of Mcl-1 by quizartinib may be through the caspase cleavage. This would make the down regulation of Mcl-1 a consequence of quizartinib-induced cell death rather than a causative event. This would still cause an imbalance between Bim and Mcl-1 potentially controlling the ITD cells sensitivity to apoptosis following inhibition.

To confirm a role further for Mcl-1 in FLT3L signalling we used siRNA to specifically knockdown the expression of Mcl-1 in the ITD cells and then tested

their sensitivity toward quizartinib and potential rescue by FLT3L. Transfection of MV4-11 and MOLM-13 cells with Mcl-1 specific siRNA but not with control siRNA significantly reduced Mcl-1 protein whereas Bcl-2 levels were unaffected (Fig 4.7D). Mcl-1 knockdown alone induce significant cell death with about 30% apoptosis in both cell lines prior to quizartinib treatment. Consequently, upon treatment with quizartinib, there was an increase in apoptosis of both cells with Mcl-1-targeting siRNA compared to control siRNA (Fig 4.7E). To test if reduction in Mcl-1 inhibits the protective effect of FLT3L, we also treated siRNA transfected cells with quizartinib and FLT3L. FLT3L had no protective effect on Mcl-1 siRNA transfected cells compare to control siRNA or non-transfected cells. Both experiments showed that Mcl-1 knockdown renders FLT3-ITD cells more sensitive to the FLT3 inhibitor quizartinib and prevent the protective effect by FLT3 ligand.

To further establish the role of Mcl-1 in ITD-expressing AML cells we used an Mcl-1 inhibitor, S63845 (Kotschy et al., 2016). Induction of cell death following treatment with quizartinib or Mcl-1 inhibition was assessed using Annexin V/PI. Cells were treated for 24 and 48h with increasing concentrations of S63845 (10 – 200 nM) or quizartinib (100 nM) or the two drugs in combination. A dose-dependent induction of apoptosis was seen in MV4-11 and MOLM-13 cells following treatment with S63845. In MOLM-13s, treatment with S63845 in combination with quizartinib appeared to have an additive effect compared to the compounds as single agents. This additive effect was not observed in MV4-11 cells which were more sensitive to S63845 alone (Fig 4.6F).

Upregulation of Mcl-1 in both cell lines could potentially provide an explanation for the protection observed with FLT3L. We therefore hypothesized that Mcl-1 inhibition would prevent the FLT3L-induced resistance in ITD cells treated with quizartinib. We chose the lowest concentration of S63845 (10 nM) and treated the cells with quizartinib and FLT3L for 24 and 72h. As before, FLT3L reduced quizartinib-induced apoptosis in both cell lines (Fig 4.6G). Apoptosis induced by combination of quizartinib and S63845 was not reduced with FLT3L suggesting that Mcl-1 could be important for the protective effect.

This was further confirmed by analysis of PARP and procaspase-3 cleavage. Quizartinib caused processing of PARP and procaspase-3 that was abrogated when co-treated with FLT3L (Fig 4.6H). Processing was also observed in both cell lines in combination of quizartinib with S63845 as this was not rescued with FLT3L. Collectively, these data support the importance of Mcl-1 for survival of the ITD cells and give a rational for targeting Mcl-1 in AML including the patient who represents with high FLT3L plasma level after starting the FLT3 targeted therapy.

A)

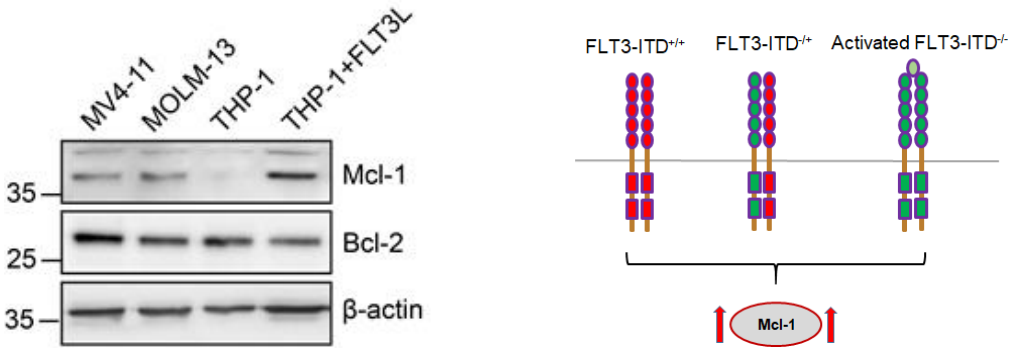
MV4-11
MOLM-13
THP-1
THP-1+FLT3L
35
Mcl-1
25
Bcl-2
35
β-actin
FLT3-ITD+/+
FLT3-ITD-/+
Activated FLT3-ITD-/-
Mcl-1

B)

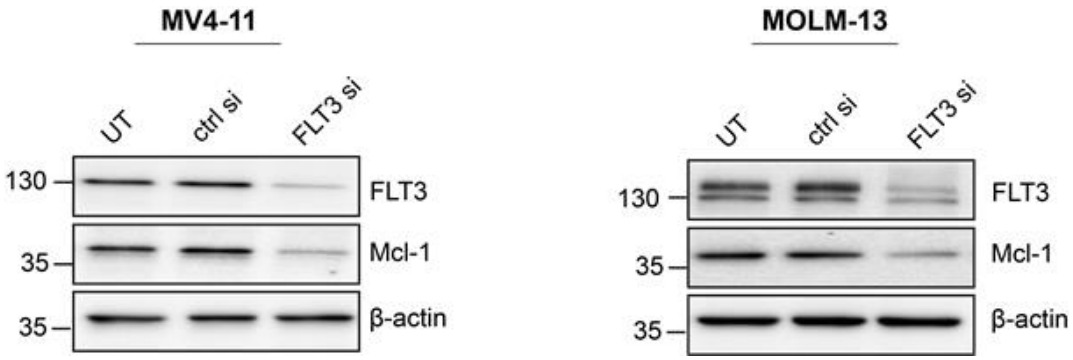
MV4-11
UT
ctrl si
FLT3 si
130
FLT3
35
Mcl-1
35
β-actin
MOLM-13
UT
ctrl si
FLT3 si
130
FLT3
35
Mcl-1
35
β-actin

C)

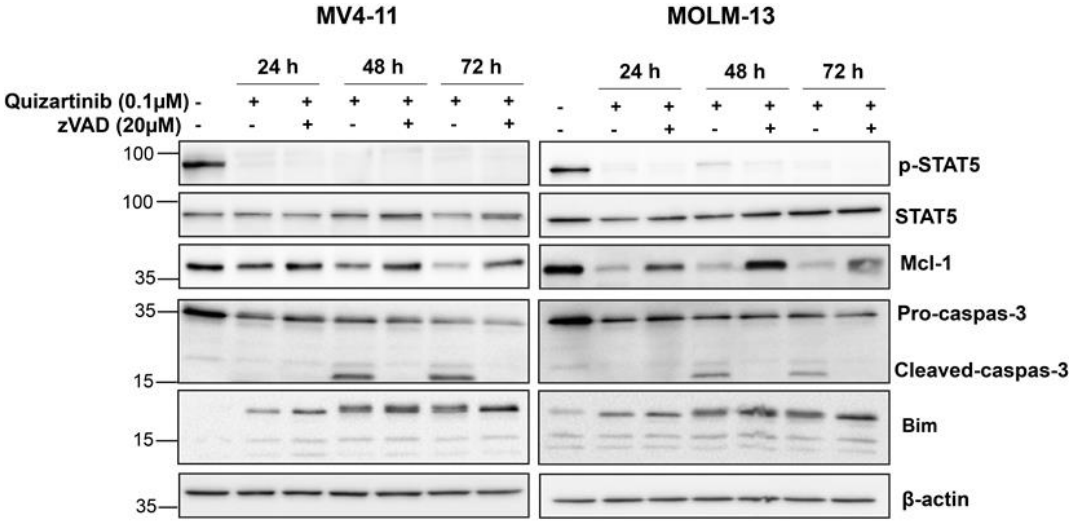
MV4-11
MOLM-13
24 h
48 h
72 h
Quizartinib (0.1μM)
zVAD (20μM)
100
p-STAT5
100
STAT5
35
Mcl-1
35
Pro-caspas-3
15
Cleaved-caspas-3
15
Bim
35
β-actin

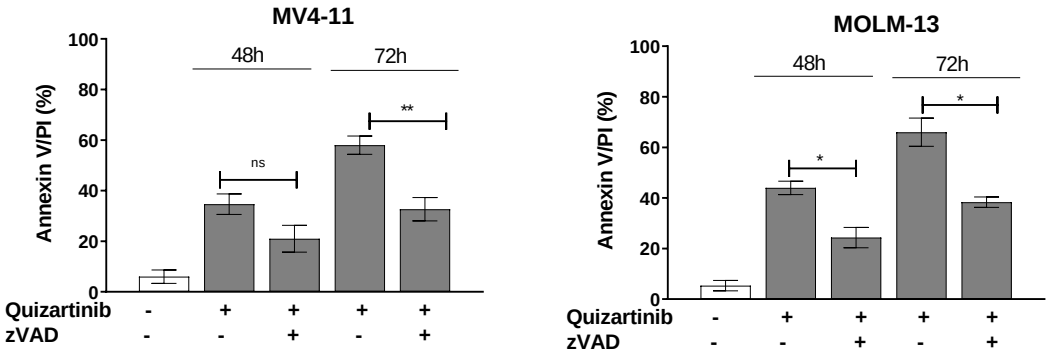
MV4-11
MOLM-13
Annexin V/PI (%)
48h
72h
ns
**
*
Quizartinib
zVAD

D)

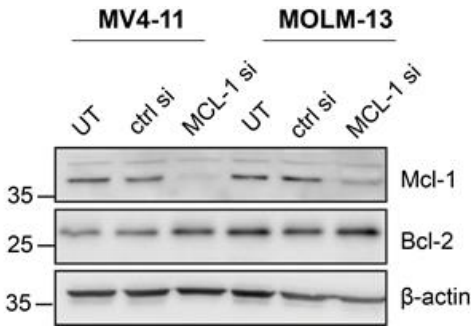
MV4-11
MOLM-13
UT
ctrl si
MCL-1 si
Mcl-1
Bcl-2
β-actin
35
25

E)

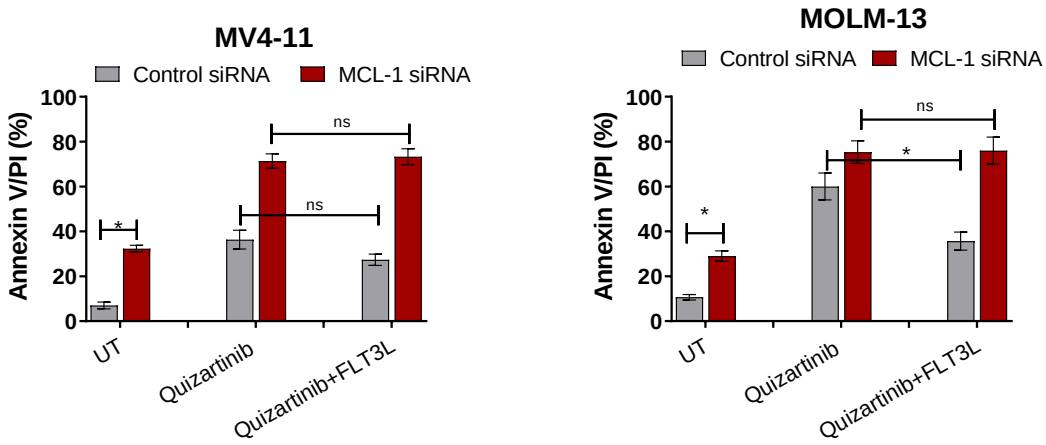
MV4-11
MOLM-13
Control siRNA
MCL-1 siRNA
Annexin V/PI (%)
ns
*
UT
Quizartinib
Quizartinib+FLT3L

F)

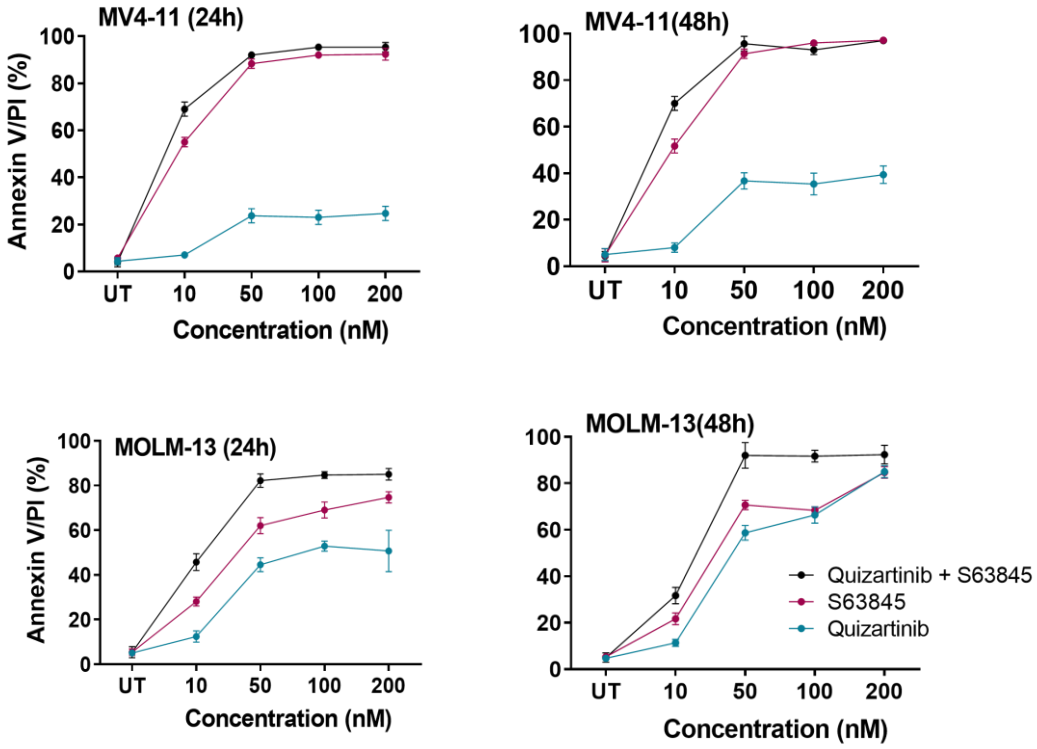
MV4-11 (24h)
MV4-11(48h)
MOLM-13 (24h)
MOLM-13(48h)
Annexin V/PI (%)
Concentration (nM)
UT
10
50
100
200
Quizartinib + S63845
S63845
Quizartinib

G)

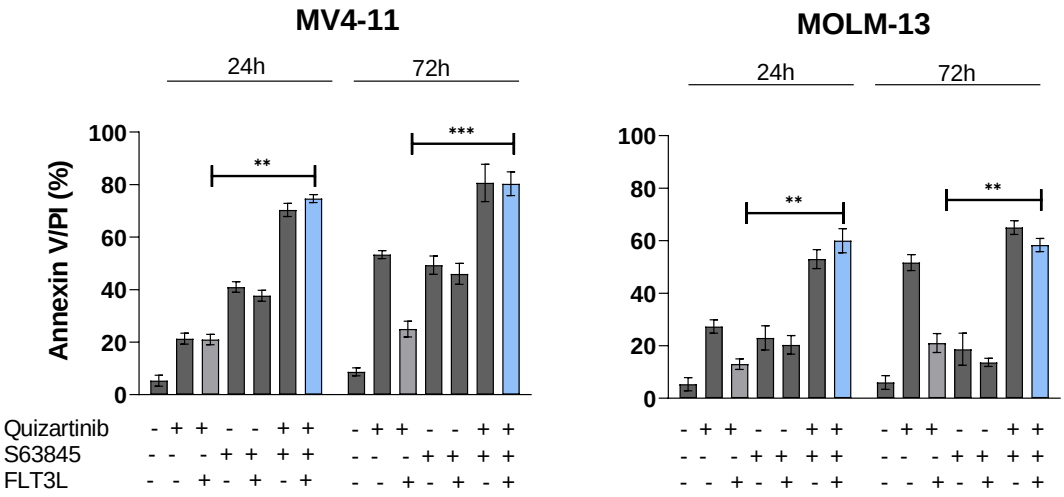
MV4-11
MOLM-13
24h
72h
Annexin V/PI (%)
**
***
Quizartinib
S63845
FLT3L

H)

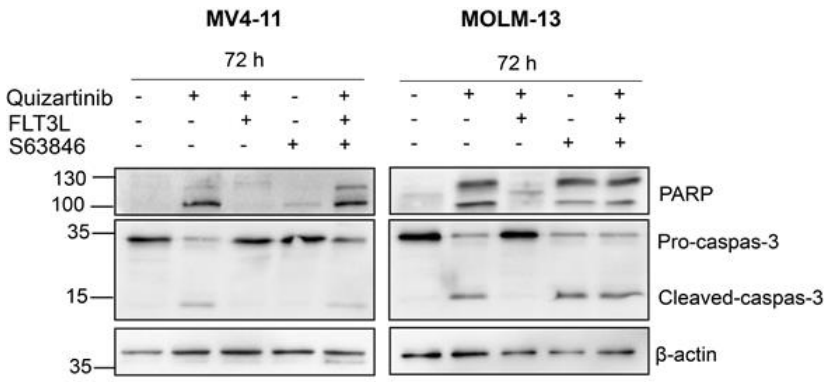

Figure 4.7: Role of Mcl-1 in quizartinib-mediated cell death and FLT3L-mediated resistance – A) Mcl-1 expression in ITD-expressing cells and THP-1 cells treated with FLT3L (100 ng/ml, 6h) was analysed by immunoblotting. Whole cell lysates were analysed for Mcl-1 and Bcl-1 expression. β-actin was used as a loading control. **B)** ITD-expressing cell lines were transfected with FLT3 siRNA (10 nM) for 72h before cells were harvested and analysed by Western blotting. **C**) Cell lines were treated with quizartinib (0.1 µM) and zVAD (20 µM) for indicated times after which lysates were analysed by Western blotting and apoptosis was measured using Annexin V/PI staining. **D)** MV4-11 and MOLM-13 were transfected with Mcl-1 specific or control siRNAs (10 nM). Whole cell lysates were analysed for Mcl-1 protein expression. β-actin was used as a loading control. **E)** Cells were transfected with Ctrl or Mcl-1 siRNA for 72h. For quizartinib/FLT3L experiments cells were treated, 24h after transfection with quizartinib (0.1 µM) with or without FLT3L for a further 48h. Apoptosis was measured using Annexin V/PI staining. **F)** Apoptosis following quizartinib (0.1 µM) and S63845 (10-200 nM) or combination treatment was assessed by Annexin V/PI staining. **G)** Cell lines were incubated for 24 – 72h with quizartinib (0.1 µM), S63845 (10 nM) and/or FLT3L (100 ng/ml) and apoptosis measured using Annexin V/PI staining. **H)** Caspase-3 activation and PARP cleavage following quizartinib and S63846 treatment. Results represent the mean +/- SEM for 3 independent experiments. Significance testing was done by two-tailed paired *t*-test (n=3), *$P \leq 0.05$, **$P \leq 0.01$, ***$P \leq 0.001$ and *and ns, not significant.*

4.2.7 Role of Bim in quizartinib-induced apoptosis

Despite our efforts to implicate Mcl-1 in FLT3L-mediated resistance to quizartinib its role is still somewhat obscure since inhibition or knockdown is cytotoxic even before quizartinib treatment. For this reason, it remains unclear whether the downregulation seen following inhibition of FLT3 is simply a result of Mcl-1 cleavage during apoptosis rather than a mechanism of quizartinib inducing cell death or protection afforded by FLT3L. We also observed that the proapoptotic BH3-only protein Bim is significantly upregulated following FLT3 inhibition, this was independent of cell death as it was unaffected by z-VAD. To further understand any potential role for Bim in quizartinib-mediated cell death we used Bim siRNA to assess its role in apoptosis following FLT3 inhibition.

MV4-11 cells were transfected with Bim siRNA for 48h followed by quizartinib for 24h. As we had observed previously Bim expression was very low in untreated cells but was significantly increased following quizartinib treatment. This upregulation was blocked by the Bim-specific siRNA indicating it was successfully targeting Bim (Fig 4.8A). siRNA transfected cells were then treated with quizartinib to assess the effects of Bim knock-down on ITD-inhibition. As we have seen before quizartinib induced apoptosis in cells treated with a control siRNA but this was blocked in cells treated with the Bim siRNA (Fig 4.8B). Taken together, these results suggest that upregulation of Bim is a key mechanism of quizartinib-mediated apoptosis in ITD-expressing cells.

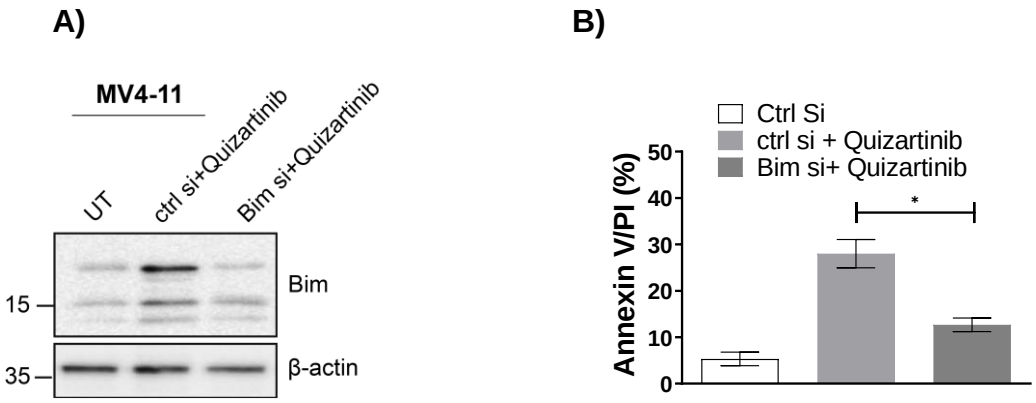

Figure 4.8: siRNA-mediated knockdown of Bim inhibits quizartinib-induced apoptosis – MV4-11 cells were transfected with Bim specific or control siRNAs (10 nM) for 48h before treatment with quizartinib (100 nM) for 24h. **A)** Transfected cells were analysed by Western blotting to validate Bim knockdown. **B)** Apoptosis measured by Annexin V/PI staining. Results represent the mean +/- SEM for 3 independent experiments. Significance testing was done by two-tailed paired *t*-test (n=3), *$P \leq 0.05$.

4.2.8 Activation of FLT3 signalling pathways by FLT3L following quizartinib treatment in FLT3-ITD cells

Based on our earlier results, phosphorylation of ERK1/2, AKT and STAT5 were decreased in ITD-expressing cells treated with quizartinib. We next investigated potential survival signalling pathways activated in these cells by FLT3L following ITD inhibition.

MV4-11 and MOLM-13 cells were treated with quizartinib or FLT3L or a combination for 24h following which the phosphorylation status of downstream signalling proteins was assessed by Western blot. FLT3 is active in both cells due to the presence of the ITD which results in constitutive phosphorylation of

ERK/12, AKT, and STAT5. Treatment with quizartinib blocked all these pathways in both cells (Fig 4.9A). In MOLM-13 cells, ERK1/2 and AKT phosphorylation could still be induced by FLT3L even in the presence of quizartinib. By contract, ERK1/2 and AKT phosphorylation status were not changed by FLT3L in the MV4-11s.

As we have observed before, In MV4-11 cells there appeared to be a delay in protection afforded by FLT3L which only started to reduce quizartinib-mediated apoptosis after 48h (Fig 4.1D). We therefore treated MV4-11s with quizartinib and FLT3L simultaneously for 48h before downstream signalling activation was assessed. Under these conditions, ERK1/2 phosphorylation was restored but not AKT or STAT5 phosphorylation (Fig 4.9B). This indicates that FLT3L reactivates ERK1/2 and to lesser extent AKT through WT-FLT3 in MOLM-13, and only ERK1/2 in MV4-11 resulting in reduced sensitivity to quizartinib. These observations implicate ERK1/2 and AKT pathways as being responsible for the protective effect of FLT3L.

We next investigated whether ERK1/2 or AKT inhibition by selective inhibitors could abrogate this resistance and restore quizartinib cytotoxicity in the FLT3-ITD cells. We used U0126, a MEK1/2 inhibitor to inhibit ERK1/2 and IPI-145, a PI3-Kinase inhibitor for the AKT pathway (KERR et al., 2003, Pillinger et al., 2016). MOLM-13 cells were treated with quizartinib and FLT3L in the presence of either U0126 or IPI-145 before pathway analysis by Western blotting and cell death analysis. The selectivity of MEK1/2 and AKT inhibitors was

confirmed as U0126 inhibited only ERK1/2 phosphorylation, whereas, IPI-145 inhibits only AKT (Fig 4.9C).

FLT3L can activate ERK1/2 even in the presence of quizartinib however, in cells treated with a U0126, FLT3L could not restore ERK1/2 phosphorylation (Fig 4.9C). However, Inhibition of AKT with IPI-145 only partially attenuated the protective effect of FLT3L. Annexin V/PI results showed that treatment of the cells with U0126 alone only caused slight cytotoxicity on its own, however it reversed the protective effect of FLT3L. This indicates that inactivation of ERK1/2 is sufficient to counteract the protective effect of FLT3L. This effect was also observed with U0126 in MV4-11 treated for 48h (Fig 4.9D). This data suggests that the protective effect of FLT3L appears to be predominately through the ERK1/2 pathway.

As we described earlier, only the type II inhibitors (sorafenib and quizartinib) but not type I inhibitors (midostaurin and gilteritinib) could be affected by FLT3L (Fig 4.1). We therefore further tested FLT3 signalling in MOLM-13 cells treated with FLT3 inhibitors in combination with FLT3L. We also investigated the effect of combining type II inhibitors sorafenib and quizartinib with the MEK inhibitor, trametinib which is used to treat metastatic melanoma (Thota et al., 2015).

All inhibitors blocked constitutive activation of ERK1/2 and AKT (Fig 4.9E). FLT3L was able to restore ERK1/2 phosphorylation only following sorafenib or quizartinib but not gilteritinib. Co-treatment of sorafenib or quizartinib with

trametinib inhibited FLT3L-induced ERK1/2 activation, and interestingly also protect the cells from FLT3L-induced Mcl-1 overexpression. The cell death results were consistent with those obtained with U0126 and demonstrated that FLT3L inhibition of apoptosis induction by type II inhibitors can be restored by adding the MEK inhibitor, trametinib (Fig 4.9F). Furthermore, ERK1/2 inhibition increased the sensitivity of cells to FLT3 inhibitors-induced apoptosis induction. This was not observed with gilteritinib (Appendix Fig A4). Inhibition of ERK1/2 phosphorylation was observed at trametinib concentration used in the experiment without affecting cell viability (Appendix Fig A5). These results confirmed that inhibition of MEK/ERK1/2 inhibits the protective effect of FLT3L and provides a rationale for overcoming FLT3L-mediated resistance in ITD patients with high FLT3L plasma levels using a combination of FLT3 and MEK/ERK1/2 inhibition.

A)

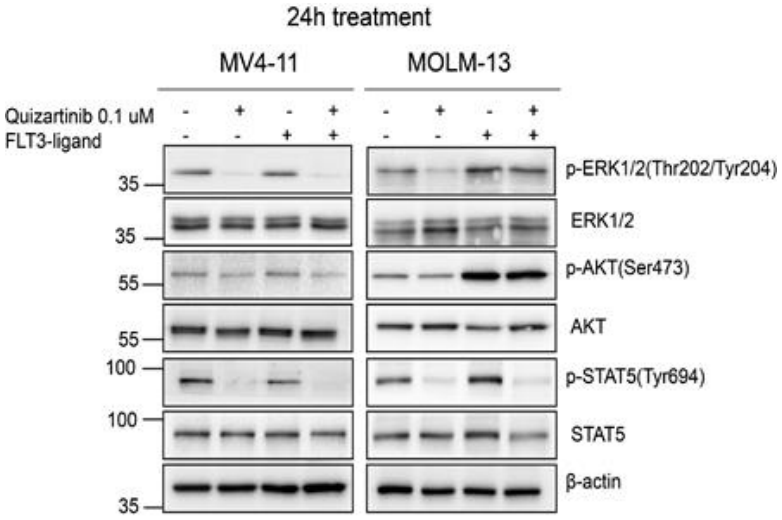

B)

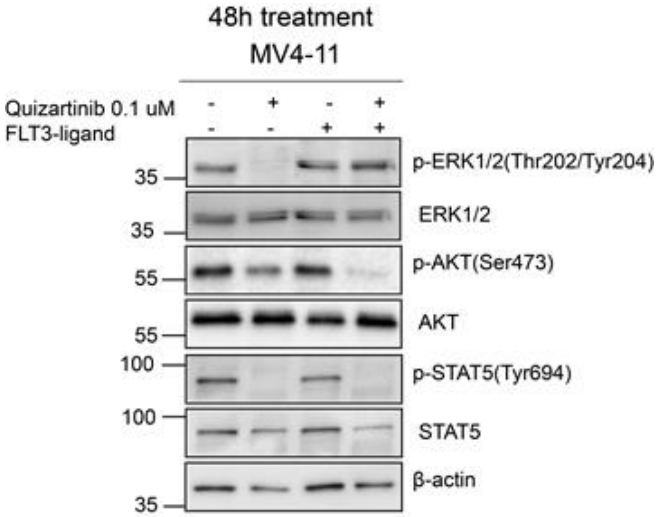
48h treatment
MV4-11
Quizartinib 0.1 uM
FLT3-ligand
p-ERK1/2(Thr202/Tyr204)
ERK1/2
p-AKT(Ser473)
AKT
p-STAT5(Tyr694)
STAT5
β-actin
35
35
55
55
100
100
35

C)

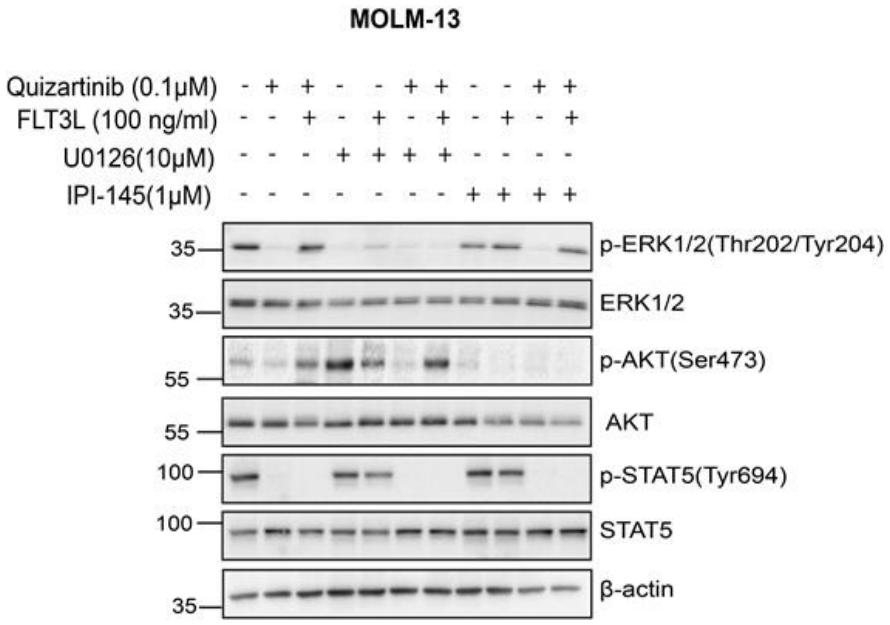
MOLM-13
Quizartinib (0.1μM)
FLT3L (100 ng/ml)
U0126(10μM)
IPI-145(1μM)
p-ERK1/2(Thr202/Tyr204)
ERK1/2
p-AKT(Ser473)
AKT
p-STAT5(Tyr694)
STAT5
β-actin
35
35
55
55
100
100
35

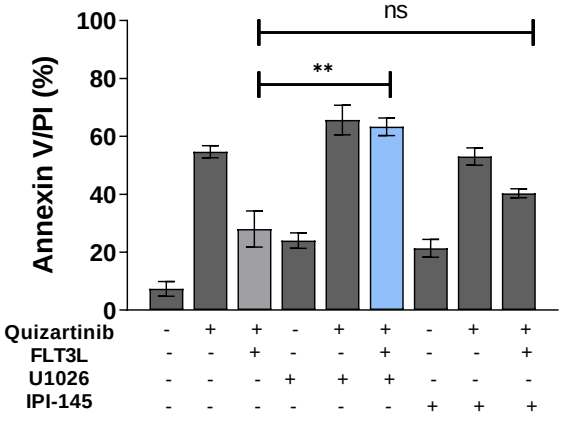
Annexin V/PI (%)
ns
**
100
80
60
40
20
0
Quizartinib
FLT3L
U1026
IPI-145

D)

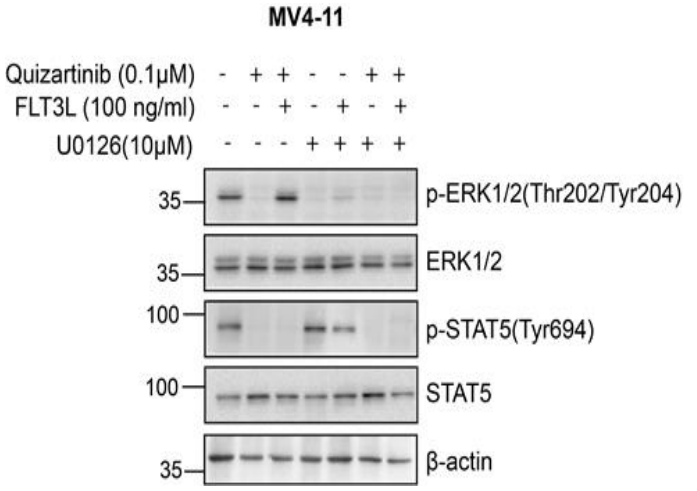
MV4-11
Quizartinib (0.1μM) - + + - - + +
FLT3L (100 ng/ml) - - + - + - +
U0126(10μM) - - - + + + +
35
p-ERK1/2(Thr202/Tyr204)
35
ERK1/2
100
p-STAT5(Tyr694)
100
STAT5
35
β-actin

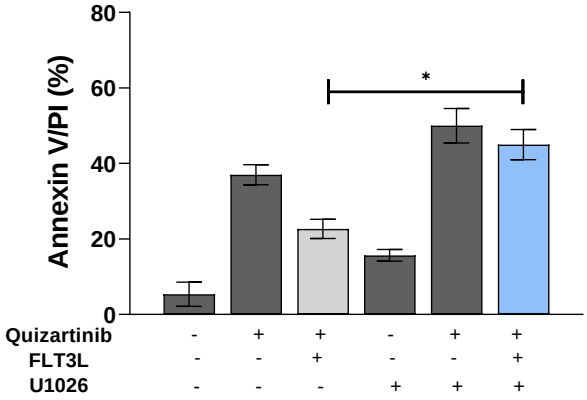
Annexin V/PI (%)
80
60
40
20
0
*
Quizartinib - + + - + +
FLT3L - - + - - +
U1026 - - - + + +

E)

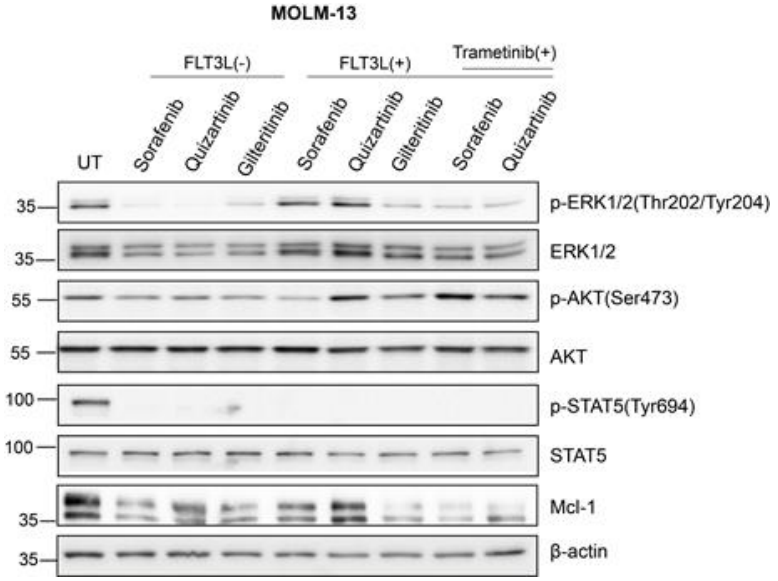

F)

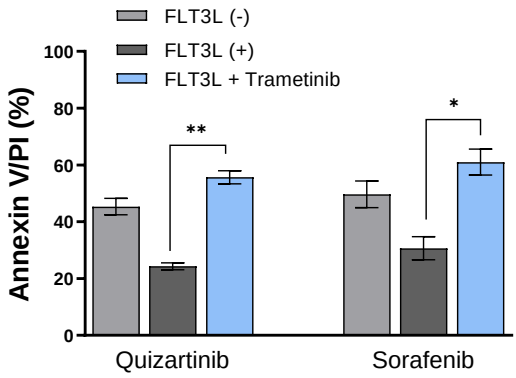

Figure 4.9: ERK1/2 is crucial for FLT3L to render the FLT3-ITD inhibition – A-B) MV4-11, and MOLM-13 cells were treated with quizartinib (0.1 µM) and FLT3L (100 ng/ml) for up to 48h. Total cellular extracts were separated by 10% SDS-PAGE and subjected to immunoblot analysis with phospho- STAT5, -AKT, -ERK1/2, and their unphosphorylated forms. β-actin was used as a loading control. **C)** MOLM-13 cells were treated with indicated treatment for 48 h, followed by immunoblotting with the indicated antibodies, apoptosis assessed by Annexin V staining. **D)** MV4-11 cells were treated with indicated treatment for 48h, followed by immunoblotting with the indicated antibodies, apoptosis was assessed by Annexin V. **E)** MOLM-13 cells were treated with quizartinib (0.1 µM), sorafenib (1 µM), gilteritinib (0.1 µM), trametinib (0.05 µM) and/or FLT3L (100 ng/ml) for 48h, followed by immunoblotting with the

indicated antibodies. **F)** Apoptosis was assessed by Annexin V staining. Results represent the mean +/- SEM for 3 independent experiments. Significance testing was done by two-tailed paired *t*-test (n=3), **P ≤ 0.05, **P ≤ 0.01,* and *and ns, not significant.*

4.2.9 Mcl-1 Expression Is Up-Regulated by the MAPK/ERK Pathway

We have demonstrated that Mcl-1 is the main anti-apoptotic protein downregulated upon FLT3 inhibition by quizartinib, and FLT3L reduces the cytotoxicity of FLT3 inhibitors through Mcl-1 upregulation. Also, we showed that ERK1/2 and to a lesser extent AKT pathways play an essential role for modulation of FLT3 inhibition in the presence of FLT3L. The involvement of main FLT3 signalling in Mcl-1 upregulation was examined.

Our previous result indicated that STAT5 remains inhibited either with quizartinib treatment or quizartinib plus FLT3L (Fig 4.9A-B), so it's not act as a modulator for FLT3L to induce drug resistance in ITD cells and may not be essentially involved in the regulation of Mcl-1. Indeed, we have shown that WT-FLT3 does not activate STAT5 even after stimulation with FLT3L and this suggest that Mcl-1 upregulation in THP-1 cells stimulated with FLT3L as shown in (Fig 4.7A) is linked to other pathways. In contrast to WT, ITD cause a constitutive activation of STAT5 and further activation of ITD by FLT3L has no effect on p-STAT5 status. To test whether or not STAT5 is necessary in ITD to induce Mcl-1 expression we knocked down STAT5 in MV4-11. STAT5 silencing lead to Mcl-1 downregulation at protein level, however, this could be related to cell death observed as a result of the knockdown rather than direct regulation of Mcl-1 by STAT5 (Appendix Fig A6). We were not able to use

selective STAT5 inhibitor (Ruxolitinib) as the cells maintained STAT5 phosphorylation throughout experiments. Taken together, STAT5 appears to not play an essential role in Mcl-1 upregulation mediated by FLT3 signalling.

As the Mcl-1 downregulation by quizartinib is not a functional effect rather than a cell death consequence, we were interested to study if Mcl-1 is regulated by MAPK/ERK pathway. First, we checked the apoptosis induction by U0126 (MEK inhibitor) and IPI-145 (AKT inhibitor) for different time points in MOLM-13 cells. For both inhibitors, induction of apoptosis has started after 24h treatment (Fig 4.10A). To examine which pathway is more implicated in the regulation of Mcl-1, we treat MOLM-13 with these two inhibitors for 12h, a time point prior to the induction of apoptosis, and Mcl-1 expression was checked by immunoblotting. As expected, U0126 treatment inhibits only ERK1/2, and IPI-145 inhibits only AKT. Treatment with MEK inhibitor but not AKT inhibitor leads to a decrease in the expression of Mcl-1 (Fig 4.10B).

To confirm further the reduction of Mcl-1 protein by ERK inhibition is not a consequence of cell death, cells were pre-treated with the pan-caspase inhibitor Z-VAD-FMK and MEK inhibitor for 48h. The MEK inhibitor U0126 reduced the Mcl-1 protein level despite the presence of the caspase inhibitor. Together, these results suggest that the Mcl-1 reduction by MEK inhibitor is not a result of cell death; however, the MAPK/ERK pathway seems to play a crucial role in the regulation of Mcl-1 in AML cells at the protein level (Fig 4.10B).

Among the anti-apoptotic Bcl-2 family protein, Mcl-1 is known to have a much shorter half-life (Brunelle et al., 2009). Down-regulation of Mcl-1 is thought to be regulated by protein degradation through the ubiquitination pathway (Wu et al., 2020). MOLM-13 cells treated with the proteasome inhibitor MG132 for up to 6h lead to the increase and stabilization of Mcl-1 protein level (Fig 4.10C).

To study if the downregulation of Mcl-1 by ERK1/2 inhibition is mediated through the proteasome pathway by enhancing Mcl-1 turnover, cells were treated with the MG132 (proteasome inhibitor) for 2h before added MEK inhibitor U0126 for 4h. U0126 reduced Mcl-1 protein level even in the proteasomal inhibition condition (Fig 4.10C). This result suggests that ERK1/2 pathway regulates the Mcl-1 protein level in different mechanisms to protein stabilization through proteasome pathway.

A)

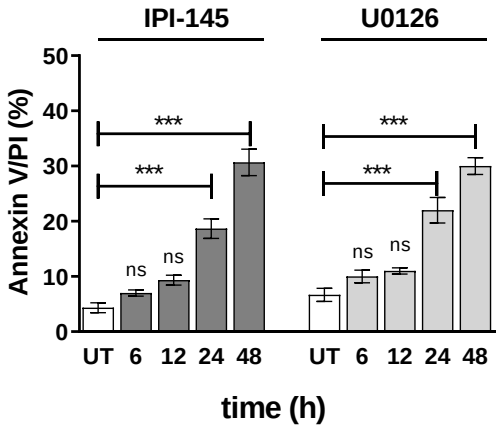

B)

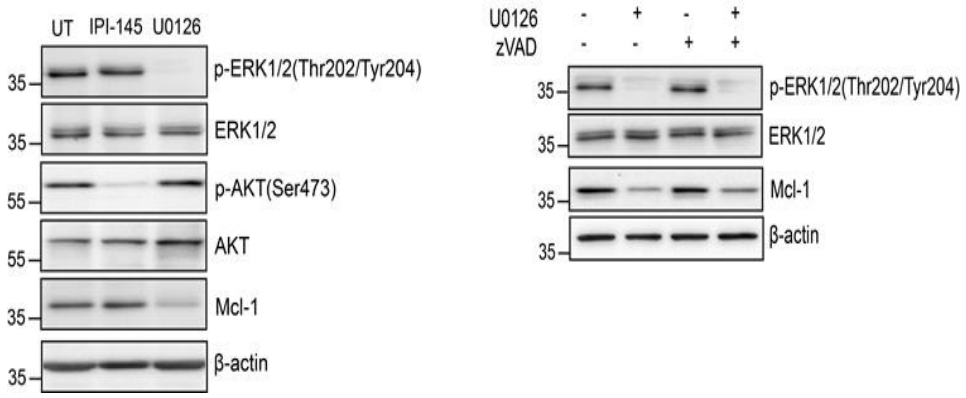

C)

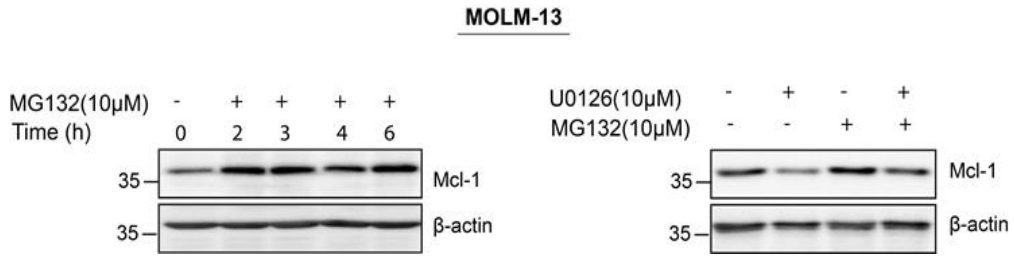

Figure 4.10: MAPK/ERK pathway regulate Mcl-1 expression in FLT3-ITD – A) MOLM-13 cells were treated with U0126 or IPI-145 for indicated times following which apoptosis was assessed by Annexin V/PI staining. Significance testing was done by one-way ANOVA with Dunnette's multiple comparison test (n=3), ****P ≤0.001, ns, not significant.* **B)** MOLM-13 cell were treated with U0126 (10 μM) or IPI-145 (1 μM) for 12h, followed by immunoblotting with the indicated antibodies. Cells were also treated with U0126 with or zVAD (20 μM) for 48h followed by immunoblotting analysis. **C)** Cells were treated with MG132 for up to 6h, or pretreated with MG132 for 2h and then treated with U0126 for 4h followed by immunoblotting analysis. β-actin was used as a loading control.

4.3 Discussion:

Over the last decade, FLT3 has been considered a potential molecular target in a subset of AML cases. The therapeutic effects of several FLT3 inhibitors possessing different characteristics have been reported in AML patients harbouring FLT3 mutations (Assi and Ravandi, 2018). With the early generation of FLT3 inhibitors, the peripheral AML blasts percentages were reduced transiently with limited effect on the percentages of bone marrow AML blast (Smith et al., 2004). Lacking the specificity of these multi-targeted TKIs for FLT3-ITD may explain their transient anti-leukemic activity, especially when used as monotherapy (Fischer et al., 2010). Therefore, next-generation FLT3 inhibitors with greater specificity for FLT3 have been developed and shown promising single-agent anti-leukemic activity in clinical trials (Perl et al., 2017, Cortes et al., 2018a). Despite the higher response rate of selective ITD inhibitors, one of the major obstacles with the use of newest FLT3 inhibitors in AML is drug-resistance which has been observed even with more recent inhibitors such as quizartinib (Dumas et al., 2019, Smith et al., 2017, Moore et al., 2020, Alvarado et al., 2014). Although several mechanisms of resistance have been identified such as secondary mutations (Smith et al., 2012a), elevated levels of FLT3L appears to be particularly problematic especially as most FLT3 mutations are heterozygous meaning a WT allele is still present (Sato et al., 2011). Therefore, further elucidating the resistance mechanisms that can be emerged during FLT3 inhibitors treatment is inevitable.

Human AML stem cells residing in the endosteal niche of the bone marrow are relatively chemoresistant (Ishikawa et al., 2007). Indeed, bone marrow microenvironment confers a protection to leukaemia cells as a result of different survival cues, either through cytokines/growth factors such as (PDGF, IL-3, SCF, and FLT3L) or through cell-cell surface contact such as SDF1 and CXCR4 (Sison and Brown, 2011, Lane et al., 2009). It has been reported that the FLT3-ITD AML blasts circulating in the peripheral circulation are sensitive to FLT3 inhibitors, however, FLT3-ITD AML blasts that residing within BM exhibit some degree of resistance to FLT3 inhibitors (Smith et al., 2004). Moreover, studies also suggest that FLT3-ITD leukaemia stem cells but not FLT3-WT leukaemia cells can be protected by stromal niche cells and reduce the efficacy of first-generation FLT3 tyrosine kinase inhibitor SU5614 (Parmar et al., 2011). However, the overexpression of FLT3 receptor in AML patients, the different allelic ration of ITD/WT, and the releasing of FLT3L may have changed the responsiveness of AML cells to all types of FLT3 inhibitors. All of these studies suggest that leukaemia niches can provide a protective effect on the FLT3-ITD AML blasts from being eradicated by the FLT3 inhibitors. Sato et al has demonstrated that FLT3-ITD AML cells are still responsive to exogenous FLT3 ligand, and also that the FLT3 ligand that is expressed in the marrow microenvironment increases the resistance of FLT3-ITD AML cells to the FLT3 inhibitors (Sato et al., 2011). They also showed that the FLT3L levels are routinely elevated in AML patients undergoing therapy which also can be a major obstacle when combined with the protective stromal effects and so promote resistance to FLT3 inhibitors. Another cytokines, Fibroblast growth factor 2 (FGF2), also found to protects FLT3-ITD AML cells

from quizartinib treatment through binding to FGFR1 receptor, and the MAPK signalling pathway was consistently restored in all FGF2 dependent resistant cultures (Traer et al., 2016). Additionally, the FLT3 inhibitor MLN518 lost its kinase inhibition activity significantly in the presence of FLT3L in heterozygous ITD cells, MOLM-13 and MOLM-14 but not against FLT3-ITD homozygous MV4-11 cells (Wang et al., 2016a). The inhibitory effects of MLN518 were decreased for FLT3 phosphorylation and/or c-MYC expression and increased for pS6K phosphorylation upon FLT3 ligand stimulation, and using dual inhibitor of AKT/FLT3-ITD, A674563, was able to overcome FLT3 ligand induced drug resistance in vitro and in xenograft models. This subsequently led to development of novel FLT3 kinase inhibitor such as G-749 which could the next generation of FLT3 inhibitor with an ability to overcome other drug resistances conferred by patient plasma, FLT3 ligand, and stromal cells (Lee et al., 2014). All of the these studies indicate that the effect of FLT3L is depend on the type of AML cells genotype, the cells model, as well as the type of FLT3 inhibitors being used as there was different mechanism has been proposed for the FLT3L mediated-resistance. Given that FLT3-ITD cells have different protection and sensitivity towards FLT3 tyrosine kinase inhibitors, it was crucial to understand how the cytokines and growth factor like FLT3L could interfere in this process and how they can derive resistance to FLT3 inhibitors. Therefore, to address these discrepancies in the role of FLT3L, we investigated the effect of exogenous FLT3L on the efficacy of different types of FLT3 inhibitors using AML cell lines model of WT-FLT3, homozygous and heterozygous ITD mutations and provide a novel strategy to overcome this emerging resistance mechanism. Although four different FLT3 inhibitors were

initially evaluated, we mainly focussed on quizartinib to delineate the resistance mechanism mediated by FLT3L. In the previous chapter, we demonstrated that quizartinib cause cell cycle arrest, inhibit cell proliferation and induces apoptosis. To explore the mechanism by which FLT3L reduce the cytotoxicity effect of quizartinib, we investigated the effects of FLT3L on cell cycle, cell proliferation and apoptosis. The FLT3L has no effect on G1 cell cycle arrest induced by quizartinib but it decease the sub-G1 population starting from day 2 of cell cycle analysis. FLT3L also has no effect on the cell proliferation inhibition induce by quizartinib. This indicate that FLT3L mainly working against quizartinib through apoptosis pathway. This was confirmed by Annexin V/PI and by the previous observation of reducing sub-G1 population.

We demonstrated that FLT3L can attenuate the inhibitory effect of type II FLT3 inhibitors such as quizartinib and sorafenib in both homozygous and heterozygous ITD-expressing cells. By contrast, no such effect was seen with the type I inhibitors gilteritinib or midostaurin. Type I inhibitors exhibit a similar potency against both WT and ITD-FLT3 and this is likely the reason why FLT3L has less effect in a homozygous ITD mutation background (Daver et al., 2019). Quizartinib and sorafenib tend to be more selective for ITD-FLT3 therefore FLT3L-mediated attenuation of quizartinib and sorafenib is a result of their weaker inhibitory effect on WT-FLT3 (Levis, 2014, Antar et al., 2017). This was clearly seen in the MOLM-13s as the effect of FLT3L on type II FLT3 inhibitors was more pronounced than that in the MV4-11s. Our result was similar to Sato et al work in terms of the effect of FLT3L on FLT3 inhibitors, however, by employing AV/PI technique we also showed that only type II but

not type I inhibitors can be affected by the presence of FLT3L. This was shown as all FLT3 inhibitors can be modulated by FLT3L using MTT assay in Sato et al work. We also found that cytotoxicity of type II inhibitors not only reduced by FLT3L in heterozygous cells like MOLM-13 or MOLM-14, but also in homozygous ITD mutated cells, MV4-11. These results suggest the mechanism by which FLT3L decreases the efficacy of FLT3 inhibitors is likely due to FLT3L dependent activation of WT-FLT3 as well as with long exposure to FLT3L this also can affect to less extent FLT3-ITD receptor. This effect is only seen against ITD-selective FLT3 inhibitors such as quizartinib and sorafenib. Given that most of AML patients present with heterozygous ITD mutations, non-selective FLT3 inhibitors such as midostaurin may be of more therapeutic benefit as they can also overcome any protective effect afforded by endogenous FLT3L. Therefore, tyrosine kinase genotyping and selection of FLT3 inhibitors types may become a prerequisite for optimal clinical use of this agent in patients with ITD mutation.

The glycosylation changes in the post translated protein FLT3 has pronounced effect on its kinase activity and downstream signalling cascades (Choudhary et al., 2009a). Mass spectrometry analysis revealed nine potential N-glycosylation sites in the extracellular domain of FLT3 indicating the critical roles of glycosylation in folding, stability, and functions of FLT3 (Verstraete et al., 2011, Pinho and Reis, 2015). Different glycosylation of FLT3 resulted in different patterns of FLT3 on Western blots. It is known that there are two forms of human FLT3. One appears around 150-160 kDa, and it’s thought to be the mature form of the receptor which reside on the cell surface. The other one is

an immature form which appears around 130 kDa and mainly localised in the ER (Schmidt-Arras et al., 2005). To confirm the heterogeneous pattern of FLT3 on Western blots, we checked cell lysates of FLT3-WT (THP-1) and ITD-FLT3 (MV4-11) for total FLT3 expression. The mutant FLT3 presented with one band at 130 kDa, and WT-FLT3 presented with two bands at 130 and 160 kDa. A lower third band was observed in untreated THP-1s which may be a non-specific band or could represent the immature unglycosylated form that would appear around 110-120 kDa. Cells were treated with two glycosylation inhibitors; tunicamycin and BFA and analysed for FLT3 expression pattern and activation status of STAT5, AKT, and ERK1/2, which are important pathways for FLT3 WT and mutant downstream signalling. In THP-1 (FLT3-WT), treatment with both inhibitors lead to decrease in 130-160 kDa forms and this suggest that the receptor tend to be retained intracellularly. This was accompanied by ERK1/2 and AKT inhibition indicating that surface localisation of FLT3 is required for activation of ERK1/2 and AKT which may be a problematic when surface FLT3 exposed to FLT3L. In MV4-11 cells with homozygous ITD we interestingly found that BFA, which only prevent the maturation form of FLT3 (160 kDa), lead to decrease in surface localised FLT3. From FACS experiment, we know that there is a minimal level of FLT3 on the surface of MV4-11 cells and this pool was not detectable by Western blotting. The ERK1/2 was more inhibited than AKT by treatment with glycosylation inhibitors suggesting that surface localised FLT3-ITD is mainly required for ERK1/2 activation. This result suggests that glycosylation is an important for FLT3 trafficking to the cell surface, and the surface localisation of FLT3 is important for activation of ERK1/2 and AKT in WT as well as ITD

FLT3. It also confirmed that STAT5 is mainly activated by intracellularly retained ITD not WT receptor, and support the finding of (Schmidt-Arras et al., 2009b) in which the intracellularly retained FLT3-ITD reduces ERK1/2 and AKT activation and further activate STAT5.

We next wanted to investigate the role of surface localised WT or ITD on the FLT3L-mediated resistance in our cell lines model taking the advantage of several published works suggested targeting proteins such as FLT3 on glycosylation process. This basically might be a tool to study the glycosylation inhibition rather than a therapeutic molecules as these inhibitors can affect any protein folding not just FLT3. Tunicamycin inhibits the transfer of active sugars to dolichol phosphate, which is an important step in the N-glycosylation of proteins at endoplasmic reticulum, and found to induced a cytotoxic effects and enhanced the susceptibility of several cancer cell lines such as head and neck carcinoma and lung cancer via glycosylation inhibition (Ahsan et al., 2010). Furthermore, a recent work showed that interference in FLT3-ITD glycoprotein maturation using tunicamycin has an anti-proliferative and pro-apoptotic effects on FLT3ITD-expressing human cells, and the combination of tunicamycin with FLT3-ITD kinase inhibitors caused synergistic cell death especially in ITD-expressing cells (Tsitsipatis et al., 2017). Fluvastatin and 2-deoxy-D-glucose are another examples of drugs that have been used to target FLT3 glycosylation and now being evaluated in clinical trial phase I (Williams et al., 2012, Larrue et al., 2015). We are aware that these inhibitors can induce cytotoxicity through ER stress. Therefore, we realised that further work need to be done in order to study the ER stress that can be caused by theses

inhibitors and looking for several UPR adaptive activation readouts such as, phosphorylation of PERK or IRE1, XBP1 splicing or processing of ATF6 (Oslowski and Urano, 2011). The question was if we manipulate the surface localisation of ITD and WT using low dose of BFA and tunicamycin ,which apparently attenuating FLT3ITD-driven AKT and ERK signalling, can lead to abrogate the FLT3L-mediated resistance to quizartinib. To determine the lowest concentration which can prevent surface localisation of FLT3 but at the same time does not induce significant apoptosis, we tested different concentrations varying from 0.01 µM to 10 µM for several time points. The dose response curve of tunicamycin and BFA indicate that these inhibitors caused cell death in both cell lines (MV4-11 and MOLM-13) to different extent. For this reason we checked the dose that required to inhibit the surface localisation of FLT3, and FACS results showed that 0.1 µM but not 0.01 µM can decrease surface localised FLT3. The 0.1 µM of BFA and tunicamycin induce ~10-20% cell death after 24h treatment. Therefore, we picked this concentration for MOLM-13 immunoblotting experiment and treat the cells with quizartinib plus BFA for 24h, a time we can start observe the effect of FLT3L on quizartinib, following by 2 minutes activation by FLT3L in order to study the possible rescued downstream cascades. The FLT3L was not able to restore ERK1/2 or AKT in the presence of BFA. This give an indication that the low dose of BFA prevent signalling rescued and could inhibit the resistance mediated by FLT3L. We observed that with BFA treatment in the presence of quizartinib and FLT3L, total FLT3 levels decreased. Quizartinib has been shown to increase the 160 kDa surface localised FLT3 species, and that BFA can prevent maturation of the 130 kDa form into 160 kDa form. We also know

that FLT3L will bind to any trace of surface localised FLT3 that is not prevented by BFA, and all of these factors could have an implication in the decreasing level of total FLT3 we observed in the plot. In order to study if the ERK/12 and AKT rescued prevention by BFA treatment would have an effect on the cell viability induced by FLT3L in the presence of quizartinib, we treat the cells with quizartinib, BFA or tunicamycin with or without FLT3L for 24h-48h. Similarly, we used a concentrations (0.1 μM) that has shown the ability to prevent the majority of surface localised FLT3 in FACS experiment and also induce the minimal cytotoxicity to the cells. Linking the effect of glycosylation inhibitors to FLT3-ITD is somehow unreliable for the experiments we have done as THP-1 total FLT3 surface localised respond to these inhibitors. Whether or not the THP-1 cells have the same sensitivity towards these inhibitors is need more investigation. However, we can clearly suggest that heterozygous cells as MOLM-13 cells are sensitive to BFA and tunicamycin. Generally, results showed that preventing FLT3 maturation and as a result trafficking to the cell surface using glycosylation inhibitors inhibits the effect of FLT3L on both WT and ITD FLT3 and consequently the resistance to quizartinib. We also observed that the STAT5, a specific downstream target of ITD activation did not change following inhibition of glycosylation indicating that cell surface FLT3 and so ERK1/2 and AKT is critical for FLT3L to mediate resistance to FLT3 inhibition. Although tunicamycin is currently not a clinically studying molecule, it was reported tunicamycin is well-tolerated in mouse models (Hou et al., 2013). As a result, the possibility of using tunicamycin in more pre-clinical and clinical setting is expected in future.

The Bcl-2 family members have been studied extensively for its role in leukemic pathogenesis and drug resistance. Anti-apoptotic protein BCL2 found to be highly expressed in AML leukaemia stem cells (LSC) and contribute to chemotherapy resistant (Carter et al., 2016). A recent study employed BH3 profiling to assessed dependence on anti-apoptotic pathways showed that co-inhibition of BCL2 with ABT-199 in addition to tyrosine kinase inhibitors enhanced eradication of diverse co-existing mutations AML in patient-derived xenograft (PDX) models (Saito et al., 2017). As different cell types can be relay on certain anti-apoptotic proteins for their survival, it's crucial to study each AML cells model with certain genetic abnormalities to determine which bcl-2 proteins required for cells survival or for drug sensitivity. Venetoclax lack the ability to inhibit MCL1, this leads to resistance in leukaemia cells that are depend on MCL1 for survival (Lin et al., 2016). Other anti-apoptotic member of the BCL2 family proteins is myeloid leukaemia cell differentiation protein 1 (MCL1), and it's commonly upregulated in AML cells, especially in relapsed patients (Kaufmann et al., 1998). A recent study provide a rationale for initiating a clinical study evaluating the combination of MCL1 inhibitor S63845 and MEK-inhibitor trametinib, and showed that haematological cells with elevated MCL1- and MEK-protein levels were most sensitive to the combined treatment (Seipel et al., 2019). While it is clear that inhibiting anti-apoptotic proteins is important for the synergistic killing of leukaemia cells, the mechanism how FLT3L promotes quizartinib resistance in the context of BCL-2 proteins is not clear. Therefore, in order to understand how quizartinib induces cytotoxicity and how FLT3L-mediated its resistance, we looked at the role of Bcl-2 family members in MV4-11 and MOLM-13 cell

lines. We identified the anti-apoptotic protein Mcl-1 as promising target in ITD-expressing cells, and this was consistent with the data showed that 32D cells transfected with ITD mutations induced a dramatic up-regulation of the anti-apoptotic myeloid cell leukaemia 1 protein (Mcl-1) (Breitenbuecher et al., 2009b). Another work showed that Mcl-1 is upregulated in FLT3-ITD-positive cell lines and primary AML cells and that Mcl-1 is a downstream target of FLT3L-stimulated FLT3 signalling (Kasper et al., 2012). In the context of our project, looking into BCL-2 apoptotic proteins will help to provide a rational approach to improve the therapeutic outcome of quizartinib and also to prevent the resistance mechanism that can be emerged by FLT3L. The expression level of Mcl-1 in MV4-11 and MOLM-13 was high compared with THP-1s and the expression was found to be regulated either through the ITD or WT-FLT3 stimulated with FLT3L. This observation was confirmed by inhibiting ITD signalling with quizartinib or by siRNA-mediated suppression of FLT3. This data confirmed what has been shown in the literature that Mcl-1 is regulated by FLT3L acting upon WT-FLT3 in non-ITD AML lines, and also that the high basal expression in the MV4-11 and MOLM-13 cell lines is likely due to the presence of ITD-FLT3. We next showed that quizartinib modulate Mcl-1 and Bim, but not other BCL-2 proteins in ITD cells, and FLT3L itself can induce Mcl-1 upregulation in WT-FLT3, and as a result this finding may be clinically meaningful for patients who develop resistance to type II FLT3 inhibitors like quizartinib and present with high FLT3L plasma level. The issue of mechanistically implicating Mcl-1 in survival signalling in the AML cells lines is that both the Mcl-1 inhibitor and the siRNA induced apoptosis as single agents. They both increased the effects of quizartinib but at times this appeared

additive rather than a true synergism. So Mcl-1 inhibition alone is clearly a therapeutically relevant for treatment of AML. The other Bcl-2 protein we found to be regulated by FLT3 is the pro-apoptotic BH3-only Bim. Bim levels were significantly increased following treatment with quizartinib suggesting that ITD signalling is responsible for suppression of its expression. We subsequently found this effect was not limited to ITD signalling as when cells were treated with quizartinib in combination with FLT3L upregulation of Bim was inhibited. This only occurred in the MOLM-13 cells as these cells also express WT-FLT3 as well as the ITD allele. Therefore, FLT3 signalling (both WT and ITD) appears to regulate negatively Bim expression. What is clear from these data is that both quizartinib and FLT3L can modulate Bim and Mcl-1 at protein levels. Quizartinib appears to cause an upregulation of Bim with a concomitant downregulation of Mcl-1. FLT3L, which has a protective effect following ITD inhibition can modulate Mcl-1 in both lines but appears to suppress Bim in the MOLM-13s. Given these cells also express WT-FLT3, which cannot be inhibited by quizartinib, it is likely that the upregulation of Bim, following ITD inhibition, was being reversed by FLT3L through WT- FLT3. This suggests that the imbalance between Mcl-1 and Bim expression may play a major role in ITD inhibition and in the resistance induced by FLT3L. These findings provide a rationale for a combination strategy targeting both FLT3-ITD and Mcl-1 to overcome drug resistance induced by FLT3L.

Downstream pathways activated by FLT3 play an important role in modulating the efficacy of FLT3 inhibitors. Major pathways activated are PI3K, MAPK and, at least in ITD-expressing cells, the STAT5 pathway. In the previous chapter,

we showed that short term FLT3L stimulation (2 -10 minutes) does not prevent quizartinib inhibition of FLT3 signalling in MV4-11 even though there was an internalization of ITD receptor, however, it rescued ERK1/2 and AKT in MOLM-13 cells. This variation in the quick response to FLT3L can rely on several factors including; the initial localised cell surface FLT3, the extent of re-localisation of FLT3 upon quizartinib treatment and the time point used for FLT3L stimulation. Sato it all shows that FLT3L maintains p-FLT3 levels in MOLM-14 cells upon several TKIs treatment. Even though we were not able to detect p-FLT3 level using several antibodies and therefore we did not interpret the phosphorylation status of FLT3, our results were in consistent with Sato it all in which the FLT3L restored ERK1/2 and AKT in MOLM-13 cell (similar to MOLM-14 cells) assuming this was as a result of FLT3 phosphorylation and activation. Interestingly, we showed that MV4-11 cells are response to long exposure of FLT3L in the presence of quizartinib and start to restore ERK1/2 but not AKT within 48h of co-treatment. This observation has not been shown by Sato et al as only p-FLT3 was studied but not it's downstream signalling ERK1/2, AKT and STAT5.

It has been well established that the PI3K/AKT signalling pathway plays an important role in FLT3 oncogenic signalling, however, we observed a different AKT response to FLT3L in AML cells treated with various FLT3 inhibitors. This was not consistent with the inhibition of apoptosis induced by FLT3 inhibitors. Using PI3K/AKT inhibitor dose not rescue the effect of FLT3L on quizartinib treated cells to the same extent as MEK inhibitor does. This suggest that AKT has less effect on the mechanism of resistance caused by FLT3L. The MAPK

pathway does appear to be important for both WT- and ITD-FLT3 signalling in the AML cells. Using MEK and PI3K/AKT inhibitors, we showed that the expression of Mcl-1 by the ITD is regulated by the MAPKs suggesting a role for this pathway in cell survival. These results are consistent with the fact that FLT3L mediates its resistance through the MAPK pathway. The mechanisms by which the MAPKs regulate the expression of Mcl-1 are still under investigation. We have shown that inhibition of the MAPKs decreases the Mcl-1 protein level, however, further experiments need to be done to study the transcriptional level of Mcl-1 following MAPKs inhibition. One protein which is well known to be regulated by the MAPK pathway is Bim (Ley et al., 2003, Balmanno and Cook, 2009). This appears to be a key mediator of ITD-induced apoptosis as siRNA blocked cell death by quizartinib. We demonstrated that activation of MAPK/ERK pathway by FLT3L is responsible for the inhibition of cell apoptosis induced by quizartinib. Therefore, a strategy for targeting both FLT3 and MEK/ERK could enhance the apoptotic effect of FLT3 inhibitors even in the presence of FLT3L. Indeed, we observed targeting FLT3 with quizartinib or sorafenib in combination with MEK inhibitors such as U0126 or trametinib restored cell death induced by FLT3 inhibitors overcoming FLT3L-mediated resistance. The fact that this was not observed with gilteritinib further confirmed the role of WT-FLT3 in this resistance.

Unfortunately, due to the absence of commercial STAT5 inhibitors we were unable to fully examine the role of this pathway. However, several pieces of information would suggest that its role in apoptosis suppression through ITD signalling is less important than other pathways. It also cannot be involved in

FLT3L-medited resistance as it cannot be activated by WT-FLT3 (Spiekermann et al., 2003b). Also, STAT5 phosphorylation did not restore as a result of ligand stimulation in both cell lines, and this is in agreement with Choudhary et al findings, in which STAT5 is activated by the intracellular pool of ITD receptor and therefore cannot response to exogenous ligand (Choudhary et al., 2009a). While, silencing STAT5 has been shown to regulate Mcl-1 and Bcl-2 expression at least in ALL, our data suggests the MAPK pathway is much more important to mediate FLT3L resistance mechanism (Minieri et al., 2018). This observation is likely a result of WT-FLT3 expression in the MOLM-13s which is available on the surface for ligand binding and activation by FLT3L and is unaffected by quizartinib. This is further supported by the fact that quizartinib abolished STAT5 phosphorylation and this could not be restored by FLT3L. STAT5 phosphorylation is specifically activated by ITD-FLT3 not FLT3L acting on the WT receptor.

In summary, we demonstrate that elevated FLT3L levels may correlate with resistance to FLT3 inhibition. FLT3L reduces the inhibitory effects of quizartinib by activation of surface localised wild-type FLT3 receptor through the MAPK/ERK pathway and subsequently Mcl-1 overexpression. This also can be observed with prolong activation of ITD-FLT3. We also indicate that inhibition of upregulated Mcl-1 in the ITD model might be a promising therapeutic approach to sensitize cells to targeted therapy and to overcome the resistance induced by FLT3L. Given most patients present with a heterozygous mutation and elevated plasma FLT3L levels following chemotherapy, midostaurin and gilteritinib should be favoured over quizartinib.

These multi-kinase type I inhibitors dephosphorylate ERK1/2 even in the presence of FLT3L. On the other side, using multi-kinase inhibitor as midostaurin have a risk for inducing adverse effects as a result of its off-target effects. Finally, the combination of FLT3-ITD selective drugs such as quizartinib with MAPK/ERK inhibitors, glycosylation inhibitors, or Mcl-1 inhibitors can be a putative therapeutic approach and need more investigation.

Chapter V

==========

Validation of STAT5 knock-out strategy in HEK-293T cells

5.1 Introduction

Over recent years, genome-editing using programmable nucleases has become a significant technological breakthrough in the field of molecular biology that enables targeted gene disruption both in *vitro* and in *vivo*. Custom nucleases such as Zinc fingers (ZFNs), transcription activator like effectors (TALENs), and the “clustered regularly interspaced short palindromic repeats” (CRISPR)/“CRISPR-associated genes 9” (Cas9) have all been used for genetic modification. The CRISPR/Cas9 system has become the most popular technique due to the fact it is easy to use and readily re-taskable with simple cloning protocols. Indeed, the 2020 Nobel Prize in Chemistry was awarded to Emmanuelle Charpentier and Jennifer Doudna for their discovery of the CRISPR-Cas9 system. CRISPR-Cas9 is also less sensitive to epigenetic modifications and can be incorporated into viral vectors or delivered as a ribonucleoprotein complex (Lino et al., 2018). As discussed in Section 1.5, Genome editing technologies have advanced significantly over the past few years allowing us to manipulate precisely specific loci within the genome. These approaches using programmable nucleases can potentially correct or delete single genes responsible for disease (Capecchi, 1989, Capecchi, 2005).

Several CRISPR/Cas systems have been developed and characterised from different bacteria with each of them having their own application-specific advantages. The most commonly used Cas nuclease, is SpCas9 derived from *Streptococcus pyogenes* (Jinek et al., 2013). One advantage of SpCas9 is that its required Protospacer adjacent motif (PAM) for DNA binding, 3’ NGG,

occurs frequently in most genomes, resulting in many available target sites (Cong et al., 2013). This protein has been subjected to a large number of mutagenesis studies which have sought to widen its PAM recognition and also enhance its activity resulting in a number of new variants hfCas9, eSpCas9 and xCas9 (Hu et al., 2018). The large size of the Cas9 endonuclease is a major disadvantage, restricting some delivery methods. There has therefore been a great interest in identifying smaller orthologues, and these include SaCas9 from Staphylococus, LsCas9 from Leptotrichia and CjCas9 from Campylobacter (Ran et al., 2015). The disadvantage of all of these orthologues is that they use more restrictive PAM sequences meaning more limited genomic targeting (Cebrian-Serrano and Davies, 2017). Gene-editing has difficulties in application terms in leukaemia research. This is down to *in vitro* selection protocols, which are exclusively on suspension cell types. Similar difficulties are observed with gene editing in other leukaemia models and species utilised. A recent work revealed the importance of CRISPR-cas9 as a tool for studying a key regulators of AML stem cells. In this work, an *in vivo* pooled CRISPR-Cas9 screen that targeted selected cell surface genes has been performed in order to identify the top regulator of leukaemia-initiating cells. Using CRISPR single guide RNA (sgRNA) library that targeting 96 cell surface genes, scientists were able to identify the critical role of CXCR4 in AML cell growth and survival *in vivo* (Ramakrishnan et al., 2020).

The aim of this chapter is to establish a CRISPR-Cas9 strategy to use in the MV4-11 cells to establish further the role STAT5 plays in ITD signalling. The tools developed could allow the FLT3-ITD pathway, which is pathologically

implicated in acute myeloid leukaemia (AML), to be further interrogated in the hope of finding novel therapeutic targets.

STAT5 plays a critical role in a variety of developmental processes such as proliferation and differentiation, and it is also constitutively phosphorylated in a number of haematological disorders (Yamada et al., 2017). Several reports have described STAT5 as protein activated by FLT3-ITD which promotes an aggressive form of acute myeloid leukaemia (AML) (Choudhary et al., 2007). High STAT5 phosphorylation have been associated with tyrosine kinase inhibitor (TKI)-resistance (Warsch et al., 2011). In our cells model, we were unable to directly inhibit STAT5 as we have done with ERK1/2 or AKT, as a result suggesting STAT5 possible role in FLT3L resistance or Mcl-1 regulation has been challenging in FLT3-ITD cells. How STAT5 activated in FLT3-ITD signalling remains controversial. It has been suggested that STAT5 is activated in ITD by Jak1/2 kinases, Src family kinases (SFK) or directly by RTK receptor such as mutated FLT3 (Choudhary et al., 2007). As STAT5 has two isoforms (STAT5A and STAT5B) with a high degree of similarity (Ambrosio et al., 2002), we were interested to knock-out the most relevant isoform in ITD cells and study the role (canonical and non-canonical function) of this isoform in the pathogenesis of AML and drug resistance. To date, STAT5 has not been targeted using the CRISPR/Cas system in AML cells. The CRISPR/Cas system was chosen as the preferred method over other genome editing technologies due to its simplicity and efficiency. Comparing CRISPR/Cas with RNA interference to disrupt gene expression, CRISPR/Cas is more consistent allowing complete knockout thereby eliminating low-level protein expression

that can remain using RNA interference (Gilbert et al., 2014, Gilbert et al., 2013).

5.1.1 Aims

- Design a gene-editing strategy to investigate the role of STAT5A in FLT3 signalling. This will be used as a basis for further gene-editing studies to investigate clinically-relevant mutations in vitro.

- Establish tools and cell lines that could be used to further study the role of FLT3 in AML.

5.2 Results:

5.2.1 mRNA and protein levels of STAT5A and STAT5B in AML cell lines

STAT5A, and the closely related protein, STAT5B were first reported in 1995 by 3 different groups (Azam et al., 1995, LIu et al., 1995, Mui et al., 1995). Although they share 96% homology, they exhibit different expression patterns. In most AML studies, the effect of p-STAT5 has been extensively investigated, however, non-phosphorylated STAT5 is mostly evaluated without distinguishing between STAT5A and STAT5B.

We first compared STAT5A and STAT5B mRNA levels in the AML cell lines. The mRNA levels expression of both STAT5A and B were higher in WT-FLT3 expressing cells (THP-1s) compared to FLT3-ITD cells. STAT5A mRNA levels appeared higher than STAT5B in all cells (Fig 5.1A).

To analyse the expression and phosphorylation status in the different AML cells, proteins were extracted and subjected to immunoblotting. All cells expressed both forms of STAT5 and expression appeared to be higher in the ITD-expressing cells (Fig 5.1B). As expected, phosphorylation of STAT5 was only seen in the ITD-expressing cells (MV4-11 and MOLM-13). To test whether STAT5 could be phosphorylated in WT-FLT3, THP-1s cells were treated for 30 minutes with GM-CSF, a potent activator of STAT5. STAT5 was inactive in these cells but could activated following treatment with GM-CSF.

These results suggest that STAT5A and B are differentially expressed among the AML cell lines and appears higher in the ITD cells despite these cells expressing lower mRNA levels (Fig 5.1A).

A)

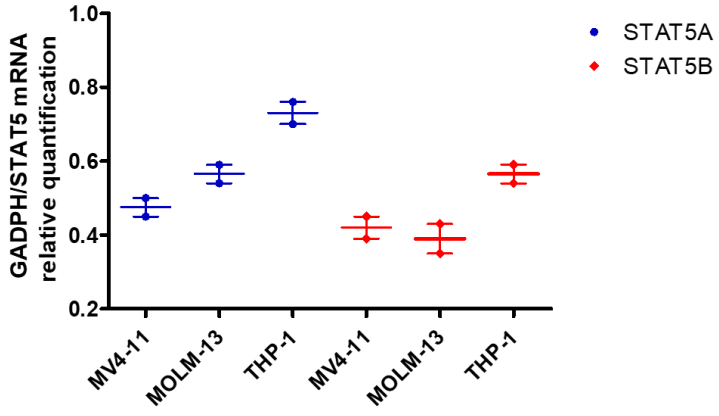

B)

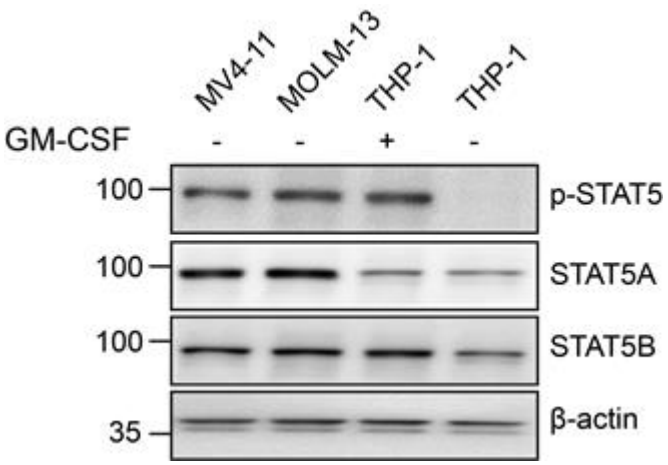

Figure 5.1: STAT5A/B expression in AML cells – A) mRNA expression of STAT5A/B genes was analysed by RT-qPCR. Data were normalized to GAPDH. Results represent the mean +/- SEM for 2 independent experiments. **B)** Total cellular protein (30 µg) from the AML cell lines was separated by SDS-PAGE and subjected to immunoblot analysis with indicated antibodies. THP-1 cells were treated with GM-CSF for 30 minutes and β-actin was used as a loading control.

5.2.2 Functional Effects of STAT5A/B knockdown in MV4-11 cells

It has been reported that STAT5A is more important than STAT5B for FLT3 signalling (Zhang et al., 2000). Our results show that AML cells appear to express more STAT5A mRNA than STAT5B and levels of both are higher in WT than ITD-expressing cells (Fig 5.1A). At the protein level, STAT5A but not STAT5B was more highly expressed in ITD-expressing cells (Fig 5.1B). The variation in protein and mRNA levels could be related to the activity of STAT5A in ITD cells.

To further analyze the role of STAT5A/B in FLT3 signalling, we knocked down STAT5A/B in MV4-11 cells using siRNA. Firstly, validation of knockdown was evaluated at the protein level by immunoblotting (Fig 5.2). Both siRNA appeared to cause significant STAT5 knockdown in the MV4-11s, although the knockdown of STAT5A appeared more complete.

Knockdown of STAT5A or STAT5B caused an increase in cell death compared to untreated cells. This increase was more pronounced with the STAT5A

siRNA. We also found that siRNA targeting STAT5A led to an increase in sensitivity of MV4-11s to quizartinib although this effect appeared at most additive (Fig 5.2). This effect was not seen with the STAT5B siRNA.

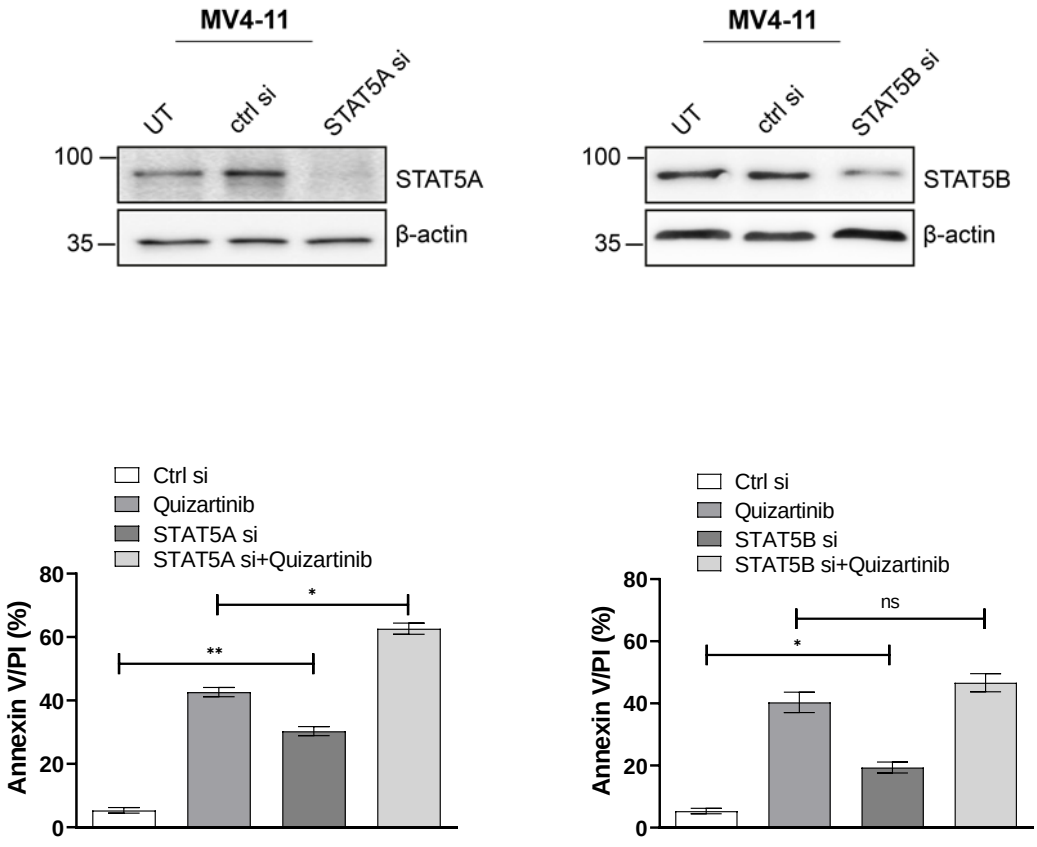

Figure 5.2: Apoptosis in MV4-11 cells following STAT5 knockdown – MV4-11 cells were transfected with STAT5A or STAT5B siRNA (10 nM) for 72h before cells were harvested and analysed by Western blotting. siRNA transfected cells were transfected for 24h before being treated with quizartinib (100 nM) for 48h. Apoptosis was measured using Annexin V/PI staining. Results represent the mean +/- SEM for 3 independent experiments. Significance testing was done by two-tailed paired *t*-test (n=3),**P*≤0.05, ***P* *≤0.01, ns, not significant.*

5.2.3 Design of STAT5A CRISPR

Our results appeared to show a potential role for STAT5A in ITD-expressing cell survival (Fig 5.2). Given the limitations of siRNA in the AML lines we wanted to explore a CRISPR-based system to further study the role of STAT5A in the AML cell lines. These reagents could subsequently be adapted to generate Mcl-1 and Bim-null cell lines to validate their role in FLT3 signalling and quizartinib cytotoxicity.

The STAT5A gene is located on the human chromosome 17 and consists of 20 exons (794 amino acids). To knockout STAT5A we designed three different guides targeting exon 1. A double-guide system was employed in which 2 guides are chosen which span the region of interest. Work in our laboratory has shown that this results in the deletion of a fragment of DNA between each Cas9 cleavage site. This makes identification of edited cells much easier than when using single guides as it is unnecessary to use DNA mismatch assays, such as Surveyor^{TM}, to identify edited clones. Genomic PCR across the edited region is sufficient to distinguish heterozygous and homozygous edits. Additionally, evidence suggests that paired guides are more efficient at editing than when used singly (Nicholas Harper personal communication). The cDNA sequence for STAT5A was obtained from the NCBI Unigene database (https://www.ncbi.nlm.nih.gov/unigene).Guide RNAs targeting the STAT5A gene were designed using CRISPoR (http://crispor.tefor.net/). A region spanning the ATG site was used. Guide sequences and their binding location can be found in (Fig 5.3). All guides are immediately 5' to the Streptococcus pyogenes Cas9 (SpCas9) PAM sequence 5' NGG 3' (highlighted in red). The

PAM sequence serves as a Cas9 binding site and the double-strand break (DSB) will occur 3 nucleotides 5' to the PAM site. Guide #1 was chosen to be in the intergenic region upstream of the Exon 1 ATG site and the other two in Exon 1.

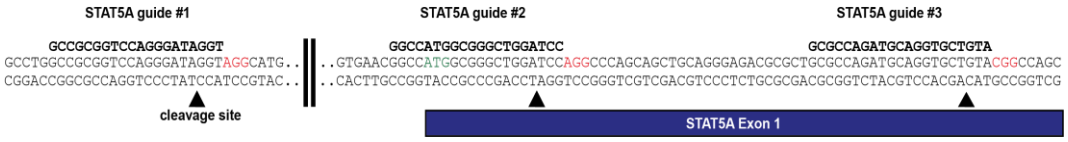

Figure 5.3: STAT5A guide selection – Cartoon of partial Exon 1 and region upstream of ATG in STAT5A gene showing binding of guide RNAs and Cas9 cleavage sites. 5' PAM sequences are depicted in red and ATG is in green.

STAT5A and STAT5B are highly related (96% similar at the amino acid level) and to efficiently target only the STAT5A gene, guides were chosen to be unable to bind STAT5B (Fig 5.4). Whilst there was no homology in the intergenic region of both genes (so guide #1 can only bind the STAT5A gene) the coding region of Exon 1 has similarity so guides were designed at position where their binding to STAT5B would be disrupted while still exhibiting low off-target effects according to the CRISPoR tool.

Figure 5.4: STAT5A and STAT5B Exon 1 alignments and guide binding – Alignment of Exon 1 of STAT5A and B. Guides were chosen such that they failed to target STAT5B. There is no similarity between STAT5A and B in the region upstream of the ATG therefore guide 1 cannot be shown.

5.2.4 Cloning of guide RNA plasmids

To generate the guide RNA plasmids, we used LentiCRISPR (Addgene - #52961) as a backbone. This plasmid contains a human U6 promoter and spCas9 together with a puromycin selection marker. The original EF-1α core promoter was replaced with a spleen focus-forming virus (SFFV) promoter as this has previously been shown to work well in haematopoietic cells lines.

For guide cloning the CRISPoR-designed oligos were phosphorylated with T4 Polynucleotide Kinase and annealed. The plasmid was digested with BsmB1 to remove the stuffer leaving 3’ and 5’ overhangs. Guide oligos were also designed with overhangs already present when annealed. Following ligation, transformation, and screening (as described in Materials and Methods) plasmids were sequenced to ensure correct guide incorporation. The plasmid map and cloning strategy for LentiCRISPR is shown in (Fig 5.5).

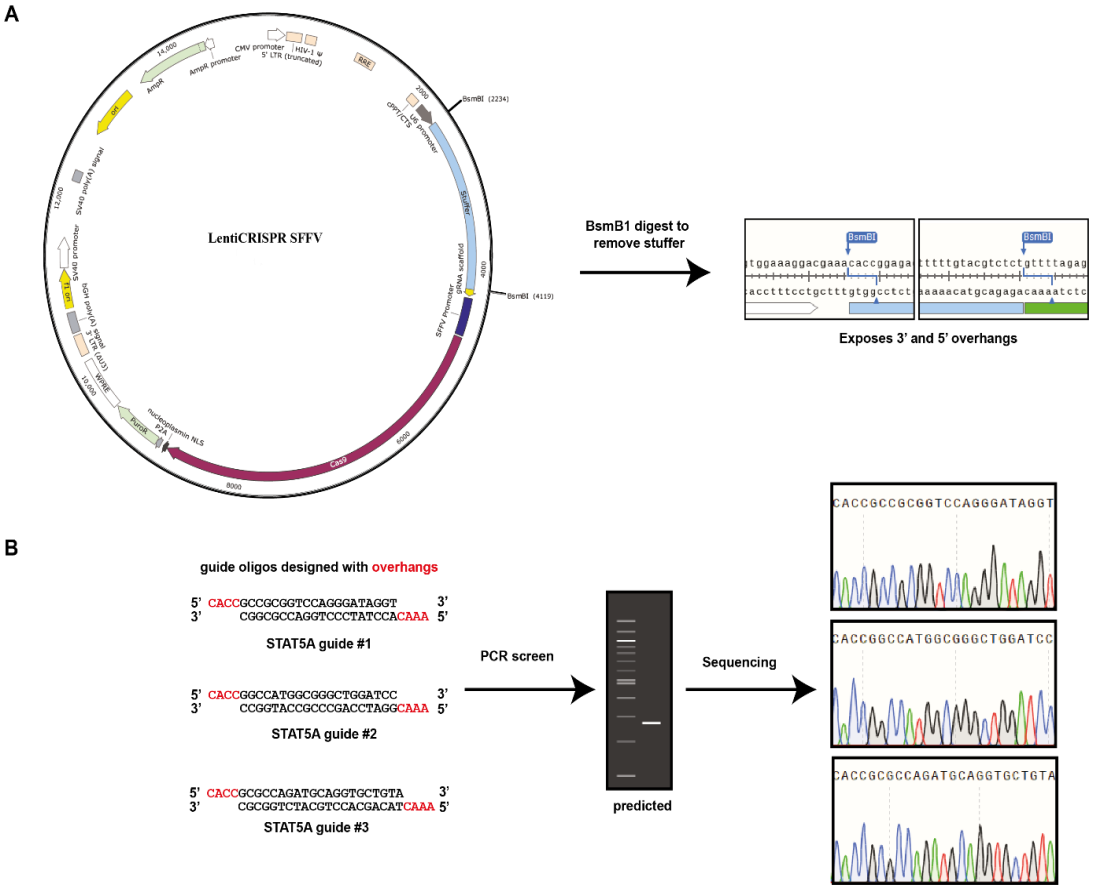

Figure 5.5: Cloning STAT5A guides into modified LentiCRISPR plasmid – A) Schematic of modified LentiCRISPR plasmid used for guide cloning. Digestion with BsmB1 results in removal of stuffer region and exposure of compatible overhangs. **B)** Ligation of annealed guide oligonucleotides containing compatible overhangs, followed by PCR screening and sequencing.

5.2.5 STAT5A Exon 1 genotyping

Before testing the guide plasmids, we needed to design and optimise primers to detect the genomic regions being targeting (Exon 1 in STAT5A). We designed several primers spanning the targeted region ensuring the guide sequences and PAM sites were within the amplified region. A schematic of the primers and their location with respect to the guide sequences is shown in (Fig 5.6A). All primers sets were checked using the NCBI BLAST algorithm (https://blast.ncbi.nlm.nih.gov/Blast.cgi) to ensure specificity.

All combination of primer sets were tested on genomic DNA extracted from HEK-293T cells. Multiple PCR products were detected in the genotyping PCR for STAT5A Exon 1. No difference was observed between the predicted product size and that found when carrying out the PCR, indicating all tested primers worked successfully (Fig 5.6B).

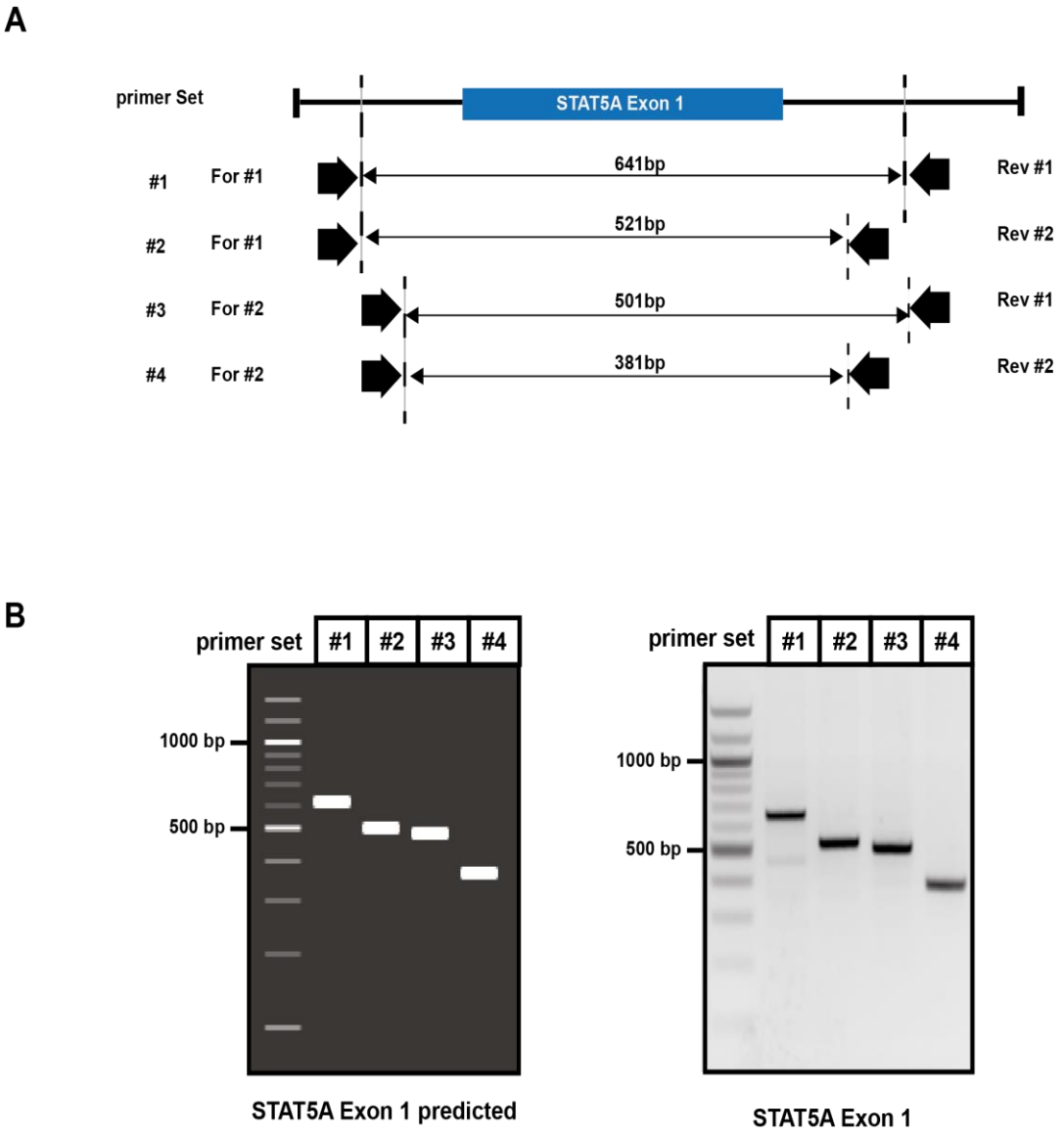

Figure 5.6: STAT5A Exon 1 genotyping PCR – A) Schematic of genotyping primer pair combinations for screening Exon 1 of STAT5A gene. **B)** Predicted products using Snapgene™ and PCR on HEK-293T genomic DNA using paired primer sets.

5.2.6 Validation of CRISPR plasmids

Guide plasmids were validated by transfection in pairs. Our lab has previously noted that when two guide plasmids are transfected a fragment of DNA between both guide cleavage sites is released. If guides are chosen sufficiently far apart this can simplify screening for knock-out alleles.

A schematic of the guide sequences and adjacent PAM sites can be seen for STAT5A Exon 1 (Fig 5.7A). Guide #1 in the intergenic region 5' to the ATG is paired with either guide #2 or #3 in Exon 1. This would be predicted to produce deleted fragments of sizes 104 and 153bp respectively (Fig 5.7A). HEK-293T cells were used for guide validation as they are easy to transfect. Two clones of each plasmid (A and B) were chosen for each guide to ensure no artefacts had been introduced when cloning and cells harvested for genotyping 72h after transfection. Figure 5.7B shows the predicted agarose gel of PCR products expected from transfected cells. Figure 5.7C shows the results in untransfected (ut) and transfected HEK-293T cells. As predicted the exon-spanning primer set 2 gives a 521 bp product in all cells acting as a control for the genotyping PCR. The lower bands only occur in transfected cells and directly correlate with the sizes of the predicted deletion fragments. The two guides would produce site-specific DSBs at the two loci and thus remove the section of DNA between the two guides. The bp deletion products between the two guides was predicted to be 153 bp and 104 bp which is confirmed by the lower bands shown on the gel (Fig 5.7C). Deletion fragments in all transfected cells confirmed that all 3 guide sequences were able to target and cut within the Exon 1 region of STAT5A.

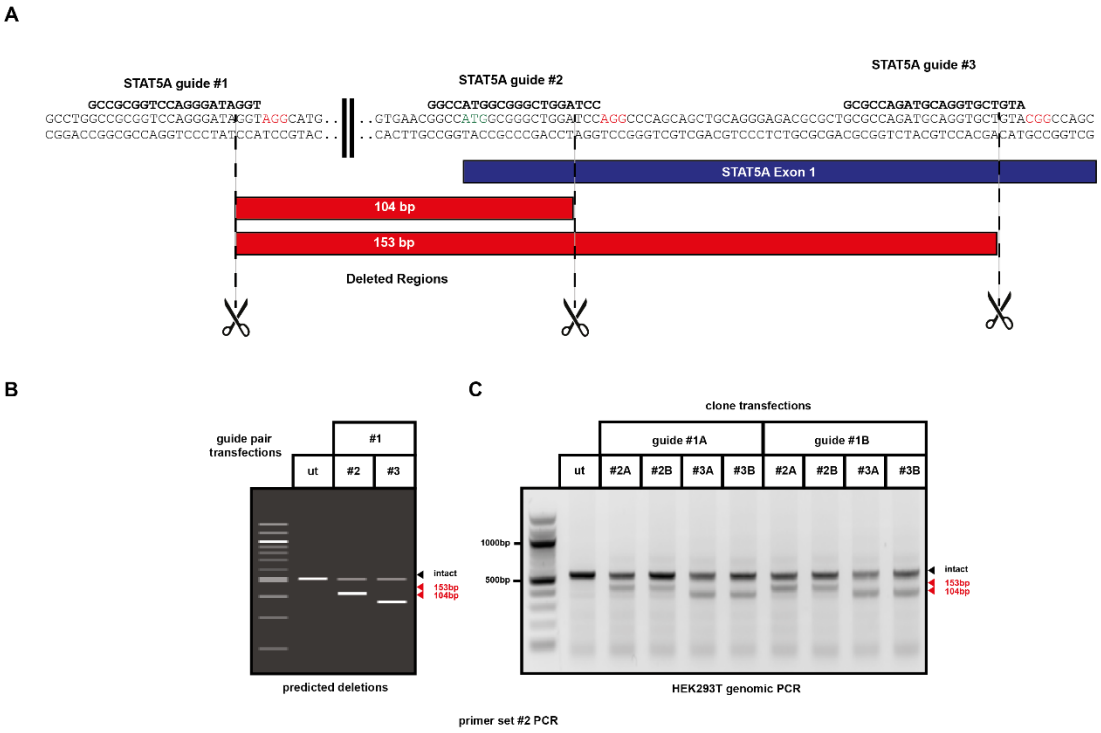

Figure 5.7: Validation of STAT5A guides in HEK293Ts – A) Schematic of STAT5A Exon 1 and ATG upstream sequence. Indicated are guides, PAMs and Cas9 cleavage sites. 2 different guides result in a "double-cut" and the removal of a "chunk" of DNA in between the cleavage sites (pictured in red). **B)** Predicted PCR products obtained from double-guide transfection. **C)** Validation of guides pairs in HEK293Ts. HEK293T cells were transfected with indicated guide plasmids for 72h following which genomic DNA was isolated and CRISPR cleavage efficiency validated by PCR.

To further confirm the exact deleted region the 3 bands obtained from transfection (untransfected, guide #1/2, guides #1/3) were amplified, extracted and Sanger sequenced. Results confirm that primers are amplifying Exon 1 of STAT5A (Fig 5.8). Sequencing of guide transfected cells shows that fragments are excised from the region surrounding Exon 1 exactly as predicted with flanking regions corresponding exactly to the guide RNA and Cas9 cleavage sites (3 bp 5' to the PAM sequence).

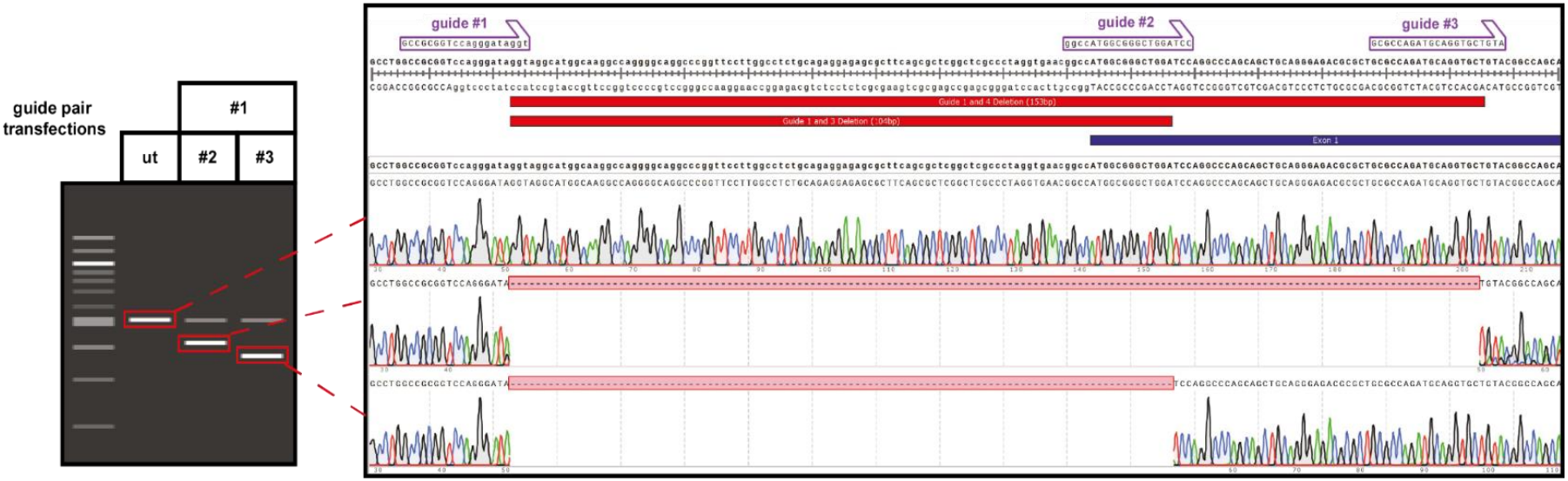

Figure 5.8: STAT5A Exon 1 deletion sequencing – PCR products from indicated guide pair transfections were amplified, extracted and subjected to Sanger sequencing to identify deleted regions and Cas9 cut sites.

5.2.7 CRISPR-Based Lethality Assay

The LentiCRISPR plasmids we used to validate the guide sequences are an example of an all-in-one plasmid as they also contain the Cas9 endonuclease. Lentivirus packaging constraints preclude us from adding an additional guide cassette therefore validated guide cassettes (U6 promoter, gRNA and tracr RNA) needed to be transferred to a smaller plasmid. Our preliminary siRNA results indicate that knocking-down (or knock-out) of STAT5A may be lethal in ITD-expressing cells in which case we would be unable to derive any knockouts. We therefore designed a CRISPR-based lethality assay which could be performed in cells that already express Cas9 (see later section 5.2.9) under the control of an inducible promoter. We would only need to supply the 2 guides to edit STAT5A in the cells. The plasmid would require visualization (EGFP) and a selection marker (puromycin) and be introduced using an integration competent virus (Fig 5.9A). If lethality was not observed, knockouts could be made using the same plasmid in an integration deficient virus (IDLV) which would still allow us to use the markers for selection, but they would only be transiently expressed.

The double guides would be inserted into a custom pLeGO plasmid generated in our lab (Addgene # 27341) which had been modified to include an EGFP marker fused to a puromycin resistance gene using a viral 2A peptide. Two MCS sites for guide cassette cloning had also been inserted flanking the selection markers (Fig 5.9B).

A

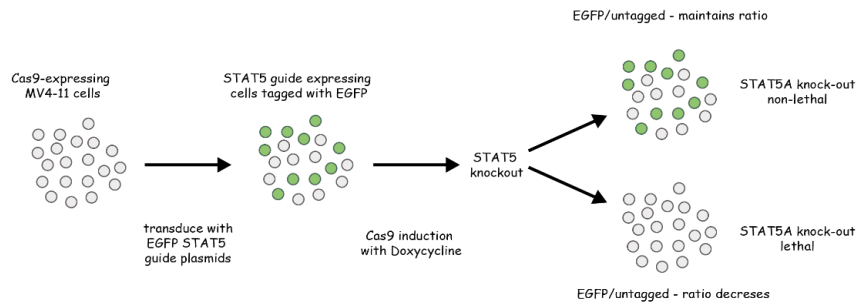

B

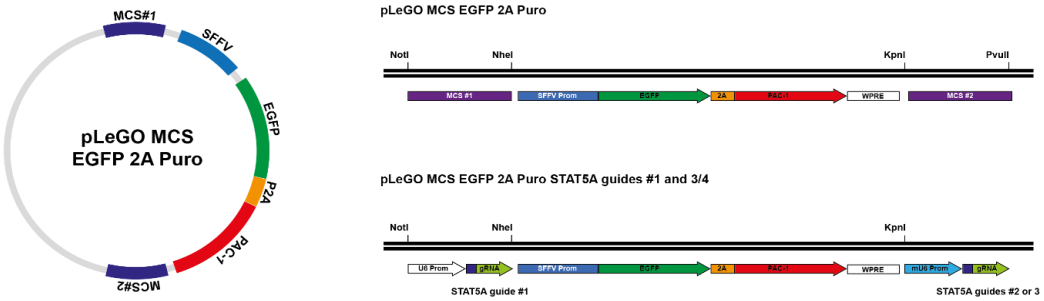

Figure 5.9: A CRISPR-based STAT5A Lethality Assay – A) Cartoon of a CRISPR-based lethality assay. Tetracycline-dependent Cas9-expressing MV4-11 cells are transduced with lentivirus containing STAT5A guides together with EGFP and puromycin markers. Cells are selected with puromycin to enrich transduced cells (to ~ 50% of population). Cas9 is then induced using Doxycycline. STAT5A will only be edited in the EGFP-positive cells and these will be removed from the population if its deletion is lethal. Maintenance of EGFP/non-transduced cell ratio means STAT5A is non-lethal. **B)** Custom plasmid for double guide and marker expression for lethality assay. The modified pLeGO lentiviral plasmid contains 2 multiple cloning sites for cloning guides cassettes (promoter and sgRNA) and EGFP and PAC-1 (puromycin resistance) markers for checking transduction efficiency and selection.

5.2.8 Double-guide cloning and validation

To avoid potential recombination issues due to the presence of 2 similar U6 promoters we cloned guides #2 and 3 into a LentiCRISPR plasmid containing a murine U6 promoter in place of the human variant (gift from Nicholas Harper, University of Liverpool). The double guide plasmids were then synthesised first by amplifying guide cassette #1 by PCR then cloning this into the first MCS of the modified pLeGO plasmid using the Not1 and Nhe1 sites. pLeGO MCS was digested with Not1 and Nhe1 and gel extracted. After ligation and PCR screening, clones were verified for insertion by Sanger sequencing (Fig 5.10A).

The second guide containing the mU6 promoter was amplified from LentiCRISPR mU6 and inserted into MCS#2 using the Kpn1 and PvuII sites. pLeGO MCS STAT5A guide #1 was digested with Kpn1 and PvuII and following gel extraction either guide cassette #2 or #3 inserted. Positive clones were identified by colony PCR and cassettes vefieid by sequencing (Fig 5.10B).

A)

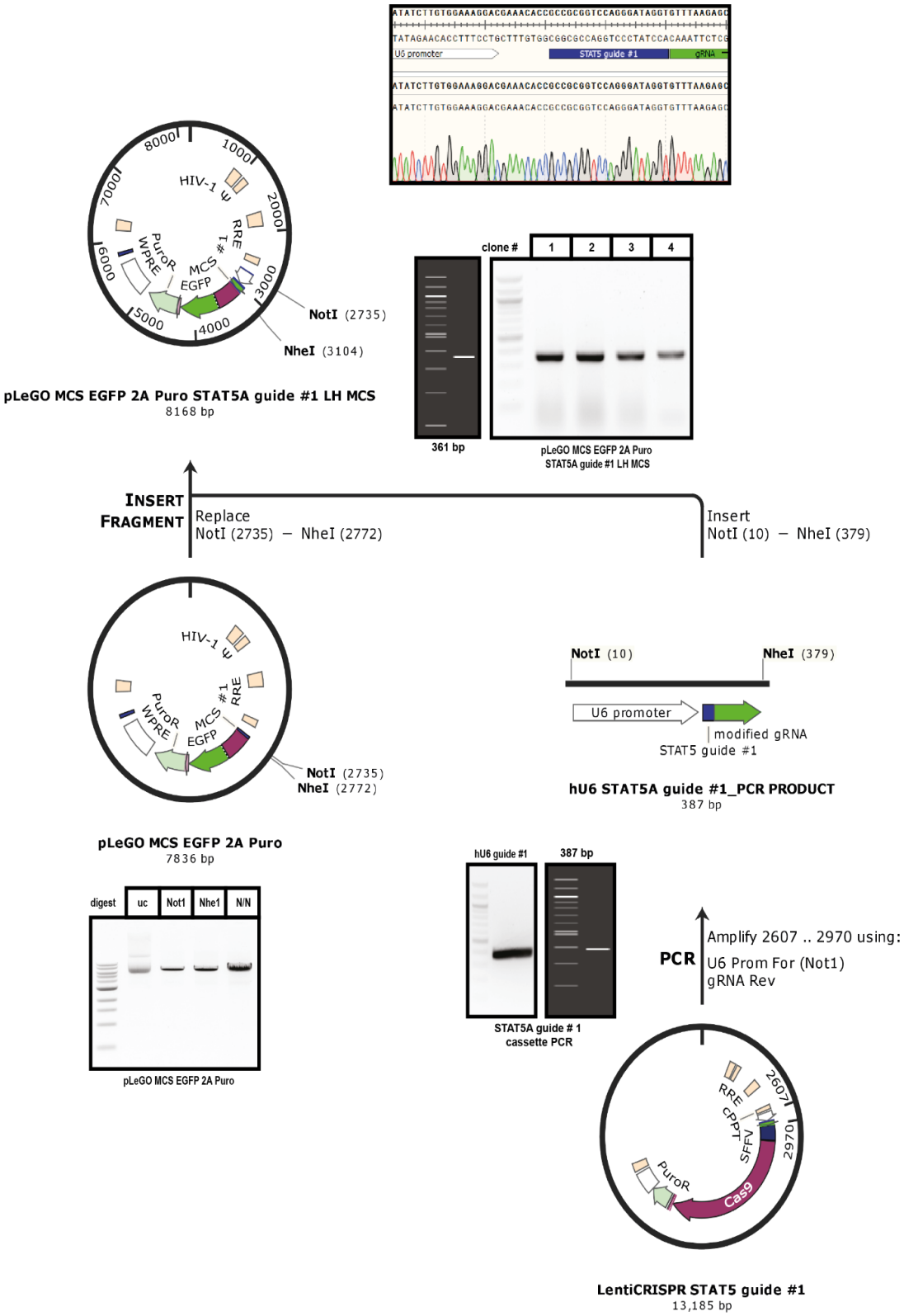
U6 promoter
STAT5 guide #1
gRNA
clone #
1
2
3
4
361 bp
pLeGO MCS EGFP 2A Puro
STAT5A guide #1 LH MCS
HIV-1 Ψ
RRE
cPPT
SFFV
MCS
EGFP
PuroR
WPRE
NotI (2735)
NheI (3104)
pLeGO MCS EGFP 2A Puro STAT5A guide #1 LH MCS
8168 bp
INSERT FRAGMENT
Replace
NotI (2735) – NheI (2772)
Insert
NotI (10) – NheI (379)
NotI (2735)
NheI (2772)
pLeGO MCS EGFP 2A Puro
7836 bp
NotI (10)
NheI (379)
U6 promoter
modified gRNA
STAT5 guide #1
hU6 STAT5A guide #1_PCR PRODUCT
387 bp
digest
uc
Not1
Nhe1
N/N
pLeGO MCS EGFP 2A Puro
hU6 guide #1
387 bp
STAT5A guide # 1
cassette PCR
PCR
Amplify 2607 .. 2970 using:
U6 Prom For (Not1)
gRNA Rev
2607
2970
Cas9
LentiCRISPR STAT5 guide #1
13,185 bp

B)

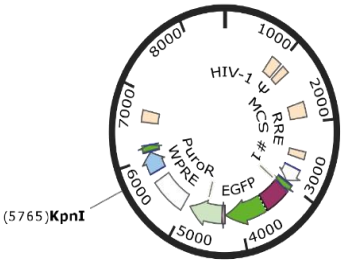

pLeGO MCS EGFP 2A Puro STAT5A guides #1 and 3
8566 bp

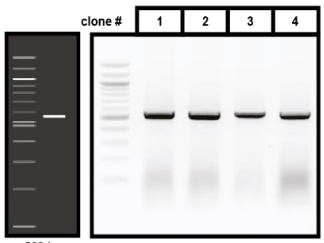

INSERT FRAGMENT
Replace
KpnI (5765) – PvuII (5814)

Insert
KpnI (8) – End (455)

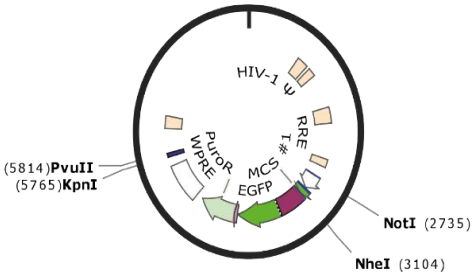

pLeGO MCS EGFP 2A Puro STAT5A guide #1 LH MCS
8168 bp

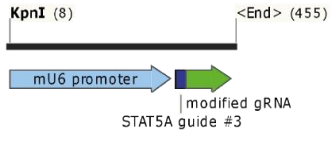

mU6 STAT5A guide #3_PCR PRODUCT
455 bp

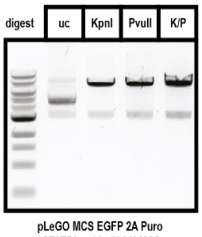

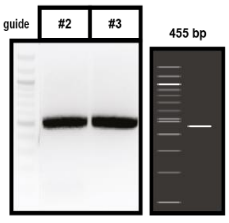

PCR
Amplify 2602 .. 3053 using:
mU6 Prom For (KpnI)
gRNA Rev (blunt)

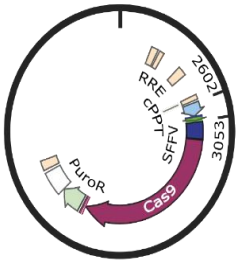

LentiCRISPR mU6 guide #3
13,284 bp

Figure 5.10: Cloning STAT5A double guides (pLeGO) – A) STAT5A guide #1 was inserted into the left-hand MCS of pLeGO MCS EGFP 2A Puro. The human U6 (hU6) promoter and guide #1 sgRNA cassette was first amplified from LentiCRISPR, purified, and digested together with the plasmid with NotI and NheI. Digested vector and insert were ligated and transformed, and clones screened for insertion by colony PCR. Clones were sequenced verified before use. **B)** Guides #2 and 3 insertion into right-hand MCS. A guide cassette containing a murine U6 promoter (mU6) and either STAT5A guides #2 or 3 was amplified from LentiCRISPR mU6 then inserted into the previous guide #1 plasmid by KpnI and PvuII digestion and ligation. Following colony screening several clones were sequence verified before use.

Double-guide plasmids were validated in HEK293T cells. Cells were transfected with each plasmid in combination with empty LentiCRISPR (to supply the Cas9 enzyme). 72h after transfection cells were imaged to visualise the EGFP marker then harvested for genotyping. Again 2 clones of each plasmid were verified for activity. As expected, all plasmids resulted in EGFP positive cells following transfection (Fig 5.11A). Transfection of these plasmids should also lead to the deletion fragments we observed previously. Genotyping indicated that both combinations of guides #1/2 and those of #1/3 resulted in the expected deletion fragments (Fig 5.11B) with the combination of guides#1 and 3 being the more efficient pairing. This shows that duplexing of both guides into the marker plasmid still results in the expected editing.

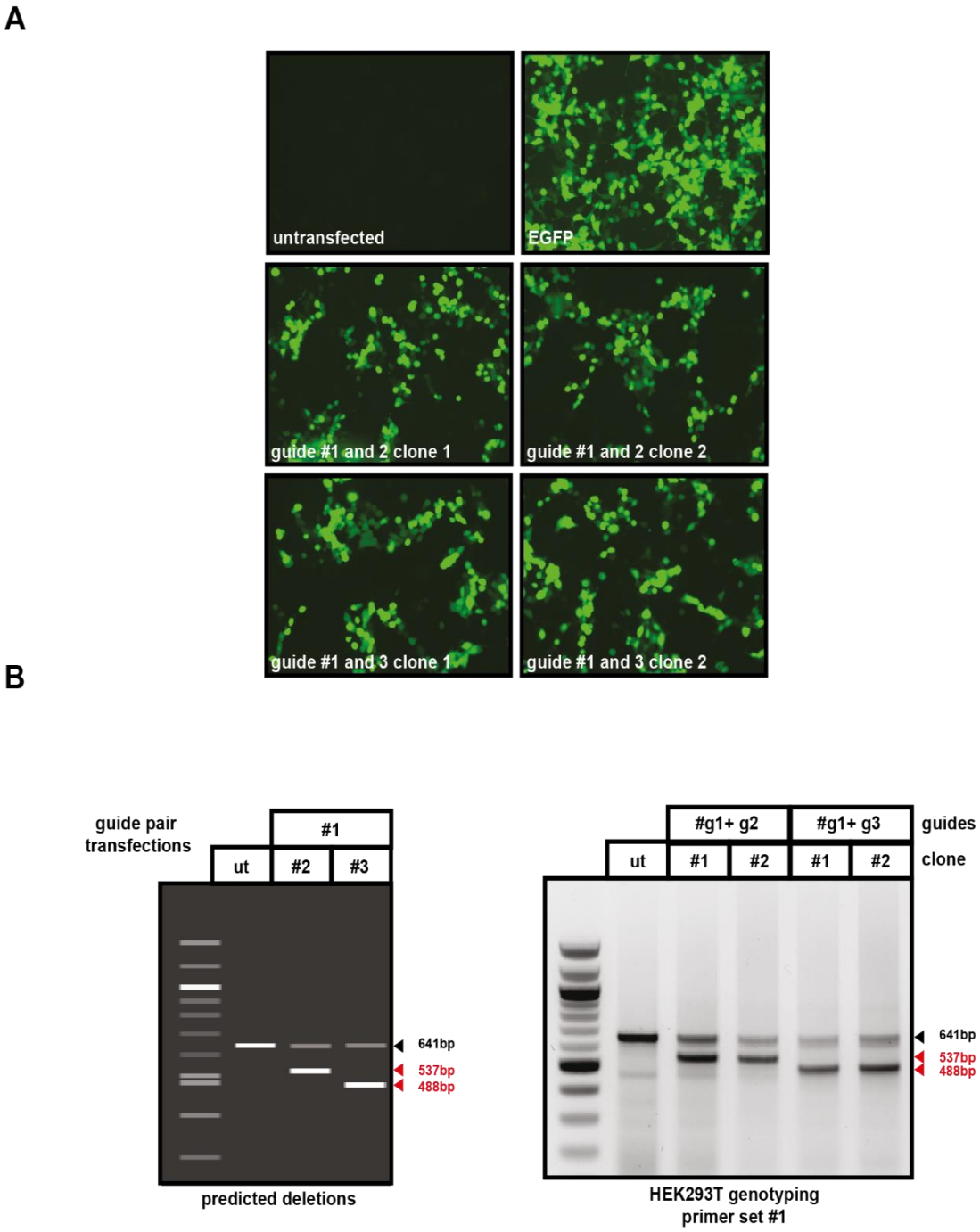

Figure 5.11: Validation of STAT5A double guide plasmids – Double-guide plasmids were transfected into HEKs together with an "empty" LentiCRISPR plasmid (to provide spCas9) for 72h. **A)** Cells were first analysed for EGFP expression. **B)** Cells were harvested, genomic DNA extracted, and deletion efficiency assessed by genotyping with primer set #1.

5.2.9 Generation of MV4-11 cells expressing inducible Cas9

The double-guide plasmids we generated to edit the STAT5A gene will require the presence of the Cas9 endonuclease for editing in our target cells. It would therefore be useful to have MV4-11 cell lines that already expressed Cas9 to use with these plasmids and any future editing studies (Bim and Mcl-1 etc). Puromycin was chosen for the guide plasmids as it kills quickly in the AML cell lines. We therefore needed to utilise a different antibiotic for production of stable Cas9-expressing cells. Additionally, it would be better if the Cas9 protein was under an inducible promoter and not constitutively expressed. As mentioned previously the use of an IDLV would ensure the guide and markers are not integrated into the host cell genome.

We chose the pCW Cas9 plasmid (Addgene # 50661) which was modified by replacing the PAC-1 puromycin resistance gene with a Blasticidin resistance marker (Fig 5.12A). Transfection of the original and modified plasmid into HEKs followed by Doxycycline treatment showed Cas9 induction with both plasmids as detected by Western blot (Fig 5.12B). MV4-11 cells were transduced with Lentivirus expressing the Cas9-blast plasmid and selected for 7-10days with Blasticidin. We wished to generate clonal cells from this population so after freezing down an initial pool, selected cells were plated into 6-well plates in Methylcellulose-containing RPMI. This semi-solid medium enables cell clones to form “clumps” within ~10 days after which they are picked and expanded, first in 96 well plates then bulked up as required. Clones are tested for Cas9 expression following Doxycyline treatment a soon as is possible to avoid growing negative or low-expression clones (Fig 5.12C).

Positive clones are further expanded for freezing and Cas9 induction re-checked as before (Fig. 5.12D). As mentioned previously these cells can be used for numerous editing studies as they only require transduction with different guide-containing plasmids.

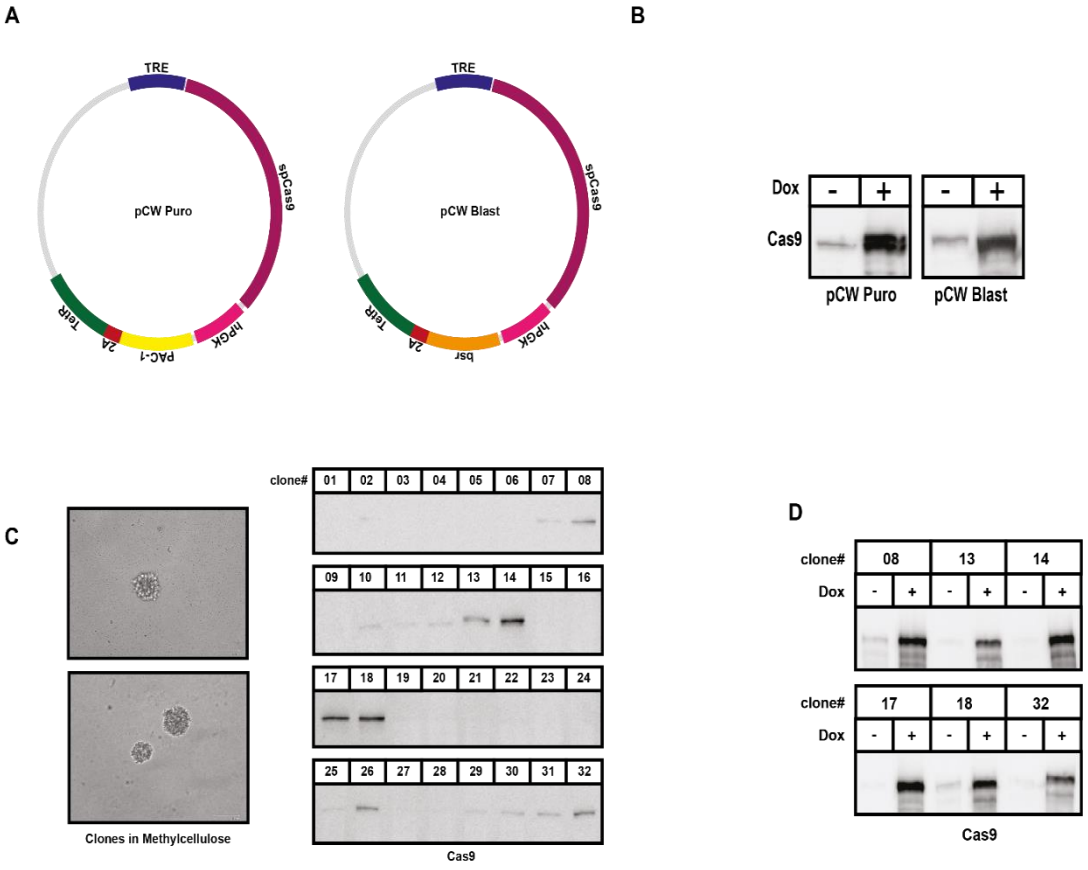

Figure 5.12: Generation of Cas9-inducible MV4-11 clones – A) Schematic of pCW Blast derived from pCW (AddGene #50661). The original pCW contains the puromycin resistance gene PAC-1 which has been replaced with the Blasticidin S-resistance gene (bsr) in pCW Blast. **B)** Validation of plasmids in HEK293Ts. pCW plasmids were transfected into HEK293T cells, 24h later Cas9 expression was induced with Doxycycline (2 µg/ml) for 72h after which cells were harvested and lysates subjected to Western blotting for spCas9. **C)** Generation of Cas9-expressing cells. Lentivirus was generated from pCW Cas9 and used to transduce low passage MV4-11 cells in the presence of

polybrene (1 µg/ml) for 72h, cells were then passaged and subjected to selection with Blasticidin (7.5 µg/ml) for 7 days. Clonal isolation of Cas9-expressing MV4-11 cells was performed by culturing the cells in Methycellulose (2.5 %). 7-10 days following plating clones were isolated from the semi-solid medium and transferred to 96-well plates for expansion and expression analysis by Western blot. **D)** Western blot verification of inducible Cas9 expression in a sample of expanded clones.

5.3 Discussion

Given the role of STAT5 activation in mediating the oncogenic effects of FLT3-ITD, it is expected that STAT5 gene editing may modulate AML cells survival and proliferation. In this chapter, we were interested to establish a strategy to knock out STAT5 in MV4-11 cells and study whether its expression is required for maintenance of AML cells. Initially, it was an important to explore the function of two members of the protein: STAT5A and STAT5B. Experiments suggested that STAT5A is more critical for AML mediating leukemogenesis. STAT5A mRNA expression was significantly higher in FLT3-ITD cells, which express pSTAT5, compared STAT5B. To validate this, we decided to evaluate the role of total STAT5A by performing the siRNA knock-out experiments in FLT3-ITD cells. The data also suggested that STAT5A knocked down can induce apoptosis to a greater extent compare to STAT5B.

Gene editing using site-directed nucleases such CRISPR-Cas9 can be used to target specific regions of DNA leading to gene disruption. The discovery of the CRISPR/Cas9 system as a gene editing tool is revolutionizing many areas of biomedical research including gene therapy, model cell line development, disease target identification and genomic screening. Its simplicity and flexibility to target nearly any location within the genome explains its popularity and widespread use. While other genome editing tools such as ZFNs and TALENs, have their own advantages, they lack the versatility of CRISPR and require more molecular biology expertise.

Due to their “programmable” nature theoretically any area of the genome is targetable, and we wished to see whether we could use these targeted nucleases to disrupt STAT5A in AML cells. We successfully validated double guide RNA constructs targeting Exon 1 of STAT5A in HEK-293T cells. We cloned CRISPR guides targeting Exons 1, of STAT5A and observed editing in this Exon. Our results show a promising method of using what we describe as a double-guide system to validate the ability of guide sequences to target Cas9 to the correct loci.

In AML, heterozygous rather than homozygous modification of FLT3 alleles is more likely to present in patients. The double-guide system also allows us to easily screen clones for complete knockout (a single band) as well as heterozygosity (would produce a double-band on genomic PCR). It also appears to be more efficient than using single guides (Nicholas Harper personal communication).

The lethality assay is a novel way of using CRISPR to determine whether genes are lethal (prior to making knockouts). These assays would initially be performed with a wt Lentivirus first to assess when a gene was lethal and if not, the knockout lines would be generated using an integration-deficient lentivirus to avoid integration and expression of the EGFP marker.

The Cas9-inducible MV4-11 clones will be of great use in looking at other proteins involved both in ITD signalling and in FLT3L-mediated resistance.

Haemopoietic cell lines in general have proved difficult to clone out and the semi-solid medium strategy used here has been particularly successful. The MOLM-13s should be similarly transduced and single clones isolated.

Clearly, these techniques and tools could be used further study the role of Mcl-1 and Bim in FLT3 inhibition and FLT3L-mediated resistance. It is also possible to introduce mutations within endogenous proteins to model different FLT3 mutations and genotypes.

Chapter VI

==========

General Discussion

6.1 Final Discussion

6.1.1 The ITD mutation affects FLT3 expression and cell surface localisation, resulting in dysregulation of downstream signalling cascades

The identification of mutations in FLT3 and their consequences on its expression and signalling offers new opportunities for targeted therapy in AML. During the past decade, the biology and function of mutated FLT3 and the WT receptor have become clearer. One challenge for AML treatment is the high degree of heterogeneity with respect to mutations and changes in FLT3 expression (Kumar, 2011b). The majority of the mutations involve an ITD, which is associated with poor prognosis and an increased incidence of relapse (DiNardo and Cortes, 2016). Differences in the downstream signalling pathways of ITD- versus WT-FLT3 and how these receptor types respond to stimulation (from endogenous FLT3L) or inhibition (with drugs) would present a better understanding of the disease and its treatment options.

In the first part of this thesis we characterised FLT3 signalling using cell line models with different FLT3 genotypes. ITD-FLT3 exclusively activates STAT5, and this was confirmed using the ITD inhibitor (quizartinib) which led to STAT5 dephosphorylation only in ITD-expressing cells. Other signalling pathways such as MAPK and AKT were activated both by ITD and the ligand-activated WT receptor**.** While our data indicated that ITD-FLT3 can respond to FLT3L resulting in additional activation of ERK1/2 and AKT, this was relatively modest in comparison with its effect on the WT receptor. Notably, STAT5 was not activated by FLT3L in both WT and ITD AML cells. As FLT3L binds and

activates cell surface localised FLT3, the results suggest that activation of ERK1/2, AKT and STAT5 is likely a consequence of differential receptor localisation in addition to mutational status (Takahashi, 2020). The differences observed in signalling present an attractive target for therapeutic intervention.

This led us to next focus on the localisation of the WT and ITD receptors in respond to TKIs or FLT3L and how this influences downstream signalling. Despite the clinical importance of FLT3, the role of subcellular receptor compartmentalisation needs to be further elucidated. We have demonstrated that a particular FLT3 mutation may not only differentially activate downstream pathways, but it also affects the subcellular localisation of the receptor. In our study, we confirmed intracellular accumulation of ITD-FLT3 in both homozygous and heterozygous ITD cells, MV4-11 and MOLM-13 respectively.

When we compared cell surface ITD to WT staining, the latter was mainly localised at the cell surface. Our data also suggests that the intracellular ITD-FLT3 activates STAT5, while ERK1/2 and AKT are activated at the plasma membrane. Inhibition of ITD signalling by quizartinib resulted in the rapid relocalisation of receptor to the plasma membrane which is consistent with an activation-induced internalization model seen in other RTKs such as c-kit (Yee et al., 1994). The fact that cells harbouring homozygous ITD mutations displayed a greater cell surface redistribution than those with heterozygous mutations following quizartinib treatment supports this. By contrast midostaurin (a type I inhibitor) has less effect on redistribution irrespective of

FLT3 genotype which is consistent with it being a poor ITD selective inhibitor. Taken together this data suggests the response to quizartinib depends on a cell's FLT3 genotype. Increased cell surface localisation in FLT3-ITD cells is a likely mechanism for quizartinib to inhibit STAT5 phosphorylation. This may also be linked to the increase in the mature, fully glycosylated form of FLT3 in ITD-expressing cells observed following quizartinib treatment. This result suggests that the ITD mutation may prevent the maturation of FLT3 required for its surface expression and the nature of signalling by the ITD could change upon trafficking of the receptor from the cytoplasmic space to the cell surface.

To confirm this, we re-stimulated FLT3 with FLT3L following quizartinib treatment and assessed the phosphorylation of ERK1/2, AKT and STAT5. Stimulation of surface localised ITD-FLT3 led to activation of ERK1/2 and AKT but not STAT5. Differential signalling as a result of altered localisation in other oncogenic RTKs like c-KIT can be applied to other cancers in order to ascertain if their signalling is similarly affected.

This data not only provides insights into effect of TKIs on the cellular localisation of FLT3 and how this affects the spatial regulation of oncogenic signalling but it also allows us to understand how FLT3-targeted therapy in the presence of FLT3L could lead to an altered biological response. Taken together, the main findings include: deactivation of STAT5 by quizartinib is a result of a change in subcellular localisation of FLT3 from an intracellular space to the cell surface. Secondly, both ERK1/2 and AKT can be activated by ligand

stimulation of cell surface localised WT and ITD-FLT3. An explanatory model is presented in Figure 6.1.

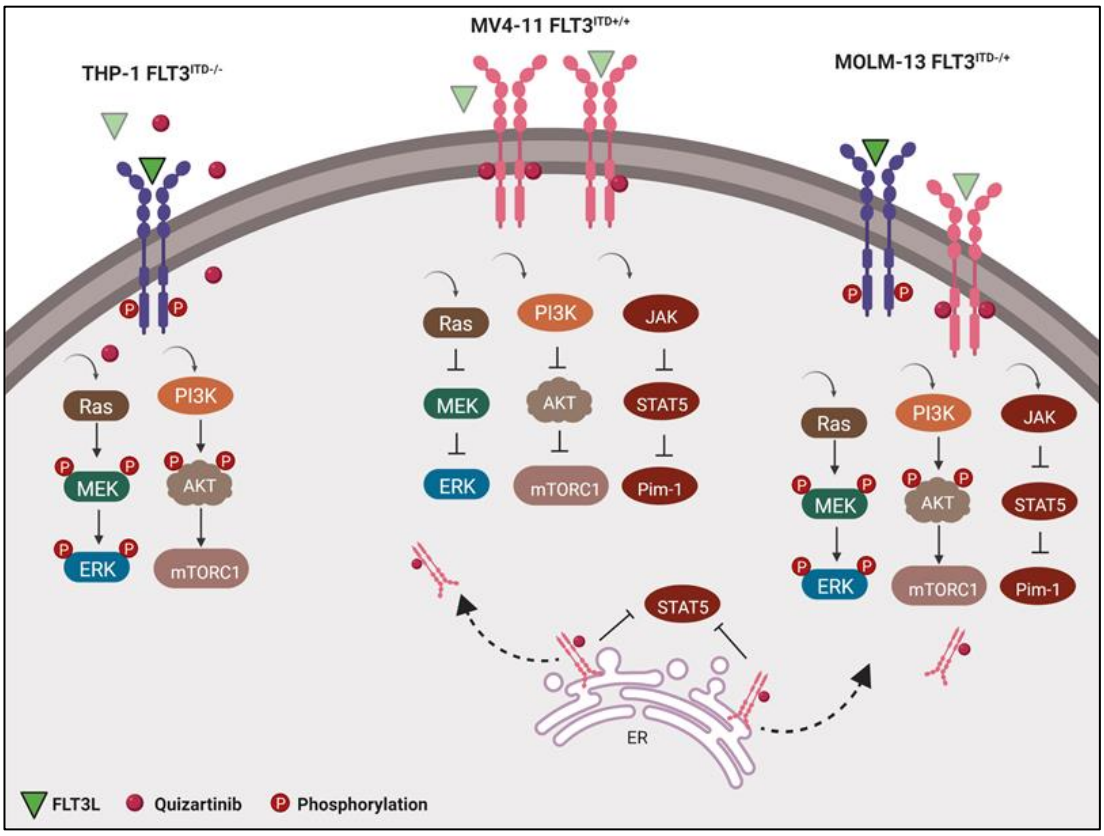

Figure 6.1: Signalling by different FLT3 genotypes in AML.

The loss of the WT allele in ITD patients affects FLT3 dimerization, signalling and clinical outcome. In one study, a high ITD-to-WT ratio in patients was associated with a significantly worse prognosis (Thiede et al., 2002). However, the presence of the WT allele could also modulate receptor activation and therefore affect sensitivity to chemotherapy. In this situation the WT and ITD forms may act independently of one another but it would be interesting to ascertain whether the WT receptor could heterodimerize with the ITD form and what the consequences would be for downstream signalling. Investigating the

role of the WT receptor in FLT3-ITD leukemia will help to understand its prognostic implications and better tailor therapeutic options for leukemogenesis caused by FLT3-ITD mutations.

6.1.2 Targeting the MAPK pathway may overcome FLT3L-mediated resistance to FLT inhibitors in patients with ITD mutations

With the identification of the ITD and other FLT3 mutations as a target for AML therapy, several drugs have advanced into clinical trials, either as monotherapy or in combination with other chemotherapies. Despite the initial clinical efficacy of FLT3 inhibitors, resistance to single agents develops after only a few months of therapy, which can limit their use.

One of the extrinsic resistance mechanisms to FLT3 inhibitors such as quizartinib is the crosstalk between the bone marrow microenvironment and leukemic cells which confers protection and can modulate drug responses. The stromal cells are a source of numerous cytokines that have been shown to support AML growth and proliferation including FLT3L (Wilson et al., 2012). Increased FLT3L levels have been observed in AML patients following treatment with FLT3 inhibitors or conventional chemotherapy and this could potentially play a role in relapse (Stirewalt and Radich, 2003).

Single cell genotyping of FLT3 in AML blasts from patients indicates they express both ITD and WT-FLT3 complicating therapy (Stirewalt et al., 2014). In one study, WT- but not ITD phosphorylation was detectable in plasma

samples from quizartinib treated patients, and this could be augmented by FLT3L reducing the efficacy of FLT3 inhibitors in these patients (Cortes et al., 2013). We found that ITD cells were still responsive to exogenous FLT3L and this could in turn antagonise type II FLT3 inhibitors. The elevated FLT3L levels in patients could act on WT-FLT3 leading to the restoration of signalling which would represent a significant obstacle to the clinical efficacy of some FLT3 inhibitors.

To begin to address the protective mechanisms of FLT3L we looked at the effects of FLT3L on four AML cell lines with varying FLT3 mutational status. We noticed that in the presence of FLT3L, the ITD-cell lines demonstrated varying degrees of resistance to quizartinib, suggesting that both homozygous and heterozygous genotypes can be affected. As would be expected AML cells with heterozygous mutations (MOLM-13) displayed a stronger response to FLT3L and this resulted in increased resistance to quizartinib compared to the homozygous cells. This was confirmed as the IC50 increased significantly with the addition of FLT3L. It was highly likely that this would also occur with other type II inhibitors, and agreeing with this both ITD cells displayed a similar resistance to sorafenib. Despite this, the cells retained their sensitivity to type I inhibitors, gilteritinib and midostaurin, under the same conditions. Given FLT3 mutations are largely heterozygous, this suggests that type I inhibitors or some other way of co-targeting FLT3L signalling when using ITD selective inhibitors would be a preferred treatment.

To investigate the signalling changes associated with FLT3L-mediated response, we looked at survival signalling pathways commonly engaged by FLT3. Reactivation of both AKT and ERK1/2 was associated with inhibition of apoptosis and occurred even in the presence of quizartinib. STAT5 is exclusively activated through ITD-FLT3 so does not play a role in ligand-mediated protection (Piloto et al., 2007). Our results demonstrate that MAPK/ERK likely represents a nexus in the resistance conferred by FLT3L towards FLT3 inhibition. This result is in consistent with other works that have shown the implication of ERK activation in FLT3 inhibitors resistance. The high levels of phosphorylated ERK in leukemia blasts after treatment with sorafenib has been reported and this was despite the continued suppression of p-FLT3 (Borthakur et al., 2011). High ERK activation was also observed in the sorafenib–resistant cell lines and concomitantly targeting FLT3 and MEK with crenolanib and the MEK inhibitor CI1040 induced marked apoptosis (Zhang et al., 2014).

While using pan-kinase inhibitors abrogates this resistance, patient tolerance remains an issue. Given that only type II inhibitors are affected by FLT3L, we propose the combination of type II FLT3 inhibitors (with more selectivity towards the ITD mutation) and MEK inhibitors such as trametinib, U0126 or imatinib may represent a novel approach in AML patients with FLT3 mutations who also present with elevated plasma levels of FLT3L. This combination triggered a dramatic pro-apoptotic effect in the ITD cells treated with FLT3L. This strategy may not only overcome the limitation of FLT3L reduced drug efficacy in ITD cells but could also prevent adaptive TKI-resistance, a frequent

problem in single agent TKI-treatment. Further preclinical models and clinical trials are needed to translate these findings into novel therapeutic approaches. It would be of interest to investigate the role of RAS protein in FLT3L-mediated resistance. ERK1/2 is a downstream protein of RAS, and RAS mutation has been shown to cause a persistent activation of ERK1/2 and limit the efficacy FLT3 inhibitors (McMahon et al., 2019). The long exposure of AML cell line to FLT3L or FGF2 lead to acceleration of resistance development. Indeed, removing FLT3L or FGF2 greatly accelerated the acquisition of KRAS mutations which means upon removal of cytokines the resistant cultures are not depended on the presence of the cytokines/growth factors anymore (Traer et al., 2016). RAS protein is not mutated in MV4-11 or MOLM-13, and if RAS mutation can be developed to quizartinib (second generation-type II) and sorafenib (first generation-type I) as a result of FLT3L treatment for long time needs more investigation with all downstream cascades related to RAS activation. This actually may be related to late rescue of ERK1/2 in MV4-11we observed in our study.

6.1.3 Role of Bcl-2 family members in FLT3 signalling and Quizartinib cytotoxicity

The Bcl-2 family play a crucial role in both promoting and inhibiting cell death in many tumor types (Warren et al., 2019). Mcl-1 is overexpressed in most bone marrow cell samples taken from newly diagnosed AML patients (Xiang et al., 2009). Additionally, Mcl-1 overexpression has been identified as contributing to the development of resistance to the Bcl-2 inhibitor venetoclax in relapsed AML (Kaufmann et al., 1998). Therefore, Mcl-1 is involved not just

in promoting AML survival, but also promoting drug resistance (Glaser et al., 2012). We were interested to establish if Mcl-1 played a role in FLT3 signalling and FLT3L-mediated resistance. We have shown that in AML cells the expression of Mcl-1 is regulated by FLT3 signalling through the MAPK pathway. Both ITD and WT-FLT3 could induce Mcl-1 expression implicating it in FLT3L-mediated resistance and suggesting that targeting Mcl-1 may offer a potential avenue for therapy in AML.

The efficacy of S63845, a potent selective Mcl-1 inhibitor, was evaluated in the ITD-expressing cells. Selective inhibition of Mcl-1 by S63845 was effective in ITD cells when used alone as the viability of MOLM-13 and MV4-11 cells was significantly decreased. Co-treatment with quizartinib abrogated the protective effect of FLT3L but cell death was only slightly increased compared to Mcl-1 inhibition alone. Mcl-1 knockdown by siRNA sensitized MV4-11 cells to quizartinib and prevented resistance mediated by FLT3L. Therefore, targeting Mcl-1 alone may be a potential option for AML treatment. These results indicate that S63845 not just used as a combination with quizartinib to abrogate FLT3L effect but also acted as a single agent to counteract FLT3L in ITD cells.

By using cBioportal database and TCGA data sets in the cBioPortal for Cancer Genomics (Figure A8, A-D), we showed that FLT3 is significantly mutated in AML with about 28% of patients have somatic mutations in FLT3, compared with other types of cancer. This is in consistent with the data showed that

FLT3-ITD is found in approximately 25-30% of adult patients over 55 years of age (Stirewalt et al., 2001). Furthermore, this mutations is associated with the overexpression of FLT3 that observed in AML patients. TCGA data also indicated that FLT3 is significantly overexpressed in AML compared to other cancer types. Supporting the data we showed and others for the role of Mcl-1 in AML, the TCGA data show that AML patents also express a high level of Mcl-1 among 33 cancer cell types. The higher levels of Mcl-1 expression have been associated with poor prognosis and can be used for disease monitoring (Li et al., 2019). Indeed, there was a positive correlation between FLT3 and Mcl-1 expression in AML patients, and this can be further investigated for the rational of co-targeting FLT3 and Mcl-1 as this be can a potential therapeutic target in the treatment of newly diagnosed and relapsed AML (Gao et al., 2013, Cerami et al., 2012, Network, 2013).

Sorafenib is type 2 first generation FLT3 inhibitor and has been shown to downregulate Mcl-1 and upregulate Bim in FLT3-ITD AML clinical trials (Zhang et al., 2008). Quizartinib is second generation with more selectivity toward mutant FLT3. We were interested to observe quizartinib exhibited the same effect in the context of our project and what pathway was involved. Perhaps the most profound effect we saw was on the pro-apoptotic Bcl-2 family member Bim. Following quizartinib treatment there was a significant increase in Bim expression, and this could be clearly antagonised in a heterozygous cell line by the addition of FLT3L. The importance of Bim was further supported with siRNA which abrogated quizartinib-mediated cell death.

Our data indicates a model whereby constitutive MAPK signalling through ITD-FLT3 supresses Bim expression effectively protecting the cells from apoptosis. This is further aided by upregulation of Mcl-1 (Fig 4.6). Inhibition of FLT3 with quizartinib causes Bim upregulation and possibly downregulation of Mcl-1 leading to apoptosis. This is antagonised in heterozygous cells by the presence of FLT3L which, as its unaffected by quizartinib, can still signal through MAPKs to supress Bim expression, protecting the cells. We were able to counteract this with the MEK inhibitor trametinib or U0126 which acted to inhibit the effect of FLT3L. This provides a potential novel therapeutic option when using type II inhibitors in patients with high plasma levels of FLT3L. An explanatory model for the role of Mcl-1 and Bim in ITD and FLT3L signalling is presented in Figure 6.2.

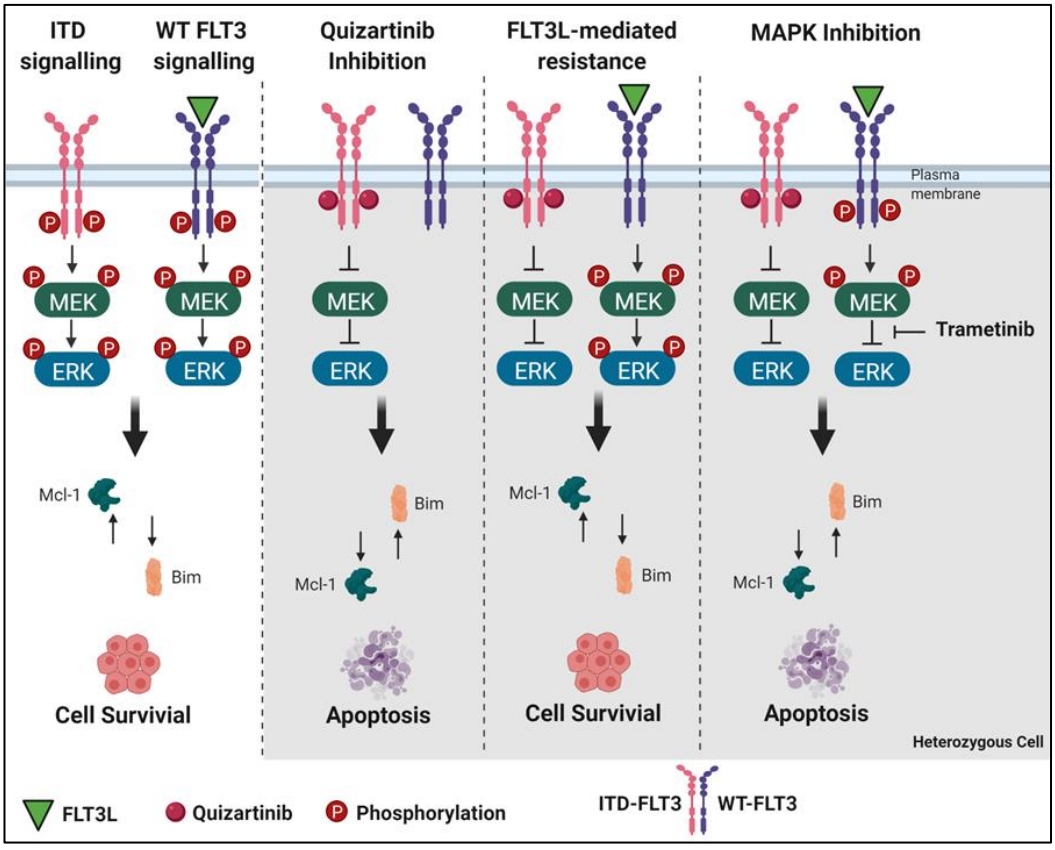

Figure 6.2: ITD regulation of Mcl-1 and Bim.

6.1.4 Gene Editing STAT5A using a double-guide RNA CRISPR-Cas9 system

CRISPR is a powerful tool to precisely change the DNA sequence at a target location or prevent gene expression by disruption of genes. “Knock-outs” have several advantages over transient knockdown methods such as siRNA or shRNAs the main ones being the changes are permanent and following selection of clones, complete, whereas the knock-down efficiency can vary.

A number of studies have used CRISPR library screening in AML to investigate drug mechanisms including examining factors required for quizartinib toxicity (Hou et al., 2017, Tzelepis et al., 2016). Despite this manipulating individual proteins in haematopoietic cells is still in its infancy probably due to the difficulty in introducing the components at sufficient efficiency to cause editing and the difficulty in the subsequent isolation of clonal cells. While we were unable to realise fully the potential of our CRISPR experiments, the tools generated will be of great use for further dissecting the role of FLT3 in AML. We generated Cas9-expressing MV4-11 cells and a lab colleague has done the same for the MOLM-13s. This enables us to study uniquely the effect of FLT3 genotype on the efficacy of inhibitors.

One way of avoiding, at least the cell line-to-cell line heterogeneity would have been to use CRISPR to introduce reciprocal mutations into the MV4-11 and MOLM-13s or in the WT-FLT3 THP-1 cell lines. This would have the additional benefit of resulting in cells with what we would predict as endogenous

expression levels of FLT3 assuming the mutations introduced did not somehow affect protein stability. At least they would be subject to the control of the endogenous human FLT3 promoter. It would be of interest to pursue such experiments in future studies. It will be possible to target specifically mutated alleles and therefore an ITD allele in MV4-11s could be reverted to WT to observe whether the protective effects of FLT3L are reproducible in another cell background. In a similar way the ITD allele in the MOLM-13s could be mutated to WT variant. Whilst we identified two distinct ITDs in our cell line models, many others exist and these could all be modelled using the cell lines and tools we generated, again to ascertain the efficacy of inhibition and protection afforded through the WT receptor. Additionally, as FLT3 is not the only protein mutated in AML, these lines could also be used to investigate ITD signalling and the role of FLT3L on the background of other AML mutations such as those in NPM-1 and DNMT3A.

The main objective of this work is to highlight that careful treatment strategies are needed for targeted FLT3 therapy in order to increase the efficacy and decrease resistance. The current approach in drug development is to enhance drug efficacy and selectivity. However, these factors are not sufficient to achieve remission and does not preclude development of resistance even with the newer highly selective FLT3 inhibitors. When using FLT3 inhibitors in patients presenting with ITD mutations three factors need to be closely monitored: FLT3 genotype, type of FLT3 inhibitors and FLT3L plasma levels. Our data suggests that the efficacy of the type II inhibitors in patients with heterozygous mutations and high plasma levels of FLT3L will be improved by

co-administration with a MAPK inhibitors, Mcl-1 inhibitor or, glycosylation inhibitors (summarised in Figure 6.3).

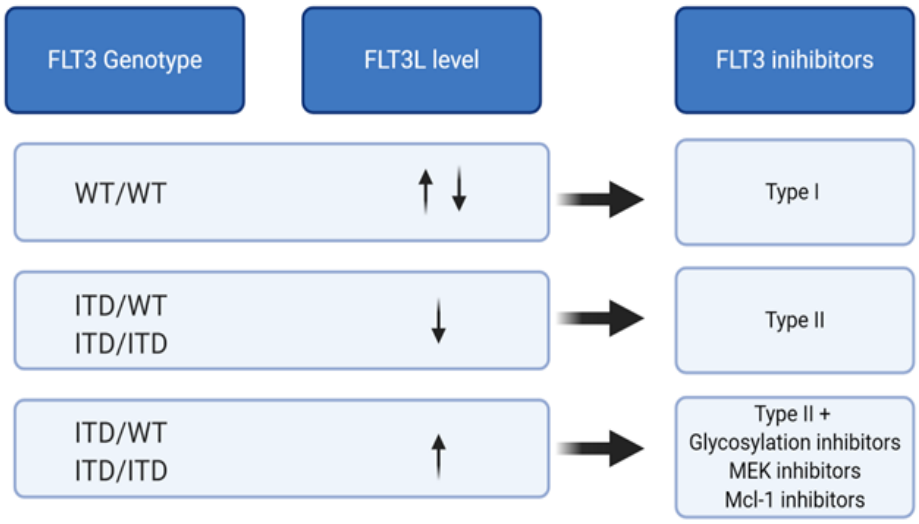

Figure 6.3: Suggested summary of using FLT3 inhibitors

6.2 Future work

Expanding the cell line models

Unfortunately during the course of this study, we were unable access primary patient samples, so it would be of great interest to characterise the response to FLT3L and FLT3 inhibition in actual patient samples expressing homozygous or heterozygous ITD-FLT3. As we already had two human lines containing differing ITD mutations and zygosity available it was decided to use these for the study. I would have preferred to have used primary patient samples for some of these experiments (this was the original idea) but unfortunately none are available in Liverpool. Obviously, there would have been heterogeneity across samples/lines due to differing mutational

“landscapes”, but it would have been nice to have had the samples to reinforce some of the results seen in the cell lines. Also, in this study we are assuming that the effect we have seen is related to FLT3 with no other RTKs involved. To further expand this, we could use FLT3 null cells such as BaF3, 32D and U937 cells, and introduce constructs expressing ITD, wild-type, and other FLT3 mutations in order to assess their response to inhibition and FLT3L.

The Kinome and cellular adaptation to drug resistance

Based on our results, activation of MAPKs is implicated in drug resistance as these kinases can activate alternate survival and proliferation pathways. It would be interesting to look at global kinase expression and phosphorylation state and how this is altered by modulating FLT3, especially on the background of differing FLT3 genotypes and in different cell models. To track possible pathways of drug-resistance, large-scale proteomics studies are needed. We were hoping to investigate the kinome profile of MV4-11, MOLM-13 and patient samples exposed to FLT3L and quizartinib by nanostring (mRNA) and phospho-proteomics (protein level). This will allow us to validate dysregulated proteins by flow cytometry, qPCR, and Western blotting using strategies established in Chapter III/IV. Other kinases could be potential targets in AML might be identified and should be studied further to explore their potential for combination therapy.

Another area of interest is the differential response of AML cells to FLT3 inhibitors and why only type I is affected by FLT3L. Our data suggests that the FLT3 mutational status might not be the only factor predicting response to

FLT3 inhibitors. The activation of other protein kinases besides FLT3 may provide further insight into the AML cell responsiveness to FLT3 inhibition and activation. A well establish approach to investigate this is to apply mass spectrometry-based proteomics to monitor and quantify all phosphorylation sites in a single experiment. Indeed, we can apply a phosphoproteome analysis to study the effects of type I/II inhibitors on panel of multiple AML cell line models. This might open a new window for understanding different mechanisms of action and resistance pathways and so predicting the responsiveness of AML cells.

Genome editing AML cells

In this thesis, we successfully established a CRISPR/Cas9-based strategy to knock-out STAT5A gene. The strategy was established and validated in HEK-293T cells. Due to time constraints we were not able to use the same strategy in AML cell lines e.g. MV4-11. This should be done in future experiments as it allows us to use these cells to elucidate the role of STAT5A in AML. The same strategy could be applied to understand better the role of Mcl-1 and Bim and their potential as an essential target in AML. Generating AML Mcl-1 or Bim knock-out cells is a good starting point. MOLM-13 cells that contain heterozygous FLT3-ITD mutation are of interest seeing that FLT3L has more effect of reducing apoptosis in these cells.

Appendix

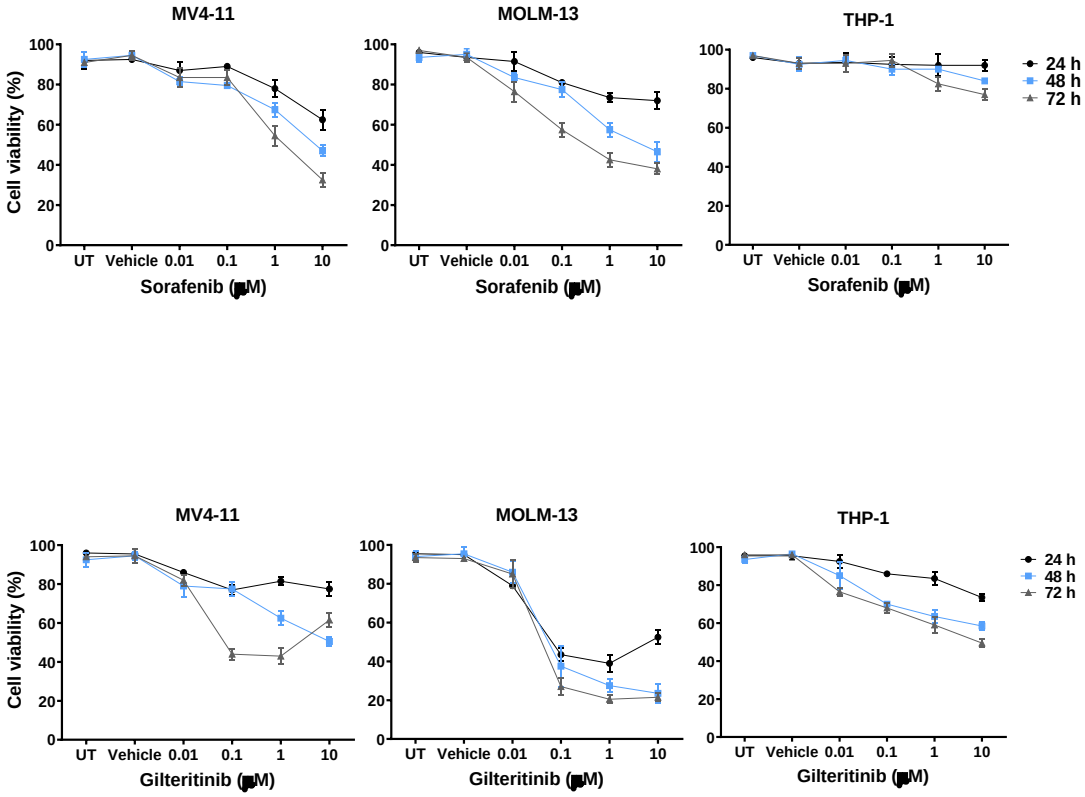

Figure A1 – MV4-11, MOLM-13, and THP-1, cells were incubated with increasing concentrations of sorafenib or gilteritinib. Apoptosis was measured at indicated times using Annexin-V/PI staining. Results represent the mean +/- SEM for 2 independent experiments.

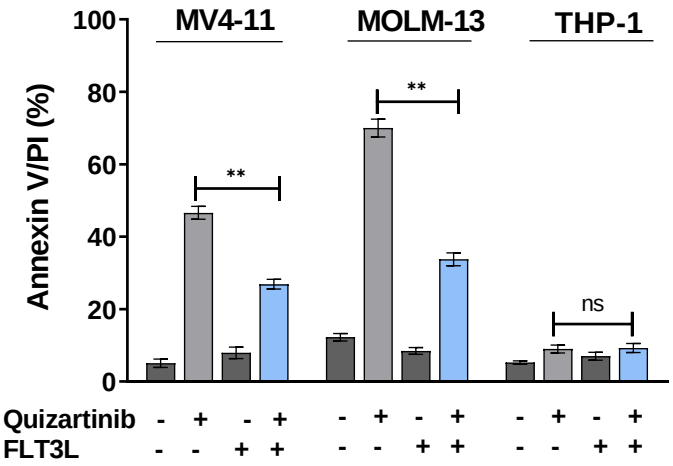

Figure A2 – MV4-11, MOLM-13, and THP-1 were treated with quizartinib (0.1 µM) in the presence of FLT3L (100 ng/ml) for 72h. Apoptosis was measured at indicated times using Annexin V/PI. Results represent the mean +/- SEM of 5 independent experiments. Significance testing was done by two-tailed paired *t*-test (n=5), ***P ≤0.01, and ns, not significant.*

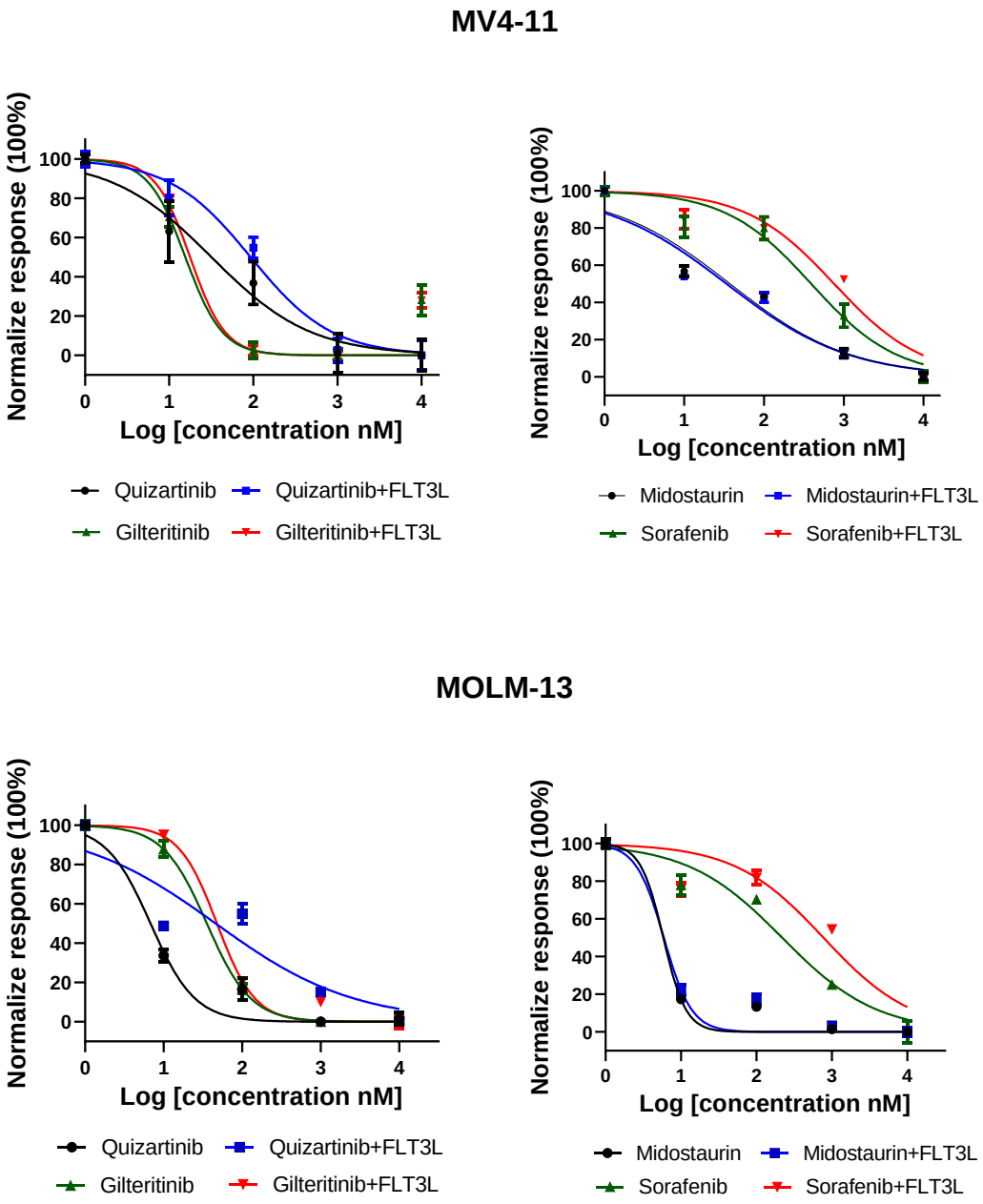

Figure A3 – Dose–response curve indicating viability of FLT3-ITD expressing cells, MV4-11 and MOLM-13 treated with different concentrations of FLT3 inhibitors alone and in combination with FLT3L for 72h. The resulting dose-response curves were fitted by nonlinear regression using GraphPad program.

Cell line and ITD status	compound	IC50 (72h) nM

MV4-11(FLT3-ITD$^{+/+}$)	Quizartinib	31
	Quizartinib + FLT3L	97
	Gilteritinib	11
	Gilteritinib+ FLT3L	16
	Midostaurin	37
	Midostaurin+ FLT3L	34
	Sorafenib	385
	Sorafenib + FLT3L	749
MOLM-13 (FLT3-ITD$^{-/+}$)	Quizartinib	6
	Quizartinib + FLT3L	49
	Gilteritinib	35
	Gilteritinib+ FLT3L	47
	Midostaurin	5
	Midostaurin+ FLT3L	5
	Sorafenib	210
	Sorafenib + FLT3L	780

Table A1: IC50 of FLT3 inhibitors on ITD expressing cells

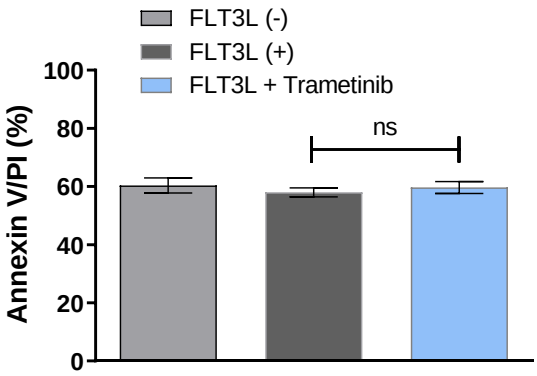

Figure A4 – MOLM-13 cells were treated with gilteritinib (0.1 µM) and/or FLT3L (100 ng/ml) for 48h and apoptosis was assessed by Annexin V staining. Results represent the mean +/- SEM for 3 independent experiments. Significance testing was done by two-tailed paired *t*-test (n=3), *ns, not significant.*

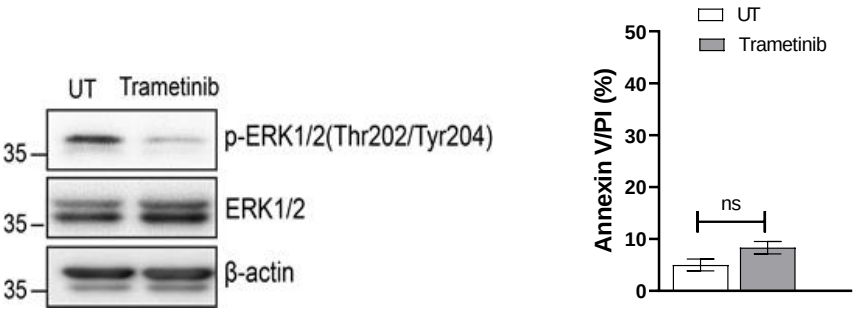

Figure A5 – MOLM-13 cells were treated with trametinib (0.05 µM) for 48h, followed by immunoblotting with the indicated antibodies. Apoptosis was assessed by Annexin V staining. Results represent the mean +/- SEM for 3 independent experiments. Significance testing was done by two-tailed paired *t*-test (n=3), *ns, not significant.*

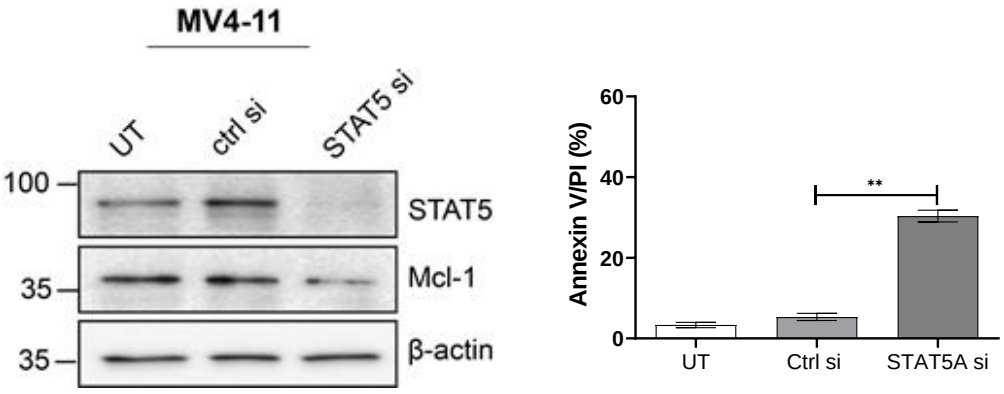

Figure A6 – MV4-11 cells were transfected with STAT5A (10 nM) for 72h before cells were harvested and analysed by Western blotting. Apoptosis was assessed by Annexin V staining. Results represent the mean +/- SEM for 3 independent experiments. Significance testing was done by two-tailed paired *t*-test (n=3), ***P ≤0.01.*

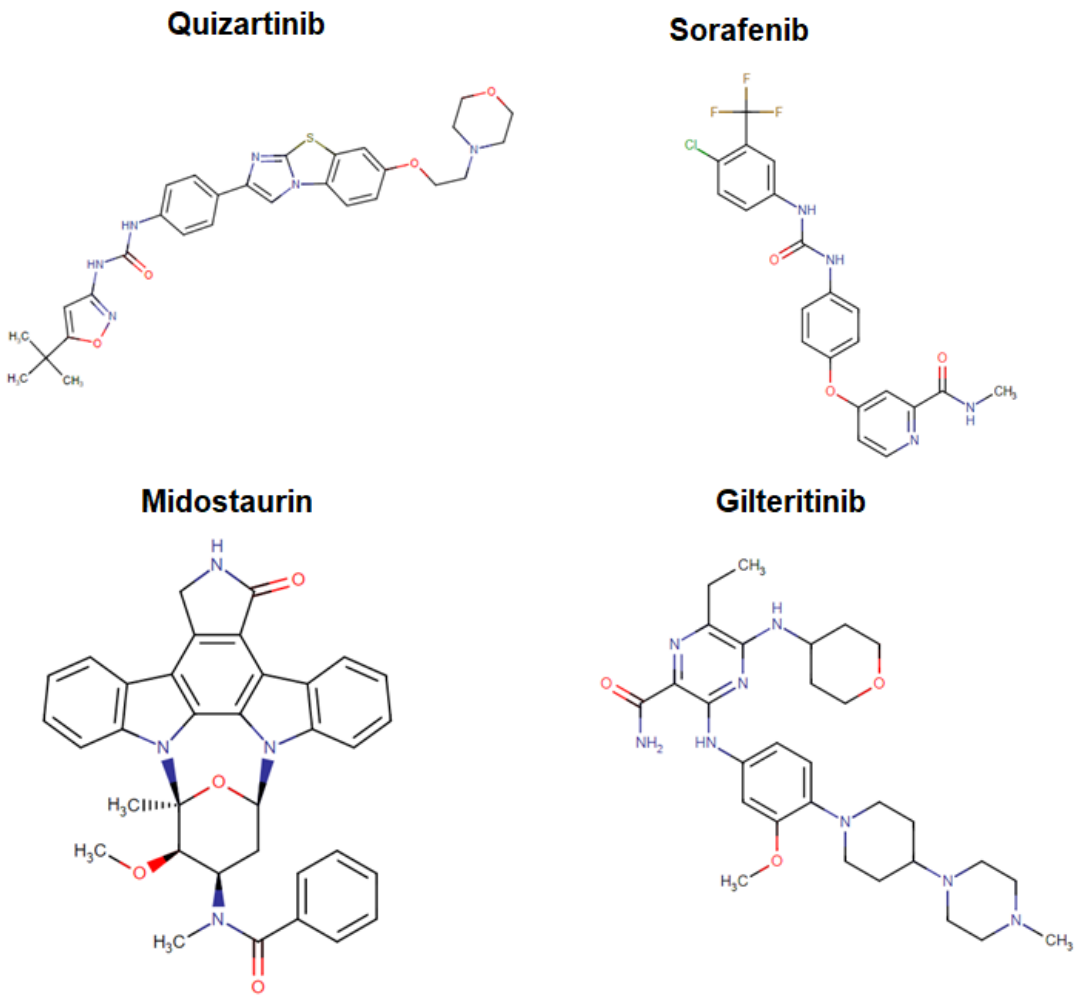

Figure A7 – Chemical structure of FLT3 inhibitors used in this study.

A)

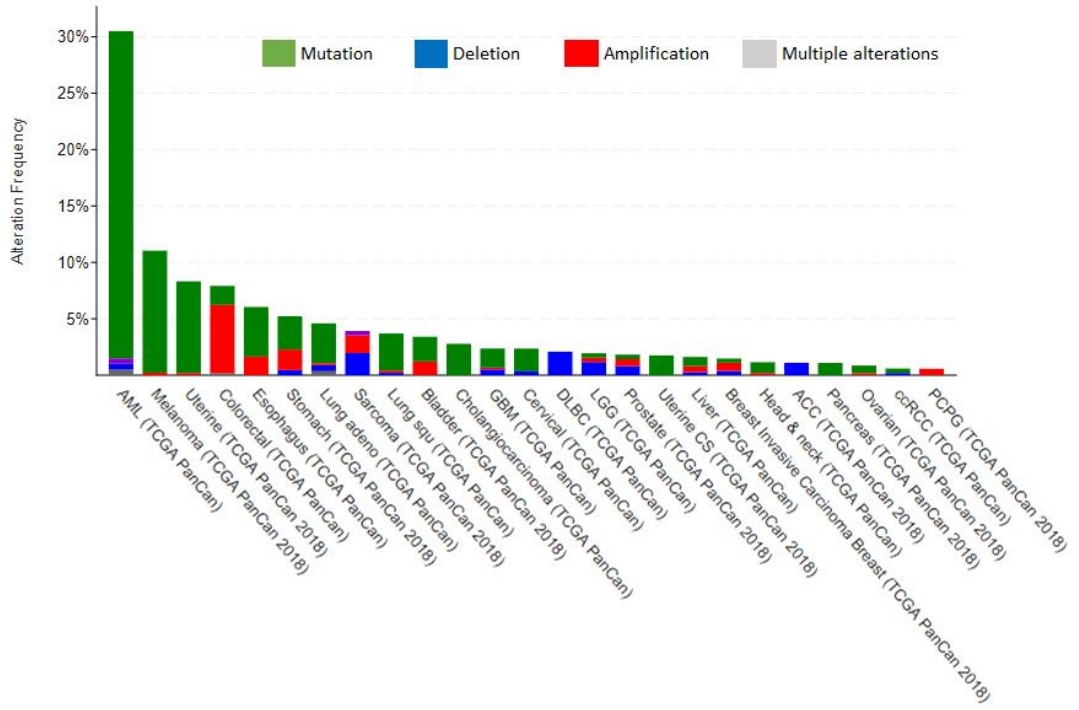
Mutation
Deletion
Amplification
Multiple alterations
Alteration Frequency
30%
25%
20%
15%
10%
5%
AML (TCGA PanCan)
Melanoma (TCGA PanCan 2018)
Uterine (TCGA PanCan 2018)
Colorectal (TCGA PanCan)
Esophagus (TCGA PanCan)
Stomach (TCGA PanCan)
Lung adeno (TCGA PanCan 2018)
Sarcoma (TCGA PanCan)
Lung squ (TCGA PanCan)
Bladder (TCGA PanCan 2018)
Cholangiocarcinoma (TCGA PanCan 2018)
GBM (TCGA PanCan)
Cervical (TCGA PanCan)
DLBC (TCGA PanCan)
LGG (TCGA PanCan)
Prostate (TCGA PanCan)
Uterine CS (TCGA PanCan 2018)
Liver (TCGA PanCan)
Breast Invasive Carcinoma (TCGA PanCan 2018)
Head & neck (TCGA PanCan)
ACC (TCGA PanCan 2018)
Pancreas (TCGA PanCan 2018)
Ovarian (TCGA PanCan 2018)
ccRCC (TCGA PanCan)
PCPG (TCGA PanCan 2018)

B)

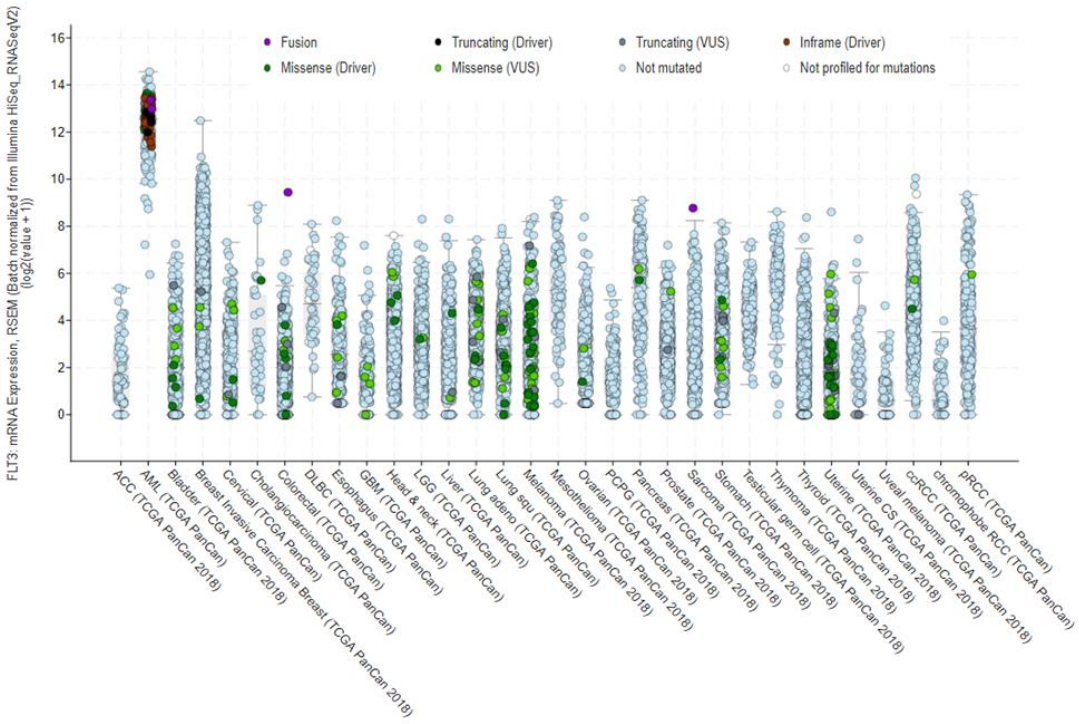
Fusion
Truncating (Driver)
Truncating (VUS)
Inframe (Driver)
Missense (Driver)
Missense (VUS)
Not mutated
Not profiled for mutations
FLT3: mRNA Expression, RSEM (Batch normalized from Illumina HiSeq_RNASeqV2) (log2(value + 1))
16
14
12
10
8
6
4
2
0
ACC (TCGA PanCan 2018)
AML (TCGA PanCan)
Bladder (TCGA PanCan 2018)
Breast Invasive Carcinoma (TCGA PanCan)
Cervical (TCGA PanCan)
Cholangiocarcinoma (TCGA PanCan 2018)
Colorectal (TCGA PanCan)
DLBC (TCGA PanCan)
Esophagus (TCGA PanCan)
GBM (TCGA PanCan)
Head & neck (TCGA PanCan)
LGG (TCGA PanCan)
Liver (TCGA PanCan)
Lung adeno (TCGA PanCan)
Lung squ (TCGA PanCan)
Melanoma (TCGA PanCan 2018)
Mesothelioma (TCGA PanCan 2018)
Ovarian (TCGA PanCan 2018)
PCPG (TCGA PanCan 2018)
Pancreas (TCGA PanCan 2018)
Prostate (TCGA PanCan 2018)
Sarcoma (TCGA PanCan 2018)
Stomach (TCGA PanCan 2018)
Testicular germ cell (TCGA PanCan 2018)
Thymoma (TCGA PanCan 2018)
Thyroid (TCGA PanCan 2018)
Uterine (TCGA PanCan 2018)
Uterine CS (TCGA PanCan 2018)
Uveal melanoma (TCGA PanCan 2018)
ccRCC (TCGA PanCan)
chromophobe RCC (TCGA PanCan)
pRCC (TCGA PanCan)

C)

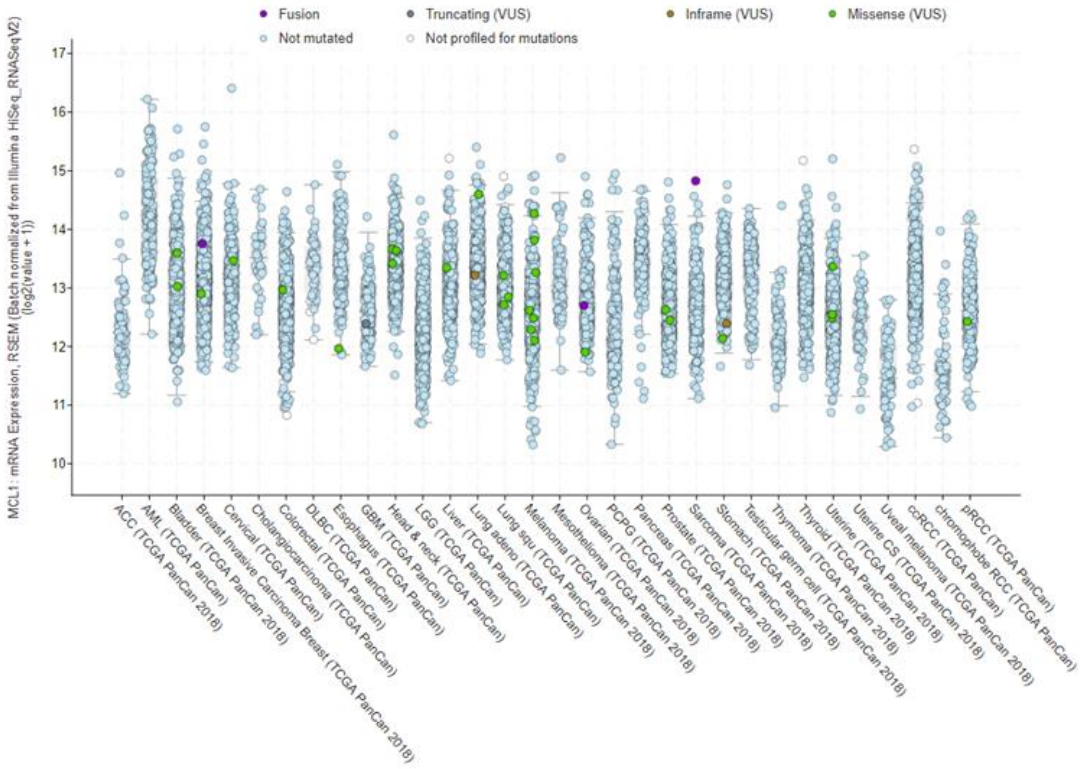
Fusion
Truncating (VUS)
Inframe (VUS)
Missense (VUS)
Not mutated
Not profiled for mutations
MCL1 : mRNA Expression, RSEM (Batch normalized from Illumina HiSeq_RNASeqV2) (log2(value + 1))
17
16
15
14
13
12
11
10
ACC (TCGA PanCan 2018)
AML (TCGA PanCan)
Bladder (TCGA PanCan 2018)
Breast Invasive Carcinoma (TCGA PanCan)
Cervical (TCGA PanCan 2018)
Cholangiocarcinoma (TCGA PanCan)
Colorectal (TCGA PanCan)
DLBC (TCGA PanCan)
Esophagus (TCGA PanCan)
GBM (TCGA PanCan)
Head & neck (TCGA PanCan)
LGG (TCGA PanCan)
Liver (TCGA PanCan)
Lung adeno (TCGA PanCan)
Lung squ (TCGA PanCan)
Melanoma (TCGA PanCan)
Mesothelioma (TCGA PanCan 2018)
Ovarian (TCGA PanCan 2018)
PCPG (TCGA PanCan 2018)
Pancreas (TCGA PanCan 2018)
Prostate (TCGA PanCan 2018)
Sarcoma (TCGA PanCan 2018)
Stomach (TCGA PanCan 2018)
Testicular germ cell (TCGA PanCan 2018)
Thymoma (TCGA PanCan 2018)
Thyroid (TCGA PanCan 2018)
Uterine (TCGA PanCan 2018)
Uterine CS (TCGA PanCan 2018)
Uveal melanoma (TCGA PanCan 2018)
ccRCC (TCGA PanCan)
chromophobe RCC (TCGA PanCan)
pRCC (TCGA PanCan)

D)

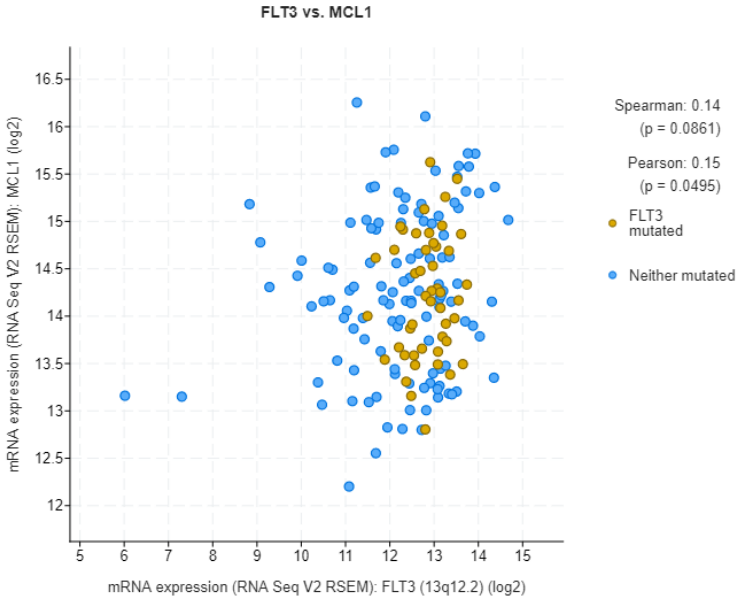
FLT3 vs. MCL1
mRNA expression (RNA Seq V2 RSEM): MCL1 (log2)
16.5
16
15.5
15
14.5
14
13.5
13
12.5
12
5
6
7
8
9
10
11
12
13
14
15
mRNA expression (RNA Seq V2 RSEM): FLT3 (13q12.2) (log2)
Spearman: 0.14
(p = 0.0861)
Pearson: 0.15
(p = 0.0495)
FLT3 mutated
Neither mutated

Figure A8 – A) cBioportal database was used to analyse mutations and copy number alterations of FLT3. Genetic alterations of FLT3 in different types of cancer showed that FLT3 was significantly mutated in AML. Expression of FLT3 mRNA **(B)** and Mcl-1 **(C)** in different tumours was analysed using cBioportal database. **D)** cBioportal result showed the expression of FLT3 was positively correlated with Mcl-1 expression in AML (TCGA, NEJM 2013 dataset).

Figure A9 – Flow cytometry Gating:

Cell cycle analysis: MV4-11 A) UT (untreated), B) quizartinib (0.1 µM), 24h.

A)

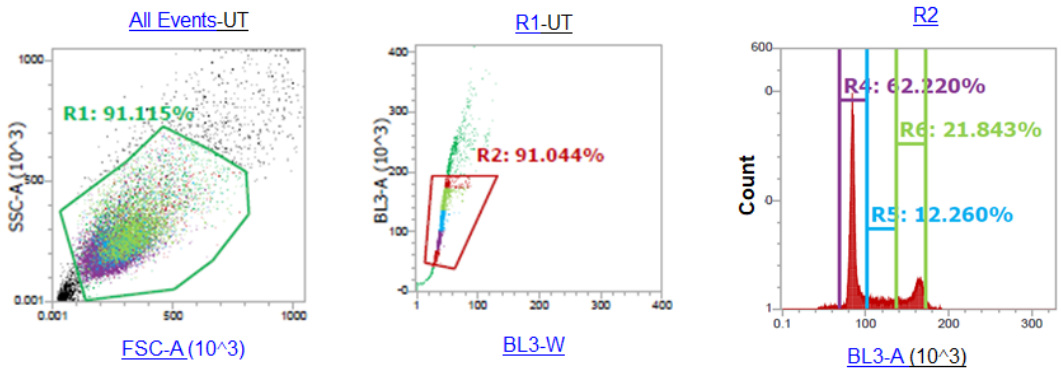

B)

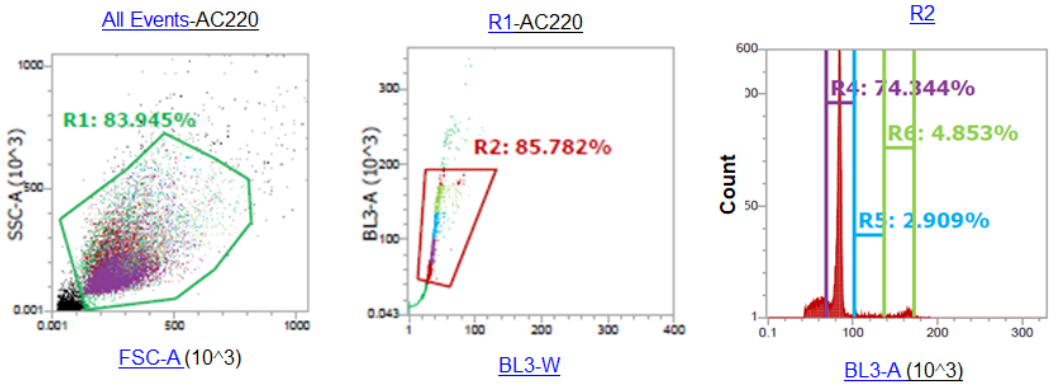

Cell cycle analysis: MOLM-13 A) UT (untreated), B) quizartinib (0.1 µM), 24h.

A)

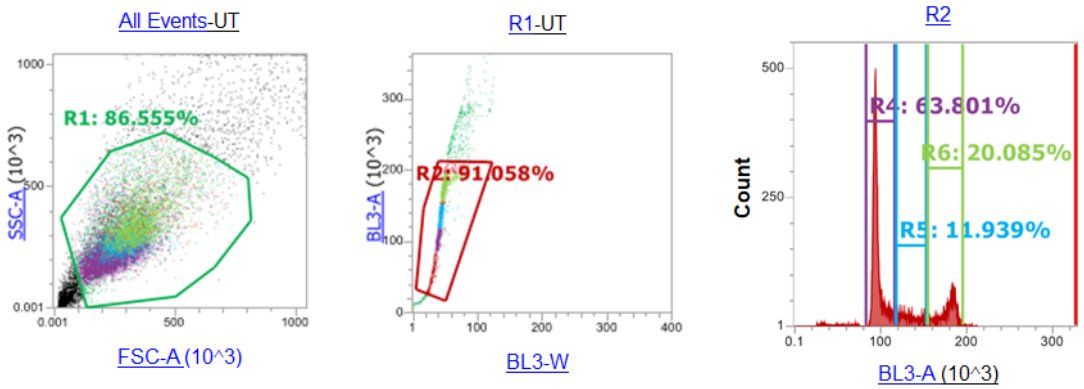

B)

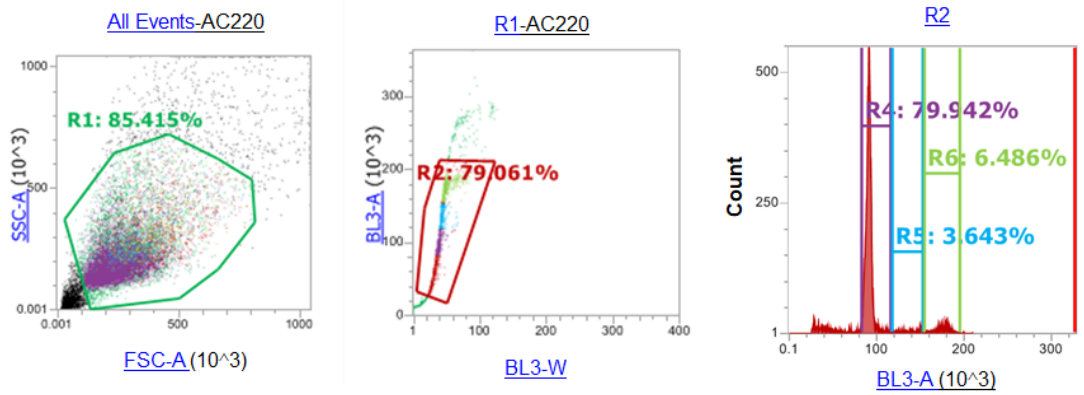

Cell cycle analysis: THP-1 A) UT (untreated), B) quizartinib (0.1 µM), 24h.

A)

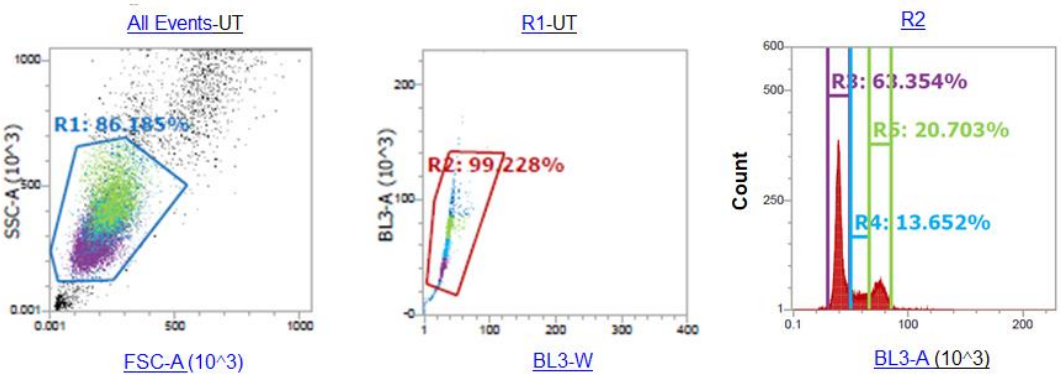

B)

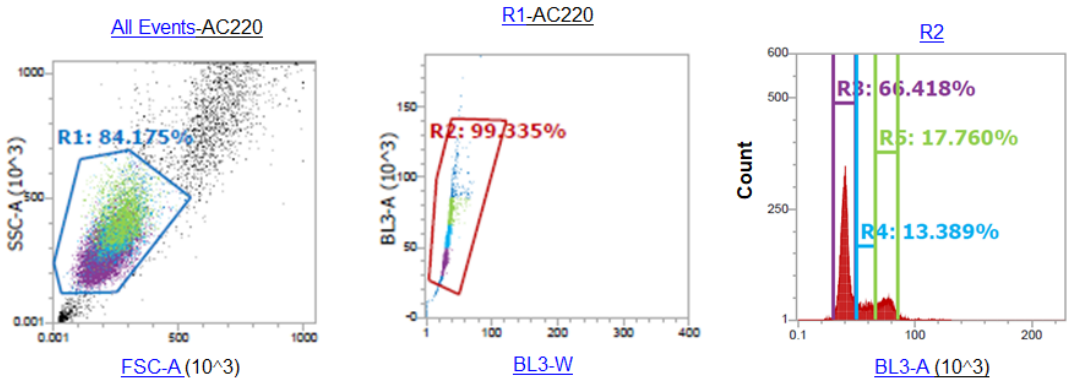

Cell cycle analysis: U937 A) UT (untreated), B) quizartinib (0.1 µM), 24h.

A)

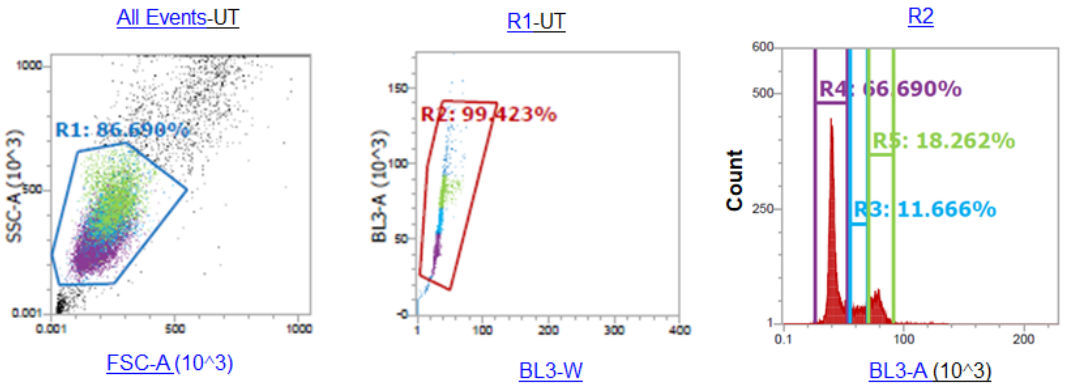

B)

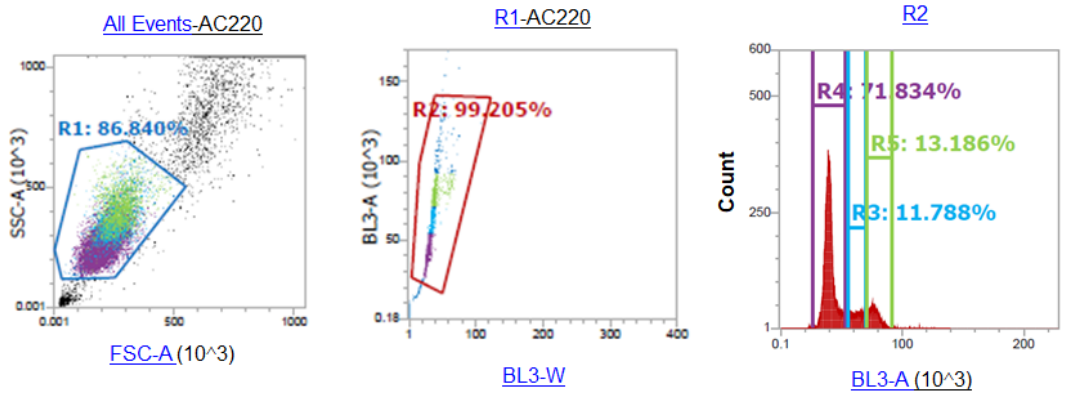

CFSE staining: MV4-11 untreated (UT) **A)** 24 h, **B)** 72 h and **C)** quizartinib (0.1 µM), 72h.

A)

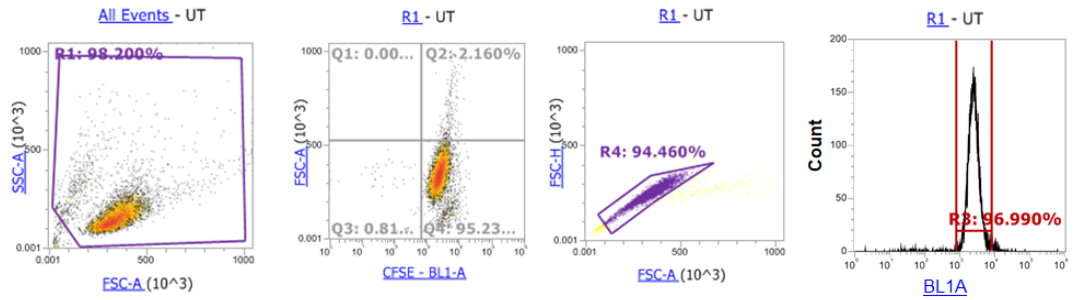

B)

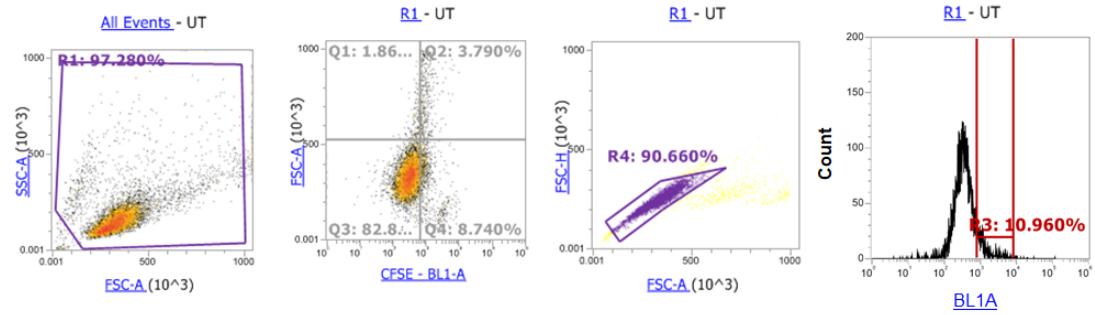

C)

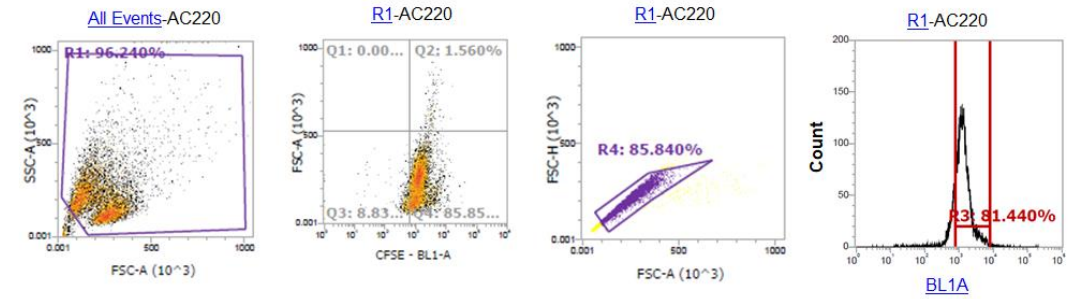

CFSE staining: MOLM-13 untreated (UT) **A)** 24 h, **B)** 72 h and **C)** quizartinib (0.1 µM), 72h.

A)

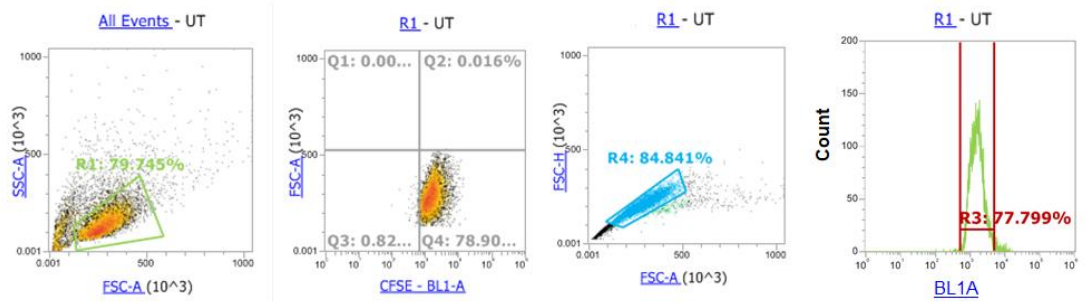

B)

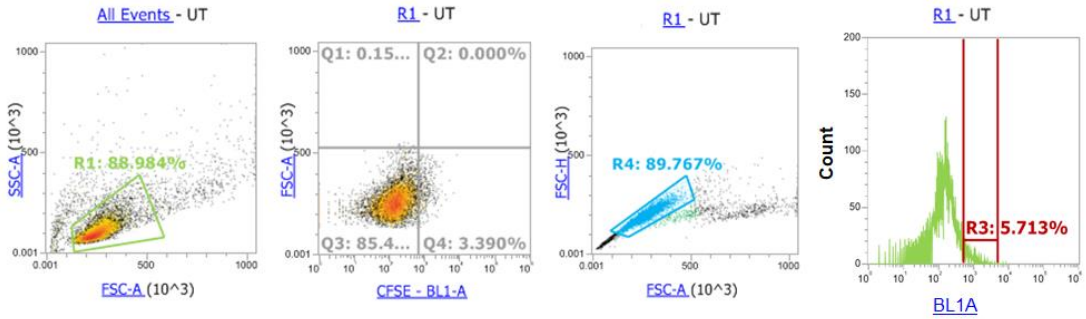

C)

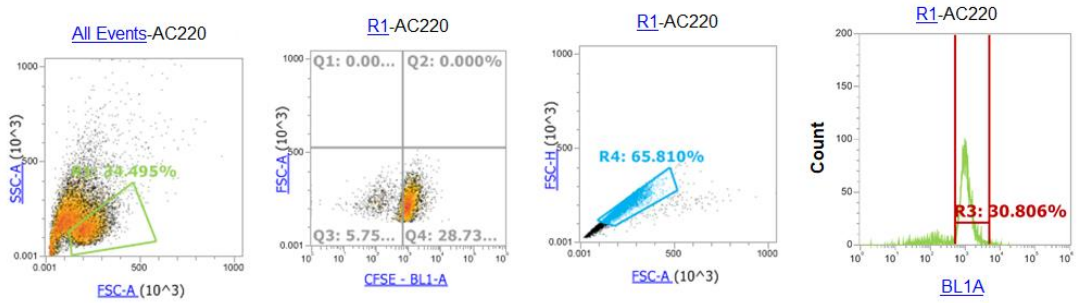

Cell apoptosis assay: **A)** Representative plots of MV4-11 cells treated with the following for 24h.

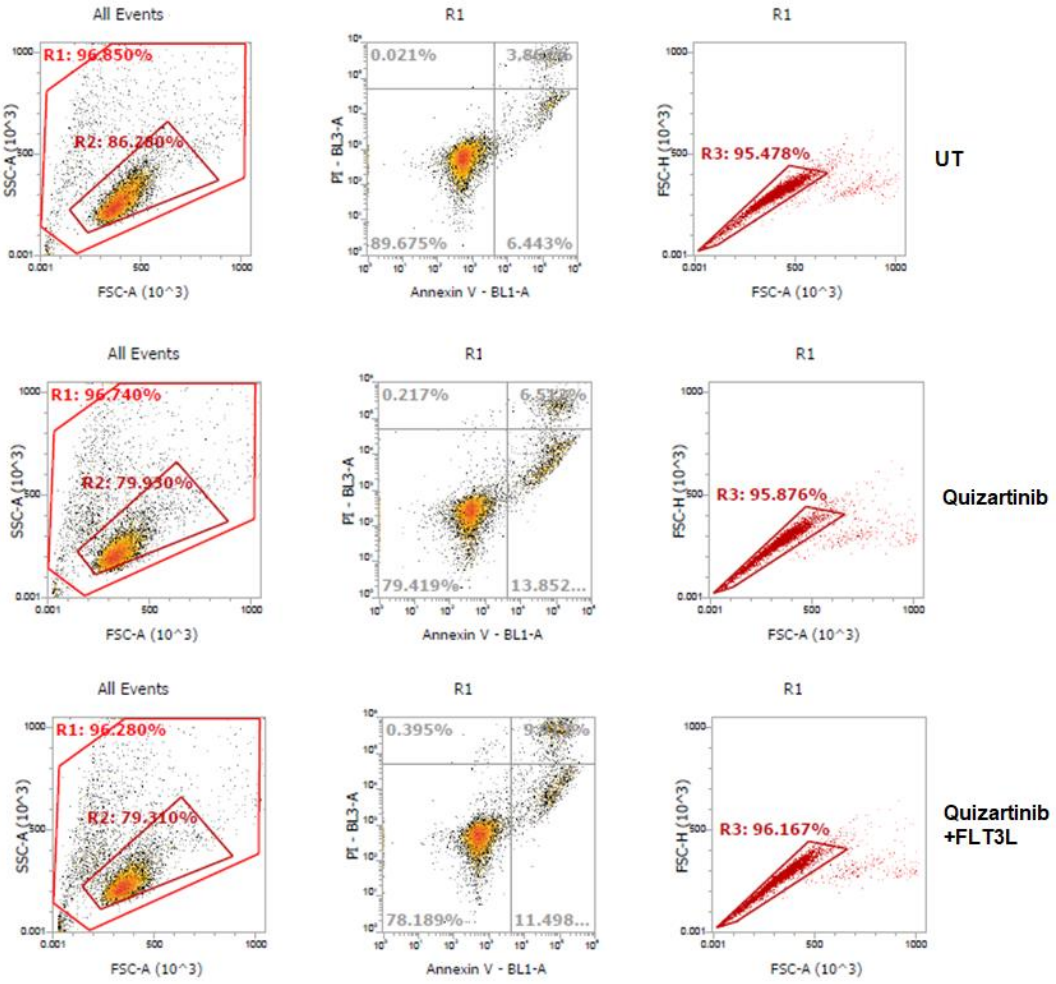

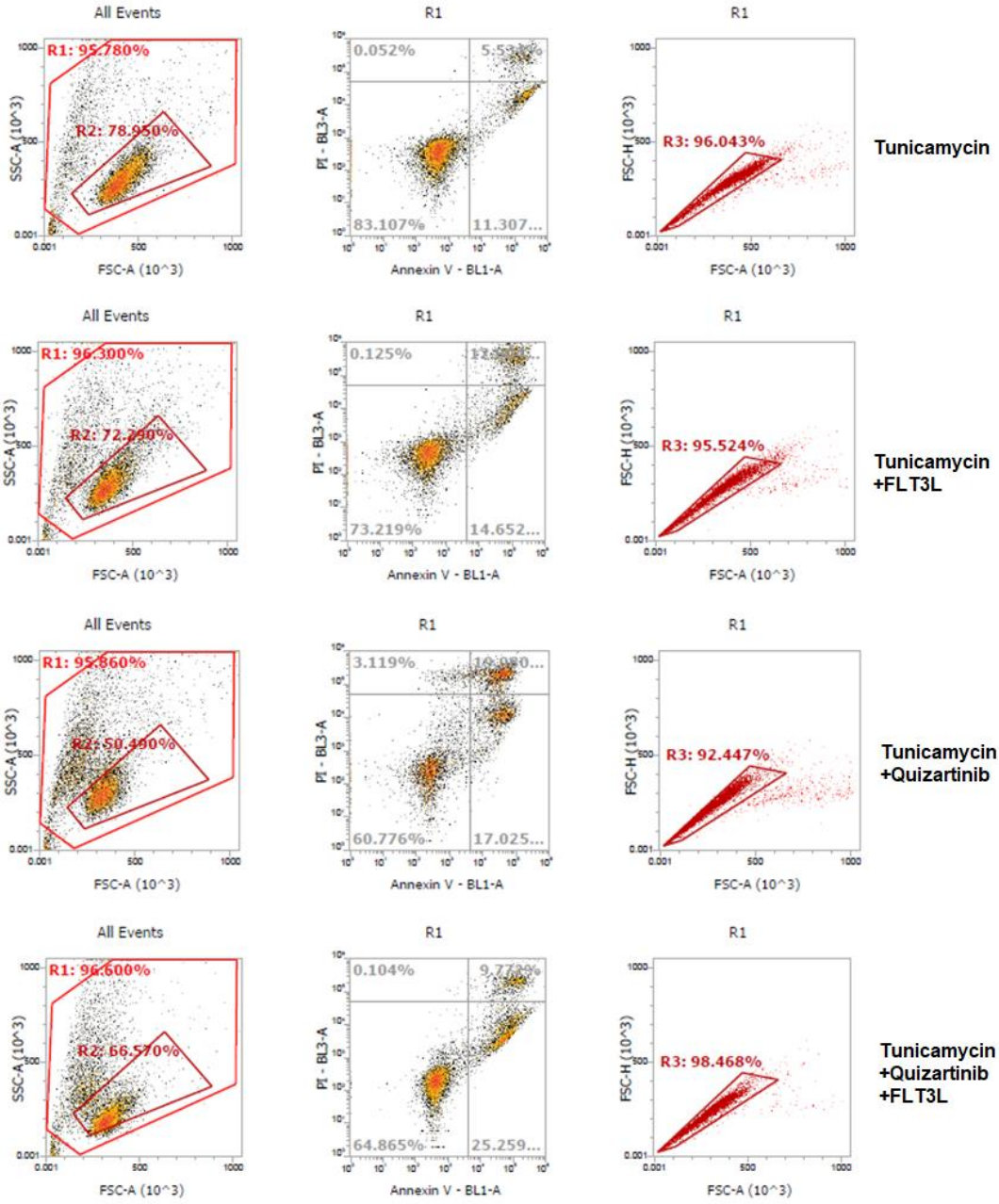
All Events
R1: 95.780%
R2: 78.950%
SSC-A (10^3)
FSC-A (10^3)
R1
0.052%
83.107%
11.307...
PI - BL3-A
Annexin V - BL1-A
R1
R3: 96.043%
FSC-H (10^3)
FSC-A (10^3)
Tunicamycin
All Events
R1: 96.300%
R2: 72.290%
SSC-A (10^3)
FSC-A (10^3)
R1
0.125%
73.219%
14.652...
PI - BL3-A
Annexin V - BL1-A
R1
R3: 95.524%
FSC-H (10^3)
FSC-A (10^3)
Tunicamycin
+FLT3L
All Events
R1: 95.860%
R2: 50.490%
SSC-A (10^3)
FSC-A (10^3)
R1
3.119%
60.776%
17.025...
PI - BL3-A
Annexin V - BL1-A
R1
R3: 92.447%
FSC-H (10^3)
FSC-A (10^3)
Tunicamycin
+Quizartinib
All Events
R1: 96.600%
R2: 66.570%
SSC-A (10^3)
FSC-A (10^3)
R1
0.104%
64.865%
25.259...
PI - BL3-A
Annexin V - BL1-A
R1
R3: 98.468%
FSC-H (10^3)
FSC-A (10^3)
Tunicamycin
+Quizartinib
+FLT3L

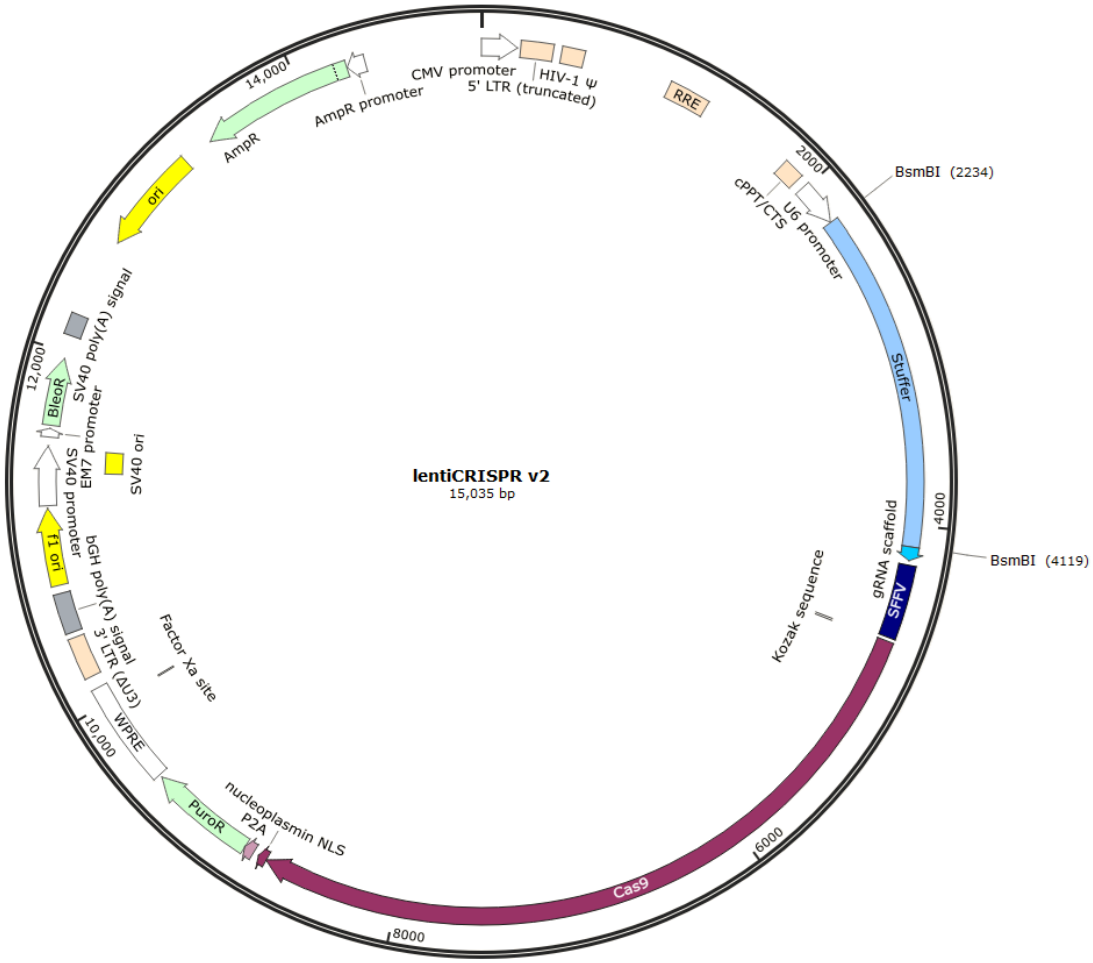

Figure A10 – LentiCRISPR v2 plasmid

LentiCRISPR v2 plasmid is a lentiviral SpCas9-expressing plasmid and was purchased from Addgene (#52961). The original EF-1α core promotor was replaced with a SFFV promotor. For guide cloning, plasmid was digested with BsmbI to remove the stuffer region and annealed guide oligos were ligated into the plasmid.

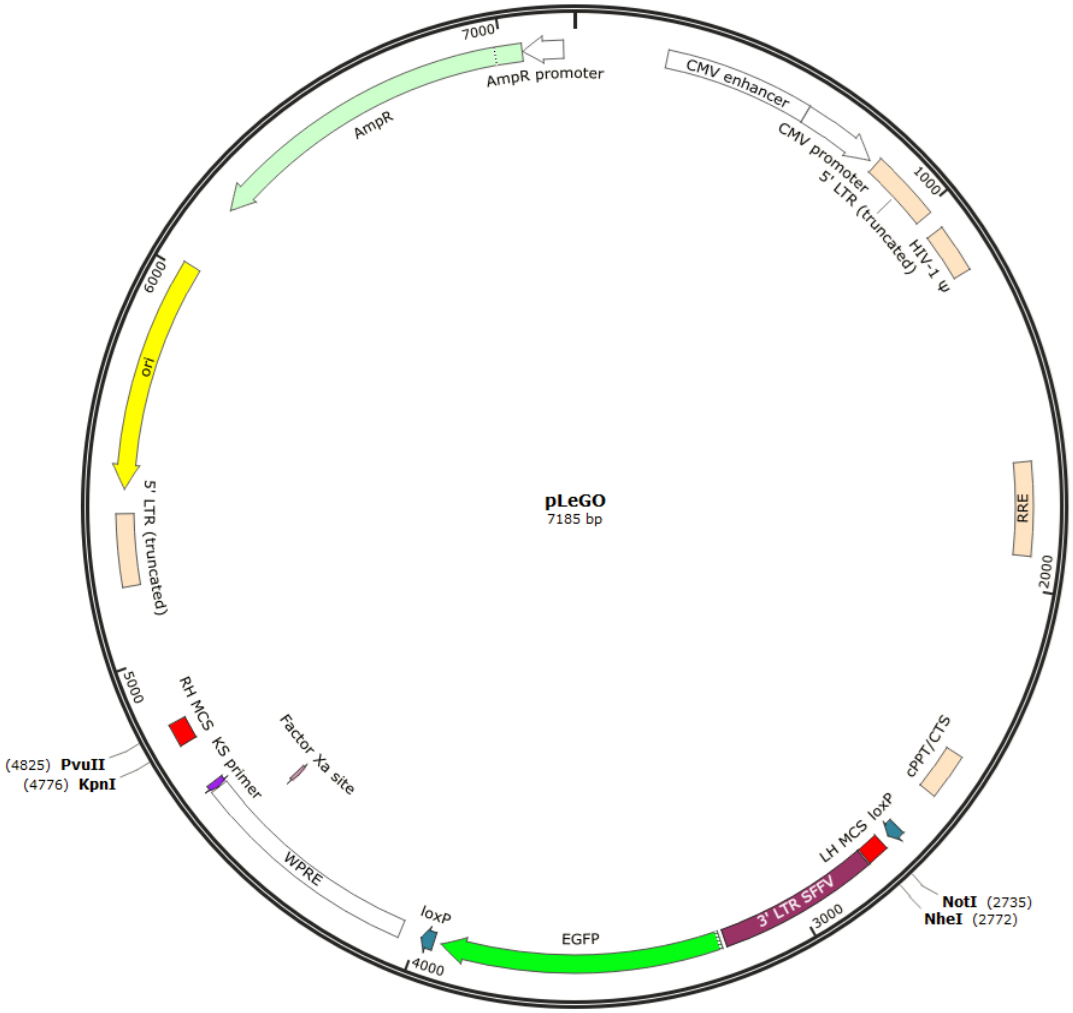

Figure A11 – pLeGO plasmid

pLeGO is a lentiviral plasmid purchased from Addgene (#27341) that expresses EGFP under the control of a SFFV promotor. This plasmid was modified by adding two multiple cloning sites (LH and RH MCS depicted in red).

Table A2– Purchased Reagents and Kits

Name	Supplier
Tween-20	Thermo Fisher Scientific™ (Loughborough, UK)
sodium dodecyl sulphate (SDS)	Thermo Fisher Scientific™ (Loughborough, UK)
page ruler plus protein ladder	Thermo Fisher Scientific™ (Loughborough, UK)
glycine	Thermo Fisher Scientific™ (Loughborough, UK)
sodium chloride tris-base	Thermo Fisher Scientific™ (Loughborough, UK)
ammonium peroxodisulphate (APS)	Thermo Fisher Scientific™ (Loughborough, UK)
Bovine Serum Albumin (BSA)	Sigma-Aldrich (Poole, UK)
tetramethylethylenediamine (TEMED)	Sigma-Aldrich (Poole, UK)
dimethyl sulphoxide (DMSO)	Sigma-Aldrich (Poole, UK)
ethylenediaminetetraacetic acid (EDTA)	Sigma-Aldrich (Poole, UK)
Luria Bertani (LB)	Sigma-Aldrich (Poole, UK)
Phosphate buffered saline (PBS)	Sigma-Aldrich (Poole, UK)
Propidium Iodide (PI)	Sigma-Aldrich (Poole, UK)
Trypsin/EDTA (0.25%)	Sigma-Aldrich (Poole, UK)
β-Mercaptoethanol	Sigma-Aldrich (Poole, UK)
Hybond ECL nitrocellulose membrane	GE Healthcare (Amersham, UK)
Ultrapure ProtoGel® solution	Geneflow Ltd
Acrylamide	Geneflow Ltd
Fetal bovine serum (FBS)	Invitrogen
Dulbecco's Modified Eagle's Medium (DMEM)	Invitrogen

Opti-MEM	Invitrogen
Penicillin, Streptomycin (10 mg/ mL)	Invitrogen
Roswell Park Memorial Institute (RPMI)	Invitrogen
Protease Inhibitor Cocktail	Roche
PhosSTOPTM Phosphatase Inhibitor	Roche
Immobilon Western Chemiluminescent HRP substrate	Millipore

References

ABDEL-WAHAB, O. & LEVINE, R. L. 2013. Mutations in epigenetic modifiers in the pathogenesis and therapy of acute myeloid leukemia. *Blood, The Journal of the American Society of Hematology,* 121**,** 3563-3572.

ABU-DUHIER, F., GOODEVE, A., WILSON, G., CARE, R., PEAKE, I. & REILLY, J. 2001. Identification of novel FLT-3 Asp835 mutations in adult acute myeloid leukaemia. *British journal of haematology,* 113**,** 983-988.

AHSAN, A., HINIKER, S. M., RAMANAND, S. G., NYATI, S., HEGDE, A., HELMAN, A., MENAWAT, R., BHOJANI, M. S., LAWRENCE, T. S. & NYATI, M. K. 2010. Role of epidermal growth factor receptor degradation in cisplatin-induced cytotoxicity in head and neck cancer. *Cancer research,* 70**,** 2862-2869.

ALESSI, D. R., DEAK, M., CASAMAYOR, A., CAUDWELL, F. B., MORRICE, N., NORMAN, D. G., GAFFNEY, P., REESE, C. B., MACDOUGALL, C. N. & HARBISON, D. 1997. 3-Phosphoinositide-dependent protein kinase-1 (PDK1): structural and functional homology with the Drosophila DSTPK61 kinase. *Current biology,* 7**,** 776-789.

ALMEIDA, A. M. & RAMOS, F. 2016. Acute myeloid leukemia in the older adults. *Leukemia research reports,* 6**,** 1-7.

ALVARADO, Y., KANTARJIAN, H. M., LUTHRA, R., RAVANDI, F., BORTHAKUR, G., GARCIA-MANERO, G., KONOPLEVA, M., ESTROV, Z., ANDREEFF, M. & CORTES, J. E. 2014. Treatment with FLT3 inhibitor in patients with FLT3-mutated acute myeloid leukemia is associated with development of secondary FLT3–tyrosine kinase domain mutations. *Cancer,* 120**,** 2142-2149.

AMBROSIO, R., FIMIANI, G., MONFREGOLA, J., SANZARI, E., DE FELICE, N., SALERNO, M. C., PIGNATA, C., D'URSO, M. & URSINI, M. V. 2002. The structure of human STAT5A and B genes reveals two regions of nearly identical sequence and an alternative tissue specific STAT5B promoter. *Gene,* 285**,** 311-318.

ANDERSON, K. E. & JACKSON, S. P. 2003. Class I phosphoinositide 3-kinases. *The international journal of biochemistry & cell biology,* 35**,** 1028-1033.

ANTAR, A., OTROCK, Z., EL-CHEIKH, J., KHARFAN-DABAJA, M., BATTIPAGLIA, G., MAHFOUZ, R., MOHTY, M. & BAZARBACHI, A. 2017. Inhibition of FLT3 in AML: a focus on sorafenib. *Bone marrow transplantation,* 52**,** 344-351.

ARBER, D. A., ORAZI, A., HASSERJIAN, R., THIELE, J., BOROWITZ, M. J., LE BEAU, M. M., BLOOMFIELD, C. D., CAZZOLA, M. & VARDIMAN, J. W. 2016. The 2016 revision to the World Health Organization classification of myeloid neoplasms and acute leukemia. *Blood,* 127**,** 2391-405.

ASHKENAZI, A., FAIRBROTHER, W. J., LEVERSON, J. D. & SOUERS, A. J. 2017. From basic apoptosis discoveries to advanced selective BCL-2 family inhibitors. *Nature Reviews Drug Discovery,* 16**,** 273.

ASSI, R. & RAVANDI, F. 2018. FLT3 inhibitors in acute myeloid leukemia: Choosing the best when the optimal does not exist. *American journal of hematology,* 93**,** 553-563.

AZAM, M., ERDJUMENT-BROMAGE, H., KREIDER, B., XIA, M., QUELLE, F., BASU, R., SARIS, C., TEMPST, P., IHLE, J. & SCHINDLER, C.

1995. Interleukin-3 signals through multiple isoforms of Stat5. *The EMBO Journal,* 14**,** 1402-1411.

BADAR, T., KANTARJIAN, H. M., NOGUERAS-GONZALEZ, G. M., BORTHAKUR, G., GARCIA MANERO, G., ANDREEFF, M., KONOPLEVA, M., KADIA, T. M., DAVER, N. & WIERDA, W. G. 2015. Improvement in clinical outcome of FLT3 ITD mutated acute myeloid leukemia patients over the last one and a half decade. *American journal of hematology,* 90**,** 1065-1070.

BALMANNO, K. & COOK, S. 2009. Tumour cell survival signalling by the ERK1/2 pathway. *Cell Death & Differentiation,* 16**,** 368-377.

BANKER, D. E., RADICH, J., BECKER, A., KERKOF, K., NORWOOD, T., WILLMAN, C. & APPELBAUM, F. R. 1998. The t (8; 21) translocation is not consistently associated with high Bcl-2 expression in de novo acute myeloid leukemias of adults. *Clinical Cancer Research,* 4**,** 3051-3062.

BAUM, C. M., WEISSMAN, I. L., TSUKAMOTO, A. S., BUCKLE, A.-M. & PEAULT, B. 1992. Isolation of a candidate human hematopoietic stem-cell population. *Proceedings of the National Academy of Sciences,* 89**,** 2804-2808.

BEINORTAS, T., TAVORIENĖ, I., ŽVIRBLIS, T., GERBUTAVIČIUS, R., JURGUTIS, M. & GRIŠKEVIČIUS, L. 2016. Chronic myeloid leukemia incidence, survival and accessibility of tyrosine kinase inhibitors: a report from population-based Lithuanian haematological disease registry 2000–2013. *BMC cancer,* 16**,** 198.

BENEKLI, M., BAER, M. R., BAUMANN, H. & WETZLER, M. 2003. Signal transducer and activator of transcription proteins in leukemias. *Blood, The Journal of the American Society of Hematology,* 101**,** 2940-2954.

BENNETT, J. M., CATOVSKY, D., DANIEL, M. T., FLANDRIN, G., GALTON, D. A., GRALNICK, H. R. & SULTAN, C. 1976. Proposals for the classification of the acute leukaemias. French-American-British (FAB) co-operative group. *Br J Haematol,* 33**,** 451-8.

BENNETT, J. M., CATOVSKY, D., DANIEL, M. T., FLANDRIN, G., GALTON, D. A., GRALNICK, H. R. & SULTAN, C. 1985. Proposed revised criteria for the classification of acute myeloid leukemia. A report of the French-American-British Cooperative Group. *Ann Intern Med,* 103**,** 620-5.

BESBES, S., MIRSHAHI, M., POCARD, M. & BILLARD, C. 2015. New dimension in therapeutic targeting of BCL-2 family proteins. *Oncotarget,* 6**,** 12862.

BESLU, N., LAROSE, J., CASTERAN, N., BIRNBAUM, D., LECOCQ, E., DUBREUIL, P. & ROTTAPEL, R. 1996. Phosphatidylinositol-3′ kinase is not required for mitogenesis or internalization of the Flt3/Flk2 receptor tyrosine kinase. *Journal of Biological Chemistry,* 271**,** 20075-20081.

BLOOMFIELD, C. D., ESTEY, E., PLEYER, L., SCHUH, A. C., STEIN, E. M., TALLMAN, M. S. & WEI, A. 2018. Time to repeal and replace response criteria for acute myeloid leukemia? *Blood reviews,* 32**,** 416-425.

BLUME-JENSEN, P., CLAESSON-WELSH, L., SIEGBAHN, A., ZSEBO, K. M., WESTERMARK, B. & HELDIN, C.-H. 1991. Activation of the human c-kit product by ligand-induced dimerization mediates circular actin reorganization and chemotaxis. *The EMBO journal,* 10**,** 4121-4128.

BODDU, P. C., KADIA, T. M., GARCIA-MANERO, G., CORTES, J., ALFAYEZ, M., BORTHAKUR, G., KONOPLEVA, M., JABBOUR, E. J., DAVER, N. G. & DINARDO, C. D. 2019. Validation of the 2017 European LeukemiaNet classification for acute myeloid leukemia with NPM1 and FLT3-internal tandem duplication genotypes. *Cancer,* 125**,** 1091-1100.

BORTHAKUR, G., KANTARJIAN, H., RAVANDI, F., ZHANG, W., KONOPLEVA, M., WRIGHT, J. J., FADERL, S., VERSTOVSEK, S., MATHEWS, S. & ANDREEFF, M. 2011. Phase I study of sorafenib in patients with refractory or relapsed acute leukemias. *Haematologica,* 96**,** 62-68.

BOUDEWIJN, M. T. & COFFER, P. J. 1995. Protein kinase B (c-Akt) in phosphatidylinositol-3-OH kinase signal transduction. *Nature,* 376**,** 599-602.

BRADBURY, D. & RUSSELL, N. 1995. Comparative quantitative expression of bcl-2 by normal and leukaemic myeloid cells. *British journal of haematology,* 91**,** 374-379.

BRANDTS, C. H., SARGIN, B., RODE, M., BIERMANN, C., LINDTNER, B., SCHWÄBLE, J., BUERGER, H., MÜLLER-TIDOW, C., CHOUDHARY, C. & MCMAHON, M. 2005. Constitutive activation of Akt by Flt3 internal tandem duplications is necessary for increased survival, proliferation, and myeloid transformation. *Cancer research,* 65**,** 9643-9650.

BRASEL, K., ESCOBAR, S., ANDERBERG, R., DE VRIES, P., GRUSS, H. J. & LYMAN, S. D. 1995. Expression of the flt3 receptor and its ligand on hematopoietic cells. *Leukemia,* 9**,** 1212-8.

BRATTON, S. B., WALKER, G., SRINIVASULA, S. M., SUN, X. M., BUTTERWORTH, M., ALNEMRI, E. S. & COHEN, G. M. 2001. Recruitment, activation and retention of caspases-9 and-3 by Apaf-1 apoptosome and associated XIAP complexes. *The EMBO journal,* 20**,** 998-1009.

BREITENBUECHER, F., MARKOVA, B., KASPER, S., CARIUS, B., STAUDER, T., BÖHMER, F. D., MASSON, K., RÖNNSTRAND, L., HUBER, C. & KINDLER, T. 2009a. A novel molecular mechanism of primary resistance to FLT3-kinase inhibitors in AML. *Blood, The Journal of the American Society of Hematology,* 113**,** 4063-4073.

BREITENBUECHER, F., MARKOVA, B., KASPER, S., CARIUS, B., STAUDER, T., BÖHMER, F. D., MASSON, K., RÖNNSTRAND, L., HUBER, C. & KINDLER, T. 2009b. A novel molecular mechanism of primary resistance to FLT3-kinase inhibitors in AML. *Blood,* 113**,** 4063-4073.

BRUNELLE, J. K., RYAN, J., YECIES, D., OPFERMAN, J. T. & LETAI, A. 2009. MCL-1–dependent leukemia cells are more sensitive to chemotherapy than BCL-2–dependent counterparts. *Journal of Cell Biology,* 187**,** 429-442.

BRUNET, A., BONNI, A., ZIGMOND, M. J., LIN, M. Z., JUO, P., HU, L. S., ANDERSON, M. J., ARDEN, K. C., BLENIS, J. & GREENBERG, M. E. 1999. Akt promotes cell survival by phosphorylating and inhibiting a Forkhead transcription factor. *cell,* 96**,** 857-868.

BRUNNER, A. M., CAMPIGOTTO, F., SADRZADEH, H., DRAPKIN, B. J., CHEN, Y. B., NEUBERG, D. S. & FATHI, A. T. 2013. Trends in all-cause mortality among patients with chronic myeloid leukemia: a

Surveillance, Epidemiology, and End Results database analysis. *Cancer,* 119**,** 2620-2629.
BUITENHUIS, M. & COFFER, P. J. 2009. The role of the PI3K-PKB signaling module in regulation of hematopoiesis. *Cell cycle,* 8**,** 560-566.
BURCHERT, A., BUG, G., FINKE, J., STELLJES, M., ROLLIG, C., WÄSCH, R., BORNHÄUSER, M., BERG, T., LANG, F. & EHNINGER, G. 2018. Sorafenib as maintenance therapy post allogeneic stem cell transplantation for FLT3-ITD positive AML: results from the randomized, double-blind, placebo-controlled multicentre sormain trial. *Blood,* 132**,** 661-661.
CALÒ, V., MIGLIAVACCA, M., BAZAN, V., MACALUSO, M., BUSCEMI, M., GEBBIA, N. & RUSSO, A. 2003. STAT proteins: from normal control of cellular events to tumorigenesis. *Journal of cellular physiology,* 197**,** 157-168.
CAO, T., JIANG, N., LIAO, H., SHUAI, X., SU, J. & ZHENG, Q. 2019. The FLT3-ITD mutation and the expression of its downstream signaling intermediates STAT5 and Pim-1 are positively correlated with CXCR4 expression in patients with acute myeloid leukemia. *Scientific reports,* 9**,** 1-10.
CAPECCHI, M. R. 1989. Altering the genome by homologous recombination. *Science,* 244**,** 1288-1292.
CAPECCHI, M. R. 2005. Gene targeting in mice: functional analysis of the mammalian genome for the twenty-first century. *Nature Reviews Genetics,* 6**,** 507-512.
CAROW, C. E., LEVENSTEIN, M., KAUFMANN, S. H., CHEN, J., AMIN, S., ROCKWELL, P., WITTE, L., BOROWITZ, M. J., CIVIN, C. I. & SMALL, D. 1996. Expression of the hematopoietic growth factor receptor FLT3 (STK-1/Flk2) in human leukemias. *Blood,* 87**,** 1089-96.
CARROLL, D. 2011. Genome engineering with zinc-finger nucleases. *Genetics,* 188**,** 773-782.
CARTER, B. Z., MAK, P. Y., MU, H., ZHOU, H., MAK, D. H., SCHOBER, W., LEVERSON, J. D., ZHANG, B., BHATIA, R. & HUANG, X. 2016. Combined targeting of BCL-2 and BCR-ABL tyrosine kinase eradicates chronic myeloid leukemia stem cells. *Science translational medicine,* 8**,** 355ra117-355ra117.
CASTAIGNE, S., PAUTAS, C., TERRÉ, C., RAFFOUX, E., BORDESSOULE, D., BASTIE, J.-N., LEGRAND, O., THOMAS, X., TURLURE, P. & REMAN, O. 2012. Effect of gemtuzumab ozogamicin on survival of adult patients with de-novo acute myeloid leukaemia (ALFA-0701): a randomised, open-label, phase 3 study. *The Lancet,* 379**,** 1508-1516.
CAUCHY, P., JAMES, S. R., ZACARIAS-CABEZA, J., PTASINSKA, A., IMPERATO, M. R., ASSI, S. A., PIPER, J., CANESTRARO, M., HOOGENKAMP, M. & RAGHAVAN, M. 2015. Chronic FLT3-ITD signaling in acute myeloid leukemia is connected to a specific chromatin signature. *Cell reports,* 12**,** 821-836.
CEBRIAN-SERRANO, A. & DAVIES, B. 2017. CRISPR-Cas orthologues and variants: optimizing the repertoire, specificity and delivery of genome engineering tools. *Mammalian Genome,* 28**,** 247-261.
CERAMI, E., GAO, J., DOGRUSOZ, U., GROSS, B. E., SUMER, S. O., AKSOY, B. A., JACOBSEN, A., BYRNE, C. J., HEUER, M. L. &

LARSSON, E. 2012. The cBio cancer genomics portal: an open platform for exploring multidimensional cancer genomics data. AACR.
CHAGASTELLES, P. C. & NARDI, N. B. 2011. Biology of stem cells: an overview. *Kidney international supplements,* 1**,** 63-67.
CHAN, P. M., ILANGUMARAN, S., LA ROSE, J., CHAKRABARTTY, A. & ROTTAPEL, R. 2003. Autoinhibition of the kit receptor tyrosine kinase by the cytosolic juxtamembrane region. *Molecular and cellular biology,* 23**,** 3067-3078.
CHAN, S. L. & YU, V. C. 2004. Proteins of the bcl-2 family in apoptosis signalling: from mechanistic insights to therapeutic opportunities. *Clinical and Experimental Pharmacology and Physiology,* 31**,** 119-128.
CHAO, Q., SPRANKLE, K. G., GROTZFELD, R. M., LAI, A. G., CARTER, T. A., VELASCO, A. M., GUNAWARDANE, R. N., CRAMER, M. D., GARDNER, M. F., JAMES, J., ZARRINKAR, P. P., PATEL, H. K. & BHAGWAT, S. S. 2009. Identification of N-(5-tert-butyl-isoxazol-3-yl)-N'-{4-[7-(2-morpholin-4-yl-ethoxy)imidazo[2,1-b][1 ,3]benzothiazol-2-yl]phenyl}urea dihydrochloride (AC220), a uniquely potent, selective, and efficacious FMS-like tyrosine kinase-3 (FLT3) inhibitor. *J Med Chem,* 52**,** 7808-16.
CHAUDRY, S. F. & CHEVASSUT, T. J. 2017. Epigenetic guardian: a review of the DNA methyltransferase DNMT3A in acute myeloid leukaemia and clonal haematopoiesis. *BioMed research international,* 2017.
CHEN, C., LIU, Y., LIU, R., IKENOUE, T., GUAN, K.-L., LIU, Y. & ZHENG, P. 2008. TSC–mTOR maintains quiescence and function of hematopoietic stem cells by repressing mitochondrial biogenesis and reactive oxygen species. *The Journal of experimental medicine,* 205**,** 2397-2408.
CHENG, H., ZHENG, Z. & CHENG, T. 2020. New paradigms on hematopoietic stem cell differentiation. *Protein & cell,* 11**,** 34-44.
CHKLOVSKAIA, E., JANSEN, W., NISSEN, C., LYMAN, S. D., RAHNER, C., LANDMANN, L. & WODNAR-FILIPOWICZ, A. 1999. Mechanism of flt3 ligand expression in bone marrow failure: translocation from intracellular stores to the surface of T lymphocytes after chemotherapy-induced suppression of hematopoiesis. *Blood, The Journal of the American Society of Hematology,* 93**,** 2595-2604.
CHOI, Y., ZHANG, J., MURGA, C., YU, H., KOLLER, E., MONIA, B. P., GUTKIND, J. S. & LI, W. 2002. PTEN, but not SHIP and SHIP2, suppresses the PI3K/Akt pathway and induces growth inhibition and apoptosis of myeloma cells. *Oncogene,* 21**,** 5289-5300.
CHONG, H. & GUAN, K.-L. 2003. Regulation of Raf through phosphorylation and N terminus-C terminus interaction. *Journal of Biological Chemistry,* 278**,** 36269-36276.
CHOUDHARY, C., BRANDTS, C., SCHWABLE, J., TICKENBROCK, L., SARGIN, B., UEKER, A., BÖHMER, F.-D., BERDEL, W. E., MÜLLER-TIDOW, C. & SERVE, H. 2007. Activation mechanisms of STAT5 by oncogenic Flt3-ITD. *Blood, The Journal of the American Society of Hematology,* 110**,** 370-374.
CHOUDHARY, C., OLSEN, J. V., BRANDTS, C., COX, J., REDDY, P. N., BÖHMER, F. D., GERKE, V., SCHMIDT-ARRAS, D.-E., BERDEL, W. E. & MÜLLER-TIDOW, C. 2009a. Mislocalized activation of oncogenic

RTKs switches downstream signaling outcomes. *Molecular cell,* 36**,** 326-339.

CHOUDHARY, C., OLSEN, J. V., BRANDTS, C., COX, J., REDDY, P. N., BOHMER, F. D., GERKE, V., SCHMIDT-ARRAS, D. E., BERDEL, W. E., MULLER-TIDOW, C., MANN, M. & SERVE, H. 2009b. Mislocalized activation of oncogenic RTKs switches downstream signaling outcomes. *Mol Cell,* 36**,** 326-39.

CHOUDHARY, C., SCHWÄBLE, J., BRANDTS, C., TICKENBROCK, L., SARGIN, B. L., KINDLER, T., FISCHER, T., BERDEL, W. E., MÜLLER-TIDOW, C. & SERVE, H. 2005. AML-associated Flt3 kinase domain mutations show signal transduction differences compared with Flt3 ITD mutations. *Blood,* 106**,** 265-273.

CHRISTIN, J. R. & BECKERT, M. V. 2016. Origins and Applications of CRISPR-Mediated Genome Editing. *The Einstein journal of biology and medicine: EJBM,* 31**,** 2.

CLAESSON-WELSH, L., ERIKSSON, A., WESTERMARK, B. & HELDIN, C.-H. 1989. cDNA cloning and expression of the human A-type platelet-derived growth factor (PDGF) receptor establishes structural similarity to the B-type PDGF receptor. *Proceedings of the National Academy of Sciences,* 86**,** 4917-4921.

COLE, S., AYLETT, G., HARVEY, N., CAMBARERI, A. & ASHMAN, L. 1996. Increased expression of c-kit or its ligand Steel factor is not a common feature of adult acute myeloid leukaemia. *Leukemia,* 10**,** 288-296.

CONG, L., RAN, F. A., COX, D., LIN, S., BARRETTO, R., HABIB, N., HSU, P. D., WU, X., JIANG, W. & MARRAFFINI, L. A. 2013. Multiplex genome engineering using CRISPR/Cas systems. *Science,* 339**,** 819-823.

CORTES, J., PERL, A. E., DÖHNER, H., KANTARJIAN, H., MARTINELLI, G., KOVACSOVICS, T., ROUSSELOT, P., STEFFEN, B., DOMBRET, H. & ESTEY, E. 2018a. Quizartinib, an FLT3 inhibitor, as monotherapy in patients with relapsed or refractory acute myeloid leukaemia: an open-label, multicentre, single-arm, phase 2 trial. *The Lancet Oncology,* 19**,** 889-903.

CORTES, J. E., ALTMAN, J., RITCHIE, E. K., LARSON, R. A., CLAXTON, D., MINDEN, M. D., GOLDENBERG, A., NAOE, T., YOON, S.-S. & ROUSSELOT, P. H. 2017. A phase II/III, multicenter, open-label, 3-arm study of gilteritinib, gilteritinib plus azacitidine, or azacitidine alone in the treatment of newly diagnosed FLT3 mutation-positive acute myeloid leukemia (AML) patients ineligible for intensive induction chemotherapy. American Society of Clinical Oncology.

CORTES, J. E., KANTARJIAN, H., FORAN, J. M., GHIRDALADZE, D., ZODELAVA, M., BORTHAKUR, G., GAMMON, G., TRONE, D., ARMSTRONG, R. C. & JAMES, J. 2013. Phase I study of quizartinib administered daily to patients with relapsed or refractory acute myeloid leukemia irrespective of FMS-like tyrosine kinase 3–internal tandem duplication status. *Journal of clinical oncology,* 31**,** 3681.

CORTES, J. E., KHALED, S., MARTINELLI, G., PERL, A. E., GANGULY, S., RUSSELL, N., KRÄMER, A., DOMBRET, H., HOGGE, D. & JONAS, B. A. 2019. Quizartinib versus salvage chemotherapy in relapsed or refractory FLT3-ITD acute myeloid leukaemia (QuANTUM-R): a

multicentre, randomised, controlled, open-label, phase 3 trial. *The Lancet Oncology,* 20**,** 984-997.

CORTES, J. E., KHALED, S. K., MARTINELLI, G., PERL, A. E., GANGULY, S., RUSSELL, N. H., KRAMER, A., DOMBRET, H., HOGGE, D. & JONAS, B. A. 2018b. Efficacy and safety of single-agent quizartinib (Q), a potent and selective FLT3 inhibitor (FLT3i), in patients (pts) with FLT3-internal tandem duplication (FLT3-ITD)-mutated relapsed/refractory (R/R) acute myeloid leukemia (AML) enrolled in the global, phase 3, randomized controlled quantum-R trial. *Blood,* 132**,** 563-563.

COUSSENS, L., VAN BEVEREN, C., SMITH, D., CHEN, E., MITCHELL, R. L., ISACKE, C. M., VERMA, I. M. & ULLRICH, A. 1986. Structural alteration of viral homologue of receptor proto-oncogene fms at carboxyl terminus. *Nature,* 320**,** 277-280.

CZABOTAR, P. E., LEE, E. F., VAN DELFT, M. F., DAY, C. L., SMITH, B. J., HUANG, D. C., FAIRLIE, W. D., HINDS, M. G. & COLMAN, P. M. 2007. Structural insights into the degradation of Mcl-1 induced by BH3 domains. *Proceedings of the National Academy of Sciences,* 104**,** 6217-6222.

CZABOTAR, P. E., LESSENE, G., STRASSER, A. & ADAMS, J. M. 2014. Control of apoptosis by the BCL-2 protein family: implications for physiology and therapy. *Nature reviews Molecular cell biology,* 15**,** 49-63.

DAVER, N., CORTES, J., RAVANDI, F., PATEL, K. P., BURGER, J. A., KONOPLEVA, M. & KANTARJIAN, H. 2015. Secondary mutations as mediators of resistance to targeted therapy in leukemia. *Blood, The Journal of the American Society of Hematology,* 125**,** 3236-3245.

DAVER, N., SCHLENK, R. F., RUSSELL, N. H. & LEVIS, M. J. 2019. Targeting FLT3 mutations in AML: review of current knowledge and evidence. *Leukemia,* 33**,** 299-312.

DE KOUCHKOVSKY, I. & ABDUL-HAY, M. 2016. 'Acute myeloid leukemia: a comprehensive review and 2016 update'. *Blood Cancer J,* 6**,** e441.

DEL POETA, G., VENDITTI, A., DEL PRINCIPE, M. I., MAURILLO, L., BUCCISANO, F., TAMBURINI, A., COX, M. C., FRANCHI, A., BRUNO, A. & MAZZONE, C. 2003. Amount of spontaneous apoptosis detected by Bax/Bcl-2 ratio predicts outcome in acute myeloid leukemia (AML) Presented in part at the 42nd annual meeting of the American Society of Hematology, San Francisco, CA, December 1-5, 2000.46. *Blood, The Journal of the American Society of Hematology,* 101**,** 2125-2131.

DELBRIDGE, A. R., GRABOW, S., STRASSER, A. & VAUX, D. L. 2016. Thirty years of BCL-2: translating cell death discoveries into novel cancer therapies. *Nature reviews Cancer,* 16**,** 99.

DELIA, D., AIELLO, A., SOLIGO, D., FONTANELLA, E., MELANI, C., PEZZELLA, F., PIEROTTI, M. A. & DELLA PORTA, G. 1992. bcl-2 proto-oncogene expression in normal and neoplastic human myeloid cells.

DELTCHEVA, E., CHYLINSKI, K., SHARMA, C. M., GONZALES, K., CHAO, Y., PIRZADA, Z. A., ECKERT, M. R., VOGEL, J. & CHARPENTIER, E. 2011. CRISPR RNA maturation by trans-encoded small RNA and host factor RNase III. *Nature,* 471**,** 602-607.

DINARDO, C., DE BOTTON, S., POLLYEA, D. A., STEIN, E. M., FATHI, A. T., ROBOZ, G. J., COLLINS, R., SWORDS, R. T., FLINN, I. W. & ALTMAN, J. K. 2015. Molecular profiling and relationship with clinical response in patients with IDH1 mutation-positive hematologic malignancies receiving AG-120, a first-in-class potent inhibitor of mutant IDH1, in addition to data from the completed dose escalation portion of the phase 1 study. *Blood,* 126.

DINARDO, C. D. & CORTES, J. E. 2016. Mutations in AML: prognostic and therapeutic implications. *Hematology 2014, the American Society of Hematology Education Program Book,* 2016**,** 348-355.

DINARDO, C. D., PRATZ, K., PULLARKAT, V., JONAS, B. A., ARELLANO, M., BECKER, P. S., FRANKFURT, O., KONOPLEVA, M., WEI, A. H. & KANTARJIAN, H. M. 2019. Venetoclax combined with decitabine or azacitidine in treatment-naive, elderly patients with acute myeloid leukemia. *Blood,* 133**,** 7-17.

DÖHNER, H., ESTEY, E., GRIMWADE, D., AMADORI, S., APPELBAUM, F. R., BÜCHNER, T., DOMBRET, H., EBERT, B. L., FENAUX, P. & LARSON, R. A. 2017. Diagnosis and management of AML in adults: 2017 ELN recommendations from an international expert panel. *Blood,* 129**,** 424-447.

DOHNER, H., ESTEY, E. H., AMADORI, S., APPELBAUM, F. R., BUCHNER, T., BURNETT, A. K., DOMBRET, H., FENAUX, P., GRIMWADE, D., LARSON, R. A., LO-COCO, F., NAOE, T., NIEDERWIESER, D., OSSENKOPPELE, G. J., SANZ, M. A., SIERRA, J., TALLMAN, M. S., LOWENBERG, B., BLOOMFIELD, C. D. & EUROPEAN, L. 2010. Diagnosis and management of acute myeloid leukemia in adults: recommendations from an international expert panel, on behalf of the European LeukemiaNet. *Blood,* 115**,** 453-74.

DREXLER, H. 1996. Expression of FLT3 receptor and response to FLT3 ligand by leukemic cells. *Leukemia,* 10**,** 588-599.

DRUKER, B. J., TAMURA, S., BUCHDUNGER, E., OHNO, S., SEGAL, G. M., FANNING, S., ZIMMERMANN, J. & LYDON, N. B. 1996. Effects of a selective inhibitor of the Abl tyrosine kinase on the growth of Bcr–Abl positive cells. *Nature medicine,* 2**,** 561-566.

DU, C., FANG, M., LI, Y., LI, L. & WANG, X. 2000. Smac, a mitochondrial protein that promotes cytochrome c–dependent caspase activation by eliminating IAP inhibition. *Cell,* 102**,** 33-42.

DUMAS, P.-Y., NAUDIN, C., MARTIN-LANNERÉE, S., IZAC, B., CASETTI, L., MANSIER, O., ROUSSEAU, B., ARTUS, A., DUFOSSÉE, M. & GIESE, A. 2019. Hematopoietic niche drives FLT3-ITD acute myeloid leukemia resistance to quizartinib via STAT5-and hypoxia-dependent upregulation of AXL. *haematologica,* 104**,** 2017-2027.

ERBA, H. P., LEVIS, M. J., SEKERES, M. A., DOMBRET, H., AMADORI, S., ZERNOVAK, O., MIRES, D. E., GE, N., HANYOK, J. & MACINTYRE, S. 2016. Phase 3 (P3) study of quizartinib (Q) or placebo (P) with induction (IND) and consolidation chemotherapy (CON) and as maintenance (MN) in patients (pts) with newly diagnosed (NDx) FLT3-ITD–positive acute myeloid leukemia (AML): the QuANTUM-First study. American Society of Clinical Oncology.

ESTEY, E. H. 2018. Acute myeloid leukemia: 2019 update on risk-stratification and management. *Am J Hematol,* 93**,** 1267-1291.

FAN, J., LI, L., SMALL, D. & RASSOOL, F. 2010. Cells expressing FLT3/ITD mutations exhibit elevated repair errors generated through alternative NHEJ pathways: implications for genomic instability and therapy. *Blood, The Journal of the American Society of Hematology,* 116**,** 5298-5305.

FATHI, A. T. & CHEN, Y.-B. 2011. Treatment of FLT3-ITD acute myeloid leukemia. *American journal of blood research,* 1**,** 175.

FENAUX, P., MUFTI, G. J., HELLSTROM-LINDBERG, E., SANTINI, V., FINELLI, C., GIAGOUNIDIS, A., SCHOCH, R., GATTERMANN, N., SANZ, G. & LIST, A. 2009. Efficacy of azacitidine compared with that of conventional care regimens in the treatment of higher-risk myelodysplastic syndromes: a randomised, open-label, phase III study. *The lancet oncology,* 10**,** 223-232.

FERNANDEZ, S., DESPLAT, V., VILLACRECES, A., GUITART, A. V., MILPIED, N., PIGNEUX, A., VIGON, I., PASQUET, J.-M. & DUMAS, P.-Y. 2019. Targeting tyrosine kinases in acute myeloid leukemia: why, who and how? *International journal of molecular sciences,* 20**,** 3429.

FISCHER, T., STONE, R. M., DEANGELO, D. J., GALINSKY, I., ESTEY, E., LANZA, C., FOX, E., EHNINGER, G., FELDMAN, E. J. & SCHILLER, G. J. 2010. Phase IIB trial of oral Midostaurin (PKC412), the FMS-like tyrosine kinase 3 receptor (FLT3) and multi-targeted kinase inhibitor, in patients with acute myeloid leukemia and high-risk myelodysplastic syndrome with either wild-type or mutated FLT3. *Journal of clinical oncology,* 28**,** 4339.

FLEISCHER, A., REBOLLO, A. & AYLLÓN, V. 2003. BH3-only proteins: the lords of death. *ARCHIVUM IMMUNOLOGIAE ET THERAPIAE EXPERIMENTALIS-ENGLISH EDITION-,* 51**,** 9-18.

FLETCHER, L., JOSHI, S. K. & TRAER, E. 2020. Profile of quizartinib for the treatment of adult patients with relapsed/refractory FLT3-ITD-positive acute myeloid leukemia: evidence to date. *Cancer Management and Research,* 12**,** 151.

FUKUDA, S., BROXMEYER, H. E. & PELUS, L. M. 2005. Flt3 ligand and the Flt3 receptor regulate hematopoietic cell migration by modulating the SDF-1α (CXCL12)/CXCR4 axis. *Blood,* 105**,** 3117-3126.

GAJ, T., GERSBACH, C. A. & BARBAS III, C. F. 2013. ZFN, TALEN, and CRISPR/Cas-based methods for genome engineering. *Trends in biotechnology,* 31**,** 397-405.

GALKIN, M. & JONAS, B. A. 2019. Enasidenib in the treatment of relapsed/refractory acute myeloid leukemia: an evidence-based review of its place in therapy. *Core evidence,* 14**,** 3.

GALLOWAY, J. L. & ZON, L. I. 2003. Ontogeny of hematopoiesis: examining the emergence of hematopoietic cells in the vertebrate embryo. *Current topics in developmental biology,* 53**,** 139-158.

GAO, J., AKSOY, B. A., DOGRUSOZ, U., DRESDNER, G., GROSS, B., SUMER, S. O., SUN, Y., JACOBSEN, A., SINHA, R. & LARSSON, E. 2013. Integrative analysis of complex cancer genomics and clinical profiles using the cBioPortal. *Science signaling,* 6**,** pl1-pl1.

GARCIA, J. S. & STONE, R. M. 2017. The development of FLT3 inhibitors in acute myeloid leukemia. *Hematology/Oncology Clinics,* 31**,** 663-680.
GARG, M., NAGATA, Y., KANOJIA, D., MAYAKONDA, A., YOSHIDA, K., HARIDAS KELOTH, S., ZANG, Z. J., OKUNO, Y., SHIRAISHI, Y. & CHIBA, K. 2015. Profiling of somatic mutations in acute myeloid leukemia with FLT3-ITD at diagnosis and relapse. *Blood, The Journal of the American Society of Hematology,* 126**,** 2491-2501.
GASSON, J. C. 1991. Molecular physiology of granulocyte-macrophage colony-stimulating factor.
GILBERT, L. A., HORLBECK, M. A., ADAMSON, B., VILLALTA, J. E., CHEN, Y., WHITEHEAD, E. H., GUIMARAES, C., PANNING, B., PLOEGH, H. L. & BASSIK, M. C. 2014. Genome-scale CRISPR-mediated control of gene repression and activation. *Cell,* 159**,** 647-661.
GILBERT, L. A., LARSON, M. H., MORSUT, L., LIU, Z., BRAR, G. A., TORRES, S. E., STERN-GINOSSAR, N., BRANDMAN, O., WHITEHEAD, E. H. & DOUDNA, J. A. 2013. CRISPR-mediated modular RNA-guided regulation of transcription in eukaryotes. *Cell,* 154**,** 442-451.
GILL, S., TASIAN, S. K., RUELLA, M., SHESTOVA, O., LI, Y., PORTER, D. L., CARROLL, M., DANET-DESNOYERS, G., SCHOLLER, J. & GRUPP, S. A. 2014. Preclinical targeting of human acute myeloid leukemia and myeloablation using chimeric antigen receptor–modified T cells. *Blood, The Journal of the American Society of Hematology,* 123**,** 2343-2354.
GILLILAND, D. G. & GRIFFIN, J. D. 2002a. The roles of FLT3 in hematopoiesis and leukemia. *Blood,* 100**,** 1532-42.
GILLILAND, D. G. & GRIFFIN, J. D. 2002b. The roles of FLT3 in hematopoiesis and leukemia. *Blood, The Journal of the American Society of Hematology,* 100**,** 1532-1542.
GLASER, S. P., LEE, E. F., TROUNSON, E., BOUILLET, P., WEI, A., FAIRLIE, W. D., IZON, D. J., ZUBER, J., RAPPAPORT, A. R. & HEROLD, M. J. 2012. Anti-apoptotic Mcl-1 is essential for the development and sustained growth of acute myeloid leukemia. *Genes & development,* 26**,** 120-125.
GORES, G. J. & KAUFMANN, S. H. 2012. Selectively targeting Mcl-1 for the treatment of acute myelogenous leukemia and solid tumors. *Genes & development,* 26**,** 305-311.
GRAHAM, D. B. & ROOT, D. E. 2015. Resources for the design of CRISPR gene editing experiments. *Genome biology,* 16**,** 260.
GREEN, A. S., MACIEL, T. T., YIN, C., MAZED, F., TOWNSEND, E. C., PILORGE, S., LAMBERT, M., PAUBELLE, E., JACQUEL, A. & ZYLBERSZTEJN, F. 2015. Pim kinases modulate resistance to FLT3 tyrosine kinase inhibitors in FLT3-ITD acute myeloid leukemia. *Science advances,* 1**,** e1500221.
GREEN, D. R. & REED, J. C. 1998. Mitochondria and apoptosis. *science,* 281**,** 1309-1312.
GRIFFITH, J., BLACK, J., FAERMAN, C., SWENSON, L., WYNN, M., LU, F., LIPPKE, J. & SAXENA, K. 2004. The structural basis for autoinhibition of FLT3 by the juxtamembrane domain. *Molecular cell,* 13**,** 169-178.

GRIMWADE, D., HILLS, R. K., MOORMAN, A. V., WALKER, H., CHATTERS, S., GOLDSTONE, A. H., WHEATLEY, K., HARRISON, C. J., BURNETT, A. K. & GROUP, N. C. R. I. A. L. W. 2010. Refinement of cytogenetic classification in acute myeloid leukemia: determination of prognostic significance of rare recurring chromosomal abnormalities among 5876 younger adult patients treated in the United Kingdom Medical Research Council trials. *Blood, The Journal of the American Society of Hematology,* 116**,** 354-365.

GRIMWADE, D., WALKER, H., OLIVER, F., WHEATLEY, K., HARRISON, C., HARRISON, G., REES, J., HANN, I., STEVENS, R. & BURNETT, A. 1998. The importance of diagnostic cytogenetics on outcome in AML: analysis of 1,612 patients entered into the MRC AML 10 trial. *Blood, The Journal of the American Society of Hematology,* 92**,** 2322-2333.

GROVE, C. S. & VASSILIOU, G. S. 2014. Acute myeloid leukaemia: a paradigm for the clonal evolution of cancer? *Dis Model Mech,* 7**,** 941-51.

GRUNDLER, R., BRAULT, L., GASSER, C., BULLOCK, A. N., DECHOW, T., WOETZEL, S., POGACIC, V., VILLA, A., EHRET, S. & BERRIDGE, G. 2009. Dissection of PIM serine/threonine kinases in FLT3-ITD–induced leukemogenesis reveals PIM1 as regulator of CXCL12–CXCR4-mediated homing and migration. *Journal of experimental medicine,* 206**,** 1957-1970.

GRUNDLER, R., MIETHING, C., THIEDE, C., PESCHEL, C. & DUYSTER, J. 2005. FLT3-ITD and tyrosine kinase domain mutants induce 2 distinct phenotypes in a murine bone marrow transplantation model. *Blood,* 105**,** 4792-4799.

GRUNWALD, M. R. & LEVIS, M. J. 2013. FLT3 inhibitors for acute myeloid leukemia: a review of their efficacy and mechanisms of resistance. *International journal of hematology,* 97**,** 683-694.

GUERROUAHEN, B. S., AL-HIJJI, I. & TABRIZI, A. R. 2011. Osteoblastic and vascular endothelial niches, their control on normal hematopoietic stem cells, and their consequences on the development of leukemia. *Stem cells international,* 2011.

HANAHAN, D. & WEINBERG, R. A. 2000. The hallmarks of cancer. *cell,* 100**,** 57-70.

HANNUM, C., CULPEPPER, J., CAMPBELL, D., MCCLANAHAN, T., ZURAWSKI, S., KASTELEIN, R., BAZAN, J., HUDAK, S., WAGNER, J. & MATTSON, J. 1994. Ligand for FLT3/FLK2 receptor tyrosine kinase regulates growth of haematopoietic stem cells and is encoded by variant RNAs. *Nature,* 368**,** 643-648.

HATA, A. N., ENGELMAN, J. A. & FABER, A. C. 2015. The BCL2 family: key mediators of the apoptotic response to targeted anticancer therapeutics. *Cancer discovery,* 5**,** 475-487.

HAYAKAWA, F., TOWATARI, M., KIYOI, H., TANIMOTO, M., KITAMURA, T., SAITO, H. & NAOE, T. 2000. Tandem-duplicated Flt3 constitutively activates STAT5 and MAP kinase and introduces autonomous cell growth in IL-3-dependent cell lines. *Oncogene,* 19**,** 624-631.

HECKER, J., MILLER, I., GÖTZE, K. S. & VERBEEK, M. 2018. Bridging strategies to allogeneic transplant for older AML patients. *Cancers,* 10**,** 232.

HECKL, D., KOWALCZYK, M. S., YUDOVICH, D., BELIZAIRE, R., PURAM, R. V., MCCONKEY, M. E., THIELKE, A., ASTER, J. C., REGEV, A. & EBERT, B. L. 2014. Generation of mouse models of myeloid malignancy with combinatorial genetic lesions using CRISPR-Cas9 genome editing. *Nature biotechnology,* 32**,** 941.

HELENIUS, A. & AEBI, M. 2004. Roles of N-linked glycans in the endoplasmic reticulum. *Annual review of biochemistry,* 73**,** 1019-1049.

HIRADE, T., ABE, M., ONISHI, C., TAKETANI, T., YAMAGUCHI, S. & FUKUDA, S. 2016. Internal tandem duplication of FLT3 deregulates proliferation and differentiation and confers resistance to the FLT3 inhibitor AC220 by Up-regulating RUNX1 expression in hematopoietic cells. *International journal of hematology,* 103**,** 95-106.

HOPPE, P. S., SCHWARZFISCHER, M., LOEFFLER, D., KOKKALIARIS, K. D., HILSENBECK, O., MORITZ, N., ENDELE, M., FILIPCZYK, A., GAMBARDELLA, A. & AHMED, N. 2016. Early myeloid lineage choice is not initiated by random PU. 1 to GATA1 protein ratios. *Nature,* 535**,** 299-302.

HOU, H., SUN, H., LU, P., GE, C., ZHANG, L., LI, H., ZHAO, F., TIAN, H., ZHANG, L. & CHEN, T. 2013. Tunicamycin potentiates cisplatin anticancer efficacy through the DPAGT1/Akt/ABCG2 pathway in mouse Xenograft models of human hepatocellular carcinoma. *Molecular cancer therapeutics,* 12**,** 2874-2884.

HOU, P., WU, C., WANG, Y., QI, R., BHAVANASI, D., ZUO, Z., DOS SANTOS, C., CHEN, S., CHEN, Y. & ZHENG, H. 2017. A genome-wide CRISPR screen identifies genes critical for resistance to FLT3 inhibitor AC220. *Cancer research,* 77**,** 4402-4413.

HSU, C.-L., KIKUCHI, K. & KONDO, M. 2007. Activation of mitogen-activated protein kinase kinase (MEK)/extracellular signal–regulated kinase (ERK) signaling pathway is involved in myeloid lineage commitment. *Blood, The Journal of the American Society of Hematology,* 110**,** 1420-1428.

HU, J. H., MILLER, S. M., GEURTS, M. H., TANG, W., CHEN, L., SUN, N., ZEINA, C. M., GAO, X., REES, H. A. & LIN, Z. 2018. Evolved Cas9 variants with broad PAM compatibility and high DNA specificity. *Nature,* 556**,** 57-63.

HUANG, J., ZHANG, Y., BERSENEV, A., O'BRIEN, W. T., TONG, W., EMERSON, S. G. & KLEIN, P. S. 2009. Pivotal role for glycogen synthase kinase–3 in hematopoietic stem cell homeostasis in mice. *The Journal of clinical investigation,* 119**,** 3519-3529.

ISHIKAWA, F., YOSHIDA, S., SAITO, Y., HIJIKATA, A., KITAMURA, H., TANAKA, S., NAKAMURA, R., TANAKA, T., TOMIYAMA, H. & SAITO, N. 2007. Chemotherapy-resistant human AML stem cells home to and engraft within the bone-marrow endosteal region. *Nature biotechnology,* 25**,** 1315-1321.

IWASAKI, H., SOMOZA, C., SHIGEMATSU, H., DUPREZ, E. A., IWASAKI-ARAI, J., MIZUNO, S.-I., ARINOBU, Y., GEARY, K., ZHANG, P. & DAYARAM, T. 2005. Distinctive and indispensable roles of PU. 1 in maintenance of hematopoietic stem cells and their differentiation. *Blood,* 106**,** 1590-1600.

JAGANNATHAN-BOGDAN, M. & ZON, L. I. 2013. Hematopoiesis. *Development,* 140**,** 2463-2467.

JETANI, H., GARCIA-CADENAS, I., NERRETER, T., THOMAS, S., RYDZEK, J., MEIJIDE, J. B., BONIG, H., HERR, W., SIERRA, J. & EINSELE, H. 2018. CAR T-cells targeting FLT3 have potent activity against FLT3−ITD+ AML and act synergistically with the FLT3-inhibitor crenolanib. *Leukemia,* 32**,** 1168-1179.

JIANG, F. & DOUDNA, J. A. 2017. CRISPR-Cas9 Structures and Mechanisms. *Annu Rev Biophys,* 46**,** 505-529.

JINEK, M., CHYLINSKI, K., FONFARA, I., HAUER, M., DOUDNA, J. A. & CHARPENTIER, E. 2012. A programmable dual-RNA-guided DNA endonuclease in adaptive bacterial immunity. *Science,* 337**,** 816-21.

JINEK, M., EAST, A., CHENG, A., LIN, S., MA, E. & DOUDNA, J. 2013. RNA-programmed genome editing in human cells. *elife,* 2**,** e00471.

JOUNG, J. K. & SANDER, J. D. 2013. TALENs: a widely applicable technology for targeted genome editing. *Nature reviews Molecular cell biology,* 14**,** 49-55.

JUNTILLA, M. M., PATIL, V. D., CALAMITO, M., JOSHI, R. P., BIRNBAUM, M. J. & KORETZKY, G. A. 2010. AKT1 and AKT2 maintain hematopoietic stem cell function by regulating reactive oxygen species. *Blood, The Journal of the American Society of Hematology,* 115**,** 4030-4038.

KAKAROUGKAS, A., ISMAIL, A., CHAMBERS, A. L., RIBALLO, E., HERBERT, A. D., KÜNZEL, J., LÖBRICH, M., JEGGO, P. A. & DOWNS, J. A. 2014. Requirement for PBAF in transcriptional repression and repair at DNA breaks in actively transcribed regions of chromatin. *Molecular cell,* 55**,** 723-732.

KALE, J., OSTERLUND, E. J. & ANDREWS, D. W. 2018. BCL-2 family proteins: changing partners in the dance towards death. *Cell Death & Differentiation,* 25**,** 65-80.

KAMPA-SCHITTENHELM, K. M., HEINRICH, M. C., AKMUT, F., DÖHNER, H., DÖHNER, K. & SCHITTENHELM, M. M. 2013. Quizartinib (AC220) is a potent second generation class III tyrosine kinase inhibitor that displays a distinct inhibition profile against mutant-FLT3,-PDGFRA and-KIT isoforms. *Molecular cancer,* 12**,** 19.

KANNAN, R. & VENTURA, A. 2015. The CRISPR revolution and its impact on cancer research. *Swiss medical weekly,* 145**,** w14230.

KASPER, S., BREITENBUECHER, F., HEIDEL, F., HOFFARTH, S., MARKOVA, B., SCHULER, M. & FISCHER, T. 2012. Targeting MCL-1 sensitizes FLT3-ITD-positive leukemias to cytotoxic therapies. *Blood cancer journal,* 2**,** e60-e60.

KASTAN, M. B., ONYEKWERE, O., SIDRANSKY, D., VOGELSTEIN, B. & CRAIG, R. W. 1991. Participation of p53 protein in the cellular response to DNA damage. *Cancer research,* 51**,** 6304-6311.

KAUFMANN, S. H., KARP, J. E., SVINGEN, P. A., KRAJEWSKI, S., BURKE, P. J., GORE, S. D. & REED, J. C. 1998. Elevated expression of the apoptotic regulator Mcl-1 at the time of leukemic relapse. *Blood, The Journal of the American Society of Hematology,* 91**,** 991-1000.

KAUSHANSKY, K. 1995. Thrombopoietin: the primary regulator of megakaryocyte and platelet production. *Thrombosis and haemostasis,* 73**,** 521-525.
KAZI, J. U., CHOUGULE, R. A., LI, T., SU, X., MOHARRAM, S. A., RUPAR, K., MARHÄLL, A., GAZI, M., SUN, J. & ZHAO, H. 2017. Tyrosine 842 in the activation loop is required for full transformation by the oncogenic mutant FLT3-ITD. *Cellular and Molecular Life Sciences,* 74**,** 2679-2688.
KAZI, J. U. & RÖNNSTRAND, L. 2019. FMS-like tyrosine kinase 3/FLT3: from basic science to clinical implications. *Physiological reviews,* 99**,** 1433-1466.
KE, Y.-Y., SINGH, V. K., COUMAR, M. S., HSU, Y. C., WANG, W.-C., SONG, J.-S., CHEN, C.-H., LIN, W.-H., WU, S.-H. & HSU, J. T. 2015. Homology modeling of DFG-in FMS-like tyrosine kinase 3 (FLT3) and structure-based virtual screening for inhibitor identification. *Scientific reports,* 5**,** 11702.
KELLY, L. M. & GILLILAND, D. G. 2002. Genetics of myeloid leukemias. *Annual review of genomics and human genetics,* 3**,** 179-198.
KERR, A. J., JAMES, J. A., SMITH, M. A., WILLSON, C., COURT, E. L. & SMITH, J. G. 2003. An investigation of the MEK/ERK inhibitor U0126 in acute myeloid leukemia. *Annals of the New York Academy of Sciences,* 1010**,** 86-89.
KHURANA, A. & SHAFER, D. A. 2019. MDM2 antagonists as a novel treatment option for acute myeloid leukemia: perspectives on the therapeutic potential of idasanutlin (RG7388). *OncoTargets and therapy,* 12**,** 2903.
KIHARA, R., NAGATA, Y., KIYOI, H., KATO, T., YAMAMOTO, E., SUZUKI, K., CHEN, F., ASOU, N., OHTAKE, S. & MIYAWAKI, S. 2014. Comprehensive analysis of genetic alterations and their prognostic impacts in adult acute myeloid leukemia patients. *Leukemia,* 28**,** 1586-1595.
KIM, K. H. & SEDERSTROM, J. M. 2015. Assaying cell cycle status using flow cytometry. *Current protocols in molecular biology,* 111**,** 28.6. 1-28.6. 11.
KIYOI, H., KAWASHIMA, N. & ISHIKAWA, Y. 2020. FLT3 mutations in acute myeloid leukemia: Therapeutic paradigm beyond inhibitor development. *Cancer Science,* 111**,** 312.
KIYOI, H., OHNO, R., UEDA, R., SAITO, H. & NAOE, T. 2002. Mechanism of constitutive activation of FLT3 with internal tandem duplication in the juxtamembrane domain. *Oncogene,* 21**,** 2555-2563.
KIYOI, H., TOWATARI, M., YOKOTA, S., HAMAGUCHI, M., OHNO, R., SAITO, H. & NAOE, T. 1998a. Internal tandem duplication of the FLT3 gene is a novel modality of elongation mutation which causes constitutive activation of the product. *Leukemia,* 12**,** 1333-1337.
KIYOI, H., TOWATARI, M., YOKOTA, S., HAMAGUCHI, M., OHNO, R., SAITO, H. & NAOE, T. 1998b. Internal tandem duplication of the FLT3 gene is a novel modality of elongation mutation which causes constitutive activation of the product. *Leukemia,* 12**,** 1333-7.
KNAPPER, S. 2007. FLT3 inhibition in acute myeloid leukaemia. *Br J Haematol,* 138**,** 687-99.
KNAPPER, S., RUSSELL, N., GILKES, A., HILLS, R. K., GALE, R. E., CAVENAGH, J. D., JONES, G., KJELDSEN, L., GRUNWALD, M. R. &

THOMAS, I. 2017. A randomized assessment of adding the kinase inhibitor lestaurtinib to first-line chemotherapy for FLT3-mutated AML. *Blood, The Journal of the American Society of Hematology,* 129**,** 1143-1154.

KOHL, T., HELLINGER, C., AHMED, F., BUSKE, C., HIDDEMANN, W., BOHLANDER, S. & SPIEKERMANN, K. 2007. BH3 mimetic ABT-737 neutralizes resistance to FLT3 inhibitor treatment mediated by FLT3-independent expression of BCL2 in primary AML blasts. *Leukemia,* 21**,** 1763-1772.

KOJIMA, K., KONOPLEVA, M., SAMUDIO, I. J., SHIKAMI, M., CABREIRA-HANSEN, M., MCQUEEN, T., RUVOLO, V., TSAO, T., ZENG, Z. & VASSILEV, L. T. 2005. MDM2 antagonists induce p53-dependent apoptosis in AML: implications for leukemia therapy. *Blood,* 106**,** 3150-3159.

KONDO, M., WEISSMAN, I. L. & AKASHI, K. 1997. Identification of clonogenic common lymphoid progenitors in mouse bone marrow. *Cell,* 91**,** 661-672.

KONOPLEVA, M., POLLYEA, D. A., POTLURI, J., CHYLA, B. J., BUSMAN, T., MCKEEGAN, E., SALEM, A., ZHU, M., RICKER, J. L. & BLUM, W. 2014. A phase 2 study of ABT-199 (GDC-0199) in patients with acute myelogenous leukemia (AML). American Society of Hematology Washington, DC.

KONOPLEVA, M. Y. & JORDAN, C. T. 2011. Leukemia stem cells and microenvironment: biology and therapeutic targeting. *Journal of clinical oncology,* 29**,** 591.

KOONIN, E. V., MAKAROVA, K. S. & ZHANG, F. 2017. Diversity, classification and evolution of CRISPR-Cas systems. *Current opinion in microbiology,* 37**,** 67-78.

KOONIN, E. V. & WOLF, Y. I. 2015. Evolution of the CRISPR-Cas adaptive immunity systems in prokaryotes: models and observations on virus–host coevolution. *Molecular BioSystems,* 11**,** 20-27.

KORNBLAU, S. M., THALL, P. F., ESTROV, Z., WALTERSCHEID, M., PATEL, S., THERIAULT, A., KEATING, M. J., KANTARJIAN, H., ESTEY, E. & ANDREEFF, M. 1999. The prognostic impact of BCL2 protein expression in acute myelogenous leukemia varies with cytogenetics. *Clinical Cancer Research,* 5**,** 1758-1766.

KORNEV, A. P., HASTE, N. M., TAYLOR, S. S. & TEN EYCK, L. F. 2006. Surface comparison of active and inactive protein kinases identifies a conserved activation mechanism. *Proceedings of the National Academy of Sciences,* 103**,** 17783-17788.

KÖTHE, S., MÜLLER, J. P., BÖHMER, S.-A., TSCHONGOV, T., FRICKE, M., KOCH, S., THIEDE, C., REQUARDT, R. P., RUBIO, I. & BÖHMER, F. D. 2013. Features of Ras activation by a mislocalized oncogenic tyrosine kinase: FLT3 ITD signals through K-Ras at the plasma membrane of acute myeloid leukemia cells. *Journal of Cell Science,* 126**,** 4746-4755.

KOTSCHY, A., SZLAVIK, Z., MURRAY, J., DAVIDSON, J., MARAGNO, A. L., LE TOUMELIN-BRAIZAT, G., CHANRION, M., KELLY, G. L., GONG, J.-N. & MOUJALLED, D. M. 2016. The MCL1 inhibitor S63845 is tolerable and effective in diverse cancer models. *Nature,* 538**,** 477-482.

KOTTARIDIS, P. D., GALE, R. E., FREW, M. E., HARRISON, G., LANGABEER, S. E., BELTON, A. A., WALKER, H., WHEATLEY, K., BOWEN, D. T., BURNETT, A. K., GOLDSTONE, A. H. & LINCH, D. C. 2001. The presence of a FLT3 internal tandem duplication in patients with acute myeloid leukemia (AML) adds important prognostic information to cytogenetic risk group and response to the first cycle of chemotherapy: analysis of 854 patients from the United Kingdom Medical Research Council AML 10 and 12 trials. *Blood,* 98**,** 1752-9.

KREMER, K. N., DUDAKOVIC, A., MCGEE-LAWRENCE, M. E., PHILIPS, R. L., HESS, A. D., SMITH, B. D., VAN WIJNEN, A. J., KARP, J. E., KAUFMANN, S. H. & WESTENDORF, J. J. 2014. Osteoblasts protect AML cells from SDF-1-induced apoptosis. *Journal of cellular biochemistry,* 115**,** 1128-1137.

KUMAR, C. C. 2011a. Genetic abnormalities and challenges in the treatment of acute myeloid leukemia. *Genes Cancer,* 2**,** 95-107.

KUMAR, C. C. 2011b. Genetic abnormalities and challenges in the treatment of acute myeloid leukemia. *Genes & cancer,* 2**,** 95-107.

LANE, S. W., SCADDEN, D. T. & GILLILAND, D. G. 2009. The leukemic stem cell niche: current concepts and therapeutic opportunities. *Blood, The Journal of the American Society of Hematology,* 114**,** 1150-1157.

LARROSA-GARCIA, M. & BAER, M. R. 2017. FLT3 inhibitors in acute myeloid leukemia: current status and future directions. *Molecular cancer therapeutics,* 16**,** 991-1001.

LARRUE, C., SALAND, E., VERGEZ, F., SERHAN, N., DELABESSE, E., MANSAT-DE MAS, V., TAMBURINI, J., MANENTI, S., SARRY, J. E. & RÉCHER, C. 2015. Antileukemic activity of 2-deoxy-d-glucose through inhibition of N-linked glycosylation in acute myeloid leukemia with FLT3-ITD or c-KIT mutations. *Molecular cancer therapeutics,* 14**,** 2364-2373.

LEE, E. F., CZABOTAR, P. E., YANG, H., SLEEBS, B. E., LESSENE, G., COLMAN, P. M., SMITH, B. J. & FAIRLIE, W. D. 2009. Conformational changes in Bcl-2 pro-survival proteins determine their capacity to bind ligands. *Journal of Biological Chemistry,* 284**,** 30508-30517.

LEE, H. K., KIM, H. W., LEE, I. Y., LEE, J., LEE, J., JUNG, D. S., LEE, S. Y., PARK, S. H., HWANG, H. & CHOI, J.-S. 2014. G-749, a novel FLT3 kinase inhibitor, can overcome drug resistance for the treatment of acute myeloid leukemia. *Blood,* 123**,** 2209-2219.

LESSENE, G., CZABOTAR, P. E. & COLMAN, P. M. 2008. BCL-2 family antagonists for cancer therapy. *Nature reviews Drug discovery,* 7**,** 989-1000.

LEVERSON, J., ZHANG, H., CHEN, J., TAHIR, S., PHILLIPS, D., XUE, J., NIMMER, P., JIN, S., SMITH, M. & XIAO, Y. 2015. Potent and selective small-molecule MCL-1 inhibitors demonstrate on-target cancer cell killing activity as single agents and in combination with ABT-263 (navitoclax). *Cell death & disease,* 6**,** e1590-e1590.

LEVIS, M. 2014. Quizartinib for the treatment of FLT3/ITD acute myeloid leukemia. *Future oncology,* 10**,** 1571-1579.

LEVIS, M., RAVANDI, F., WANG, E. S., BAER, M. R., PERL, A., COUTRE, S., ERBA, H., STUART, R. K., BACCARANI, M. & CRIPE, L. D. 2011. Results from a randomized trial of salvage chemotherapy followed by

lestaurtinib for patients with FLT3 mutant AML in first relapse. *Blood, The Journal of the American Society of Hematology,* 117**,** 3294-3301.
LEY, R., BALMANNO, K., HADFIELD, K., WESTON, C. & COOK, S. J. 2003. Activation of the ERK1/2 signaling pathway promotes phosphorylation and proteasome-dependent degradation of the BH3-only protein, Bim. *Journal of Biological Chemistry,* 278**,** 18811-18816.
LI, H., ZHU, H., XU, C.-J. & YUAN, J. 1998. Cleavage of BID by caspase 8 mediates the mitochondrial damage in the Fas pathway of apoptosis. *Cell,* 94**,** 491-501.
LI, X.-X., ZHOU, J.-D., WEN, X.-M., ZHANG, T.-J., WU, D.-H., DENG, Z.-Q., ZHANG, Z.-H., LIAN, X.-Y., HE, P.-F. & YAO, X.-Y. 2019. Increased MCL-1 expression predicts poor prognosis and disease recurrence in acute myeloid leukemia. *OncoTargets and therapy,* 12**,** 3295.
LIEVENS, P. M.-J., RONCADOR, A. & LIBOI, E. 2006. K644E/M FGFR3 mutants activate Erk1/2 from the endoplasmic reticulum through FRS2α and PLCγ-independent pathways. *Journal of molecular biology,* 357**,** 783-792.
LIN, K. H., WINTER, P. S., XIE, A., ROTH, C., MARTZ, C. A., STEIN, E. M., ANDERSON, G. R., TINGLEY, J. P. & WOOD, K. C. 2016. Targeting MCL-1/BCL-X L forestalls the acquisition of resistance to ABT-199 in acute myeloid leukemia. *Scientific reports,* 6**,** 27696.
LINCH, D. C., HILLS, R. K., BURNETT, A. K., KHWAJA, A. & GALE, R. E. 2014. Impact of FLT3ITD mutant allele level on relapse risk in intermediate-risk acute myeloid leukemia. *Blood,* 124**,** 273-276.
LINDBLAD, O., CORDERO, E., PUISSANT, A., MACAULAY, L., KABIR, N. N., SUN, J., HARALDSSON, K., BORG, Å., LEVANDER, F. & STEGMAIER, K. 2015. Aberrant Activation of the PI3K/mTOR Pathway Promotes Resistance to Sorafenib in AML. American Society of Hematology Washington, DC.
LING, Y., ZHANG, Z., ZHANG, H. & HUANG, Z. 2017. Protein Kinase Inhibitors as Therapeutic Drugs in AML: Advances and Challenges. *Current pharmaceutical design,* 23**,** 4303-4310.
LINO, C. A., HARPER, J. C., CARNEY, J. P. & TIMLIN, J. A. 2018. Delivering CRISPR: a review of the challenges and approaches. *Drug delivery,* 25**,** 1234-1257.
LIPKA, D. B., WAGNER, M.-C., DZIADOSZ, M. & FISCHER, T. 2016. Prolonged cellular midostaurin retention suggests potential alternative dosing strategies for FLT3-ITD-positive leukemias. *Leukemia,* 30**,** 2090-2093.
LIU, X., ROBINSON, G. W., GOUILLEUX, F., GRONER, B. & HENNIGHAUSEN, L. 1995. Cloning and expression of Stat5 and an additional homologue (Stat5b) involved in prolactin signal transduction in mouse mammary tissue. *Proceedings of the National Academy of Sciences,* 92**,** 8831-8835.
LUSKIN, M. R., LEE, J.-W., FERNANDEZ, H. F., ABDEL-WAHAB, O., BENNETT, J. M., KETTERLING, R. P., LAZARUS, H. M., LEVINE, R. L., LITZOW, M. R. & PAIETTA, E. M. 2016. Benefit of high-dose daunorubicin in AML induction extends across cytogenetic and molecular groups. *Blood,* 127**,** 1551-1558.

LYMAN, S. D. & JACOBSEN, S. E. W. 1998. c-kit ligand and Flt3 ligand: stem/progenitor cell factors with overlapping yet distinct activities. *Blood, The Journal of the American Society of Hematology,* 91**,** 1101-1134.

LYMAN, S. D., JAMES, L., BOS, T. V., DE VRIES, P., BRASEL, K., GLINIAK, B., HOLLINGSWORTH, L., PICHA, K. S., MCKENNA, H. J. & SPLETT, R. R. 1993. Molecular cloning of a ligand for the flt3flk-2 tyrosine kinase receptor: A proliferative factor for primitive hematopoietic cells. *Cell,* 75**,** 1157-1167.

LYMAN, S. D., SEABERG, M., HANNA, R., ZAPPONE, J., BRASEL, K., ABKOWITZ, J., PRCHAL, J., SCHULTZ, J. & SHAHIDI, N. 1995. Plasma/serum levels of flt3 ligand are low in normal individuals and highly elevated in patients with Fanconi anemia and acquired aplastic anemia.

MACKAREHTSCHIAN, K., HARDIN, J. D., MOORE, K. A., BOAST, S., GOFF, S. P. & LEMISCHKA, I. R. 1995. Targeted disruption of the flk2/flt3 gene leads to deficiencies in primitive hematopoietic progenitors. *Immunity,* 3**,** 147-161.

MAKAROVA, K. S., WOLF, Y. I., ALKHNBASHI, O. S., COSTA, F., SHAH, S. A., SAUNDERS, S. J., BARRANGOU, R., BROUNS, S. J., CHARPENTIER, E. & HAFT, D. H. 2015. An updated evolutionary classification of CRISPR–Cas systems. *Nature Reviews Microbiology,* 13**,** 722-736.

MALI, P., YANG, L., ESVELT, K. M., AACH, J., GUELL, M., DICARLO, J. E., NORVILLE, J. E. & CHURCH, G. M. 2013. RNA-guided human genome engineering via Cas9. *Science,* 339**,** 823-826.

MANNING, B. D. & CANTLEY, L. C. 2007. AKT/PKB signaling: navigating downstream. *Cell,* 129**,** 1261-1274.

MANZ, M. G., MIYAMOTO, T., AKASHI, K. & WEISSMAN, I. L. 2002. Prospective isolation of human clonogenic common myeloid progenitors. *Proceedings of the National Academy of Sciences,* 99**,** 11872-11877.

MARCHESI, F., MONTI, P., LEONE, B. E., ZERBI, A., VECCHI, A., PIEMONTI, L., MANTOVANI, A. & ALLAVENA, P. 2004. Increased survival, proliferation, and migration in metastatic human pancreatic tumor cells expressing functional CXCR4. *Cancer research,* 64**,** 8420-8427.

MARDIROS, A., DOS SANTOS, C., MCDONALD, T., BROWN, C. E., WANG, X., BUDDE, L. E., HOFFMAN, L., AGUILAR, B., CHANG, W.-C. & BRETZLAFF, W. 2013. T cells expressing CD123-specific chimeric antigen receptors exhibit specific cytolytic effector functions and antitumor effects against human acute myeloid leukemia. *Blood, The Journal of the American Society of Hematology,* 122**,** 3138-3148.

MASSON, K., LIU, T., KHAN, R., SUN, J. & RÖNNSTRAND, L. 2009. A role of Gab2 association in Flt3 ITD mediated Stat5 phosphorylation and cell survival. *British journal of haematology,* 146**,** 193-202.

MATTHEWS, W., JORDAN, C. T., WIEGAND, G. W., PARDOLL, D. & LEMISCHKA, I. R. 1991. A receptor tyrosine kinase specific to hematopoietic stem and progenitor cell-enriched populations. *Cell,* 65**,** 1143-1152.

MCCLANAHAN, T., CULPEPPER, J., CAMPBELL, D., WAGNER, J., FRANZ-BACON, K., MATTSON, J., TSAI, S., LUH, J., GUIMARAES, M. & MATTEI, M. 1996. Biochemical and genetic characterization of multiple splice variants of the Flt3 ligand.

MCKENNA, H. J., STOCKING, K. L., MILLER, R. E., BRASEL, K., DE SMEDT, T., MARASKOVSKY, E., MALISZEWSKI, C. R., LYNCH, D. H., SMITH, J. & PULENDRAN, B. 2000. Mice lacking flt3 ligand have deficient hematopoiesis affecting hematopoietic progenitor cells, dendritic cells, and natural killer cells. *Blood, The Journal of the American Society of Hematology,* 95**,** 3489-3497.

MCMAHON, C. M., FERNG, T., CANAANI, J., WANG, E. S., MORRISSETTE, J. J., EASTBURN, D. J., PELLEGRINO, M., DURRUTHY-DURRUTHY, R., WATT, C. D. & ASTHANA, S. 2019. Clonal selection with Ras pathway activation mediates secondary clinical resistance to selective FLT3 inhibition in acute myeloid leukemia. *Cancer discovery,* 9**,** 1050-1063.

MEAD, A. J., NEO, W. H., BARKAS, N., MATSUOKA, S., GIUSTACCHINI, A., FACCHINI, R., THONGJUEA, S., JAMIESON, L., BOOTH, C. A. & FORDHAM, N. 2017. Niche-mediated depletion of the normal hematopoietic stem cell reservoir by Flt3-ITD–induced myeloproliferation. *Journal of Experimental Medicine,* 214**,** 2005-2021.

MEDEIROS, B. C., CHAN, S. M., DAVER, N. G., JONAS, B. A. & POLLYEA, D. A. 2019. Optimizing survival outcomes with post-remission therapy in acute myeloid leukemia. *American journal of hematology,* 94**,** 803-811.

MEHTA, S., SHUKLA, S. & VORA, H. 2013. Overexpression of Bcl2 protein predicts chemoresistance in acute myeloid leukemia: its correlation with FLT3. *Neoplasma,* 60**,** 666-675.

MEIERHOFF, G., DEHMEL, U., GRUSS, H. J., ROSNET, O., BIRNBAUM, D., QUENTMEIER, H., DIRKS, W. & DREXLER, H. G. 1995. Expression of FLT3 receptor and FLT3-ligand in human leukemia-lymphoma cell lines. *Leukemia,* 9**,** 1368-72.

MEISSNER, T. B., MANDAL, P. K., FERREIRA, L. M., ROSSI, D. J. & COWAN, C. A. 2014. Genome editing for human gene therapy. *Methods in enzymology.* Elsevier.

MESHINCHI, S. & APPELBAUM, F. R. 2009. Structural and functional alterations of FLT3 in acute myeloid leukemia. *Clin Cancer Res,* 15**,** 4263-9.

MESHINCHI, S., WOODS, W. G., STIREWALT, D. L., SWEETSER, D. A., BUCKLEY, J. D., TJOA, T. K., BERNSTEIN, I. D. & RADICH, J. P. 2001. Prevalence and prognostic significance of Flt3 internal tandem duplication in pediatric acute myeloid leukemia. *Blood, The Journal of the American Society of Hematology,* 97**,** 89-94.

MILHAS, D., CUVILLIER, O., THERVILLE, N., CLAVÉ, P., THOMSEN, M., LEVADE, T., BENOIST, H. & SÉGUI, B. 2005. Caspase-10 triggers Bid cleavage and caspase cascade activation in FasL-induced apoptosis. *Journal of Biological Chemistry,* 280**,** 19836-19842.

MINIERI, V., DE DOMINICI, M., PORAZZI, P., MARIANI, S. A., SPINELLI, O., RAMBALDI, A., PETERSON, L. F., PORCU, P., NEVALAINEN, M. T. & CALABRETTA, B. 2018. Targeting STAT5 or STAT5-regulated

pathways suppresses leukemogenesis of Ph+ acute lymphoblastic leukemia. *Cancer research,* 78**,** 5793-5807.

MIRANDA, M., MCGUIRE, T. & JOHNSON, D. 2002. Importance of MEK-1/-2 signaling in monocytic and granulocytic differentiation of myeloid cell lines. *Leukemia,* 16**,** 683-692.

MIZUKI, M., FENSKI, R., HALFTER, H., MATSUMURA, I., SCHMIDT, R., MÜLLER, C., GRÜNING, W., KRATZ-ALBERS, K., SERVE, S. & STEUR, C. 2000. Flt3 mutations from patients with acute myeloid leukemia induce transformation of 32D cells mediated by the Ras and STAT5 pathways. *Blood, The Journal of the American Society of Hematology,* 96**,** 3907-3914.

MIZUKI, M., SCHWÄBLE, J., STEUR, C., CHOUDHARY, C., AGRAWAL, S., SARGIN, B. L., STEFFEN, B. R., MATSUMURA, I., KANAKURA, Y. & BÖHMER, F. D. 2003. Suppression of myeloid transcription factors and induction of STAT response genes by AML-specific Flt3 mutations. *Blood, The Journal of the American Society of Hematology,* 101**,** 3164-3173.

MODI, V. & DUNBRACK, R. L. 2019. Defining a new nomenclature for the structures of active and inactive kinases. *Proceedings of the National Academy of Sciences,* 116**,** 6818-6827.

MOL, C. D., LIM, K. B., SRIDHAR, V., ZOU, H., CHIEN, E. Y., SANG, B.-C., NOWAKOWSKI, J., KASSEL, D. B., CRONIN, C. N. & MCREE, D. E. 2003. Structure of a c-kit product complex reveals the basis for kinase transactivation. *Journal of Biological Chemistry,* 278**,** 31461-31464.

MOONEY, C. J., CUNNINGHAM, A., TSAPOGAS, P., TOELLNER, K.-M. & BROWN, G. 2017. Selective expression of Flt3 within the mouse hematopoietic stem cell compartment. *International journal of molecular sciences,* 18**,** 1037.

MOORE, A. S., FAISAL, A., MAK, G. W., MIRAKI-MOUD, F., BAVETSIAS, V., VALENTI, M., BOX, G., HALLSWORTH, A., DE HAVEN BRANDON, A. & XAVIER, C. P. 2020. Quizartinib-resistant FLT3-ITD acute myeloid leukemia cells are sensitive to the FLT3-Aurora kinase inhibitor CCT241736. *Blood advances,* 4**,** 1478-1491.

MORITA, K., WANG, F., JAHN, K., KUIPERS, J., YAN, Y., MATTHEWS, J., LITTLE, L., GUMBS, C., CHEN, S. & ZHANG, J. 2020. Clonal evolution of acute myeloid leukemia revealed by high-throughput single-cell genomics. *bioRxiv*.

MOUJALLED, D. M., POMILIO, G., GHIURAU, C., IVEY, A., SALMON, J., RIJAL, S., MACRAILD, S., ZHANG, L., TEH, T.-C. & TIONG, S. 2019. Combining BH3-mimetics to target both BCL-2 and MCL1 has potent activity in pre-clinical models of acute myeloid leukemia. *Leukemia,* 33**,** 905-917.

MUI, A., WAKAO, H., O'FARRELL, A., HARADA, N. & MIYAJIMA, A. 1995. Interleukin-3, granulocyte-macrophage colony stimulating factor and interleukin-5 transduce signals through two STAT5 homologs. *The EMBO journal,* 14**,** 1166-1175.

MULLER, P. A. & VOUSDEN, K. H. 2013. p53 mutations in cancer. *Nature cell biology,* 15**,** 2-8.

MUPO, A., CELANI, L., DOVEY, O., COOPER, J., GROVE, C., RAD, R., SPORTOLETTI, P., FALINI, B., BRADLEY, A. & VASSILIOU, G. 2013.

A powerful molecular synergy between mutant Nucleophosmin and Flt3-ITD drives acute myeloid leukemia in mice. *Leukemia,* 27**,** 1917-1920.

NAKAO, M., YOKOTA, S., IWAI, T., KANEKO, H., HORIIKE, S., KASHIMA, K., SONODA, Y., FUJIMOTO, T. & MISAWA, S. 1996. Internal tandem duplication of the flt3 gene found in acute myeloid leukemia. *Leukemia,* 10**,** 1911-1918.

NETWORK, C. G. A. R. 2013. Genomic and epigenomic landscapes of adult de novo acute myeloid leukemia. *New England Journal of Medicine,* 368**,** 2059-2074.

O'DONNELL, M. R., TALLMAN, M. S., ABBOUD, C. N., ALTMAN, J. K., APPELBAUM, F. R., ARBER, D. A., BHATT, V., BIXBY, D., BLUM, W. & COUTRE, S. E. 2017a. Acute myeloid leukemia, version 3.2017, NCCN clinical practice guidelines in oncology. *Journal of the National Comprehensive Cancer Network,* 15**,** 926-957.

O'DONNELL, M. R., TALLMAN, M. S., ABBOUD, C. N., ALTMAN, J. K., APPELBAUM, F. R., ARBER, D. A., BHATT, V., BIXBY, D., BLUM, W., COUTRE, S. E., DE LIMA, M., FATHI, A. T., FIORELLA, M., FORAN, J. M., GORE, S. D., HALL, A. C., KROPF, P., LANCET, J., MANESS, L. J., MARCUCCI, G., MARTIN, M. G., MOORE, J. O., OLIN, R., PEKER, D., POLLYEA, D. A., PRATZ, K., RAVANDI, F., SHAMI, P. J., STONE, R. M., STRICKLAND, S. A., WANG, E. S., WIEDUWILT, M., GREGORY, K. & OGBA, N. 2017b. Acute Myeloid Leukemia, Version 3.2017, NCCN Clinical Practice Guidelines in Oncology. *J Natl Compr Canc Netw,* 15**,** 926-957.

O'FARRELL, A.-M., ABRAMS, T. J., YUEN, H. A., NGAI, T. J., LOUIE, S. G., YEE, K. W., WONG, L. M., HONG, W., LEE, L. B. & TOWN, A. 2003. SU11248 is a novel FLT3 tyrosine kinase inhibitor with potent activity in vitro and in vivo. *Blood, The Journal of the American Society of Hematology,* 101**,** 3597-3605.

OGAWA, M., MATSUZAKI, Y., NISHIKAWA, S., HAYASHI, S., KUNISADA, T., SUDO, T., KINA, T., NAKAUCHI, H. & NISHIKAWA, S. 1991. Expression and function of c-kit in hemopoietic progenitor cells. *The Journal of experimental medicine,* 174**,** 63-71.

OHANIAN, M., GARCIA-MANERO, G., LEVIS, M., JABBOUR, E., DAVER, N., BORTHAKUR, G., KADIA, T., PIERCE, S., BURGER, J. & RICHIE, M. A. 2018. Sorafenib combined with 5-azacytidine in older patients with untreated FLT3-ITD mutated acute myeloid leukemia. *American journal of hematology,* 93**,** 1136-1141.

OLTERSDORF, T., ELMORE, S. W., SHOEMAKER, A. R., ARMSTRONG, R. C., AUGERI, D. J., BELLI, B. A., BRUNCKO, M., DECKWERTH, T. L., DINGES, J. & HAJDUK, P. J. 2005. An inhibitor of Bcl-2 family proteins induces regression of solid tumours. *Nature,* 435**,** 677-681.

ORKIN, S. H. & ZON, L. I. 2008. Hematopoiesis: an evolving paradigm for stem cell biology. *Cell,* 132**,** 631-644.

OSLOWSKI, C. M. & URANO, F. 2011. Measuring ER stress and the unfolded protein response using mammalian tissue culture system. *Methods in enzymology.* Elsevier.

OZEKI, K., KIYOI, H., HIROSE, Y., IWAI, M., NINOMIYA, M., KODERA, Y., MIYAWAKI, S., KURIYAMA, K., SHIMAZAKI, C. & AKIYAMA, H. 2004.

Biologic and clinical significance of the FLT3 transcript level in acute myeloid leukemia. *Blood,* 103**,** 1901-1908.
PAGÈS, G., GUÉRIN, S., GRALL, D., BONINO, F., SMITH, A., ANJUERE, F., AUBERGER, P. & POUYSSÉGUR, J. 1999. Defective thymocyte maturation in p44 MAP kinase (Erk 1) knockout mice. *Science,* 286**,** 1374-1377.
PALIS, J. 2014. Primitive and definitive erythropoiesis in mammals. *Frontiers in physiology,* 5**,** 3.
PARK, I., MUNDY-BOSSE, B., WHITMAN, S., ZHANG, X., WARNER, S., BEARSS, D., BLUM, W., MARCUCCI, G. & CALIGIURI, M. 2015. Receptor tyrosine kinase Axl is required for resistance of leukemic cells to FLT3-targeted therapy in acute myeloid leukemia. *Leukemia,* 29**,** 2382-2389.
PARMAR, A., MARZ, S., RUSHTON, S., HOLZWARTH, C., LIND, K., KAYSER, S., DÖHNER, K., PESCHEL, C., OOSTENDORP, R. A. & GÖTZE, K. S. 2011. Stromal niche cells protect early leukemic FLT3-ITD+ progenitor cells against first-generation FLT3 tyrosine kinase inhibitors. *Cancer research,* 71**,** 4696-4706.
PASCHKA, P., MARCUCCI, G., RUPPERT, A. S., MRÓZEK, K., CHEN, H., KITTLES, R. A., VUKOSAVLJEVIC, T., PERROTTI, D., VARDIMAN, J. W. & CARROLL, A. J. 2006. Adverse prognostic significance of KIT mutations in adult acute myeloid leukemia with inv (16) and t (8; 21): a Cancer and Leukemia Group B Study. *Journal of Clinical Oncology,* 24**,** 3904-3911.
PEARSON, G., ROBINSON, F., BEERS GIBSON, T., XU, B.-E., KARANDIKAR, M., BERMAN, K. & COBB, M. H. 2001. Mitogen-activated protein (MAP) kinase pathways: regulation and physiological functions. *Endocrine reviews,* 22**,** 153-183.
PELLAGATTI, A., DOLATSHAD, H., YIP, B. H., VALLETTA, S. & BOULTWOOD, J. 2016. Application of genome editing technologies to the study and treatment of hematological disease. *Advances in biological regulation,* 60**,** 122-134.
PEMMARAJU, N., KANTARJIAN, H., RAVANDI, F. & CORTES, J. 2011. FLT3 inhibitors in the treatment of acute myeloid leukemia: the start of an era? *Cancer,* 117**,** 3293-304.
PERL, A. E., ALTMAN, J. K., CORTES, J., SMITH, C., LITZOW, M., BAER, M. R., CLAXTON, D., ERBA, H. P., GILL, S. & GOLDBERG, S. 2017. Selective inhibition of FLT3 by gilteritinib in relapsed or refractory acute myeloid leukaemia: a multicentre, first-in-human, open-label, phase 1–2 study. *The Lancet Oncology,* 18**,** 1061-1075.
PERL, A. E., ALTMAN, J. K., CORTES, J. E., SMITH, C. C., LITZOW, M., BAER, M. R., CLAXTON, D. F., ERBA, H. P., GILL, S. C. & GOLDBERG, S. L. 2016. Final results of the chrysalis trial: a first-in-human phase 1/2 dose-escalation, dose-expansion study of gilteritinib (ASP2215) in patients with relapsed/refractory acute myeloid leukemia (R/R AML). American Society of Hematology Washington, DC.
PERL, A. E., MARTINELLI, G., CORTES, J. E., NEUBAUER, A., BERMAN, E., PAOLINI, S., MONTESINOS, P., BAER, M. R., LARSON, R. A. & USTUN, C. 2019a. Abstract CT184: Gilteritinib significantly prolongs overall survival in patients with FLT3-mutated (FLT3mut+)

relapsed/refractory (R/R) acute myeloid leukemia (AML): Results from the Phase III ADMIRAL trial. AACR.

PERL, A. E., MARTINELLI, G., CORTES, J. E., NEUBAUER, A., BERMAN, E., PAOLINI, S., MONTESINOS, P., BAER, M. R., LARSON, R. A. & USTUN, C. 2019b. Gilteritinib or chemotherapy for relapsed or refractory FLT3-mutated AML. *New England Journal of Medicine,* 381**,** 1728-1740.

PIETRAS, E. M., MIRANTES-BARBEITO, C., FONG, S., LOEFFLER, D., KOVTONYUK, L. V., ZHANG, S., LAKSHMINARASIMHAN, R., CHIN, C. P., TECHNER, J.-M. & WILL, B. 2016. Chronic interleukin-1 exposure drives haematopoietic stem cells towards precocious myeloid differentiation at the expense of self-renewal. *Nature cell biology,* 18**,** 607-618.

PIETRAS, E. M., REYNAUD, D., KANG, Y.-A., CARLIN, D., CALERO-NIETO, F. J., LEAVITT, A. D., STUART, J. M., GÖTTGENS, B. & PASSEGUÉ, E. 2015. Functionally distinct subsets of lineage-biased multipotent progenitors control blood production in normal and regenerative conditions. *Cell stem cell,* 17**,** 35-46.

PILLINGER, G., LOUGHRAN, N. V., PIDDOCK, R. E., SHAFAT, M. S., ZAITSEVA, L., ABDUL-AZIZ, A., LAWES, M. J., BOWLES, K. M. & RUSHWORTH, S. A. 2016. Targeting PI3Kδ and PI3Kγ signalling disrupts human AML survival and bone marrow stromal cell mediated protection. *Oncotarget,* 7**,** 39784.

PILOTO, O., WRIGHT, M., BROWN, P., KIM, K.-T., LEVIS, M. & SMALL, D. 2007. Prolonged exposure to FLT3 inhibitors leads to resistance via activation of parallel signaling pathways. *Blood,* 109**,** 1643-1652.

PINHO, S. S. & REIS, C. A. 2015. Glycosylation in cancer: mechanisms and clinical implications. *Nature Reviews Cancer,* 15**,** 540-555.

POITRAS, J. L., HEISER, D., LI, L., NGUYEN, B., NAGAI, K., DUFFIELD, A. S., GAMPER, C. & SMALL, D. 2016. Dnmt3a deletion cooperates with the Flt3/ITD mutation to drive leukemogenesis in a murine model. *Oncotarget,* 7**,** 69124.

POLAK, R. & BUITENHUIS, M. 2012. The PI3K/PKB signaling module as key regulator of hematopoiesis: implications for therapeutic strategies in leukemia. *Blood,* 119**,** 911-23.

PORT, M., BÖTTCHER, M., THOL, F., GANSER, A., SCHLENK, R., WASEM, J., NEUMANN, A. & POURYAMOUT, L. 2014. Prognostic significance of FLT3 internal tandem duplication, nucleophosmin 1, and CEBPA gene mutations for acute myeloid leukemia patients with normal karyotype and younger than 60 years: a systematic review and meta-analysis. *Annals of hematology,* 93**,** 1279-1286.

PORTEUS, M. H. 2015. Genome editing of the blood: opportunities and challenges. *Current stem cell reports,* 1**,** 23-30.

PRATZ, K. W., CHERRY, M., ALTMAN, J. K., COOPER, B., CRUZ, J. C., JURCIC, J. G., LEVIS, M. J., LIN, T. L., PERL, A. E. & PODOLTSEV, N. A. 2018. Updated results from a phase 1 study of gilteritinib in combination with induction and consolidation chemotherapy in subjects with newly diagnosed acute myeloid leukemia (AML). *Blood,* 132**,** 564-564.

PRATZ, K. W., CORTES, J., ROBOZ, G. J., RAO, N., AROWOJOLU, O., STINE, A., SHIOTSU, Y., SHUDO, A., AKINAGA, S. & SMALL, D. 2009. A pharmacodynamic study of the FLT3 inhibitor KW-2449 yields insight into the basis for clinical response. *Blood, The Journal of the American Society of Hematology,* 113**,** 3938-3946.

PRATZ, K. W., SATO, T., MURPHY, K. M., STINE, A., RAJKHOWA, T. & LEVIS, M. 2010. FLT3-mutant allelic burden and clinical status are predictive of response to FLT3 inhibitors in AML. *Blood, The Journal of the American Society of Hematology,* 115**,** 1425-1432.

PROPPER, D., MCDONALD, A., MAN, A., THAVASU, P., BALKWILL, F., BRAYBROOKE, J., CAPONIGRO, F., GRAF, P., DUTREIX, C. & BLACKIE, R. 2001. Phase I and pharmacokinetic study of PKC412, an inhibitor of protein kinase C. *Journal of Clinical Oncology,* 19**,** 1485-1492.

QUENTMEIER, H., REINHARDT, J., ZABORSKI, M. & DREXLER, H. G. 2003. FLT3 mutations in acute myeloid leukemia cell lines. *Leukemia,* 17**,** 120-4.

RAMAKRISHNAN, R., PEÑA-MARTÍNEZ, P., AGARWAL, P., RODRIGUEZ-ZABALA, M., CHAPELLIER, M., HÖGBERG, C., ERIKSSON, M., YUDOVICH, D., SHAH, M. & EHINGER, M. 2020. CXCR4 Signaling Has a CXCL12-Independent Essential Role in Murine MLL-AF9-Driven Acute Myeloid Leukemia. *Cell Reports,* 31**,** 107684.

RAN, F. A., CONG, L., YAN, W. X., SCOTT, D. A., GOOTENBERG, J. S., KRIZ, A. J., ZETSCHE, B., SHALEM, O., WU, X. & MAKAROVA, K. S. 2015. In vivo genome editing using Staphylococcus aureus Cas9. *Nature,* 520**,** 186-191.

RAN, F. A., HSU, P. D., WRIGHT, J., AGARWALA, V., SCOTT, D. A. & ZHANG, F. 2013. Genome engineering using the CRISPR-Cas9 system. *Nature protocols,* 8**,** 2281.

RATH, D., AMLINGER, L., RATH, A. & LUNDGREN, M. 2015. The CRISPR-Cas immune system: biology, mechanisms and applications. *Biochimie,* 117**,** 119-128.

RAY, P., KRISHNAMOORTHY, N., ORISS, T. B. & RAY, A. 2010. Signaling of c-kit in dendritic cells influences adaptive immunity. *Annals of the New York Academy of Sciences,* 1183**,** 104.

REARDON, S. 2015. Leukaemia success heralds wave of gene-editing therapies. *Nature News,* 527**,** 146.

REITER, K., POLZER, H., KRUPKA, C., MAISER, A., VICK, B., ROTHENBERG-THURLEY, M., METZELER, K., DÖRFEL, D., SALIH, H. & JUNG, G. 2018. Tyrosine kinase inhibition increases the cell surface localization of FLT3-ITD and enhances FLT3-directed immunotherapy of acute myeloid leukemia. *Leukemia,* 32**,** 313-322.

ROCNIK, J. L., OKABE, R., YU, J.-C., LEE, B. H., GIESE, N., SCHENKEIN, D. P. & GILLILAND, D. G. 2006. Roles of tyrosine 589 and 591 in STAT5 activation and transformation mediated by FLT3-ITD. *Blood,* 108**,** 1339-1345.

RODGERS, K. & MCVEY, M. 2016. Error-prone repair of DNA double-strand breaks. *Journal of cellular physiology,* 231**,** 15-24.

ROSNET, O., BÜHRING, H.-J., DELAPEYRIÈRE, O., BESLU, N., LAVAGNA, C., MARCHETTO, S., RAPPOLD, I., DREXLER, H. G., BIRG, F. &

ROTTAPEL, R. 1996a. Expression and signal transduction of the FLT3 tyrosine kinase receptor. *Acta haematologica,* 95**,** 218-223.
ROSNET, O., BÜHRING, H., MARCHETTO, S., RAPPOLD, I., LAVAGNA, C., SAINTY, D., ARNOULET, C., CHABANNON, C., KANZ, L. & HANNUM, C. 1996b. Human FLT3/FLK2 receptor tyrosine kinase is expressed at the surface of normal and malignant hematopoietic cells. *Leukemia,* 10**,** 238-248.
ROSNET, O., MARCHETTO, S., DELAPEYRIERE, O. & BIRNBAUM, D. 1991a. Murine Flt3, a gene encoding a novel tyrosine kinase receptor of the PDGFR/CSF1R family. *Oncogene,* 6**,** 1641-1650.
ROSNET, O., MATTEÏ, M.-G., MARCHETTO, S. & BIRNBAUM, D. 1991b. Isolation and chromosomal localization of a novel FMS-like tyrosine kinase gene. *Genomics,* 9**,** 380-385.
ROSNET, O., SCHIFF, C., PEBUSQUE, M., MARCHETTO, S., TONNELLE, C., TOIRON, Y., BIRG, F. & BIRNBAUM, D. 1993. Human FLT3/FLK2 gene: cDNA cloning and expression in hematopoietic cells.
ROTTAPEL, R., TURCK, C. W., CASTERAN, N., LIU, X., BIRNBAUM, D., PAWSON, T. & DUBREUIL, P. 1994. Substrate specificities and identification of a putative binding site for PI3K in the carboxy tail of the murine Flt3 receptor tyrosine kinase. *Oncogene,* 9**,** 1755-1765.
SAELENS, X., FESTJENS, N., WALLE, L. V., VAN GURP, M., VAN LOO, G. & VANDENABEELE, P. 2004. Toxic proteins released from mitochondria in cell death. *Oncogene,* 23**,** 2861-2874.
SAITO, Y., MOCHIZUKI, Y., OGAHARA, I., WATANABE, T., HOGDAL, L., TAKAGI, S., SATO, K., KANEKO, A., KAJITA, H. & UCHIDA, N. 2017. Overcoming mutational complexity in acute myeloid leukemia by inhibition of critical pathways. *Science translational medicine,* 9**,** eaao1214.
SAKAGUCHI, M., YAMAGUCHI, H., NAJIMA, Y., USUKI, K., UEKI, T., OH, I., MORI, S., KAWATA, E., UOSHIMA, N. & KOBAYASHI, Y. 2018. Prognostic impact of low allelic ratio FLT3-ITD and NPM1 mutation in acute myeloid leukemia. *Blood advances,* 2**,** 2744-2754.
SÁNCHEZ-AGUILERA, A. & MÉNDEZ-FERRER, S. 2017. The hematopoietic stem-cell niche in health and leukemia. *Cellular and Molecular Life Sciences,* 74**,** 579-590.
SANJUAN-PLA, A., MACAULAY, I. C., JENSEN, C. T., WOLL, P. S., LUIS, T. C., MEAD, A., MOORE, S., CARELLA, C., MATSUOKA, S. & JONES, T. B. 2013. Platelet-biased stem cells reside at the apex of the haematopoietic stem-cell hierarchy. *Nature,* 502**,** 232-236.
SARBASSOV, D. D., GUERTIN, D. A., ALI, S. M. & SABATINI, D. M. 2005. Phosphorylation and regulation of Akt/PKB by the rictor-mTOR complex. *Science,* 307**,** 1098-1101.
SATO, T., YANG, X., KNAPPER, S., WHITE, P., SMITH, B. D., GALKIN, S., SMALL, D., BURNETT, A. & LEVIS, M. 2011. FLT3 ligand impedes the efficacy of FLT3 inhibitors in vitro and in vivo. *Blood, The Journal of the American Society of Hematology,* 117**,** 3286-3293.
SCHEIJEN, B., NGO, H. T., KANG, H. & GRIFFIN, J. D. 2004. FLT3 receptors with internal tandem duplications promote cell viability and proliferation by signaling through Foxo proteins. *Oncogene,* 23**,** 3338-3349.

SCHLENK, R. F., DÖHNER, K., KRAUTER, J., FRÖHLING, S., CORBACIOGLU, A., BULLINGER, L., HABDANK, M., SPÄTH, D., MORGAN, M. & BENNER, A. 2008. Mutations and treatment outcome in cytogenetically normal acute myeloid leukemia. *New England Journal of Medicine,* 358**,** 1909-1918.

SCHLENK, R. F., FIEDLER, W., SALIH, H. R., WULF, G., THOL, F., KÜNDGEN, A., KINDLER, T., SALWENDER, H.-J., LÜBBERT, M. & BROSSART, P. 2016. Impact of age and midostaurin-dose on response and outcome in acute myeloid leukemia with FLT3-ITD: interim-analyses of the AMLSG 16-10 Trial. American Society of Hematology Washington, DC.

SCHLENK, R. F., WEBER, D., FIEDLER, W., SALIH, H. R., WULF, G., SALWENDER, H., SCHROEDER, T., KINDLER, T., LÜBBERT, M. & WOLF, D. 2019. Midostaurin added to chemotherapy and continued single-agent maintenance therapy in acute myeloid leukemia with FLT3-ITD. *Blood,* 133**,** 840-851.

SCHMIDT-ARRAS, D.-E., BÖHMER, A., MARKOVA, B., CHOUDHARY, C., SERVE, H. & BÖHMER, F.-D. 2005. Tyrosine phosphorylation regulates maturation of receptor tyrosine kinases. *Molecular and cellular biology,* 25**,** 3690-3703.

SCHMIDT-ARRAS, D., BÖHMER, S.-A., KOCH, S., MÜLLER, J. P., BLEI, L., CORNILS, H., BAUER, R., KORASIKHA, S., THIEDE, C. & BÖHMER, F.-D. 2009a. Anchoring of FLT3 in the endoplasmic reticulum alters signaling quality. *Blood, The Journal of the American Society of Hematology,* 113**,** 3568-3576.

SCHMIDT-ARRAS, D., BÖHMER, S.-A., KOCH, S., MÜLLER, J. P., BLEI, L., CORNILS, H., BAUER, R., KORASIKHA, S., THIEDE, C. & BÖHMER, F.-D. 2009b. Anchoring of FLT3 in the endoplasmic reticulum alters signaling quality. *Blood,* 113**,** 3568-3576.

SCHUTTE, B., NUYDENS, R., GEERTS, H. & RAMAEKERS, F. 1998. Annexin V binding assay as a tool to measure apoptosis in differentiated neuronal cells. *Journal of neuroscience methods,* 86**,** 63-69.

SCHWARTZ, P. A. & MURRAY, B. W. 2011. Protein kinase biochemistry and drug discovery. *Bioorganic chemistry,* 39**,** 192-210.

SEEDHOUSE, C. H., PALLIS, M., GRUNDY, M., SHANG, S. & RUSSELL, N. H. 2009. FLT3-ITD expression levels and their effect on STAT5 in AML with and without NPM mutations. *British journal of haematology,* 147**,** 653-661.

SEGER, R. & KREBS, E. G. 1995. The MAPK signaling cascade. *The FASEB journal,* 9**,** 726-735.

SEIPEL, K., SCHMITTER, K., BACHER, U. & PABST, T. 2019. Rationale for a Combination Therapy Consisting of MCL1-and MEK-Inhibitors in Acute Myeloid Leukemia. *Cancers,* 11**,** 1779.

SENGUPTA, S., PETERSON, T. R. & SABATINI, D. M. 2010. Regulation of the mTOR complex 1 pathway by nutrients, growth factors, and stress. *Molecular cell,* 40**,** 310-322.

SERVE, H., KRUG, U., WAGNER, R., SAUERLAND, M. C., HEINECKE, A., BRUNNBERG, U., SCHAICH, M., OTTMANN, O., DUYSTER, J. & WANDT, H. 2013. Sorafenib in combination with intensive

chemotherapy in elderly patients with acute myeloid leukemia: results from a randomized, placebo-controlled trial. *Journal of Clinical Oncology,* 31**,** 3110-3118.

SEVAL, G. C. & OZCAN, M. 2015. Treatment of Acute Myeloid Leukemia in Adolescent and Young Adult Patients. *J Clin Med,* 4**,** 441-59.

SHAMAS-DIN, A., KALE, J., LEBER, B. & ANDREWS, D. W. 2013. Mechanisms of action of Bcl-2 family proteins. *Cold Spring Harbor perspectives in biology,* 5**,** a008714.

SHEIKH, M. S. & HUANG, Y. 2004. Death receptors as targets of cancer therapeutics. *Current cancer drug targets,* 4**,** 97-104.

SHIH, A. H., ABDEL-WAHAB, O., PATEL, J. P. & LEVINE, R. L. 2012. The role of mutations in epigenetic regulators in myeloid malignancies. *Nature reviews Cancer,* 12**,** 599-612.

SILL, H., OLIPITZ, W., ZEBISCH, A., SCHULZ, E. & WÖLFLER, A. 2011. Therapy-related myeloid neoplasms: pathobiology and clinical characteristics. *British journal of pharmacology,* 162**,** 792-805.

SISON, E. A. R. & BROWN, P. 2011. The bone marrow microenvironment and leukemia: biology and therapeutic targeting. *Expert review of hematology,* 4**,** 271-283.

SKAYNEH, H., JISHI, B., HLEIHEL, R., HAMIEH, M., DARWICHE, N., BAZARBACHI, A., EL SABBAN, M. & EL HAJJ, H. 2019. A Critical Review of Animal Models Used in Acute Myeloid Leukemia Pathophysiology. *Genes,* 10**,** 614.

SMALL, D. 2006. FLT3 mutations: biology and treatment. *Hematology Am Soc Hematol Educ Program***,** 178-84.

SMITH, B. D., LEVIS, M., BERAN, M., GILES, F., KANTARJIAN, H., BERG, K., MURPHY, K. M., DAUSES, T., ALLEBACH, J. & SMALL, D. 2004. Single-agent CEP-701, a novel FLT3 inhibitor, shows biologic and clinical activity in patients with relapsed or refractory acute myeloid leukemia. *Blood,* 103**,** 3669-3676.

SMITH, C. C., LIN, K., STECULA, A., SALI, A. & SHAH, N. P. 2015. FLT3 D835 mutations confer differential resistance to type II FLT3 inhibitors. *Leukemia,* 29**,** 2390-2392.

SMITH, C. C., PAGUIRIGAN, A., JESCHKE, G. R., LIN, K. C., MASSI, E., TARVER, T., CHIN, C.-S., ASTHANA, S., OLSHEN, A. & TRAVERS, K. J. 2017. Heterogeneous resistance to quizartinib in acute myeloid leukemia revealed by single-cell analysis. *Blood, The Journal of the American Society of Hematology,* 130**,** 48-58.

SMITH, C. C., WANG, Q., CHIN, C.-S., SALERNO, S., DAMON, L. E., LEVIS, M. J., PERL, A. E., TRAVERS, K. J., WANG, S. & HUNT, J. P. 2012a. Validation of ITD mutations in FLT3 as a therapeutic target in human acute myeloid leukaemia. *Nature,* 485**,** 260-263.

SMITH, C. C., WANG, Q., CHIN, C. S., SALERNO, S., DAMON, L. E., LEVIS, M. J., PERL, A. E., TRAVERS, K. J., WANG, S., HUNT, J. P., ZARRINKAR, P. P., SCHADT, E. E., KASARSKIS, A., KURIYAN, J. & SHAH, N. P. 2012b. Validation of ITD mutations in FLT3 as a therapeutic target in human acute myeloid leukaemia. *Nature,* 485**,** 260-3.

SOCOLOVSKY, M., FALLON, A. E., BRUGNARA, C. & LODISH, H. F. 1999. Fetal anemia and apoptosis of red cell progenitors in Stat5a−/− 5b−/− mice: a direct role for Stat5 in Bcl-XL induction. *Cell,* 98**,** 181-191.

SOUERS, A. J., LEVERSON, J. D., BOGHAERT, E. R., ACKLER, S. L., CATRON, N. D., CHEN, J., DAYTON, B. D., DING, H., ENSCHEDE, S. H. & FAIRBROTHER, W. J. 2013. ABT-199, a potent and selective BCL-2 inhibitor, achieves antitumor activity while sparing platelets. *Nature medicine,* 19**,** 202.

SPECK, N. A. & GILLILAND, D. G. 2002. Core-binding factors in haematopoiesis and leukaemia. *Nature Reviews Cancer,* 2**,** 502-513.

SPIEKERMANN, K., BAGRINTSEVA, K., SCHWAB, R., SCHMIEJA, K. & HIDDEMANN, W. 2003a. Overexpression and constitutive activation of FLT3 induces STAT5 activation in primary acute myeloid leukemia blast cells. *Clin Cancer Res,* 9**,** 2140-50.

SPIEKERMANN, K., BAGRINTSEVA, K., SCHWAB, R., SCHMIEJA, K. & HIDDEMANN, W. 2003b. Overexpression and constitutive activation of FLT3 induces STAT5 activation in primary acute myeloid leukemia blast cells. *Clinical Cancer Research,* 9**,** 2140-2150.

STEELMAN, L., ABRAMS, S., WHELAN, J., BERTRAND, F., LUDWIG, D., BÄSECKE, J., LIBRA, M., STIVALA, F., MILELLA, M. & TAFURI, A. 2008. Contributions of the Raf/MEK/ERK, PI3K/PTEN/Akt/mTOR and Jak/STAT pathways to leukemia. *Leukemia,* 22**,** 686-707.

STEIN, E. M., DINARDO, C., ALTMAN, J. K., COLLINS, R., DEANGELO, D. J., KANTARJIAN, H. M., SEKERES, M. A., FATHI, A. T., FLINN, I. W. & FRANKEL, A. E. 2015. Safety and efficacy of AG-221, a potent inhibitor of mutant IDH2 that promotes differentiation of myeloid cells in patients with advanced hematologic malignancies: results of a phase 1/2 trial. American Society of Hematology Washington, DC.

STERNBERG, S. H., LAFRANCE, B., KAPLAN, M. & DOUDNA, J. A. 2015. Conformational control of DNA target cleavage by CRISPR–Cas9. *Nature,* 527**,** 110-113.

STIREWALT, D., POGOSOVA-AGADJANYAN, E., TSUCHIYA, K., JOAQUIN, J. & MESHINCHI, S. 2014. Copy-neutral loss of heterozygosity is prevalent and a late event in the pathogenesis of FLT3/ITD AML. *Blood cancer journal,* 4**,** e208-e208.

STIREWALT, D. L., KOPECKY, K. J., MESHINCHI, S., APPELBAUM, F. R., SLOVAK, M. L., WILLMAN, C. L. & RADICH, J. P. 2001. FLT3, RAS, and TP53 mutations in elderly patients with acute myeloid leukemia. *Blood, The Journal of the American Society of Hematology,* 97**,** 3589-3595.

STIREWALT, D. L. & RADICH, J. P. 2003. The role of FLT3 in haematopoietic malignancies. *Nature Reviews Cancer,* 3**,** 650-665.

STÖLZEL, F., STEUDEL, C., OELSCHLÄGEL, U., MOHR, B., KOCH, S., EHNINGER, G. & THIEDE, C. 2010. Mechanisms of resistance against PKC412 in resistant FLT3-ITD positive human acute myeloid leukemia cells. *Annals of hematology,* 89**,** 653-662.

STONE, R. M., DEANGELO, D. J., KLIMEK, V., GALINSKY, I., ESTEY, E., NIMER, S. D., GRANDIN, W., LEBWOHL, D., WANG, Y., COHEN, P., FOX, E. A., NEUBERG, D., CLARK, J., GILLILAND, D. G. & GRIFFIN, J. D. 2005. Patients with acute myeloid leukemia and an activating

mutation in FLT3 respond to a small-molecule FLT3 tyrosine kinase inhibitor, PKC412. *Blood,* 105**,** 54-60.

STONE, R. M., FISCHER, T., PAQUETTE, R., SCHILLER, G., SCHIFFER, C. A., EHNINGER, G., CORTES, J., KANTARJIAN, H. M., DEANGELO, D. J. & HUNTSMAN-LABED, A. 2012. Phase IB study of the FLT3 kinase inhibitor midostaurin with chemotherapy in younger newly diagnosed adult patients with acute myeloid leukemia. *Leukemia,* 26**,** 2061-2068.

STONE, R. M., MANDREKAR, S. J., SANFORD, B. L., LAUMANN, K., GEYER, S., BLOOMFIELD, C. D., THIEDE, C., PRIOR, T. W., DÖHNER, K. & MARCUCCI, G. 2017a. Midostaurin plus chemotherapy for acute myeloid leukemia with a FLT3 mutation. *New England Journal of Medicine,* 377**,** 454-464.

STONE, R. M., MANDREKAR, S. J., SANFORD, B. L., LAUMANN, K., GEYER, S. M., BLOOMFIELD, C. D., DOHNER, K., THIEDE, C., MARCUCCI, G. & LO COCO, F. 2017b. The addition of midostaurin to standard chemotherapy decreases cumulative incidence of relapse (CIR) in the international prospective randomized, placebo-controlled, double-blind trial (CALGB 10603/RATIFY [Alliance]) for newly diagnosed acute myeloid leukemia (AML) patients with FLT3 mutations. *Blood,* 130**,** 2580-2580.

STONE, R. M., WANG, E. S., GOLDBERG, A. D., SWEET, K. L., FATHI, A. T., LIU, H. & MESSAHEL, B. 2019. Crenolanib versus midostaurin combined with induction and consolidation chemotherapy in newly diagnosed FLT3 mutated AML. American Society of Clinical Oncology.

STUBBS, M., KIM, Y., KRIVTSOV, A., WRIGHT, R., FENG, Z., AGARWAL, J., KUNG, A. & ARMSTRONG, S. 2008. MLL-AF9 and FLT3 cooperation in acute myelogenous leukemia: development of a model for rapid therapeutic assessment. *Leukemia,* 22**,** 66-77.

SWAMINATHAN, M., KANTARJIAN, H. M., DAVER, N., BORTHAKUR, G., OHANIAN, M., KADIA, T., DINARDO, C. D., JAIN, N., ESTROV, Z. & FERRAJOLI, A. 2017. The combination of quizartinib with azacitidine or low dose cytarabine is highly active in patients (Pts) with FLT3-ITD mutated myeloid leukemias: interim report of a phase I/II trial. *Blood,* 130**,** 723-723.

TABONE-EGLINGER, S., SUBRA, F., EL SAYADI, H., ALBERTI, L., TABONE, E., MICHOT, J.-P., THÉOU-ANTON, N., LEMOINE, A., BLAY, J.-Y. & EMILE, J.-F. 2008. KIT mutations induce intracellular retention and activation of an immature form of the KIT protein in gastrointestinal stromal tumors. *Clinical Cancer Research,* 14**,** 2285-2294.

TAKAHASHI, S. 2011. Current findings for recurring mutations in acute myeloid leukemia. *Journal of hematology & oncology,* 4**,** 36.

TAKAHASHI, S. 2019. Mutations of FLT3 receptor affect its surface glycosylation, intracellular localization, and downstream signaling. *Leukemia Research Reports***,** 100187.

TAKAHASHI, S. 2020. Mutations of FLT3 receptor affect its surface glycosylation, intracellular localization, and downstream signaling. *Leukemia research reports,* 13**,** 100187.

TAMAMYAN, G., KADIA, T., RAVANDI, F., BORTHAKUR, G., CORTES, J., JABBOUR, E., DAVER, N., OHANIAN, M., KANTARJIAN, H. & KONOPLEVA, M. 2017. Frontline treatment of acute myeloid leukemia in adults. *Crit Rev Oncol Hematol,* 110**,** 20-34.

TAMMA, R. & RIBATTI, D. 2017. Bone niches, hematopoietic stem cells, and vessel formation. *International journal of molecular sciences,* 18**,** 151.

TEO, Y. L., HO, H. K. & CHAN, A. 2015. Metabolism-related pharmacokinetic drug− drug interactions with tyrosine kinase inhibitors: current understanding, challenges and recommendations. *British journal of clinical pharmacology,* 79**,** 241-253.

THIEDE, C., STEUDEL, C., MOHR, B., SCHAICH, M., SCHÄKEL, U., PLATZBECKER, U., WERMKE, M., BORNHÄUSER, M., RITTER, M. & NEUBAUER, A. 2002. Analysis of FLT3-activating mutations in 979 patients with acute myelogenous leukemia: association with FAB subtypes and identification of subgroups with poor prognosisPresented in part at the 42nd Annual Meeting of the American Society of Hematology, December 1-5, 2000, San Francisco, CA (abstract 2334). *Blood,* 99**,** 4326-4335.

THOTA, R., JOHNSON, D. B. & SOSMAN, J. A. 2015. Trametinib in the treatment of melanoma. *Expert opinion on biological therapy,* 15**,** 735-747.

TOTHOVA, Z., KOLLIPARA, R., HUNTLY, B. J., LEE, B. H., CASTRILLON, D. H., CULLEN, D. E., MCDOWELL, E. P., LAZO-KALLANIAN, S., WILLIAMS, I. R. & SEARS, C. 2007. FoxOs are critical mediators of hematopoietic stem cell resistance to physiologic oxidative stress. *Cell,* 128**,** 325-339.

TRAER, E., MARTINEZ, J., JAVIDI-SHARIFI, N., AGARWAL, A., DUNLAP, J., ENGLISH, I., KOVACSOVICS, T., TYNER, J. W., WONG, M. & DRUKER, B. J. 2016. FGF2 from marrow microenvironment promotes resistance to FLT3 inhibitors in acute myeloid leukemia. *Cancer research,* 76**,** 6471-6482.

TROMPOUKI, E., BOWMAN, T. V., LAWTON, L. N., FAN, Z. P., WU, D.-C., DIBIASE, A., MARTIN, C. S., CECH, J. N., SESSA, A. K. & LEBLANC, J. L. 2011. Lineage regulators direct BMP and Wnt pathways to cell-specific programs during differentiation and regeneration. *Cell,* 147**,** 577-589.

TSAPOGAS, P., SWEE, L. K., NUSSER, A., NUBER, N., KREUZALER, M., CAPOFERRI, G., ROLINK, H., CEREDIG, R. & ROLINK, A. 2014. In vivo evidence for an instructive role of fms-like tyrosine kinase-3 (FLT3) ligand in hematopoietic development. *Haematologica,* 99**,** 638-646.

TSE, C., SHOEMAKER, A. R., ADICKES, J., ANDERSON, M. G., CHEN, J., JIN, S., JOHNSON, E. F., MARSH, K. C., MITTEN, M. J. & NIMMER, P. 2008. ABT-263: a potent and orally bioavailable Bcl-2 family inhibitor. *Cancer research,* 68**,** 3421-3428.

TSE, K., MUKHERJEE, G. & SMALL, D. 2000. Constitutive activation of FLT3 stimulates multiple intracellular signal transducers and results in transformation. *Leukemia,* 14**,** 1766-1776.

TSITSIPATIS, D., JAYAVELU, A. K., MÜLLER, J. P., BAUER, R., SCHMIDT-ARRAS, D., MAHBOOBI, S., SCHNÖDER, T. M., HEIDEL, F. & BOEHMER, F.-D. 2017. Synergistic killing of FLT3ITD-positive AML

cells by combined inhibition of tyrosine-kinase activity and N-glycosylation. *Oncotarget,* 8**,** 26613.

TURNER, A. M., LIN, N. L., ISSARACHAI, S., LYMAN, S. D. & BROUDY, V. 1996. FLT3 receptor expression on the surface of normal and malignant human hematopoietic cells.

TZELEPIS, K., KOIKE-YUSA, H., DE BRAEKELEER, E., LI, Y., METZAKOPIAN, E., DOVEY, O. M., MUPO, A., GRINKEVICH, V., LI, M. & MAZAN, M. 2016. A CRISPR dropout screen identifies genetic vulnerabilities and therapeutic targets in acute myeloid leukemia. *Cell reports,* 17**,** 1193-1205.

UENO, Y., KANEKO, N., SAITO, R., KONDOH, Y., SHIMADA, I., MORI, M. & KUROMITSU, S. 2014. ASP2215, a novel FLT3/AXL inhibitor: Preclinical evaluation in combination with cytarabine and anthracycline in acute myeloid leukemia (AML). American Society of Clinical Oncology.

VANHAESEBROECK, B., ALI, K., BILANCIO, A., GEERING, B. & FOUKAS, L. C. 2005. Signalling by PI3K isoforms: insights from gene-targeted mice. *Trends in biochemical sciences,* 30**,** 194-204.

VANHAESEBROECK, B., GUILLERMET-GUIBERT, J., GRAUPERA, M. & BILANGES, B. 2010. The emerging mechanisms of isoform-specific PI3K signalling. *Nature reviews Molecular cell biology,* 11**,** 329-341.

VELTEN, L., HAAS, S. F., RAFFEL, S., BLASZKIEWICZ, S., ISLAM, S., HENNIG, B. P., HIRCHE, C., LUTZ, C., BUSS, E. C. & NOWAK, D. 2017. Human haematopoietic stem cell lineage commitment is a continuous process. *Nature cell biology,* 19**,** 271-281.

VEMPATI, S., REINDL, C., WOLF, U., KERN, R., PETROPOULOS, K., NAIDU, V. M., BUSKE, C., HIDDEMANN, W., KOHL, T. M. & SPIEKERMANN, K. 2008. Transformation by oncogenic mutants and ligand-dependent activation of FLT3 wild-type requires the tyrosine residues 589 and 591. *Clinical Cancer Research,* 14**,** 4437-4445.

VENDITTI, A., DEL POETA, G., MAURILLO, L., BUCCISANO, F., DEL PRINCIPE, M. I., MAZZONE, C., TAMBURINI, A., COX, C., PANETTA, P. & NERI, B. 2004. Combined analysis of bcl-2 and MDR1 proteins in 256 cases of acute myeloid leukemia. *Haematologica,* 89**,** 934-939.

VERSTRAETE, K., VANDRIESSCHE, G., JANUAR, M., ELEGHEERT, J., SHKUMATOV, A. V., DESFOSSES, A., VAN CRAENENBROECK, K., SVERGUN, D. I., GUTSCHE, I. & VERGAUWEN, B. 2011. Structural insights into the extracellular assembly of the hematopoietic Flt3 signaling complex. *Blood, The Journal of the American Society of Hematology,* 118**,** 60-68.

VOLKMANN, N., MARASSI, F., NEWMEYER, D. & HANEIN, D. 2014. The rheostat in the membrane: BCL-2 family proteins and apoptosis. *Cell Death & Differentiation,* 21**,** 206-215.

WALLACH, D., VARFOLOMEEV, E., MALININ, N., GOLTSEV, Y. V., KOVALENKO, A. & BOLDIN, M. 1999. Tumor necrosis factor receptor and Fas signaling mechanisms. *Annual review of immunology,* 17**,** 331-367.

WANG, A., WU, H., CHEN, C., HU, C., QI, Z., WANG, W., YU, K., LIU, X., ZOU, F. & ZHAO, Z. 2016a. Dual inhibition of AKT/FLT3-ITD by

A674563 overcomes FLT3 ligand-induced drug resistance in FLT3-ITD positive AML. *Oncotarget,* 7**,** 29131.

WANG, C. X. & CANNON, P. M. 2016. The clinical applications of genome editing in HIV. *Blood, The Journal of the American Society of Hematology,* 127**,** 2546-2552.

WANG, E. S., TALLMAN, M. S., STONE, R. M., WALTER, R. B., KARANES, C., JAIN, V. & COLLINS, R. H. 2017. Low relapse rate in younger patients≤ 60 years old with newly diagnosed FLT3-mutated acute myeloid leukemia (AML) treated with crenolanib and cytarabine/anthracycline chemotherapy. *Blood,* 130**,** 566-566.

WANG, H., YANG, H., SHIVALILA, C. S., DAWLATY, M. M., CHENG, A. W., ZHANG, F. & JAENISCH, R. 2013. One-step generation of mice carrying mutations in multiple genes by CRISPR/Cas-mediated genome engineering. *Cell,* 153**,** 910-918.

WANG, L., LI, F., DANG, L., LIANG, C., WANG, C., HE, B., LIU, J., LI, D., WU, X., XU, X., LU, A. & ZHANG, G. 2016b. In Vivo Delivery Systems for Therapeutic Genome Editing. *Int J Mol Sci,* 17.

WARREN, C. F., WONG-BROWN, M. W. & BOWDEN, N. A. 2019. BCL-2 family isoforms in apoptosis and cancer. *Cell death & disease,* 10**,** 1-12.

WARSCH, W., KOLLMANN, K., ECKELHART, E., FAJMANN, S., CERNY-REITERER, S., HÖLBL, A., GLEIXNER, K. V., DWORZAK, M., MAYERHOFER, M. & HOERMANN, G. 2011. High STAT5 levels mediate imatinib resistance and indicate disease progression in chronic myeloid leukemia. *Blood, The Journal of the American Society of Hematology,* 117**,** 3409-3420.

WEI, Q. & FRENETTE, P. S. 2018. Niches for hematopoietic stem cells and their progeny. *Immunity,* 48**,** 632-648.

WEIS, T. M., MARINI, B. L., BIXBY, D. L. & PERISSINOTTI, A. J. 2019. Clinical considerations for the use of FLT3 inhibitors in acute myeloid leukemia. *Critical reviews in oncology/hematology,* 141**,** 125-138.

WEISBERG, E., BOULTON, C., KELLY, L. M., MANLEY, P., FABBRO, D., MEYER, T., GILLILAND, D. G. & GRIFFIN, J. D. 2002. Inhibition of mutant FLT3 receptors in leukemia cells by the small molecule tyrosine kinase inhibitor PKC412. *Cancer cell,* 1**,** 433-443.

WEISBERG, E., SATTLER, M., RAY, A. & GRIFFIN, J. 2010. Drug resistance in mutant FLT3-positive AML. *Oncogene,* 29**,** 5120-5134.

WESTON, S. A. & PARISH, C. R. 1990. New fluorescent dyes for lymphocyte migration studies: analysis by flow cytometry and fluorescence microscopy. *Journal of immunological methods,* 133**,** 87-97.

WETERINGS, E. & CHEN, D. J. 2008. The endless tale of non-homologous end-joining. *Cell research,* 18**,** 114-124.

WHITMAN, S. P., ARCHER, K. J., FENG, L., BALDUS, C., BECKNELL, B., CARLSON, B. D., CARROLL, A. J., MRÓZEK, K., VARDIMAN, J. W. & GEORGE, S. L. 2001. Absence of the wild-type allele predicts poor prognosis in adult de novo acute myeloid leukemia with normal cytogenetics and the internal tandem duplication of FLT3: a cancer and leukemia group B study. *Cancer research,* 61**,** 7233-7239.

WIEDENHEFT, B., STERNBERG, S. H. & DOUDNA, J. A. 2012. RNA-guided genetic silencing systems in bacteria and archaea. *Nature,* 482**,** 331-338.

WILLIAMS, A. B., LI, L., NGUYEN, B., BROWN, P., LEVIS, M. & SMALL, D. 2012. Fluvastatin inhibits FLT3 glycosylation in human and murine cells and prolongs survival of mice with FLT3/ITD leukemia. *Blood, The Journal of the American Society of Hematology,* 120**,** 3069-3079.

WILSON, A., LAURENTI, E., OSER, G., VAN DER WATH, R. C., BLANCO-BOSE, W., JAWORSKI, M., OFFNER, S., DUNANT, C. F., ESHKIND, L. & BOCKAMP, E. 2008. Hematopoietic stem cells reversibly switch from dormancy to self-renewal during homeostasis and repair. *Cell,* 135**,** 1118-1129.

WILSON, T. R., FRIDLYAND, J., YAN, Y., PENUEL, E., BURTON, L., CHAN, E., PENG, J., LIN, E., WANG, Y. & SOSMAN, J. 2012. Widespread potential for growth-factor-driven resistance to anticancer kinase inhibitors. *Nature,* 487**,** 505-509.

WOOD, A. J., LO, T.-W., ZEITLER, B., PICKLE, C. S., RALSTON, E. J., LEE, A. H., AMORA, R., MILLER, J. C., LEUNG, E. & MENG, X. 2011. Targeted genome editing across species using ZFNs and TALENs. *Science,* 333**,** 307-307.

WOOLLEY, J. F., NAUGHTON, R., STANICKA, J., GOUGH, D. R., BHATT, L., DICKINSON, B. C., CHANG, C. J. & COTTER, T. G. 2012. H 2 O 2 production downstream of FLT3 is mediated by p22phox in the endoplasmic reticulum and is required for STAT5 signalling. *PLoS One,* 7**,** e34050.

WU, X., LUO, Q. & LIU, Z. 2020. Ubiquitination and deubiquitination of MCL1 in cancer: deciphering chemoresistance mechanisms and providing potential therapeutic options. *Cell Death & Disease,* 11**,** 1-11.

XIANG, Z., LUO, H., PAYTON, J. E., WARTMAN, L. D., RITCHEY, J., DIPERSIO, J. F., LEY, T. J., OPFERMAN, J. T. & TOMASSON, M. 2009. MCL1 Haploinsufficiency Protects Mice From MYC-Induced Acute Myeloid Leukemia. American Society of Hematology.

XUE, W., CHEN, S., YIN, H., TAMMELA, T., PAPAGIANNAKOPOULOS, T., JOSHI, N. S., CAI, W., YANG, G., BRONSON, R. & CROWLEY, D. G. 2014. CRISPR-mediated direct mutation of cancer genes in the mouse liver. *Nature,* 514**,** 380-384.

YAMADA, M., WATANABE, Y., GOOTENBERG, J. S., HIRANO, H., RAN, F. A., NAKANE, T., ISHITANI, R., ZHANG, F., NISHIMASU, H. & NUREKI, O. 2017. Crystal structure of the minimal Cas9 from Campylobacter jejuni reveals the molecular diversity in the CRISPR-Cas9 systems. *Molecular cell,* 65**,** 1109-1121. e3.

YAMAMOTO, R., MORITA, Y., OOEHARA, J., HAMANAKA, S., ONODERA, M., RUDOLPH, K. L., EMA, H. & NAKAUCHI, H. 2013. Clonal analysis unveils self-renewing lineage-restricted progenitors generated directly from hematopoietic stem cells. *Cell,* 154**,** 1112-1126.

YAMAMOTO, Y., KIYOI, H., NAKANO, Y., SUZUKI, R., KODERA, Y., MIYAWAKI, S., ASOU, N., KURIYAMA, K., YAGASAKI, F. & SHIMAZAKI, C. 2001. Activating mutation of D835 within the activation loop of FLT3 in human hematologic malignancies. *Blood, The Journal of the American Society of Hematology,* 97**,** 2434-2439.

YAMAURA, T., NAKATANI, T., UDA, K., OGURA, H., SHIN, W., KUROKAWA, N., SAITO, K., FUJIKAWA, N., TAKASAKI, M. & TERADA, D. 2018. A novel irreversible FLT3 inhibitor, FF-10101, shows excellent efficacy against AML cells with FLT3 mutations. *Blood,* 131**,** 426-438.

YANG, L., BRYDER, D., ADOLFSSON, J. R., NYGREN, J., MÅNSSON, R., SIGVARDSSON, M. & JACOBSEN, S. E. W. 2005. Identification of Lin–Sca1+ kit+ CD34+ Flt3–short-term hematopoietic stem cells capable of rapidly reconstituting and rescuing myeloablated transplant recipients. *Blood,* 105**,** 2717-2723.

YANG, X., SEXAUER, A. & LEVIS, M. 2014. Bone marrow stroma-mediated resistance to FLT 3 inhibitors in FLT 3-ITD AML is mediated by persistent activation of extracellular regulated kinase. *British journal of haematology,* 164**,** 61-72.

YAO, Z., CUI, Y., WATFORD, W. T., BREAM, J. H., YAMAOKA, K., HISSONG, B. D., LI, D., DURUM, S. K., JIANG, Q. & BHANDOOLA, A. 2006. Stat5a/b are essential for normal lymphoid development and differentiation. *Proceedings of the National Academy of Sciences,* 103**,** 1000-1005.

YARDEN, Y., KUANG, W.-J., YANG-FENG, T., COUSSENS, L., MUNEMITSU, S., DULL, T., CHEN, E., SCHLESSINGER, J., FRANCKE, U. & ULLRICH, A. 1987. Human proto-oncogene c-kit: a new cell surface receptor tyrosine kinase for an unidentified ligand. *The EMBO journal,* 6**,** 3341-3351.

YECIES, D., CARLSON, N. E., DENG, J. & LETAI, A. 2010. Acquired resistance to ABT-737 in lymphoma cells that up-regulate MCL-1 and BFL-1. *Blood, The Journal of the American Society of Hematology,* 115**,** 3304-3313.

YEE, K. W., O'FARRELL, A. M., SMOLICH, B. D., CHERRINGTON, J. M., MCMAHON, G., WAIT, C. L., MCGREEVEY, L. S., GRIFFITH, D. J. & HEINRICH, M. C. 2002. SU5416 and SU5614 inhibit kinase activity of wild-type and mutant FLT3 receptor tyrosine kinase. *Blood, The Journal of the American Society of Hematology,* 100**,** 2941-2949.

YEE, N. S., HSIAU, C., SERVE, H., VOSSELLER, K. & BESMER, P. 1994. Mechanism of down-regulation of c-kit receptor. Roles of receptor tyrosine kinase, phosphatidylinositol 3'-kinase, and protein kinase C. *Journal of Biological Chemistry,* 269**,** 31991-31998.

YOKOTA, S., KIYOI, H., NAKAO, M., IWAI, T., MISAWA, S., OKUDA, T., SONODA, Y., ABE, T., KAHSIMA, K., MATSUO, Y. & NAOE, T. 1997. Internal tandem duplication of the FLT3 gene is preferentially seen in acute myeloid leukemia and myelodysplastic syndrome among various hematological malignancies. A study on a large series of patients and cell lines. *Leukemia,* 11**,** 1605-9.

YOSHIMOTO, G., MIYAMOTO, T., JABBARZADEH-TABRIZI, S., IINO, T., ROCNIK, J. L., KIKUSHIGE, Y., MORI, Y., SHIMA, T., IWASAKI, H. & TAKENAKA, K. 2009. FLT3-ITD up-regulates MCL-1 to promote survival of stem cells in acute myeloid leukemia via FLT3-ITD–specific STAT5 activation. *Blood, The Journal of the American Society of Hematology,* 114**,** 5034-5043.

YOULE, R. J. & STRASSER, A. 2008. The BCL-2 protein family: opposing activities that mediate cell death. *Nature reviews Molecular cell biology,* 9**,** 47-59.

ZARRINKAR, P. P., GUNAWARDANE, R. N., CRAMER, M. D., GARDNER, M. F., BRIGHAM, D., BELLI, B., KARAMAN, M. W., PRATZ, K. W., PALLARES, G. & CHAO, Q. 2009a. AC220 is a uniquely potent and selective inhibitor of FLT3 for the treatment of acute myeloid leukemia (AML). *Blood, The Journal of the American Society of Hematology,* 114**,** 2984-2992.

ZARRINKAR, P. P., GUNAWARDANE, R. N., CRAMER, M. D., GARDNER, M. F., BRIGHAM, D., BELLI, B., KARAMAN, M. W., PRATZ, K. W., PALLARES, G., CHAO, Q., SPRANKLE, K. G., PATEL, H. K., LEVIS, M., ARMSTRONG, R. C., JAMES, J. & BHAGWAT, S. S. 2009b. AC220 is a uniquely potent and selective inhibitor of FLT3 for the treatment of acute myeloid leukemia (AML). *Blood,* 114**,** 2984-92.

ZHANG, C. C. & LODISH, H. F. 2008. Cytokines regulating hematopoietic stem cell function. *Current opinion in hematology,* 15**,** 307.

ZHANG, H., SAVAGE, S., SCHULTZ, A. R., BOTTOMLY, D., WHITE, L., SEGERDELL, E., WILMOT, B., MCWEENEY, S. K., EIDE, C. A. & NECHIPORUK, T. 2019. Clinical resistance to crenolanib in acute myeloid leukemia due to diverse molecular mechanisms. *Nature communications,* 10**,** 1-13.

ZHANG, S. & BROXMEYER, H. E. 2000. Flt3 ligand induces tyrosine phosphorylation of gab1 and gab2 and their association with shp-2, grb2, and PI3 kinase. *Biochemical and biophysical research communications,* 277**,** 195-199.

ZHANG, S., FUKUDA, S., LEE, Y., HANGOC, G., COOPER, S., SPOLSKI, R., LEONARD, W. J. & BROXMEYER, H. E. 2000. Essential role of signal transducer and activator of transcription (Stat) 5a but not Stat5b for Flt3-dependent signaling. *The Journal of experimental medicine,* 192**,** 719-728.

ZHANG, W., GAO, C., KONOPLEVA, M., CHEN, Y., JACAMO, R. O., BORTHAKUR, G., CORTES, J. E., RAVANDI, F., RAMACHANDRAN, A. & ANDREEFF, M. 2014. Reversal of acquired drug resistance in FLT3-mutated acute myeloid leukemia cells via distinct drug combination strategies. *Clinical Cancer Research,* 20**,** 2363-2374.

ZHANG, W., KONOPLEVA, M., RUVOLO, V., MCQUEEN, T., EVANS, R., BORNMANN, W., MCCUBREY, J., CORTES, J. & ANDREEFF, M. 2008. Sorafenib induces apoptosis of AML cells via Bim-mediated activation of the intrinsic apoptotic pathway. *Leukemia,* 22**,** 808-818.

ZHANG, Y., GAO, S., XIA, J. & LIU, F. 2018. Hematopoietic hierarchy–an updated roadmap. *Trends in cell biology,* 28**,** 976-986.

ZHAO, J., SONG, Y. & LIU, D. 2019. Gilteritinib: a novel FLT3 inhibitor for acute myeloid leukemia. *Biomark Res,* 7**,** 19.

ZHAO, Z., WU, H., WANG, L., LIU, Y., KNAPP, S., LIU, Q. & GRAY, N. S. 2014. Exploration of type II binding mode: A privileged approach for kinase inhibitor focused drug discovery? *ACS chemical biology,* 9**,** 1230-1241.

ZHENG, R., BAILEY, E., NGUYEN, B., YANG, X., PILOTO, O., LEVIS, M. & SMALL, D. 2011. Further activation of FLT3 mutants by FLT3 ligand. *Oncogene,* 30**,** 4004-4014.

ZHENG, R., FRIEDMAN, A. D., LEVIS, M., LI, L., WEIR, E. G. & SMALL, D. 2004. Internal tandem duplication mutation of FLT3 blocks myeloid differentiation through suppression of C/EBPα expression. *Blood,* 103**,** 1883-1890.

ZHOU, J., BI, C., JANAKAKUMARA, J. V., LIU, S.-C., CHNG, W.-J., TAY, K.-G., POON, L.-F., XIE, Z., PALANIYANDI, S. & YU, H. 2009. Enhanced activation of STAT pathways and overexpression of survivin confer resistance to FLT3 inhibitors and could be therapeutic targets in AML. *Blood, The Journal of the American Society of Hematology,* 113**,** 4052-4062.

ZORN, J. A., WANG, Q., FUJIMURA, E., BARROS, T. & KURIYAN, J. 2015. Crystal structure of the FLT3 kinase domain bound to the inhibitor quizartinib (AC220). *PloS one,* 10**,** e0121177.